Imperial College
London

Water Distribution Networks with Dynamic Topology

A thesis submitted to the Imperial College of Science, Engineering and Medicine for the degree of Doctor of Philosophy

by

Robert John Wright

2016

Department of Civil and Environmental Engineering

ABSTRACT

The subdivision of water distribution networks (WDN) into zones, known as district metered areas (DMAs), is a popular approach to leakage management used by water companies. The DMAs are formed by permanently closing isolation valves at the boundaries of each zone (known as boundary valves). By forming discrete zones in the WDN, leakage estimates can be made at night when demand is low, which is used to prioritise pipe repair and replacement programmes. However, the permanent closure of boundary valves has also caused several disadvantages, including reduced network resilience to failure, sub-optimal pressure management, and water quality problems.

This thesis introduces a novel approach to the operational management of WDNs, where DMAs are dynamically aggregated for improved network resilience, pressure management and water quality, and segregated for leakage monitoring at night. This is facilitated by replacing closed boundary valves with self-powered, remote control valves (dynamic boundary valves). The operation of a dynamic topology can therefore successfully eliminate the disadvantages of conventional DMAs, whilst retaining or improving their success in leakage monitoring. The investigation is carried out both analytically and experimentally on a real, operational UK network supplying approximately 8,000 properties in order to establish the benefits and challenges of the proposed approach.

An extensive review of the current and emerging forms of pressure and DMA management from around the world is carried out. A case study using a real large scale network (3,148km of pipeline) demonstrates the current state of DMAs and their conformity to DMA design guidelines, and identifies how a dynamic DMA topology can improve network performance. A novel resilience index (the Reserve Capacity) is then used in the design of the dynamic DMA topology in the experimental programme.

The analytical and experimental investigation has demonstrated a 27% reduction in leakage using a dynamic DMA topology over the most common approach to pressure management, and strong improvements in network resilience to failure where 1,400 customers maintained a supply during a real, major burst incident that would otherwise have been disconnected. In order to actuate near optimal control in the experimental programme, a novel optimisation algorithm based on sequential convex programming (SCP) is proposed for the control of valves. The SCP method takes advantage of computationally efficient solvers that facilitate prompt and reliable convergence. The algorithm also includes the development of a novel, convex valve model that can be integrated into efficient null space algorithms. In order to actuate the control, a novel approach for valve control in DMAs with dynamic topology is proposed, where time varying flow modulation curves are used based on the dynamic connectivity of DMAs.

ACKNOWLEDGMENTS

I would like to thank everyone that has contributed to this thesis.

To my academic supervisor Ivan Stoianov and my industrial sponsor and supervisor John King, former MD of Cla-Val UK Ltd, for motivating my interest in this area, giving me the opportunity to undertake the work, and supporting me throughout. Long may our interesting discussions about the current and future operation of water supply systems continue. To my second supervisor Panos Parpas who joined the project after the first year. Your assistance with the optimisation work came at a time when I needed it most.

To the whole team at Bristol Water, in particular Kevin Henderson, Selina Ward, Richard Foster, David Watts, Nigel Colgan, Julian Woonton, Frank Van Der Kleij, Jamie Angelinetta, Mathias Pacalin, Ian Michell, and David Burnell. I thank you all for your kindness and help throughout.

To Cla-Val Ltd for the financial backing of this project and technical support. In particular, to Hugo Van Buel and David Humphrey for your assistance and our interesting meetings, to Karim Amdouni and Fabrice Largey for always being there to ensure we have communication with the valves, and to Mike Plant for ensuring the valves run like Swiss clockwork. To the Engineering and Physical Sciences Research Council for the additional financial support of the project.

To all past and present members of room 409 (*A.H.*) that I have had the pleasure of sharing an office with. In particular, to Asher Hoskins for your help with data acquisition, to Karl Smith for your, quite literally, endless words of guidance, to Edo Abraham and Manuel Herrera for your support and friendship, and to Quentin Cheok for your friendship and unassuming advice over these years.

To the members of *Under Construction*. Music is the perfect retreat.

To Christina, for helping me along the way and making the journey all the more enjoyable.

Finally to my parents Geoff & Jane Wright. Without their support I would not have been able to complete this work and it is to them that I dedicate this thesis.

DECLARATION OF ORIGINALITY

I hereby declare that all work presented in this thesis is my own, unless otherwise cited.

COPYRIGHT DECLARATION

The copyright of this thesis rests with the author and is made available under a Creative Commons Attribution Non-Commercial No Derivatives licence. Researchers are free to copy, distribute or transmit the thesis on the condition that they attribute it, that they do not use it for commercial purposes and that they do not alter, transform or build upon it. For any reuse or redistribution, researchers must make clear to others the licence terms of this work.

Contents

List of Figures **9**

List of Tables **15**

1 Introduction **16**
1.1 Background . . . 16
1.2 Water Distribution Networks with Dynamic Topology . . . 18
1.3 Objectives . . . 20
1.4 Methodology . . . 21
1.5 Publications . . . 22
1.5.1 Journal Papers . . . 22
1.5.2 Conference Papers . . . 23

2 Hydraulic Modelling **24**
2.1 Introduction . . . 24
2.2 Network Representation and Notation . . . 25
2.3 Hydraulic Equations: Mass and Energy Conservation . . . 26
2.4 Solution Methods . . . 28
2.4.1 Global Gradient Algorithm . . . 32
2.4.2 Null Space (Loop) Method . . . 34
2.5 Stopping Criterion . . . 35
2.6 Regularisation . . . 36
2.7 Modelling Control Valves . . . 37
2.8 Online Model Parameter Update . . . 42
2.9 Pressure Dependent Demand . . . 42
2.9.1 Demand-Pressure Relationships . . . 42
2.9.2 Pressure-Driven GGA . . . 44
2.10 Conclusion . . . 46

3 Design and Analysis of District Metered Areas **48**
3.1 Introduction . . . 48
3.2 DMA Description . . . 48
3.3 Advantages of the DMA . . . 49
3.3.1 Leakage Assessment . . . 49
3.3.2 Pressure Management . . . 51
3.3.3 Other Advantages . . . 53
3.4 Disadvantages of the DMA . . . 53
3.4.1 Resilience to Failure . . . 53
3.4.2 Frictional Energy Losses . . . 55
3.4.3 Other Disadvantages . . . 56
3.5 Performance Indicators . . . 57

3.5.1 Pressure and Leakage Management . . . 57
3.5.2 Resilience to Failure . . . 59
3.6 DMA Design . . . 62
3.6.1 Critical Customers and Regulations . . . 62
3.6.2 Establishing the DMA Boundary . . . 63
3.6.3 DMA Size . . . 64
3.6.4 Critical Points . . . 65
3.6.5 Flow Meter Installation . . . 65
3.6.6 Zero Pressure Test . . . 66
3.6.7 Automated DMA Design . . . 67
3.7 Approaches to Pressure Management . . . 67
3.7.1 Fixed Outlet Pressure Reducing Valve . . . 67
3.7.2 Timer Controlled Outlet Pressure . . . 69
3.7.3 Flow Modulation . . . 69
3.7.4 Closed loop . . . 72
3.7.5 Hybrid Methods . . . 72
3.8 Alternatives to the DMA . . . 72
3.9 Global Trends in DMA Installation . . . 73
3.10 Case Study: Analysis of Large Scale Networks . . . 75
3.11 Conclusion . . . 78

4 Control of Multi-feed Pressure Managed Zones 80
4.1 Introduction . . . 80
4.2 Review of Multi-feed Pressure Managed DMA Practices . . . 81
4.2.1 Multiple Flow Modulating PRVs . . . 81
4.2.2 Combining Flow Modulating and Fixed Outlet PRVs . . . 82
4.2.3 Model Predictive Control . . . 83
4.3 Control Options for WDNs with Dynamic Topology . . . 84
4.3.1 Model Predictive Control . . . 84
4.3.2 Decentralised Control . . . 85
4.4 Undesirable Valve Behaviour . . . 89
4.4.1 Valve Oscillations . . . 89
4.4.2 Interaction of Flow Modulating PRVs . . . 91
4.5 Time Varying Flow Modulation Control . . . 92
4.6 Conclusion . . . 95

5 Experimental Programme 97
5.1 Introduction . . . 97
5.2 Network Description and Motivation . . . 98
5.3 Design . . . 100
5.3.1 Initial Model Calibration . . . 100
5.3.2 Candidate Options . . . 101

5.3.3 Pressure Management . . . 108
5.3.4 Resilience to Failure . . . 110
5.3.5 Conclusions . . . 114
5.4 Technology . . . 114
5.4.1 Pilot Valve for Bidirectional Control . . . 115
5.4.2 High Speed Pressure Monitoring (128S/s) . . . 117
5.4.3 Flow Meters . . . 117
5.4.4 Turbine for Energy Harvesting . . . 117
5.4.5 ADSL and GSM Telecommunications . . . 118
5.5 Hydraulic Model Calibration . . . 120
5.6 Conclusion . . . 125

6 Control Optimisation 127
6.1 Introduction . . . 127
6.2 General Overview of Problem Formulation . . . 128
6.3 Review of Optimization Methods for Valve Control . . . 129
6.3.1 Sequential Linear Programming . . . 129
6.3.2 Sequential Quadratic Programming . . . 130
6.3.3 Other Non Linear Program Solvers . . . 131
6.3.4 Evolutionary Algorithms . . . 134
6.4 Sequential Convex Programming for PRV Control . . . 134
6.4.1 Novel Valve Model for Optimal Control . . . 135
6.4.2 Problem Formulation . . . 136
6.4.3 Remarks on Problem Formulation . . . 137
6.4.4 Sub-Problem A . . . 139
6.4.5 Sub-Problem B . . . 140
6.4.6 Full Step Sequential Convex Programming . . . 141
6.4.7 Strictly Feasible Sequential Convex Programming . . . 143
6.5 Results . . . 146
6.5.1 Small Illustrative Example . . . 146
6.5.2 Experimental Programme Network (2 PRVs + 2 PRV Boundary Valves) . . . 148
6.5.3 Experimental Programme Network (2 PRVs + 2 Position Control Boundary Valves) . . . 154
6.5.4 Experimental Programme Network (3 PRVs + 2 Position Control Boundary Valves) . . . 157
6.6 Comparison with Other Optimisation Approaches . . . 159
6.7 Conclusion . . . 162

7 Experimental Investigation of Pressure Management and Network Resilience 164
7.1 Introduction . . . 164

7.2 Pressure Management 165
7.2.1 AZP and Pressure Variability 166
7.2.2 Background Leakage Estimation 171
7.3 Flow Reversals 174
7.4 Resilience to Failure 175
7.4.1 Medium Sized Bursts (Hydrant Flushing) 175
7.4.2 Large Burst Incident 178
7.5 Conclusion 180

8 Conclusion **182**
8.1 Novel Contributions 184
8.2 Future Work 185

Bibliography **187**

Appendix A Model Calibration **201**

Appendix B Validation of Model Calibration **212**

List of Figures

1.1 Adaptive sectorisation of water distribution networks with dynamically reconfigurable topology (Wright et al., 2014*a*): (a) Segregating a supply zone into DMAs for leakage detection during a period of low demand (02:00-04:00); (b) Aggregating DMAs into a large pressure management zone (04:00-02:00). 20

1.2 Thesis structure and methodology for investigating water distribution networks with dynamic topology 22

2.1 WDN notation 26

2.2 Comparison of solution accuracy using the infinite norm of the energy conservation equations ($\|g_1\|_\infty$) and the total number of iterations k required for convergence for a regularised and non-regularised (Todini) GGA solution method 37

2.3 Simulating a PRV in the experimental programme network (Figure 5.16) with the GGA and valve settings $\eta(h, q, \hat{h})$ for flow modulation. The modelled outlet pressure matches the target (outlet) pressure of the PRV with $\|g_1\|_\infty \leq 10^{-9}$ 41

3.1 A comparison of head losses at various consumption levels for a single and multiple inlet WDN 56

3.2 The schematic of a pressure reducing valve (Cla-Val, 2015*d*) with components: (1) main valve, (2) isolation valve, (3) strainer, (4) check valve flow control for main valve opening speed, (5) pilot valve, (A) strainer, (B) isolation valve, (C) check valve flow control for main valve closing speed, (Y) strainer and (D) check valve with isolation valves. 68

3.3 An example of a flow modulation curve and a statistical approach for its calculation, where $P2$ is the PRV outlet pressure and $P3$ is the CP pressure 71

3.4 (a) A real, operational water distribution network consisting of approximately 3,148km of pipeline, (b) the DMA boundaries (red lines), (c) a breakdown of pressure differential at closed boundary valves, and (d) a breakdown of diameter at closed boundary valves 77

4.1 Using the multifunction network controllers in a model predictive control framework (Wright et al., 2014*a*) 85

4.2 Master/Slave arrangement with Flow Modulating PRVs and FCVs 86

4.3 Master/Slave arrangement with flow modulating PRVs and fixed position valves 88

4.4 Data showing a consistent flow of approximately 4l/s through the dynamic boundary valve in the experimental programme when operating as a slave controller with fixed stem position (40%), attributed to the fact that pressure variability is low in the network 88

4.5 PRV dynamic behaviour in a single-inlet DMA caused by a pressure transient (Hoskins and Stoianov, 2014) 90
4.6 Pressure monitoring at 128 samples/s at a PRV for (a) a single-inlet network and (b) multi-inlet network 91
4.7 (a) Data (outlet pressure and flow) for PRV 1 and PRV 2, showing that PRV 2 is dominant on Sun, Tue and Thur, and PRV 1 is dominant on Wed and parts of Tue. 92
4.8 (a) Fitting a single flow modulation curve to optimal open loop settings at PRV 1 and (b) pressure at the CP when using just a single flow modulation curve for PRV 1 whilst operating a dynamic topology that opens to 80% in the day and closes at night 92
4.9 In order to obtain a better fit of flow modulation curve, it is proposed that a (a) Nighttime flow modulation curve is used for when the DMA topology is closed, (b) a daytime flow modulation curve is used for when the DMA topology is open, and (c) pressure at the CP 1 which is more stable at its minimum allowable pressure 94
5.1 Network configuration of the experimental programme before installation of the dynamic boundary and associated technologies . 99
5.2 Simulation of the field lab network by the water company using Infoworks WS, prior to the installation of the dynamic boundary, that confirms low pressure complaints from customers. Low pressure is experienced in the network due to high frictional head losses in cast iron mains 100
5.3 Initial calibration of the hydraulic model for investigating the design options of the field lab site (red dots: locations where hydraulic data was acquired) 101
5.4 The distribution of pipe diameter across the experimental programme network. Larger pipes provide larger capacity for flow. . 102
5.5 Option 1: DMA rezone + 2 PRVs 103
5.6 Low pressure simulated when rezoning the DMAs in the design process for Option 1 104
5.7 Option 2: Original DMA topology (closed) + Constant Outlet PRV + Time Varying Outlet PRV 105
5.8 Option 3: Dynamic boundary valve at location V1, PRV 1 following a time varying outlet profile, and PRV 2 fixed outlet pressure 106
5.9 Option 4: Dynamic boundary valve at location V3, PRV 1 following a time varying outlet profile, and PRV 2 fixed outlet pressure 107
5.10 Option 5: 2 Dynamic boundary valves at locations V1 and V3, PRV 1 and PRV 2 following a fixed outlet profile 108
5.11 A comparison of average daytime nodal pressure (P_{av}) for the potential design options 109

5.12 A comparison of pressure variability ($\overline{P}_{var}$) for the potential design options 109
5.13 A comparison of resilience indexes: (a) Design options produced using the developed resilience index (b) Design options produced using Todini's resilience index 110
5.14 A burst simulation at 8:30am comparing a kept shut (KS) boundary valve configuration, and a dynamic boundary valve configuration 112
5.15 Pipe closure scenarios 113
5.16 An overview of the experimental programme for the investigation of dynamic topologies for adaptive networks, showing the installed equipment 115
5.17 Schematic of a position control valve set up for bidirectional flow, to be used as a dynamic boundary valve 116
5.18 Equipment installation for the experimental programme: (a) PRV 1, (b) PRV 2, (c) DBV 1, (d) DBV 2, (e) PRV chamber and empty kiosk and (f) the kiosk fully equipped with ADSL, mains power and real-time pressure sensing 119
5.19 The locations of InfraSense TS pressure loggers (black triangles) sampling at up to 128S/s and used for hydraulic model calibration and insight into the hydraulic behaviour of the experimental programme during normal operation and failure situations. Control valves have two loggers installed, where the number notation is: First number (inlet), second number (outlet), both boundary valves have flow directions northerly 121
5.20 Calibrating demand profiles with inlet flow data 122
6.1 A convex set example taken from (Boyd and Vandenberghe, 2004, Sec. 2.1.4). 138
6.2 Demonstrating that the NLP in (6.14) is non-convex. In (a), The contours represent the objective function (AZP) and hydraulically feasible set $\mathbb{E}$, where PRV settings η are varied along each axis. The shaded area represents the operationally and hydraulically feasible set $\mathbb{E} \cap \mathbb{F}$. A line segment between two feasible points shows that not all of the line is in $\mathbb{E} \cap \mathbb{F}$, as highlighted in (b). . 139
6.3 Visualisation of the η search space for SCP (Wright et al., 2014*a*) 142
6.4 (a) Solution space $\mathbb{E}$ and objective function f (contours), and feasible space $\mathbb{E} \cap \mathbb{F}$ (shaded areas). Cycling in convergence in the infeasible area of the search space occurs with SCP (b) Objective function f (contours) in the LP search space (Sub-problem A). The solution to a linear program results in iterations outside of the feasible area in the non-linear search space of (a) 143
6.5 (a) Cycling in convergence in an infeasible area when using SCP (b) Strictly feasible steps to aid convergence in SFSCP 145

6.6 Small illustrative example network taken from Todini (2003) . . 147
6.7 Optimisation results for small illustrative network shown in Figure 6.6 148
6.8 The hydraulic model of the network where the experimental programme is located. In this model, 2 PRVs are active. 149
6.9 Exploring the solution search space. A more optimal AZP is achieved if DBV 1 controls pressure and flow in a northwards direction. 149
6.10 Optimal PRV settings for the experimental programme operating with 2 PRVs and 2 dynamic boundary valves 150
6.11 Convergence of SFSCP plotted as (a) an extended period simulation which shows more iterations seem to be required during day time hours and (b) a histogram showing that the iterations required range from 4 to 9, with an average value of 7. 151
6.12 Optimal PRV settings 153
6.13 (a) A stem position opening schedule for the control of the dynamic boundary valves and (b) a valve model fitted to the available data points from the experimental programme 155
6.14 Optimal PRV settings for the experimental programme operating with 2 PRVs and 2 dynamic boundary valves opening to 20% as shown in Figure 6.13a. 156
6.15 Fitted flow modulation curves to PRV 1 and PRV 2 open loop settings from Figure 6.14 156
6.16 Convergence of SFSCP when DBVs follow an open loop stem position schedule. (a) An extended period simulation that shows the iterations required at each time step and (b) a histogram showing the most common number of iterations required for convergence . 157
6.17 The hydraulic model of the network where the experimental programme is located. In this model, 3 PRVs are active. 158
6.18 Search space of AZP showing the convergence properties of SCP (red line) and SFSCP (blue line) (Wright et al., 2015*d*) 158
6.19 AZP results when the SFSCP algorithm is applied to the experimental programme network for different levels of dynamic boundary valve opening %. (a) AZP over a 24 hour period and (b) average daytime AZP. 159
6.20 A comparison of optimisation methods. The contours represent the objective function (AZP) and hydraulically feasible set $\mathbb{E}$, where PRV settings η are varied along each axis. The shaded area represents the operationally and hydraulically feasible set $\mathbb{E} \cap \mathbb{F}$. The black line is the iteration path of the optimisation solver for (a) SLP-LT, (b) SLP-NR, (c) SCP-LT and (d) SFSCP. 161

7.1 (a) Elevation plot of the experimental programme network and its schematic, InfraSense TS locations (black triangle), and artificial burst locations (blue star) created by operating fire hydrants and (b) a photograph of the artificial bursts generated by operating fire hydrants. 165
7.2 Data at the control valves during phase 1. Flow data is unavailable at PRV 1 for this period. 167
7.3 Data at the control valves during phase 2. 167
7.4 Data at the control valves during phase 3 168
7.5 Pressure management comparison during the three phase experimental programme 170
7.6 Estimating a leakage-pressure relationship using the night AZP (R-square value = 0.68) 172
7.7 Demonstrating leakage in comparison to DMA input for the three phase programme 173
7.8 Analysing the flow reversals of the three phase programme 175
7.9 Analysis of network resilience to a medium burst event (Wright et al., 2014*a*) 176
7.10 Artificially generated bursts produced by operating fire hydrants under different network configurations. FM = Flow modulation and FO = Fixed Outlet (Wright et al., 2015*b*) 178
7.11 A comparison of DMA 1 and DMA 2 inlet pressure heads during the occurrence of a real burst 179
7.12 (a) An overview of the network during the real burst incident. The top DMA, which was not affected by the burst, supplies the neighbouring DMA with an alternative supply of water (b) the boundary flow at DBV 1 which supplies the affected DMA 180
A.1 InfraSense TS Logger ID 1 (See Figure 5.19, Section 5.5 for logger locations) 201
A.2 InfraSense TS Logger ID 2 (See Figure 5.19, Section 5.5 for logger locations) 201
A.3 InfraSense TS Logger ID 3 (See Figure 5.19, Section 5.5 for logger locations) 202
A.4 InfraSense TS Logger ID 4 (See Figure 5.19, Section 5.5 for logger locations) 202
A.5 InfraSense TS Logger ID 5 (See Figure 5.19, Section 5.5 for logger locations) 203
A.6 InfraSense TS Logger ID 6 (See Figure 5.19, Section 5.5 for logger locations) 203
A.7 InfraSense TS Logger ID 7 (See Figure 5.19, Section 5.5 for logger locations) 204

A.8 InfraSense TS Logger ID 8 (See Figure 5.19, Section 5.5 for logger locations) . . . 204
A.9 InfraSense TS Logger ID 9 (See Figure 5.19, Section 5.5 for logger locations) . . . 205
A.10 InfraSense TS Logger ID 10 (See Figure 5.19, Section 5.5 for logger locations) . . . 205
A.11 InfraSense TS Logger ID 11 (See Figure 5.19, Section 5.5 for logger locations) . . . 206
A.12 InfraSense TS Logger ID 12 (See Figure 5.19, Section 5.5 for logger locations) . . . 206
A.13 InfraSense TS Logger ID 13 (See Figure 5.19, Section 5.5 for logger locations) . . . 207
A.14 InfraSense TS Logger ID 14 (See Figure 5.19, Section 5.5 for logger locations) . . . 207
A.15 InfraSense TS Logger ID 15 (See Figure 5.19, Section 5.5 for logger locations) . . . 208
A.16 InfraSense TS Logger ID 16 (See Figure 5.19, Section 5.5 for logger locations) . . . 208
A.17 InfraSense TS Logger ID 17 (See Figure 5.19, Section 5.5 for logger locations) . . . 209
A.18 InfraSense TS Logger ID 18 (See Figure 5.19, Section 5.5 for logger locations) . . . 209
A.19 InfraSense TS Logger ID 19 (See Figure 5.19, Section 5.5 for logger locations) . . . 210
A.20 InfraSense TS Logger ID 20 (See Figure 5.19, Section 5.5 for logger locations) . . . 210
A.21 InfraSense TS Logger ID 21 (See Figure 5.19, Section 5.5 for logger locations) . . . 211
A.22 InfraSense TS Logger ID 22 (See Figure 5.19, Section 5.5 for logger locations) . . . 211

List of Tables

1 Water balance from the International Water Association (IWA) best practice standard, taken from (Fanner, 2010) 50
2 Network information for the case study used to analysis the current state and operation of DMA 76
3 Pressure management comparison for different design options . . 109
4 Analysing % demand met during pipe closure scenarios for the design of the experimental programme 113
5 Key for Figure 5.17, which shows a bidirectional control valve for the dynamic DMA topology 116
6 Hazen-Williams coefficients for pipes of varying age and condition (Bhave, 1991) 122
7 Summary of calibration results for the experimental programme network (Figure 5.19 124
8 Details of the nodes in the simple example shown in Figure 6.6 . 147
9 Details of the links in the simple example shown in Figure 6.6 . . 148
10 Summary of pressure management results for the operation of the experimental programme under three different configurations . . 153
11 Comparison of optimisation methods for another steady simulation where all methods except SLP-LT converge to the same local optimal point 161
12 Summary of pressure management results for the three phase operation of the experimental programme 170
13 Pressure data and model comparison. Logger locations are shown in Figure 5.19, Section 5.5 171
14 Leakage estimation using the model and data over a 5 day period 173
15 Phase 1 pressure data and model comparison. Data at Logger ID 1, 5, 6, 7 and 8 was unavailable during this period. Logger locations are shown in Figure 5.19, Section 5.5 212
16 Phase 2 pressure data and model comparison. Logger locations are shown in Figure 5.19, Section 5.5 213
17 Phase 3 pressure data and model comparison. Data at Logger ID 1, 2, and 22 was unavailable during this period. Logger locations are shown in Figure 5.19, Section 5.5 214

1 Introduction

1.1 Background

An efficient management of water resources and the provision of a satisfactory level of customer service are common objectives for all water companies. However, a complex and ageing infrastructure, with many pipes dating back to the Victorian era, presents challenges that oppose these objectives. Leakage from these mains is a financial loss for the company and puts strain on water resources particularly in times of drought, whilst new bursts that occur on the ageing pipelines disrupt the customers' supply. In addition, rising populations and climate change are contributing to the need to manage water resources more carefully on a global scale (United Nations, 2012). In Europe, the careful management of water use and loss by water utilities is now strongly encouraged in order to meet current and future demand (European Union, 2015).

Since the privatisation of water companies in the UK in the 1980s, the reduction of leakage has been a priority enforced by the economic regulator, Ofwat. In order to meet this regulation and reduce leakage, water companies extensively implemented district metered areas (DMA), which at the time was a pioneering approach in network and leakage management. A DMA is a discrete zone in the network formed by permanently closing isolation valves. Each DMA commonly has just a single inlet (feed), as recommended in DMA design practices (Morrison et al., 2007). The permanent closure of isolation valves stops flow from breaching the boundary of the DMA, and they are commonly referred to as boundary valves (BV). The two major benefits of implementing DMAs are:

- A transparent approach to derive mass balance and non-revenue water estimations by continuously monitoring flow at the inlets of DMAs. Consequently, the variability in the minimum night flow is used to (i) substantially reduce the time for leakage detection; (ii) identify areas with a rising level of water losses so that surveys for active leakage control are carried out and repair activities prioritised; (iii) detect unreported bursts; and (iv) minimise non-revenue water. The stochastic nature of customers demand significantly hinders the successful execution of these tasks outside hours of minimum (night) water demand.
- The simplistic implementation of pressure management by installing a pressure reducing valve (PRV) at the DMA inlet. Reducing the operational pressure in a WDN provides significant benefits both in terms of reducing background leakage and bursts frequency (Farley and Trow, 2003). Lalonde et al. (2008) and Fantozzi et al. (2009) report burst reductions of up to 40% following the implementation of pressure management. A basic

form of pressure management can be implemented where the PRV provides a constant pressure at all times, or more advanced options are available where the PRV varies its outlet pressure in a more optimal way in order to further reduce leakage. The PRV control process needs to be implemented with a high degree of confidence to guarantee a good quality of service and minimise the risk of customers complaints.

The implementation of DMAs has reduced leakage in the UK by over 30% in the last 25 years (Ofwat, 2007). It remains to this day the most efficient and cost effective way to detect, estimate, and reduce leakage, and prioritise mains rehabilitation (Farley and Trow, 2003; Lalonde et al., 2008; Kunkel and Sturm, 2011).

Although the DMA has provided strong improvements in leakage and pressure management, its implementation has introduced major operational constraints that affect the quality of customer service. By permanently closing boundary valves, the natural redundancy within large, looped networks is severely reduced. This causes unintended consequences which are summarised as following:

- Reduced resilience to failure. The permanent closure of boundary valves reduces the network redundancy which results in a reduced number of independent supply routes for consumers. The network is therefore less resilient to failure (Yazdani et al., 2011). For single feed DMAs, more single points of failure exist. In the event of failure, boundary valves are commonly opened manually in order to sustain pressure and keep customers in service (Drinking Water Inspectorate, 2009). A substantial amount of time is necessary to detect the incident, plan a rezone of the DMA, and travel to the affected area in order to open boundary valves, during which time the customer's service can be disrupted.

- Suboptimal pressure management due to higher frictional energy losses occurring in single-feed DMAs (Wright et al., 2014*a*). More pressure is therefore required in single-feed DMAs to provide an acceptable level of service to all customers. The higher pressure results in higher levels of leakage. The frictional head losses of an equivalent multi-feed network are lower, therefore the management of pressure and leakage is more efficient.

- Water quality incidents due to the build up of stagnant water at artificially created dead ends (World Health Organization, 2004). This problem is exacerbated when the closed boundary valves need to be opened, such as failure events (Armand et al., 2015). This can lead to the customers' water supply becoming discoloured and penalties issued by the regulator. The World Health Organization (2004) recommends that the artificial implementation of dead ends is limited in the design and operation of WDNs.

The disadvantages of implementing DMAs are now becoming more detrimental as water companies in the UK are facing severe financial penalties for poor customer service from Ofwat. These penalties fall under service frameworks such as the Service Incentive Mechanism (SIM, Ofwat (2012)) and the Guaranteed Standards Scheme (GSS, Ofwat (2008)). The size of the penalties can be as high as 1% of the water company's revenue (Ofwat, 2014*b*). Instances of poor customer service range from low pressures (GSS Regulation 10), stagnant or discoloured water at the customers supply point (Drinking Water Inspectorate, 2009), supply failure (GSS Regulation 8 and 9) as well as customers needing to contact their water companies for other reasons related to their service, which they may consider to be unsatisfactory. One example of this is high variability in diurnal pressure, which affects the perception of a good level of service. Furthermore, water companies are also rewarded up to 0.5% of their revenue for performing well in the SIM framework (Ofwat, 2014*b*), adding further incentive to provide a strong level of service. In order to address these new requirements in customer service levels, utilities need to carefully plan mitigations that are also closely linked with addressing the disadvantages of DMAs. Finally, there is still a strong emphasis being placed on further reducing leakage levels, and over the next five years UK water companies are expected to reduce leakage by 5% (Ofwat, 2014*a*).

1.2 Water Distribution Networks with Dynamic Topology

This thesis explores a novel approach to the operational management of water distribution networks, where DMAs are dynamically aggregated for improved network resilience, pressure management and water quality, and segregated for leakage monitoring periodically (e.g. each night). This is facilitated by replacing closed boundary valves with self-powered, remote control valves (dynamic boundary valves, DBV). The operation of a dynamic topology can therefore successfully eliminate the disadvantages of conventional DMAs, whilst retaining its success in leakage monitoring. Furthermore, smaller sized DMAs can be implemented for more aggressive leakage localisation whilst avoiding the negative effects in pressure management and resilience to failure associated with this. The approach is applicable for the progressive upgrade of networks that already have DMAs installed, or for networks where DMAs do not exist and require zoning.

The technology used for the implementation of a dynamic topology can be retrofitted to existing valves in the WDN and includes:

- A novel pilot valve and bypass system (Cla-Val, 2015*a*) that facilitate bidirectional flow and control at the dynamic boundary valves (DBV). The PRVs typically used in networks shut down when flow reversals occur (i.e. the PRV acts as a check valve). The ability to control flow and pressure

bidirectionally facilitates optimal pressure management and resilience to failure.

- High speed (128 samples/s) pressure monitoring with a time synchronization of 2ms (Hoskins and Stoianov, 2014). The acquisition of data at this frequency facilitates a unique insight into the hydraulic conditions of WDNs not available when using the industry standard (1 sample / 15 minutes). The data is used to ensure a stable operation of control valves and to understand the hydraulic behaviour of the network when operating a dynamic topology. The acquired data is also extensively used for performance indicates (such as the average pressure in the network) and the calibration of hydraulic models used in control optimisation.

- Telecommunications for receiving hydraulic data and updating control settings. This provides more options for the control and simulation of the WDN.

- Insertion flow meter that uses the vortex shedding phenomenon to calculate flow (Cla-Val, 2015*b*). The monitoring of flow at the control valves is used for the on-line update of model parameters and facilitates more advanced control options.

- Micro-turbine for energy harvesting using the pressure differential of the valve (Cla-Val, 2015*c*), which can be used for logging and control at dynamic boundary valves and replaces the need for mains power or non-rechargeable batteries.

Existing PRVs are also retrofitted with the technology for the improved hydraulic control of interconnected DMAs.

This thesis explores the following type of operation for a dynamic topology (Figure 1.1). The dynamic DMAs are usually aggregated by controlling the opening of the dynamic boundary valves. The aggregated DMAs become a multi-feed (inlet) network. This overcomes the disadvantages of a closed, fixed topology DMA by:

- Increasing the network's resilience to failure because multiple, independent supply paths are introduced between consumers and sources. In failure situations, these additional supply paths are available immediately and without the risk of water discolouration. This circumvents the traditional, manual approach of opening the permanently closed boundary valves.

- Reducing frictional energy losses because the network redundancy is increased. Consequently the outlet pressure settings of PRVs can be lowered, resulting in further reductions in pressure and leakage in the network.

- Reducing the number of dead ends in the network where closed boundary

valves were placed. Therefore there is less stagnant water building up at permanently closed boundary valves. The effects of a dynamic topology on water quality is not investigated in detail in this thesis. An extensive investigation into the effects of DMAs on water quality is presented by Armand et al. (2015).

For leakage detection and management, the dynamic DMAs can revert back to the original topology by closing the boundary valves automatically at periodic times (for example, between 02:00-04:00 nightly or weekly).

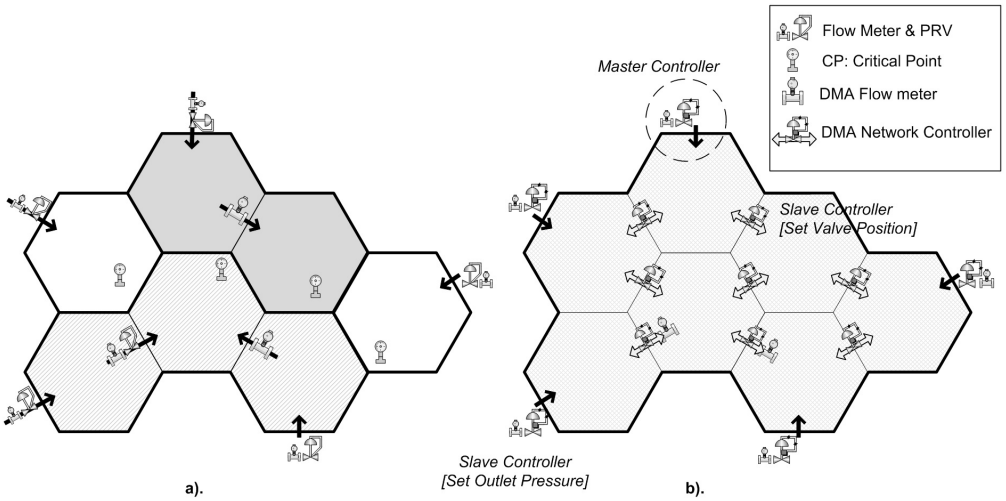


Figure 1.1: Adaptive sectorisation of water distribution networks with dynamically reconfigurable topology (Wright et al., 2014*a*): (a) Segregating a supply zone into DMAs for leakage detection during a period of low demand (02:00-04:00); (b) Aggregating DMAs into a large pressure management zone (04:00-02:00).

1.3 Objectives

The main objectives of this thesis are as follows:

1. Investigate and formalise analytical tools and control methods for the operation of water distribution networks;
2. Investigate the operation and performance of a dynamic topology in (i) resilience to failure and (ii) pressure management, and compare with other well established and emerging approaches to pressure management;
3. Validate analytical work by designing and setting up an experimental programme on a real, operational network;
4. Develop tools, if necessary, that support the analytical and experimental work.

1.4 Methodology

An analytical and experimental investigation of DMAs with dynamic topology is carried out in this thesis to understand its operation and performance, and compare this with other forms of pressure and leakage management, both established and emerging.

The dynamic aggregation of DMAs results in the formation of very large networks, complicated further by interaction between multiple sources, control valves and large consumers that impact the hydraulic conditions extensively. The focus in this thesis is therefore on computationally efficient and reliable modelling and control techniques, which can also provide the foundations for implementing real-time modelling and control. A review of hydraulic modelling principles and efficient solution methods is presented in Chapter 2. The work on hydraulic modelling supports all other chapters in the analysis of a dynamic topology.

An extensive review is undertaken in Chapter 3 on current DMA design practices and pressure management approaches. DMAs must be designed to meet the pressure requirements of its users, leakage requirements of regulators (if applicable) and with a satisfactory level of resilience to failure. A performance indicator (PI) is a commonly used metric in industry that assesses the DMA performance. This chapter reviews performance indicators relevant to a dynamic topology in pressure management and resilience to failure. The information in this chapter also feeds into the design of a dynamic DMA network. Although most DMAs are single-feed, multi-feed networks also exist. Their operation is reviewed in Chapter 4 and control options are investigated for the optimal operation of a dynamic topology.

The information acquired on DMA design, performance indications, and multi-feed network control is used to set up an experimental programme on a real, operational network supplying approximately 8,000 properties. The design and set up of this experimental programme is detailed in Chapter 5. The optimal control of the dynamic topology in the experimental programme requires an optimisation solver. In Chapter 6, a novel optimisation algorithm based on sequential convex programming (SCP) is proposed. The algorithm is applicable for networks with a dynamic topology or fixed topology networks with multiple inlets and control valves. The main benefit of the proposed SCP algorithm over other optimisation methods for valve control is its reliable convergence to an optimal point for real, complex networks. In addition, the algorithm takes advantage of fast, efficient convex problem solvers. The control is actuated within the experimental programme.

In Chapter 7, data is presented on the actuation of optimal valve control and the

performance of a dynamic topology, and compared with other well established and pioneering approaches to pressure and leakage management. The data indicates that a dynamic DMA topology facilitates a lower average zone pressure in the network and better resilience to failure due to the improvements in network redundancy.

Finally, conclusions based on all chapters, the novel contributions of this thesis, and future research avenues are discussed in Chapter 8.

The overall methodology is summarised in Figure 1.2.

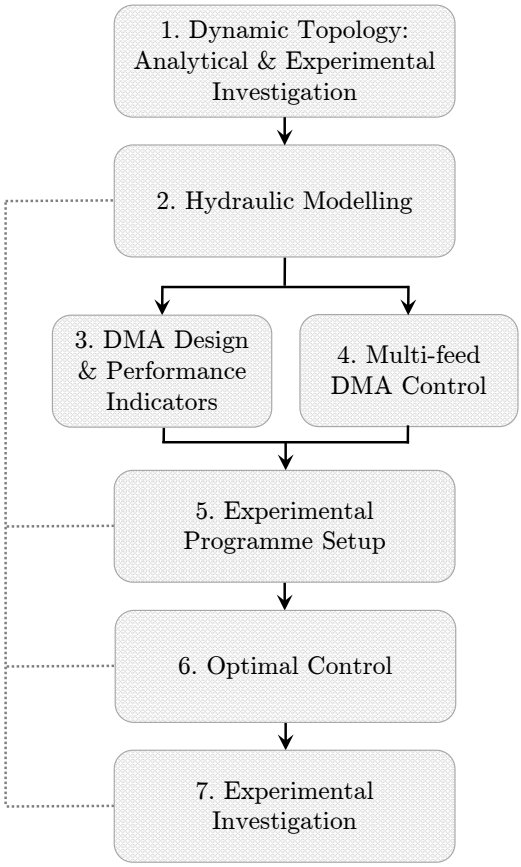


Figure 1.2: Thesis structure and methodology for investigating water distribution networks with dynamic topology

1.5 Publications

The followings papers, based on content from this thesis, have been published or accepted for publication:

1.5.1 Journal Papers

1. Wright, R., Stoianov, I., Parpas, P., Henderson, K. & King, J. (2014a), 'Adaptive water distribution networks with dynamically reconfigurable topology', *Journal of Hydroinformatics* **16**(6), 1280-1301.

2. Wright, R., Abraham, E., Stoianov, I. & Parpas, P. (2015a), 'Control of Water Distribution Networks with Dynamic Topologies using Strictly Feasible Sequential Convex Programming, *Water Resources Research* **51**(12), 9925-9941.

1.5.2 Conference Papers

1. Wright, R., Stoianov, I. & Parpas, P. (2014), 'Dynamic topology in water distribution networks', *12th Computing and Control for the Water Industry, Procedia Engineering* **70**, 1735-1744.

2. Wright, R., Stoianov, I. & Parpas, P. (2015b), 'Experimental investigation of resilience and pressure management in water distribution networks', *13th Computing and Control for the Water Industry, Procedia Engineering* **119**, 643-652.

3. Wright, R., Herrera, M., Stoianov, I. & Parpas, P. (2015c), 'Hydraulic resilience index for the critical link analysis of multi-feed water distribution networks', *13th Computing and Control for the Water Industry, Procedia Engineering* **119**, 1249-1258.

4. Wright, R., Abraham, E., Stoianov, I. & Parpas, P. (2015d), 'Optimized control of pressure reducing valves in water distribution networks with dynamic topology', *13th Computing and Control for the Water Industry, Procedia Engineering* **119**, 1003-1011.

2 Hydraulic Modelling

2.1 Introduction

Hydraulic modelling facilitates the analysis of pressure and flow in networks and is used in many aspects of water distribution. These include network design, incident management, and ensuring an acceptable level of customer service. Optimal control also uses the equations of hydraulic models as equality constraints in the problem formulation (Chapter 6). The design and optimal operation of a dynamic topology therefore requires a thorough understanding of the hydraulic equations and solution methods.

This thesis only deals with the steady state simulation and control of water distribution networks. In a steady state analysis, the rate of change of all variables with respect to time is zero. Consequently, water in the network is incompressible (i.e. water can't accelerate faster into a space than it leaves) and the instantaneous demand (water consumption) in the network is equal to the overall outflow of all tanks/reservoirs. The simulation of a network and its behaviour over a period of time is undertaken by simulating a sequence of steady state simulations. This is typically called an extended period simulation and it facilitates changes of variables in time, i.e. demand, reservoir levels, control actuation.

An extensive number of steady state hydraulic solution methods and modelling techniques exist. The hydraulic solver used for investigating the implementation and operation of a dynamic topology should include the following features:

- Computationally efficient: For calculating optimal control on large, complex networks, or for real-time control applications, it is important to have a computationally efficient hydraulic simulator due to the time constraints involved. For design or analysis purposes, where the model can be run many thousands of times, computational efficiency can make substantial savings in the time taken to retrieve a solution.
- Computationally accurate: The hydraulic solver should produce accurate solutions to the system of hydraulic equations. When error is introduced into the solutions (for example, if the system of hydraulic equations are badly conditioned), problems can be created for both decision making (i.e. design, analysis, decision support) as well as the convergence properties of optimisation solvers.
- Tractable: The hydraulic modelling should facilitate the inclusion of novel control components (i.e. advanced control valves), control approaches, and methodologies used in network analysis and optimal operation. This requirement generally omits the use of commercial hydraulic solvers, which

do not offer a transparent understanding of the hydraulics engine and offer only a limited amount of interaction between other computer coding software.

This chapter investigates the hydraulic solution methods currently available in order to establish the most appropriate approach based on the requirements listed above. All other chapters of this thesis rely in some way on the information presented in this chapter.

2.2 Network Representation and Notation

A water distribution network model with a static or dynamic topology is represented as a graph consisting of:

- A unique set of nodes N_n, where $|N_n| = n_n$
- A unique set of sources (e.g. reservoirs, tanks) N_o, where $|N_o| = n_o$
- A unique set of links N_p, where $|N_p| = n_p$
- A unique set of control valves N_v, where $|N_v| = n_v$ and $N_v \subseteq N_p$
- A non unique set of co-trees N_l, where $|N_l| = n_l$, $N_l \subseteq N_p$ and $n_l = n_p - n_n$ (Todini and Rossman, 2012; Elhay et al., 2014)

A spanning tree of a graph is a set of links that visit every node only once. The co-tree is then defined as the remaining links (Elhay et al., 2014). Therefore the co-trees close the loops, and the number of co-trees n_l can also be regarded as the number of loops in the network (Todini and Rossman, 2012).

It is convenient to represent the structure of WDNs in matrix form using incidence matrices. An incidence matrix mathematically defines the relationship between two objects. In the case of a WDN, we can define whether a link is connected to a particular node or not. The following incidence matrices are defined:

- $A_{12} \in \mathbb{R}^{n_p \times n_n}$ relates links to nodes
- $A_{10} \in \mathbb{R}^{n_p \times n_o}$ relates links to sources

The convention used is the same as (Todini and Pilati, 1988) and is detailed as:

$$A_{12}(i,j) = \begin{cases} 1 & \text{if link } i \text{ enters node } j \\ 0 & \text{if link } i \text{ is not connected to node } j \\ -1 & \text{if link } i \text{ leaves node } j \end{cases} \tag{2.1}$$

The same convention is used for A_{10}, where links are related to nodal sources.

Another representation of a WDN is an adjacency matrix. This matrix simply defines the relationship between nodes and other nodes, i.e. whether two nodes

are connected to each other or not. Each entry in the matrix is therefore a binary type, and the size of the matrix is $n_n \times n_n$. The adjacency matrix is used is some parts of this work to perform a breadth-first search, which is a graph theoretic method that can detect disconnections in a water distribution network (i.e. demand nodes that are not connected to a source node).

As an example, the graph representing a WDN in Figure 2.1 has one water source, one PRV, five nodes and five pipes. Therefore, for this WDN, $n_o = 1$, $n_v =$

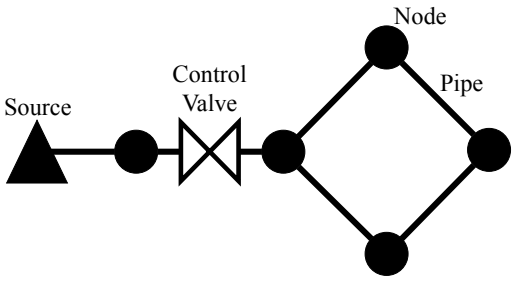


Figure 2.1: WDN notation

2.3 Hydraulic Equations: Mass and Energy Conservation

Two conservation laws are used to construct a system of equations that represents a WDN. The solution to this system includes the flow in each pipe $q \in \mathbb{R}^{n_p \times 1}$ and the hydraulic head at each node $h \in \mathbb{R}^{n_n \times 1}$ with reference to sea level, from which pressure can be found easily. The conservation laws provide the foundations for all solution methods outlined in Section 2.4.

The first conservation law is mass continuity, termed $g_2(q)$ in this thesis. This states that for an incompressible flow, the mass flow into a node must be equivalent to the mass flow out of the node. Mathematically this is defined as:

$$g_2(q) := A_{21}q - d = 0 \tag{2.2}$$

where $d \in \mathbb{R}^{n_n \times 1}$ is the demand at nodes (assumed known and constant for a demand driven simulation), and $A_{21} = A_{12}^T$. A demand-driven hydraulic analysis is the most commonly adopted analysis in industry. An alternative form of hydraulic modelling, known as pressure-driven, simulates demand at nodes as a function of the available pressure head. This approach can be useful for the simulation of leakage (which is pressure dependent), or customer demand in critical pressure (failure) scenarios. Pressure-driven simulations also use the same conservation principles as demand-driven simulations and are outlined further in Section 2.9.

The final conservation law is energy conservation, termed $g_1(q,h)$. This law uses Bernoulli's Principle and states that the energy (i.e. the hydraulic head or piezometric head) of flow between two nodes must be conserved minus any frictional head losses. Frictional energy losses can be estimated using (2.3). The total head loss over a link i due to friction ($\Delta h_i(q_i)$) is:

$$\Delta h_i(q_i) = r_i q_i |q_i|^{n_i - 1}, \ \forall i \in N_p \tag{2.3}$$

where $r \in \mathbb{R}^{n_p \times 1}$ is a vector of frictional resistance factors of the links and $n \in \mathbb{R}^{n_p \times 1}$ are exponents related to the frictional head loss. Alternatively, the frictional head loss equation (2.3) can be rearranged, as shown in (2.4), where the flow of link i is related to the head at the connected nodes j and k. However, this equation has an exponent less than 1, which can result in convergence difficulties in Newton methods (Todini and Rossman, 2012).

$$q_i = (1/r_i)(h_j - h_k)|h_j - h_k|^{\frac{1-n_i}{n_i}} \tag{2.4}$$

The conservation of hydraulic head within a network is defined as:

$$g_1(q,h) := A_{11}(q)q + A_{12}h + A_{10}h_0 = 0, \tag{2.5}$$

and the pressure head at any node in the network is defined as:

$$p_j = h_j - z_j, \ \forall j \in N_n \tag{2.6}$$

where $p \in \mathbb{R}^{n_n \times 1}$ are the pressure heads, $z \in \mathbb{R}^{n_n \times 1}$ are the nodal elevations (above some arbitrary datum), $h_0 \in \mathbb{R}^{n_o \times 1}$ are the hydraulic heads at source nodes with reference to sea level, and $A_{11}(q)$ is defined below. Whilst h_0 and h both represent nodal hydraulic head, h_0 is assumed known whereas h is an unknown to be determined. Consequently, the hydraulic head across the network is split into these two vectors accordingly. The model must have at least one source of water. This could be, for example, a reservoir, a water storage tank, a supply point from a trunk main, or a bore hole. The hydraulic head at sources is assumed known (Larock et al., 1999). The pressure head at source nodes can also be calculated in the same way as unknown head nodes using (2.6). When pressure data is available in near real-time at sources, the hydraulic head at sources is known with a high degree of confidence. Within consumer properties, storage tanks can also exist. These will not however typically affect the demand patterns of consumers if the tank fills from the main as water is used within the property.

The square matrix $A_{11} \in \mathbb{R}^{n_p \times n_p}$ is a diagonal matrix containing the frictional energy losses across each link (as a function of flow) and has elements defined as:

$$A_{11}(i,i) = r_i |q_i|^{n_i - 1}, \ \forall i \in N_p \tag{2.7}$$

i.e. (2.7) is equivalent to (2.3) when multiplied by the flow vector q.

A number of different formulae exist for estimating r and n to form a functional relationship between flow and head loss over a link. A literature review on friction factor relationships by Özger and Yıldırım (2009) found that relationships proposed by Chen (1979), Barr and Sivaloganathan (1982), Zigrang and Sylvester (1982) and Romeo et al. (2002) produced the best fit. The most popular relationships however are the Darcy-Weisbach and Hazen-Williams equations (Mays, 1999). This is also reflected in most open-source and commercially available hydraulic simulation software packages.

The Darcy-Weisbach formula is often promoted as being one of the most accurate head loss formulas available due to its analytical derivation. However, the Darcy-Weisbach formula relies on the determination of roughness values, which is essentially experimental (Mays, 1999). Mays (1999) suggests that, irrespective of the head loss relationship used, good results can be achieved in hydraulic modelling provided that the frictional resistance factors are selected appropriately. In this thesis, the Hazen-Williams formula is used. The Hazen-Williams friction formula uses the following coefficients; $n_i = 1.852$ and $r_i = \frac{10.675 L_i}{c_i^{n_i} D_i^{4.87}}$, where L_i, D_i and c_i denote the length, diameter and roughness coefficient of pipe i, respectively, and all units are SI.

A WDN model may also contain pumps, particularly on trunk mains, but also within DMAs themselves. For example, tall buildings that do not receive adequate pressure from the mains would require a booster pump. A pump curve can be used to model pumps within a network simulation (Rossman, 2000). A pump curve is similar in nature to the head loss equation, however, instead of head reducing in the direction of flow, there is a head gain. In order to model a pump, it is represented as a link, and its pump curve is stored within the A_{11} matrix. Whilst the case studies and networks considered in this thesis do not have pumps, all of the presented work is applicable to networks with pumps.

Combining the conservation laws in (2.2) and (2.5) into one system of equations gives:

$$g(q,h) := \begin{bmatrix} A_{11}(q) & A_{12} \\ A_{21} & 0 \end{bmatrix} \begin{bmatrix} q \\ h \end{bmatrix} - \begin{bmatrix} -A_{10}h_0 \\ d \end{bmatrix} = 0 \tag{2.8}$$

The system in (2.8) contains $n_p + n_n$ equations and $n_p + n_n$ unknowns. Because A_{11} is a function of q, the solution $[q^T, h^T]$ to (2.8) must be obtained iteratively.

2.4 Solution Methods

The solution to the hydraulic equations in (2.8) has been extensively studied in the literature. All methods obtain a solution by solving successive linear

approximations of (2.8). The methods can be categorised based on the type of linearisation undertaken: either the Newton method or Linear Theory (LT) method.

A Newton method uses the system of nonlinear equations and their first order derivatives to update an estimate of the solution to the system. The general form of Newton's method is defined as follows (Ryaben'kii and Tsynkov, 2006):

$$x_{k+1} = x_k - J(x_k)^{-1} F(x_k) \tag{2.9}$$

where x is a vector in the solution space, F is the system of nonlinear equations, J is the Jacobian of F, and k is the iteration number. For water distribution networks, F is the system of conservation system in (2.8) and its Jacobian, assuming the Hazen-Williams head loss model is used, is:

$$J(q) = \begin{bmatrix} NA_{11}(q) & A_{12} \\ A_{21} & 0 \end{bmatrix} \tag{2.10}$$

where $N = \texttt{diag}(n_i),\ i = 1, \ldots, n_p$, a diagonal matrix of size $n_p \times n_p$ containing the exponents of the frictional head loss equation in (2.3).

A LT method iteratively solves linear approximations of (2.8), but without information of the gradient of the system. A general form of the LT method is as follows (Todini and Rossman, 2012):

$$x_{k+1} = (1 - \vartheta)x_k + \vartheta g(x_k) \tag{2.11}$$

where g is the function of x_k and ϑ is a parameter chosen to improve convergence.

Apart from the form of linearisation used, solution methods differ based on the order in which unknowns are solved and whether the network structure is taken into account. Todini and Rossman (2012) summarises the main simulation methods found in the literature as follows:

- Newton Methods

    1. Solve for h and q: This formulation is commonly called the "Gloabal Gradient Algorithm" (GGA), and was first outlined by Todini and Pilati (1988). Although the problem formulation solves for h and q simultaneously, only a linear system (that is both sparse and positive-definite) of size $n_n \times n_n$ needs to be solved. The frictional head loss equation in (2.3) is used in this approach.

    2. Solve for q: Todini and Rossman (2012) propose this method, which solves successive linear systems of size $n_p \times n_p$ to calculate q. The frictional head loss equation in (2.3) is used in this approach. It is equivalent to the LT method that finds q, developed by Wood and Charles (1972).

3. Solve for $q_i,\ \forall i \in N_l$: These methods are often called "loop methods" or "null space" methods (Elhay et al., 2014). Epp and Fowler (1970) proposed solving for $q_i,\ \forall i \in N_l$ using a Newton method, resulting in the iterative solution of linear systems of size $n_l \times n_l$. The frictional head loss equation in (2.3) is used in this approach. Nielsen (1989) proposed a loop method for general liquid in pipe networks. One of the earliest methods for solving pipe flow problems is attributed to Cross (1936), where hydraulic equations were solved iteratively by hand. Modern computing has since made this method obsolete, although its theory still provides good insight into the flow of looped pipe systems.

4. Solve for $q_i,\ \forall i \in N_l$ and h: Osiadacz and Pienkosz (1988) uses a formulation that solves for both $q_i,\ \forall i \in N_l$ and h using a Newton method. The frictional head loss equation in (2.3) is used in this approach.

5. Solve for h: Shamir and Howard (1968); Martin and Peters (1963) proposed solving for h using a Newton method, where linear systems of size $n_n \times n_n$ are solved. This formulation eliminates q from the problem formulation by using (2.4) as the frictional head loss equation.

- Linear Theory Methods

1. Solve for h and q: Isaacs and Mills (1980) first propose linear theory to solve for both h and q simultaneously. As with the global gradient algorithm, only a system of linear equations of size $n_n \times n_n$ needs to be solved. The frictional head loss equation in (2.3) is used in this approach.

2. Solve for q: Wood and Charles (1972) first proposed solving for q using linear theory, where linear systems are solved of size $n_p \times n_p$. The frictional head loss equation in (2.3) is used in this approach.

3. Solve for $q_i,\ \forall i \in N_l$: Todini and Rossman (2012) outlined this method, which solves successive linear systems of size $n_l \times n_l$ to calculate q. The frictional head loss equation in (2.3) is used in this approach.

4. Solve for $q_i,\ \forall i \in N_l$ and h: Todini and Rossman (2012) outlined this method, which solves successive systems of size $n_n \times n_n$ to update $q_i,\ \forall i \in N_l$ and h at each iteration. The frictional head loss equation in (2.3) is used in this approach. A similar approach was proposed by Gupta and Prasad (2000), where $q_i,\ \forall i \in N_l$ was updated in the log space at each iteration.

Out of the solution methods listed above, Newton methods have been shown to reach convergence in fewer iterations than LT based methods in a case study by Todini and Rossman (2012). This is due to the fact that Newton methods use information of the function's derivative to update the root estimate, whereas linear theory only uses linear transformations of the function. In addition, Newton methods that use (2.3) for the head loss equation converged in fewer iterations than methods that used (2.4). This is because the exponent in (2.4) is less than one, which reduces the performance of the Newton method (Todini and Rossman, 2012). Another interesting result from Todini and Rossman (2012) is that all Newton methods converge in the same number of iterations. Simpson (2011) observed the same result when comparing GGA with the Newton loop method. It was proved by Elhay et al. (2014) that this result is always true because both solution methods are derived from an identical systems of non linear equations i.e. (2.8). Finally, the solution methods that only solve for q require solutions to non-symmetric systems of size $n_p \times n_p$. This is less efficient than solving symmetric systems of a similar sized $n_n \times n_n$ matrix. Therefore, out of all solution methods, the most appropriate for computationally efficiency are either the GGA or a null space algorithm.

The main strength of the GGA is that it facilitates the solution to pressure-driven demand simulations. The system of hydraulic equations in (2.8) can be modified to include this behaviour, and the derivation of the GGA is similar to the demand-driven GGA (Section 2.9). An equivalent pressure-driven null space algorithm does not exist (Elhay et al., 2014). The computation of pressure-driven demand facilitates the calculation the actual demand met during failure situations, where pressure becomes too low to supply the normal (nominal) demand. Since resilience to failure is one benefit of a dynamic DMA topology explored in this thesis, pressure-driven simulations are an important tool.

For the calculation of optimal control (Chapter 6) under normal network conditions where pressure is high enough to supply all demand, computational savings can be made by exploiting the computational efficiency of null space algorithms, where very sparse, linear systems of size $n_l \times n_l$ are solved instead of the larger systems of size $n_n \times n_n$ in the GGA (Abraham and Stoianov, 2015*b*). These savings are also beneficial for analyses involving a high number of steady state simulations. Since for most real networks the relationship $n_n \gg n_l$ is true, even for highly looped networks in North America (Elhay et al., 2014; Abraham and Stoianov, 2015*b*), these computational savings can be considerable. For example, Elhay et al. (2014) report that null space algorithms are almost twice as fast as the GGA for some networks. Abraham and Stoianov (2016) solve some networks almost four times as fast by calculating a very sparse links-loop incidence matrix. Although a loop method requires loops to be identified in the network, which has been viewed as a drawback of the approach (Todini and Rossman, 2012), this

only needs to be carried out once for most types of analysis. Efficient methods also exist for identifying the loops (Abraham and Stoianov, 2016). Finally, the GGA makes the assumption that $A_{11}(q)$ in (2.8) is invertible, an assumption that does not always need to be made for null space algorithms (Abraham and Stoianov, 2015*b*). As indicated in (2.7), this assumption is not valid when flow in a pipe is zero. Many situations can and do arise that lead to a zero flow. For example, a dead end in the network where no consumer or property is present (such as at cul-de-sacs or the permanently closed boundary valves), or at hydraulic balance points of the network. One approach to avoiding the singularity of $A_{11}(q)$ is the addition of a small arbitrary number to the link containing the zero flow (Todini and Pilati, 1988; Rossman, 2000). This can however lead to inaccuracy in the solution as well as convergence problems. An alternative remedy is the regularisation of $A_{11}(q)$ as proposed by Elhay and Simpson (2011) to guarantee that its condition number is bounded (Section 2.6).

In summary, for the analysis of critical pressure (failure) situations, a regularised form of the head-driven GGA is used in this thesis, and when efficient computational performance is required, such as within optimisation algorithms for the calculation of optimal control (Chapter 6), the null space algorithm is used. The null space algorithm is detailed in Section 2.4.2 and the head-driven GGA in Section 2.9 together with other pressure-demand principles and relationships. Since both algorithms are derived using the demand-driven GGA, this is derived in Section 2.4.1.

2.4.1 Global Gradient Algorithm

The Global Gradient Algorithm (GGA) was proposed by Todini and Pilati (1988). It was the algorithm chosen by Rossman (2000) for the popular open-source hydraulic simulation software EPANET, and is currently the most widely implemented algorithm for the simulation of WDNs.

The derivation of the GGA is undertaken by applying the Newton method in (2.9) to the partly linear, partly nonlinear system of hydraulic equations in (2.8) as follows:

$$\begin{bmatrix} NA_{11}(q_k) & A_{12} \\ A_{21} & 0 \end{bmatrix} \begin{bmatrix} q_{k+1} \\ h_{k+1} \end{bmatrix} = \begin{bmatrix} NA_{11}(q_k) & A_{12} \\ A_{21} & 0 \end{bmatrix} \begin{bmatrix} q_k \\ h_k \end{bmatrix} \ldots$$
$$\ldots - \begin{bmatrix} A_{11}(q_k) & A_{12} \\ A_{21} & 0 \end{bmatrix} \begin{bmatrix} q_k \\ h_k \end{bmatrix} - \begin{bmatrix} A_{10}h_0 \\ -d \end{bmatrix} \quad (2.12)$$

where subscript k denotes the iteration number of the Newton method. Simplifying (2.12) gives:

$$\begin{bmatrix} NA_{11}(q_k) & A_{12} \\ A_{21} & 0 \end{bmatrix} \begin{bmatrix} q_{k+1} \\ h_{k+1} \end{bmatrix} = \begin{bmatrix} NA_{11}(q_k) - A_{11}(q_k) & 0 \\ 0 & 0 \end{bmatrix} \begin{bmatrix} q_k \\ h_k \end{bmatrix} - \begin{bmatrix} A_{10}h_0 \\ -d \end{bmatrix} \quad (2.13)$$

Expanding out the matrices in (2.13) gives the following two systems. To improve readability the term $A_{11}(q_k)$ is simplified to A_{11} and we denote $NA_{11}(q_k)$ as D_{11}.

$$D_{11}q_{k+1} + A_{12}h_{k+1} = (D_{11} - A_{11})q_k - A_{10}h_0 \tag{2.14}$$

$$A_{21}q_{k+1} = d \tag{2.15}$$

In order to explicitly calculate q_{k+1}, (2.14) is rearranged and, assuming D_{11} is invertible, multiplying by its inverse:

$$q_{k+1} = D_{11}^{-1}[(D_{11} - A_{11})q_k - A_{10}h_0 - A_{12}h_{k+1}] \tag{2.16}$$

In order to explicitly calculate h_{k+1}, it is necessary to eliminate q_{k+1} from (2.14). First, (2.14) is multiplied by D_{11}^{-1} to give:

$$q_{k+1} + D_{11}^{-1}A_{12}h_{k+1} = D_{11}^{-1}[(D_{11} - A_{11})q_k - A_{10}h_0] \tag{2.17}$$

Then multiplying (2.17) by A_{21} produces:

$$A_{21}q_{k+1} + A_{21}D_{11}^{-1}A_{12}h_{k+1} = A_{21}D_{11}^{-1}[(D_{11} - A_{11})q_k - A_{10}h_0] \tag{2.18}$$

But $A_{21}q_{k+1} = d$ in (2.18) according to (2.15). Therefore:

$$A_{21}D_{11}^{-1}A_{12}h_{k+1} = A_{21}D_{11}^{-1}[(D_{11} - A_{11})q_k - A_{10}h_0] - d \tag{2.19}$$

Replacing D_{11} with its original definition, and some final tidying of (2.16) and (2.19) produces the Newton update for h_{k+1} and q_{k+1} given by Todini and Pilati (1988):

$$h_{k+1} = -(A_{21}(NA_{11})^{-1}A_{12})^{-1}... \\ ...(A_{21}N^{-1}(q_k + A_{11}^{-1}A_{10}h_0) + (d - A_{21}q_k)) \tag{2.20}$$

$$q_{k+1} = (I - N^{-1})q_k - N^{-1}A_{11}^{-1}(A_{12}h_{k+1} + A_{10}h_0) \tag{2.21}$$

Iterating between (2.20) and (2.21) is undertaken until the hydraulic equations in (2.8) are solved to a reasonable tolerance. An initial solution of h and q is required, and usually takes values that are typical of network flows and heads (Rossman, 2000). The stopping criterion is discussed more in detail in Section 2.5. In practice, the inverse in (2.20) would not be calculated. Instead, a linear system of size $n_n \times n_n$ is solved in (2.19) and of the form $Xh_{k+1} = b$ where $X = -(A_{21}(NA_{11})^{-1}A_{12})$ and $b = (A_{21}N^{-1}(q_k + A_{11}^{-1}A_{10}h_0) + (d - A_{21}q_k))$. This is one of the most computationally intensive parts of the GGA method. Other computationally intensive parts of hydraulic simulation include the calculation of head losses due to the power and log functions involved, and importing parameters and data (Michele et al., 2012).

2.4.2 Null Space (Loop) Method

A null space (or loop) method iteratively solves only for $q_i,\ \forall i \in N_l$. This is achievable due to the structure of (2.8), which is known as a saddle point problem (Benzi et al., 2005). Consider the problem where $n_p = n_n$ i.e. a tree-like network. A solution for q can be found directly from the square system (2.2), and substituted into (2.5) to find h. No Newton method is required in this process. Solving problems where $n_p > n_n$, i.e. loops are present, can be undertaken in a similar way, where a Newton method is only used on the loops. The smaller space commonly called the loops, where the solution of $q_i,\ \forall i \in N_l$ is calculated, is also called a null space (Elhay et al., 2014). Like for a problem where $n_p = n_n$, a solution is obtained to (2.2) initially. Since $n_p > n_n$, the system in (2.2) is underdetermined, therefore an infinite number of solutions exist. The solution for $q_i,\ \forall i \in (N_p \setminus N_l)$ however is unique. Any solution can therefore be used. A solution can be found, for example, using a least square method (Abraham and Stoianov, 2015*b*):

$$q_k = x^* \tag{2.22}$$

where x^* is the least square solution to (2.2) and k is the iteration number. The next iteration from (2.22) is found with:

$$q_{k+1} = x^* + Zv \tag{2.23}$$

where $Z \in \mathbb{R}^{n_p \times n_l}$ is a non-unique link-loop incidence matrix that spans the null space, and v is the (currently unknown) update to the solution of q_{k+1}. In Abraham and Stoianov (2016), a number of methods are proposed for calculating of the null space that results in a Z that is very sparse. One special property of the null space is the relationship $A_{21}Z = 0$. In order to find v, q_{k+1} in (2.23) is substituted into (2.14) of the GGA derivation in Section 2.4.1:

$$D_{11}(x^* + Zv) + A_{12}h_{k+1} = (D_{11} - A_{11})q_k - A_{10}h_0 \tag{2.24}$$

Multiplying (2.24) by Z^T gives:

$$Z^T D_{11} Z v = Z^T[(D_{11} - A_{11})q_k - A_{10}h_0 - D_{11}x^*] \tag{2.25}$$

The linear system in (2.25) is of size $n_l \times n_l$ and generally much smaller than the $(n_n \times n_n)$ systems in (2.20) of the GGA (Abraham and Stoianov, 2015*b*). The ability to invert D_{11} in (2.25) depends less on the occurrence of zero flows due to the smaller number of links involved.

A null space method therefore solves the original system of equations in (2.8) by first computing x^*, and then iteratively updating q_{k+1} in (2.23) by solving the $n_l \times n_l$ system in (2.25).

The hydraulic heads h are found by multiplying (2.5) by A_{21} and rearranging:

$$h = (A_{21}A_{12})^{-1}(-A_{11}q - A_{10}h_0) \tag{2.26}$$

Abraham and Stoianov (2015*b*) also propose that further computational savings can be made by:

- Only updating D_{11} and A_{11} for the links where flow has not converged, since head loss calculations are computationally expensive (Michele et al., 2012).
- Only computing h in (2.26), which is also computationally expensive, once q has converged. It is necessary to calculate h since it is used to ensure that the energy conservation equations in (2.5) has been solved correctly (Elhay and Simpson, 2011). Its convergence can be checked using a heuristic presented in (Abraham and Stoianov, 2015*b*).

The heuristic used for initiating the calculation of h with (2.26) is:

$$\mathbb{U} < a \times n_p \tag{2.27}$$

where $\mathbb{U}$ is the set of links where flow is still being updated in the Newton iterations, and $a \approx 0.01 - 0.1$ was found to give good computational performance, reducing the total computations by up to 20% (Abraham and Stoianov, 2015*b*). For the experimental programme network, used extensively for control optimisation in Chapter 6, $a = 0.006$ produced computational savings of this order.

2.5 Stopping Criterion

The stopping criterion used for EPANET 2.0 is defined as:

$$\frac{\sum_{i=1}^{n_p} |q_i^k - q_i^{k-1}|}{\sum_{i=1}^{n_p} |q_i^k|} \leq tol \tag{2.28}$$

where k is the iteration number and tol is a user specified tolerance. A limit of the maximum number of iterations (k_{max}) is also enforced. Another stopping criterion suggested by Elhay and Simpson (2011) to be more accurate and intuitive is the infinite norm of the energy and mass conservation equations. The infinite norm of a vector $x \in \mathbb{R}^n$ is defined as follows:

$$\|x\|_\infty = \texttt{max}(|x_i|), i = 1, \ldots, n \tag{2.29}$$

Because mass continuity converges after the first iteration of the Newton method (Abraham and Stoianov, 2015*b*), only the infinite norm of the energy conservation equations needs to be considered. The stopping criterion used in this thesis is the infinite norm of the energy conservation equations in (2.5):

$$\|g_1\|_\infty \leq \epsilon_N \tag{2.30}$$

where the stopping tolerance ϵ_N has been set to 10^{-9} in the work presented in this thesis, unless otherwise stated.

2.6 Regularisation

As shown in the derivation of GGA, the matrix $D_{11} = NA_{11}(q_k)$ that forms part of the Jacobian must not be singular, since the inverse of this term is used in (2.20) for the Newton iterations. This situation can arise if the flow of a link i becomes zero (e.g. dead ends with no customers, hydraulic balance points, closed valves).

It is important in control optimisation to ensure the hydraulic equations are correctly and accurately solved. Elhay and Simpson (2011) propose a regularisation method for D_{11} so that its condition number remains low which results in accurate Newton iterations. This method is used in this thesis. At each Newton iteration, the regularisation is as follows:

$$D_{11}(i,i) = \texttt{max}\left(D_{11}(i,i)\ ,\ \frac{D_{11}^{max}}{D_{11}(i,i)/\kappa}\right), i = 1, \ldots, n_p \tag{2.31}$$

Where κ is the bound on the condition number (see (Elhay and Simpson, 2011) for more details) and $D_{11}^{max} = \texttt{max}(D_{11})$. Abraham and Stoianov (2015*a*) propose a method for selecting an optimal value of κ. In this thesis however, κ is set to 10^5, which facilitates accuracy of the hydraulic solution of order $\mathcal{O}(10^{-11})$ for a machine precision of $\mathcal{O}(10^{-16})$.

The regularisation is tested for an extended period simulation consisting of 97 steady-state simulation using GGA on the network of the experimental programme. The iteration counter k on termination is plotted with the infinite norm of the energy equations $\|g_1\|_\infty$ in (2.30). The maximum number of iterations is set to 100. The results are shown in Figure 2.2 and compared with the method proposed by Todini and Pilati (1988). The regularisation consistently facilitates an accurate solution ($\|g_1\|_\infty < 10^{-9}$) with an average number of iterations equal to 24, whereas without regularisation the maximum number of iterations is reached, with an average $\|g_1\|_\infty = 1.3 \times 10^{-6}$.

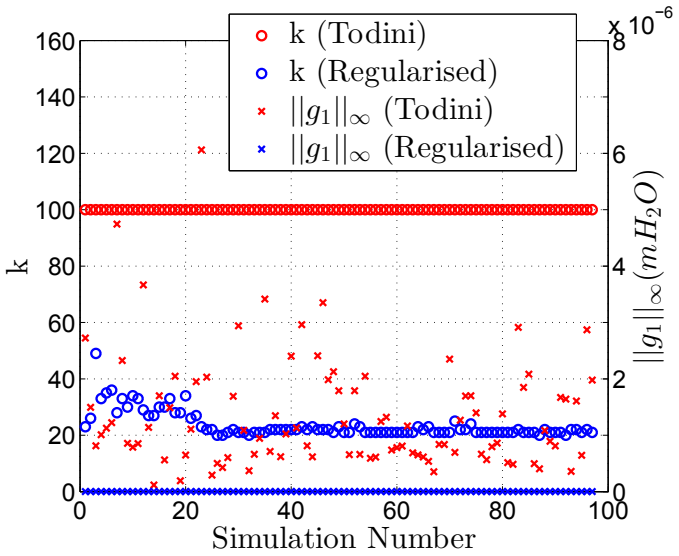


Figure 2.2: Comparison of solution accuracy using the infinite norm of the energy conservation equations ($\|g_1\|_\infty$) and the total number of iterations k required for convergence for a regularised and non-regularised (Todini) GGA solution method

2.7 Modelling Control Valves

Modelling control valves within a network simulation is a challenging problem due to the (often ad-hoc) modifications that need to be carried out to the Newton method, and the uncertainty involved with modelling multiple control valves that can interact with each other.

The modelling of a valve with a fixed stem position presents no additional challenge, since this element is effectively a pipe with a different type of head loss law. A head loss relationship for a valve i is defined as (Mays, 1999):

$$\Delta h_i = r_i |q_i| q_i \tag{2.32}$$

where the coefficient r_i is given as:

$$r_i = \frac{8\xi_i}{g_a \pi^2 d_i^4} \tag{2.33}$$

where $g_a \in \mathbb{R}$ is acceleration due to gravity and $\xi \in \mathbb{R}^{n_v}$ is a valve coefficient (available from the valve manufacturer) that is dependent on the type of valve and its opening percentage. The head loss over a valve is often referred to as a minor loss (as opposed to major losses across a network caused by friction), and (2.33) is in the minor loss equation form. An alternative definition of r_i in (2.33) is $r_i = 1/c_v^2$, where c_v is referred to as the flow coefficient, which is dependent on the valve and is also available from the manufacturer. This form is more intuitive and often used in industry, since the flow coefficient is equal to the flow through a valve with a pressure differential of $1mH_2O$. Salgado et al. (1988) describe the GGA solution method where (2.32) is used instead of (2.3) for the modelling of valves in networks.

The modelling of control valves presents more of a problem. A control valve can operate in a number of ways, as discussed in Section 3.7. For example, the valve might need to fix pressure at its downstream node (i.e. a PRV), or vary the outlet pressure based on the flow through the valve, which is called flow modulation (Section 3.7).

Bhave (1991, p. 175) outline a method for the modelling of control valves (PRVs) within network simulations, where the outlet (unknown head) node of the PRV is replaced by a fixed head node and the PRV link is removed from the simulation. For mass continuity, the inflow at the PRV inlet node must be set equal to the outflow of the PRV link fixed head node. When multiple PRVs are considered that are internal to the network (i.e. not just at the inlet of a network), a more complicated analysis is required with a new construction of equations that describe the probable PRV behaviour. A more general way of implementing this approach was outlined by Andersen and Powell (1999), with a focus on control valves being incorporated into solving hydraulic equations using a loop method. Non steady-state PRV models also exist (Prescott and Ulanicki, 2003), although these are not easily applied to steady-state network simulation approaches.

Rossman (2000) simulates PRVs in EPANET 2.0 by scaling the equations in the linear Newton systems of the GGA method (Todini and Pilati, 1988). More specifically, the $Xh_{k+1} = b$ structure of (2.20) is scaled for PRV i and outlet node j to achieve a target hydraulic head at the PRV outlet h_{set} as follows:

$$D_{11}(i,i) = 0 \tag{2.34}$$

$$b(j,j) = b(j,j) + 10^8 h_{set} \tag{2.35}$$

$$X(j,j) = X(j,j) + 10^8 \tag{2.36}$$

In addition, an algorithm consisting of a series of IF statements are used to close the PRV if the outlet head is higher than the inlet head, or fully open the PRV if the target outlet head can't be achieved due to insufficient inlet head. It is well known however that this algorithm can cause convergence problems in EPANET 2.0 when multiple PRVs are present in the network (Simpson, 1999). This problem is of particular relevance to the simulation of WDNs with a dynamic topology where multiple PRVs and other types of control valve are operating. Methods have been proposed to overcome these convergence problems by forming the hydraulics as an optimisation problem (Deuerlein et al., 2009; Piller and van Zyl, 2014), however the performance of these methods on medium or large networks have not yet been investigated.

A novel, convex approach to modelling and incorporating PRVs in a control optimisation problem was developed by Wright et al. (2014*a*). The need for the novel approach originates from the type of optimisation for valve control carried out in Chapter 6, where convex approximations are formed in order to efficiently

solve the optimisation problem. The convex approximation for a control valve is outlined in more detail in Section 6.4.1. In this section, the main emphasis is on the fact that the novel approach to modelling PRVs facilitates the use of a null space algorithm, which improves the computational efficiency of the optimisation algorithm.

The control valves are included in the hydraulic simulation through the introduction of a control valve-link incidence matrix $A_{13} \in \mathbb{R}^{n_p \times n_v}$ and an independent variable η that represents "additional" head loss across a control valve (Wright et al., 2014*a*), on top of the head loss occurring across a fully opened valve modelled by (2.32). The energy conservation equations in (2.5) are updated to reflect the presence of control valves:

$$g_1(q, h, \eta) := A_{11}(q)q + A_{12}h + A_{10}h_0 + A_{13}\eta = 0, \tag{2.37}$$

Together with certain inequality constraints, outlined in Section 6.4.1, PRV behaviour can be incorporated within a null space algorithm. The derivations of the null space algorithm with the inclusion of control valves follows the same derivation undertaken in Section 2.4.2, except (2.5) is replaced with (2.37). The final equations that are iteratively solved in the null space algorithm are as follows:

$$q_{k+1} = x^* + Zv \tag{2.38}$$

$$Z^T D_{11} Z v = Z^T[(D_{11} - A_{11})q_k - A_{10}h_0 - A_{13}\eta - D_{11}x^*] \tag{2.39}$$

The null space algorithm with control valve settings input is summarised in Algorithm 1, and used extensively in the optimisation work in Chapter 6.

Input: Valve settings (η), network parameters (A_{12}, A_{21}, A_{10}, Z, h_0, d, r)

Result: h, q

Initialization: Set $k = 1$, $q_k = x^*$;

while $k < a \times np$ *AND* $k \leq k_{max}$ **do**

Calculate A_{11}, D_{11} ;

$Z^T D_{11} Z v = Z^T[(D_{11} - A_{11})q_k - A_{10}h_0 - A_{13}\eta - D_{11}x^*]$;

$q_{k+1} = x^* + Zv$;

$k \leftarrow k + 1$;

end

while $\|g_1\|_\infty \geq \epsilon_N$ *AND* $k \leq k_{max}$ **do**

Calculate A_{11}, D_{11} ;

$g_1(q, h, \eta) = A_{11}q + A_{12}h + A_{10}h_0 + A_{13}\eta$;

$Z^T D_{11} Z v = Z^T[(D_{11} - A_{11})q_k - A_{10}h_0 - A_{13}\eta - D_{11}x^*]$;

$q_{k+1} = x^* + Zv$;

$k \leftarrow k + 1$;

end

Algorithm 1: Null space algorithm with valve settings η input, used in control optimisation (Chapter 6)

The approach used for modelling control valves can also be used in simulation, where η becomes a function of other variables in the simulation. For example, for a PRV:

$$\eta(h, q, \hat{h}) = h_{k,a} - \hat{h}_b - A_{13}^T(A_{11}q_k), \ \forall i \in N_v \tag{2.40}$$

where a and b represent the upstream and downstream node respectively of PRV i, $\hat{h} \in \mathbb{R}^{n_v}$ is the target hydraulic head at the outlet of PRVs, and k is the iteration number of the Newton method, i.e. η is updated in the iterates based on h_k and q_k. If flow modulation valves are modelled (Section 3.7.3), $\hat{h}$ becomes a function of q_k:

$$\hat{h}(q_k) = a_1 q_k^{a_2} + a_3 q_k + a_4 \tag{2.41}$$

where a are constants that represent a polynomial, which is a commonly used curve in flow modulation (Ulanicki et al., 2000).

Since η is now a function of q and h, the efficiency of the null space algorithm is reduced since h must be calculated at each stage of the Newton iterations (Algorithm 1). The GGA is therefore used when simulating PRVs. In this thesis, only the simulation of historic events is carried out (for example, in the analysis of the experimental programme network in Chapter 7, where the performance of a dynamic topology is validated). Therefore there is no need to define IF statements (Rossman, 2000) or status algorithms (Andersen and Powell, 1999) that estimate the behaviour of PRVs, this is known a priori.

The GGA with control valves is outlined in Algorithm 2. Its derivation is the same as the original GGA, except (2.5) is replaced with (2.37). A demonstration of its performance is shown in Figure 2.3, where a flow modulation PRV is simulated in an extended period simulation for a two day period. The GGA solves (2.37) with a tolerance of at least $\|g_1\|_\infty \leq 10^{-9}$ with an average of 19 iterations, and a maximum of 23 iterations.

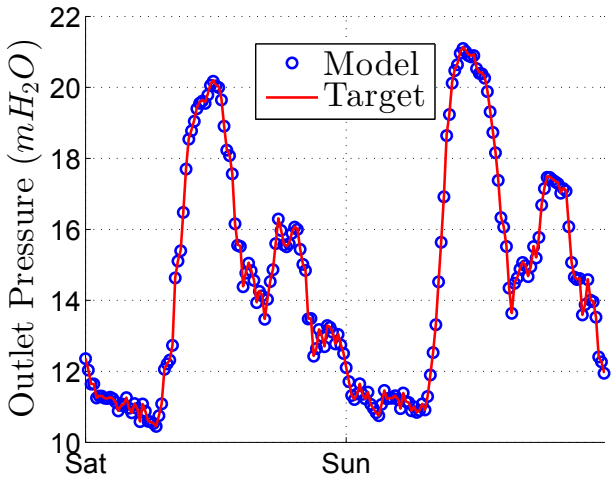


Figure 2.3: Simulating a PRV in the experimental programme network (Figure 5.16) with the GGA and valve settings $\eta(h, q, \hat{h})$ for flow modulation. The modelled outlet pressure matches the target (outlet) pressure of the PRV with $\|g_1\|_\infty \leq 10^{-9}$

.

Input: Valve settings ($\eta(h, q, \hat{h})$), network parameters (A_{12}, A_{21}, A_{10}, h_0, d, r), initial starting point (h,q)
Result: h, q
Initialization: Set $k = 1$;
while $\|g_1\|_\infty \geq \epsilon_N$ AND $k \leq k_{max}$ **do**
  Calculate A_{11}, D_{11}, $\eta_k(h_k, q_k, \hat{h})$;
  $X = A_{21}(NA_{11})^{-1}A_{12}$;
  $q_{k+1} = D_{11}^{-1}[(D_{11} - A_{11})q_k - A_{10}h_0 - A_{13}\eta - A_{12}h_{k+1}]$;
  $Xh_{k+1} = A_{21}D_{11}^{-1}[(D_{11} - A_{11})q_k - A_{10}h_0 - A_{13}\eta] - d$;
  $k \leftarrow k + 1$;
end

Algorithm 2: GGA with control valve simulation using $\eta(h, q, \hat{h})$

2.8 Online Model Parameter Update

The acquisition of hydraulic data continuously using telecommunications (Sections 1.2 and 5.4.5) facilitates the continuous update of model parameters online. The parameters include the head at inlets to DMAs (h_0) and demand profiles (d).

Let the aggregated consumer demand and leakage for all nodes n_n as a continuously expanding time series of length n_t be $d^t \in \mathbb{R}^{n_n \times n_t}$. The demand update for a discrete zone based on continuous real-time data is given by:

$$d^{t+1} = \frac{\sum_{i \in \mathcal{B}} q_{m,i}^{t+1}}{\sum_{j \in \mathcal{Z}} d_j^t} d_k^t, \ \forall k \in \mathcal{Z} \tag{2.42}$$

where $\mathcal{Z} \subseteq N_n$ is a set of nodes in a discrete zone with boundary inlets/outlets defined by the set $\mathcal{B} \subseteq N_p$, and q_m are the measured boundary flows.

The methodology for updating demand in the model is similar to the scaling method used by Davidson and Bouchart (2006). However, in the approach used by Davidson and Bouchart (2006), flow measurements were acquired for links that were not the boundary of discrete zones (such as DMAs). Consequently, just scaling all demand by the real-time inlet flow data does not result in model solutions that agree with all data points. To overcome this, Davidson and Bouchart (2006) used a least square regression method to distribute the total demand amongst nodes, weighted in a way to guarantee all flow measurements agree with the model solution. In the experimental programme, flow is monitored at the edge of all hydraulically interconnected zones (DMAs), therefore a least square regression models is not necessary.

2.9 Pressure Dependent Demand

2.9.1 Demand-Pressure Relationships

Many different demand-pressure relationships exist in the literature. For estimating how customer demand is affected during critical pressure situations (i.e. when the head at a node is insufficient to supply the normal customer demand), a relationship proposed by Wagner et al. (1988) is popular (Giustolisi and Walski, 2011):

$$d_{act,j} = \begin{cases} 0 & \text{for } h_j < z_j \\ d_j \frac{(h_j - z_j)^{0.5}}{(\underline{h}_j^* - z_j)^{0.5}} & \text{for } z_j \leq h_j < \underline{h}_j^* \ , \ \forall j \in N_n \\ d_j & \text{for } h_j \geq \underline{h}_j^* \end{cases} \tag{2.43}$$

where d_{act} is the actual demand supplied due to an insufficient head being available and $\underline{h}_j^*$ is the minimum hydraulic head required to sustain the nominal

customer demand. The demand-pressure relationship requires the definition of bounds on the head where customer demand starts to diminish ($\underline{h}_j^*$) and where customer demand becomes zero. As indicated in (2.43), if the hydraulic head is equal to the elevation at any point in the network, then no demand can be sustained. Giustolisi and Walski (2011) suggest that further research still needs to be undertaken in order to better establish $\underline{h}_j^*$. It is assumed in this thesis that $\underline{h}_j^* = z_j + 10mH_2O$ unless otherwise stated.

Another important pressure-demand relationship is the leakage that occurs on the network. Leakage is typically modelled using the following relationship:

$$l_j = \begin{cases} 0 & \text{for } p_j \leq 0 \\ \phi_j p_j^{\psi_j} & \text{for } p_j > 0 \end{cases}, \ \forall j \in N_n \tag{2.44}$$

where $l \in \mathbb{R}^{n_n}$ is the leakage, $\phi \in \mathbb{R}^{n_n}$ is a coefficient to be calibrated depending on the parameters of the network at node j (for example, Germanopoulos and Jowitt (1989) use the length of connecting pipes) and $\psi \in \mathbb{R}^{n_n}$ is an exponent that has been found to vary depending on whether background leakage or a burst is being modelled. The calibration of ϕ_j can take into account a number of pipe properties (of the pipes connected to node j) that are known to affect leakage rates. These include pipe material, age, diameter, wall thickness, soil backfill properties, replacement rates, and operational pressure (Kleiner and Rajani, 2002). Dynamic pressure (transient) conditions and pressure variability have also been linked to burst rates (Martínez-Codina et al., 2015; Hoskins, 2016). Finally, the number of customer connections is related to leakage, since a substantial amount of leakage occurs on pipes within the boundaries of properties (Tabesh et al., 2009).

The exponent ψ_j varies according to whether a burst or background leakage is modelled. For a burst, and assuming the area of the hole of the burst is constant, the exponent takes a value of 0.5 (Farley and Trow, 2003), i.e. flow is proportionate to the square root of the pressure, which can be derived from Bernoulli's principle. However for background leakage, a major study in the UK found ψ_j to take a value of 1.18 (Water Authorities Association and others, 1985) for background leakage. It is common practice to assume a constant ψ for all nodes in the area of interest when modelling leakage due to uncertainty in the model and the unavailability of data. Similar mean values of 1.13 and 1.15 were also reported in case studies in Japan and Brazil respectively (Farley and Trow, 2003), although the spread of data ranges from 0.52 to 2.79. This exponent is much higher than the theoretical value of 0.5. This phenomenon was later explained by May (1994), who proposed that the area of the holes that make up the background leakage are also pressure dependent. For networks that are predominantly plastic piping, an exponent of 1.5 is typical, whereas for metallic pipe network, an exponent from 0.5 up to 1.15 is typical, depending

on the integrity of the network. This large range in exponent can be explained by the fact that plastic piping is considerably more flexible than steel, therefore the area of the holes will be more dependent on the pressure than steel pipes. If the state of a metallic pipe network is not known, an exponent of 1.15 is recommended (Farley and Trow, 2003).

2.9.2 Pressure-Driven GGA

A null space (loop) algorithm that simulates pressure-driven demand does not exist (Elhay et al., 2014). Solution methods that use loops are less suitable for pressure-driven analyses since the loops can change between iterations (Gupta and Bhave, 1994), i.e. a null space does not exist.

Other methods however do exist for pressure driven simulations. Bhave (1991) outlines one method for when customer demand is affected by critically low pressure. The method involves running a demand-driven hydraulic simulation, and replacing critical pressure nodes with fixed-head nodes that have atmospheric pressure (i.e. the unknown is now an inflow to the fixed head node). The intuition is that, if pressure is critical enough to affect customer demand, customers will be extracting as much water as possible, which results in the pressure head at these nodes dropping to atmospheric pressure. The method involves multiple iterations of a demand-driven hydraulic simulation until all nodes have either a non-critical pressure (i.e. the full design demand is satisfied) or a critical pressure (represented by a fixed head node and a calculated outflow). This type of analysis can't be used for simulating leakage however, since leakage consists of an unknown flow rate and an unknown head.

Todini (2003) outlines two methods for pressure-driven simulations. The first one is very similar to the method proposed by Bhave (1991). The second method is based on GGA and uses mathematical pressure-demand relationships. Therefore this method can be used for simulating leakage, as undertaken by Giustolisi et al. (2008). The approach by Todini (2003) introduces a new diagonal matrix $A_{22} \in \mathbb{R}^{n_n \times n_n}$, where $A_{22}h$ is equal to a pressure-demand relationship such as (2.43) or (2.44). Updating the original demand-driven system in (2.8) to take into account head-driven demand gives:

$$g(q,h) := \begin{bmatrix} A_{11}(q) & A_{12} \\ A_{21} & A_{22}(h) \end{bmatrix} \begin{bmatrix} q \\ h \end{bmatrix} - \begin{bmatrix} -A_{10}h_0 \\ d \end{bmatrix} \tag{2.45}$$

In (2.45), d is a non-pressure dependent demand, set to zero if all demands in the network are to be simulated as pressure-driven. As in the demand-driven GGA, the derivation of the pressure-driven GGA is undertaken by applying the

Newton method in (2.9) to (2.45) as follows:

$$\begin{bmatrix} NA_{11}(q_k) & A_{12} \\ A_{21} & D_{22}(h_k) \end{bmatrix} \begin{bmatrix} q_{k+1} \\ h_{k+1} \end{bmatrix} = \begin{bmatrix} NA_{11}(q_k) & A_{12} \\ A_{21} & D_{22}(h_k) \end{bmatrix} \begin{bmatrix} q_k \\ h_k \end{bmatrix} ... \\ ... - \begin{bmatrix} A_{11}(q_k) & A_{12} \\ A_{21} & A_{22}(h_k) \end{bmatrix} \begin{bmatrix} q_k \\ h_k \end{bmatrix} - \begin{bmatrix} A_{10}h_0 \\ -d \end{bmatrix} \quad (2.46)$$

Where $D_{22}(h_k)$ is the Jacobian of $A_{22}(h)$. Simplifying (2.46) gives:

$$\begin{bmatrix} NA_{11}(q_k) & A_{12} \\ A_{21} & D_{22}(h_k) \end{bmatrix} \begin{bmatrix} q_{k+1} \\ h_{k+1} \end{bmatrix} = ... \\ ... \begin{bmatrix} NA_{11}(q_k) - A_{11}(q_k) & 0 \\ 0 & D_{22}(h_k) - A_{22}(h_k) \end{bmatrix} \begin{bmatrix} q_k \\ h_k \end{bmatrix} - \begin{bmatrix} A_{10}h_0 \\ -d \end{bmatrix} \quad (2.47)$$

Expanding out the matrices in (2.47) gives the following two systems. As before, to improve readability the term $A_{11}(q_k)$ is simplified to A_{11}, $A_{22}(h_k)$ is simplified to A_{22} and $NA_{11}(q_k)$ is replaced by D_{11}.

$$D_{11}q_{k+1} + A_{12}h_{k+1} = (D_{11} - A_{11})q_k - A_{10}h_0 \quad (2.48)$$

$$A_{21}q_{k+1} + D_{22}h_{k+1} = (D_{22} - A_{22})h_k + d \quad (2.49)$$

In order to explicitly calculate q_{k+1}, (2.48) is rearranged and multiplied by D_{11}^{-1}:

$$q_{k+1} = D_{11}^{-1}[(D_{11} - A_{11})q_k - A_{10}h_0 - A_{12}h_{k+1}] \quad (2.50)$$

In order to explicitly calculate h_{k+1}, we must eliminate q_{k+1} from (2.48). First, (2.48) is multiplied by D_{11}^{-1} to give:

$$q_{k+1} + D_{11}^{-1}A_{12}h_{k+1} = D_{11}^{-1}[(D_{11} - A_{11})q_k - A_{10}h_0] \quad (2.51)$$

Then multiply (2.51) by A_{21} to produce:

$$A_{21}q_{k+1} + A_{21}D_{11}^{-1}A_{12}h_{k+1} = A_{21}D_{11}^{-1}[(D_{11} - A_{11})q_k - A_{10}h_0] \quad (2.52)$$

Recalling that $A_{21}q_{k+1} = (D_{22} - A_{22})h_k - D_{22}h_{k+1} + d$ in (2.52) according to (2.49). Therefore:

$$A_{21}D_{11}^{-1}A_{12}h_{k+1} = A_{21}D_{11}^{-1}[(D_{11} - A_{11})q_k - A_{10}h_0]... \\ ... - (D_{22} - A_{22})h_k + D_{22}h_{k+1} - d \quad (2.53)$$

Rearranging (2.53) so that h_{k+1} is solely on one side and in the form $Ax = b$ gives:

$$(A_{21}D_{11}^{-1}A_{12} - D_{22})h_{k+1} = A_{21}D_{11}^{-1}[(D_{11} - A_{11})q_k - A_{10}h_0]... \\ ... - (D_{22} - A_{22})h_k - d \quad (2.54)$$

As in a demand-driven GGA, a linear system of size n_n needs solving in (2.54). Some final tidying of (2.50) and (2.54), and replaceing D_{11} with its definition produces the Newton update for h_{k+1} and q_{k+1} for a head-driven GGA:

$$h_{k+1} = -(A_{21}(NA_{11})^{-1}A_{12} - D_{22})^{-1}... \\ ...(A_{21}N^{-1}(q_k + A_{11}^{-1}A_{10}h_0) + d + (D_{22} - A_{22})h_k - A_{21}q_k) \quad (2.55)$$

$$q_{k+1} = (I - N^{-1})q_k - N^{-1}A_{11}^{-1}(A_{12}h_{k+1} + A_{10}h_0) \quad (2.56)$$

With an initial q_k and h_k, iterations between (2.55) and (2.56) are undertaken until $\|g\|_\infty \leq \epsilon_N$ in (2.45). Both the energy and mass norm are used for the stopping criterion because mass continuity is not automatically satisfied after the first iteration, as is the case for the demand-driven GGA and null space algorithm.

2.10 Conclusion

This chapter has reviewed hydraulic modelling principles and suitable solution methods. Out of the solution methods available, the GGA and null space algorithms are most appropriate for the work carried out in this thesis.

The null space algorithm is used in the calculation of optimal control in Chapter 6 for two reasons:

- Considerable computational savings, up to 4× that of GGA, can be made when using a null space algorithm. These savings are particularly useful when many simulations need to be undertaken. The calculation of optimal control is one example, where the evaluation of the objective function and constraint set involves solving the hydraulic equations.
- The null space does not require that D_{11} is always invertible. When a flow in a link becomes zero in the Newton iterations, D_{11} will become singular when using the Hazen-Williams head loss model, and the Newton iterations break down. Zero flows can occur for a variety of reasons, one being the full closure of valves. In valve control optimisation, this is a common occurrence.

To incorporate control valves within the null space algorithm, and retain its computational efficiency, a novel valve model is proposed (Section 2.7). The null space algorithm can then be used efficiently within control optimisation (Chapter 6).

The GGA is also used in this thesis for:

- Pressure-driven simulations, where the demand becomes a function of pressure. This is particularly important for the analysis of failure situations,

where pressure in the network can become critically low and affect the amount of water actually supplied to customers. Since resilience to failure is one benefit of a dynamic topology to be investigated in this thesis, pressure-driven simulations are highly relevant. At present, there is no pressure-driven equivalent null space algorithm.

- The simulation of networks with control valves, the control of which depends on the heads iteratively calculated in the Newton method. A null space algorithm loses some of its efficiency when the head must be calculated at each Newton iteration. The simulation of control valves is used to analyse historic events, such performance testing of a network with dynamic topology in Chapter 7. In this context, the control valve simulation is a different problem to the inclusion of valve settings in the null space algorithm and optimisation methods, as detailed above. The difference being, that in the control optimisation, the valve settings are independent variables.

3 Design and Analysis of District Metered Areas

3.1 Introduction

A key objectives of this thesis is to investigate the performance of a dynamic DMA topology and compare it with other established and emerging approaches to pressure and leakage management. An understanding of the current DMA design practices and pressure management options is therefore fundamental for the investigations carried out in this thesis. This information is also relevant for informing the design and operation of a dynamic topology.

This chapter aims to establish:

- The advantages and disadvantages of DMA operation (Sections 3.3 and 3.4) in order to establish the applicability of other approaches in pressure and leakage management.
- Performance indicators for WDN operation (Section 3.5). A performance indicator is a fundamental concept for comparing the performance of different networks and network configurations.
- Best practices in DMA design (Section 3.6), which can aid in the design of a dynamic DMA topology.
- A review of established and emerging approaches to pressure management (Section 3.7), which can be used to benchmark the performance of networks with a dynamic topology.
- Alternative forms of leakage management (Section 3.8) and global trends in the adoption of the DMA (Section 3.9). The aim is to establish whether DMAs are still relevant, despite being ubiquitous in the UK.
- An analysis on a real, operational network consisting of 245 DMAs to understand the current status of DMAs in relation to the design criteria and best practices (Section 3.6). The analysis identifies areas in the network where a dynamic topology could be beneficial.

3.2 DMA Description

A DMA is a hydraulically separated zone in a water distribution network created by permanently closing isolation valves in the network. Isolation valves are ubiquitous in most networks and are used to isolate pipes from the water source so that mains repair and replacement can be carried out. The permanently closed isolation valves that make up the boundary of the DMA are often referred to as boundary valves. The supply inlets and outlets of the DMA are monitored for flow. Most DMAs only have a single inlet, as shown in the case study in

Section 3.10. DMAs that have an outlet that forms the inlet of another DMA are known as cascading DMAs. Each DMA typically has between 500 and 3,000 customer connections (Farley and Trow, 2003), although DMA size can deviate from this. One factor that affects DMA size is the size of the mains in the DMA, which can vary globally, as discussed in Section 3.6.

3.3 Advantages of the DMA

The implementation of DMAs has two main advantages and a number of other smaller benefits. The main advantages are the ability to accurately and efficiently carry out assessments of leakage levels that help the prioritisation of pipe repair and replacement across large and complex water distribution network (Section 3.3.1) and the implementation of simplistic pressure management in DMAs through the installation of PRVs (Section 3.3.2). The benefit to cost ratio for pressure management, DMA implementation, and leakage accountability has been estimated to be 4.1 to 1 in one study (Lalonde et al., 2008), rising to 6.1 to 1 after 10 years due to the reduced need to repair bursts. Other advantages of DMA implementation are listed in Section 3.3.3.

3.3.1 Leakage Assessment

DMAs facilitate a transparent approach to derive mass balance and non-revenue estimation as the flow into and out of each DMA is continuously monitored. The measurement of flow can be used in three forms of water loss assessment: a water balance, component analysis, and minimum night flow analysis.

A water balance, sometimes called "a top-down" calculation (Puust et al., 2010), is a tally of water outputs against the total water input taken from treatment plants, as shown in Table 1 (Fanner, 2010). Leakage (real losses) can be estimated by subtracting metered or estimated water consumptions (including any errors in metering) from the the total water input. A water balance is typically carried out over a 12 month period. The accumulation of errors in all parts of the water tally, as well as a lack of information about the real loss components and how company policy affects this, makes a water balance unsuitable for leakage estimation alone (Farley and Trow, 2003).

A component analysis is the estimation of leakage through knowledge of how many bursts are repaired each year and the duration and flow rate of the bursts. The "Background and Bursts Estimates" (BABE) approach is often used in a component analysis. In BABE, leakage is categorized into background leakage and reported/unreported bursts (O'Day et al., 1982). Background leakage is defined as all leakage that is too small to be detected by current technologies ($0.25m^3/hour$ ($= 0.07l/s$) at $50mH_2O$ according to Morrison et al. (2007)), and

Table 1: Water balance from the International Water Association (IWA) best practice standard, taken from (Fanner, 2010)

<table>
<tr><td rowspan="8">System Input Volume (corrected for known errors)</td><td rowspan="4">Authorised Demand</td><td rowspan="2">Billed Authorised Demand</td><td>Billed Metered Demand (including water exported)</td><td rowspan="2">Revenue Water</td></tr>
<tr><td>Billed Unmetered Demand</td></tr>
<tr><td rowspan="2">Unbilled Unauthorised Demand</td><td>Unbilled Metered Consumption</td><td rowspan="6">Non-Revenue Water (NRW)</td></tr>
<tr><td>Unbilled Unmetered Consumption</td></tr>
<tr><td rowspan="4">Water losses</td><td rowspan="2">Apparent Losses</td><td>Unauthorised Consumption</td></tr>
<tr><td>Customer Metering Inaccuracies</td></tr>
<tr><td rowspan="3">Real Losses</td><td>Leakage on Mains</td></tr>
<tr><td>Leakage and Overflows at Utilitys Storage Tanks</td></tr>
<tr><td>Leakage on Service Connections up to Customer Meter</td></tr>
</table>

can include leakage through fittings, customer connections, joints, and smaller cracks in pipes. Although the components of background leakage are small, its total can be substantial, hence why pressure management is an efficient method of reducing background leakage. Bursts are defined as any single leak with a flow rate above background leakage flow rates (i.e. leaks that can be detected). Leakage and bursts are both pressure dependent (see Section 2.9), but have different pressure laws.

A minimum night flow analysis (also known as a "bottom-up" approach (Puust et al., 2010)) involves monitoring DMA inlet and outlet flows during low demand hours (typically 02:00 - 04:00) in order to more accurately distinguish real leakage from legitimate water use. An estimate of legitimate demand is subtracted from the minimum night flow to estimate the average night leakage ($m^3/hour$). The stochastic nature of customers demand significantly hinders the successful execution of this task outside hours of minimum (night) water demand. The estimation of total leakage in the network is carried out by multiplying the average night leakage with an "hour-day" factor which depends on the pressure variability over a 24 hour period. For a network with a moderately stable diurnal network pressure, and if the minimum night flow is measured in $m^3/hour$, the hour-day factor will be ≈ 24. A pressure step test can also be undertaken during low demand (night) hours in order to better establish the amount of night flow that is leakage (Kunkel and Sturm, 2011). This test involves incrementally increasing/decreasing pressure at night, and recording the incremental changes in minimum night flow. A similar type of analysis is carried out in Chapter 7.2.2

for the estimation of leakage in the experimental programme.

Once a water company has assessed their real losses (Table 1), it is useful to know how efficient their leakage management practices are. One methodology to do this was created by the Water Losses Task Force, and is called the "unavoidable annual real losses" (UARL). The UARL is a system of relationships and equations (based on mains lengths, customer connections etc.) that specifies the lowest technically achievable real losses for a given network (see Table 1 for information on real losses and (2.44) for leakage estimations based on network pressure). A water company can then compare this to their current annual real losses (CARL), which is estimated using ideally all of the methodologies for water loss assessment outlined in this section (water balance, component analysis, minimum night flow analysis). The ratio of CARL to UARL is called the infrastructure leakage index (ILI), and helps water companies to establish the success of their leakage management practices (Farley and Trow, 2003).

A water company has four tools available to reduce their real losses (including leakage), and achieve a better ILI score (Farley and Trow, 2003). These are:

1. Pressure management (Section 3.3.2);
2. Asset management i.e. prioritising mains replacement and repair based on the minimum night flow (if DMAs are in use);
3. Speed and quality of repairs;
4. Active leakage control (ALC), i.e. using all available information to actively locate and repair unreported bursts. This includes the minimum night flow, listening sticks, and portable noise correlators used by the leakage practitioners. ALC is in contrast to a passive approach to leakage, where mains are only repaired if a burst has been reported.

The subdivision of networks into smaller zones that are monitored for flows has substantially aided water companies to reduce the time it takes to detect and repair unreported bursts, prioritize mains replacements programmes, and operate their water networks closer to the UARL. Reductions in night flow of 50% have been reported Kunkel and Sturm (2011) by solely using DMAs to identify leaks and prioritize pipe replacement.

3.3.2 Pressure Management

Pressure management at DMA level is most commonly undertaken by installing a pressure reducing valve (PRV) at the inlet of the DMA. This will:

- Reduce the pressure downstream;
- Stop or diminish the propagation of pressure transients downstream.

Pressure management using PRVs has two main benefits. First, burst frequency can be reduced in WDNs where pressure is reduced (Farley and Trow, 2003). Lalonde et al. (2008) and Fantozzi et al. (2009) report burst reductions of up to 40% following the implementation of pressure management. Pressure variability, defined as the extent that nodes in the network differ from the average pressure in the network, has also been linked to burst frequency (Martínez-Codina et al., 2015). Second, due to the pressure-leakage relationship (Section 2.9), a reduction in pressure also results in a reduction in leakage.

Whilst these benefits in leakage and burst reduction are generally universal, the cost of PRV installation should be compared with the expected savings (for example, Awad et al. (2008)), so that the PRV installation is cost effective, particularly if the DMA to be pressure managed is small (Farley and Trow, 2003). The point at which the cost-benefit ratio becomes 1:1, i.e. where the cost of installing more pressure management or undertaking further ALC no longer returns savings from the amount of water saved, is known as the economic level of leakage (ELL). The ELL changes over time based on a number of factors such as burst rate, overall investments in monitoring, rehabilitation, pressure management and ALC, and the value of water (e.g. times of drought causes an increase in its value). Therefore, the calculation of the ELL is undertaken either in the short run (SRELL) or the long run (LRELL). The short run can be defined as a period of time where one ELL factor can be fixed and all other ELL factors vary. Examples of the short run include ALC and the speed and quality of repairs. The long run can be defined as a period of time where all factors can vary, and additional factors can be added that influence the ELL, such as the design and implementation of pressure management, or pipe replacement schemes (Pearson and Trow, 2005). In the long run therefore, a decision has to be made to invest. Since both the SRELL and LRELL are influenced by all factors that influence leakage levels, they must be calculated over a sufficiently long period of time, such that a stable ELL is found. Therefore, investment should be based on the factor that produces the best return, and once implemented, all other factors should then be reassessed.

The DMA aids in pressure management implementation by forming a boundary where flow is not breached. As pointed out by Walski (2015), a control valve (i.e. PRV) should control a discrete zone with no uncontrolled flow paths into the zone. The DMAs typically have just a single inlet as established in Section 3.10, and the PRV is commonly installed at or near the inlet in order to reduce pressure throughout the DMA. There are many commercially available pressure management solutions. Due to the widespread implementation of DMAs, pressure management options are typically installed in conjunction with DMAs. A number of different control options exist for the PRV operation in order to further reduce or optimise pressure subject to the minimum allowable

pressure that ensures an acceptable level of customer service. An investigation into pressure management technologies is presented in Section 3.7.

3.3.3 Other Advantages

Other advantages of DMAs are related to the logistical management of the network and water quality.

By subdividing a network into small discrete areas, it is easier to undertake work (mains replacement, technology installation etc.) in the DMA with the guarantee that it will not affect other DMAs that are not hydraulically connected (Farley and Trow, 2003). Man-hours can also be reduced because it is not necessary to carry out extensive investigations into how work could affect neighbouring DMAs. The complexity of sensor placement is also reduced (Fernández, 2011).

Flow reversals are more common in looped networks and can cause deposits on pipes to become suspended, leading to the discolouration of the customers water supply (World Health Organization, 2004). In a single-feed DMA, where the structure is tree-like and flow reversals are not common (Section 7.3), this is less likely to occur. There is no risk of suspended deposits if the flow reversal is a common occurrence however, since the pipe becomes well conditioned to the flow reversal.

Finally, the implementation of DMAs also reduces the extent of mixing of water from sources of different water quality. If two water sources with substantially different compositions are mixed, it might cause problems for certain industrial processes that are calibrated to the type of water they receive (World Health Organization, 2004). Contamination is also better contained when a DMA structure exists.

3.4 Disadvantages of the DMA

There are two main disadvantages associated with the implementation of DMAs. These are reduced resilience to failure due to the reduction of independent supply paths between consumers and water sources (Section 3.4.1), and sub-optimal pressure management (Section 3.3.2)

3.4.1 Resilience to Failure

Failure can be split into two types: hydraulic and mechanical. Hydraulic failure refers to unplanned consumptions that are not part of the network's normal operation. Examples include fire flow, water theft, or peaks in the stochastic nature of larger consumers. Mechanical failure refers to pipes bursts, valve or

pump failure, and other malfunctions of the WDN infrastructure. In both types of failure, pressure for customers can drop substantially either due to large demands placed on the network (fire flow, burst flow rate) or insufficient pressure at inlets (due to pump failure, trunk mains breaks, valve malfunctions etc.).

When a substantial burst occurs, and customers lose their supply for an extended period of time as a result of this, the water company often re-routes water from an alternative supply source (BBC News, 2014; Heart, 2015; Get Surrey, 2015). This process is also called "rezoning" (Drinking Water Inspectorate, 2009). The process is summarised as follows for a large burst. A large burst event is defined in this thesis as any burst where flooding is occurring, potentially causing damage to properties and infrastructure, and putting the public at risk.

1. The pipe must be isolated from the water supply. If customers are connected to the burst main, they will likely lose their supply of water. If the main is in a strategic location (i.e. a trunk main supplying many DMAs, or a distribution main at or near the inlet to the DMA), many thousands of customers can lose their water supply.

2. An analysis of the consequences of closing the pipe is undertaken, including an estimation of how many and which customers will lose their supply of water. Pressure-driven simulations are a useful tool for undertaking this type of analysis (Section 2.9).

3. Hydraulic simulations are undertaken to determine alternative supply options for the disconnected customers. Alternative supply options are made available by opening the permanently closed boundary valves, which reroutes water from unaffected DMAs or water sources. The hydraulic simulation is also used to check that customers can be reconnected without affecting neighbouring DMAs. Ideally, the minimum number of boundary valves for reconnecting customers will be identified. Other contingency options might include pumping and tank filling to improve pressure for the rezoned customers.

4. Once the boundary valves have been identified, technicians must travel to the boundary valves. Flushing is undertaken at the boundary valves to remove stagnant water before opening. There is no guarantee that flushing will fully prevent discolouration of the customers' supply however, as flow reversals will occur for the first time on pipes that have been well conditioned for only a single flow direction. It is also possible that the low network pressure caused by the failure has already caused discolouration due to ingress (Jones et al., 2014).

5. Once the boundary valves are opened, water is supplied to some customers from an alternative DMA in order to further mitigate the consequences of

the burst.

For a medium burst event, for example $2l/s - 5l/s$ (a substantial but not necessarily damaging or dangerous flow rate), isolation of the main and potential rezoning will also be carried out to avoid water losses and ensure customers receive an adequate level of service. If water is not visible at street level, it would be necessary to locate the burst using either a listening stick or portable noise correlators. The pressure for the customer might be affected during the time it takes to identify, locate and remedy this type of burst.

For smaller burst events, the water company may decide to not isolate the main until they can carry out the repair work. The pressure for customers in this situation could be lower than normal due to the continuous and additional demand placed on the pipe. For other types of failure, such as fire flow, the company might rezone customers, or intervene by manually overriding PRVs to supply more pressure for the fire flow. The use of more than one supply route in fire flow conditions is also beneficial (Kunkel and Sturm, 2011).

The execution of the above steps for re-routing water for customers during an incident is hindered by the permanent closure of boundary valves and causes higher consequences for customers and water companies in the event of failure. Furthermore, the manual opening of boundary valves also increases the risk of discoloured water reaching customers (Section 3.4.3), as well as mechanical failures caused by opening boundary valves with a high pressure differential (Section 3.10), thereby exacerbating the consequences of the original failure.

3.4.2 Frictional Energy Losses

The solution to the system of equations describing pressure and flow in a WDN is equivalent to minimising the system's "content" (Collins et al., 1978), which is a form of energy loss in the system (Strang, 1988). This describes the phenomenon of flow taking the paths that incur the least frictional energy losses. By operating a DMA with multiple sources, new paths exist between demand nodes and source nodes. This increased redundancy generally results in lower frictional energy losses, which facilitates more efficient pressure management. Figure 3.1 demonstrates this occurrence. The total head losses in a network model are summed and plotted against the corresponding total instantaneous consumptions within the network over a one day period, split into 15 minute steady state snapshots. The total head loss is calculated as $\sum_{i=1}^{n_p} A_{11}(q_i)q_i,\ \forall i \in N_p$ and the total instantaneous consumption is calculated as $\sum_{j=1}^{n_n} d_j,\ \forall j \in N_n$. Two scenarios are tested using these calculations. The first has a single source available, and the second has two sources available. All other aspects of the network model are identical. The head losses are on average 12.7% lower for the WDN with

multiple sources. The network model used to demonstrate this results is the experimental programme network (Figure 6.8, Section 6.5.2).

The reduction in frictional energy losses in a WDN with multiple sources can be used to drive more efficient, or even optimal, pressure management at PRVs. In the case of a single feed DMA, a PRV at its inlet will need to supply enough pressure to all customers within the DMA. If frictional energy losses are low, a fixed outlet PRV could be efficient enough, but if the frictional energy losses are substantial, a PRV that modulates its outlet pressure would be more appropriate to reduce leakage (see Section 3.7.1 for more details). However, if the network has multiple sources and consequently lower frictional energy losses, the PRVs do not need to supply as much pressure throughout the network in order to supply all customers with a satisfactory level of service. As discussed in Section 3.3.2, higher pressure results in higher leakage and burst frequency.

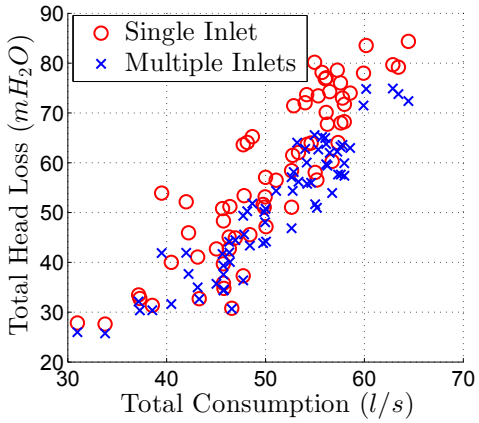


Figure 3.1: A comparison of head losses at various consumption levels for a single and multiple inlet WDN

3.4.3 Other Disadvantages

Water quality incidents are often caused by the build up of stagnant water at artificially created dead ends (World Health Organization, 2004). This problem is exacerbated when the closed boundary valves need to be opened, such as failure events as discussed in Section 3.4.1. This can lead to the customers' water supply becoming discoloured and penalties issued by the regulator. The World Health Organization (2004) recommends that the artificial implementation of dead ends is limited in the design and operation of WDNs. An investigation into the effects of DMAs on water quality is presented in (Armand et al., 2015).

Another negative effect of DMAs, related to water quality, is that they are tree-like, and the pipes have very well defined flow directions. The pipes becomes conditioned to a certain flow regime, and a change to this regime can cause discolouration of water for customers (Boxall and Saul, 2005). Therefore, if a burst

occurs that causes flow reversals in the network, there is a risk of discolouration associated with the burst, as well as the opening of any boundary valves that can restore pressure to customers. This is a well known risk in industry, and water companies will routinely carry out flushing of their pipes in order to condition them for flow reversals.

3.5 Performance Indicators

In order to assess the performance and behaviour of different networks and network configurations, performance indicators are used and defined in this subsection.

In (Alegre et al., 2006), 133 different performance indicators are outlined and used extensively by water companies and their regulators globally in order to understand and benchmark the performance of networks. The performance indicators span all operations of a water company including human resources, health and safety, asset management, water quality, and the hydraulic performance of the networks. The latter strongly focuses on two aspects: leakage statistics and the customers' level of service (i.e. the network resilience to failure, how many customers have been disconnected when failure occurs, how many customer complaints have been made). Both aspects are strongly related to the benefits of a dynamic topology investigated in this thesis.

It is strongly recommended that all performance indicators are calculated over a one year period in order to accurately assess the network with season variations. Shorter period analyses are also valid, but attention to potentional seasonal variations in the calculations should be incorporated to avoid potential bias (Alegre et al., 2006).

3.5.1 Pressure and Leakage Management

The most common forms of leakage assessment were presented in Section 3.3.1. It is common practice for a water company to assess its leakage performance as the ratio of non-revenue water (NRW, which includes leakage plus unauthorised consumption, metering errors, and unbilled consumption) to the system input (Table 1). This is called % NRW. This should be discouraged however, because the ratio can vary significantly based on the total consumption in the network (Farley and Trow, 2003). For example, high consumption decreases the % NRW, making the network appear to have less leakage. An international comparison of % NRW shows variations between approximately 5% and 50% (Farley and Trow, 2003). This range is not entirely as a result of variations in pressure management and infrastructure condition. It is therefore preferable to measure leakage based on the ILI or the previous leakage performance of the network (Farley and Trow,

2003). In Chapter 7, leakage is assessed for a dynamic topology and other configurations using this approach, i.e. the relative performance of network configurations.

In addition to leakage statistics, it is also useful to define some performance indicators related to the pressure distribution of the network, which strongly influences the total background leakage (Section 2.9.1) and has also been correlated with burst frequencies (Martínez-Codina et al., 2015). The pressure-related performance indicators used in this thesis are the average nodal pressure (P_{av}), the average zone pressure (AZP), and the average pressure variability ($\overline{P}_{var}$).

The average nodal pressure is used in the design of the experimental programme (Section 5.3) to assess different network configurations, and is defined as

$$P_{av} = \frac{1}{n_n} \sum_{j=1}^{n_n} p_j \tag{3.1}$$

where $P_{av} \in \mathbb{R}$ is the average nodal pressure. The average nodal pressure provides an approximation of the average spatial pressure in a network at a given point in time. However, in networks where nodes are not evenly distributed, the nodal pressure could give a biased approximation of average pressure in the network. Minimising the average pressure in control optimisation in order to reduce leakage could therefore give suboptimal solutions. A number of factors can affect leakage including pipe material, age, diameter, wall thickness, soil backfill properties, replacement rates, operational pressure, dynamic pressure (transient) conditions and the number of customer connections (Section 2.9). The length of main has also been used to relate pressure and leakage (Germanopoulos and Jowitt, 1989). Since leakage is one of the indicators of interest in this thesis but not exclusively the variable of interest, weighting the nodal pressure by a factor that represents both leakage in the network as well as the average pressure acting over the pipes of the network is desirable. The length of the main meets this criterion, and is used in the calculation of average zone pressure (AZP). The AZP is defined as follows:

$$AZP = \frac{1}{n_n} \sum_{j=1}^{n_n} \omega_j p_j \tag{3.2}$$

where $AZP \in \mathbb{R}$ is the average nodal pressure and the coefficients $\omega \in \mathbb{R}^{n_n}$, also in (6.14a), relate the AZP to the nodal pressures by weighting each node by the length of its incident links. That is,

$$\omega_j = \bar{L}^{-1} \sum_{i \in \mathcal{I}_j} \frac{L_i}{2}, \qquad \bar{L} = \sum_{i=1}^{n_p} L_i, \tag{3.3}$$

where $\mathcal{I}_j$ is the set of indices for links incident at node j.

The variability of pressure in the network has also been linked to burst frequency (Section 3.3.2). It is therefore useful to define an indication of pressure variability. According to Martínez-Codina et al. (2015), the pressure range was linked

to burst frequency. The pressure range was defined for a pressure time series p_{eps} as:

$$rg_p = \texttt{max}(p_{eps}) - \texttt{min}(p_{eps}) \tag{3.4}$$

where $rg_p \in \mathbb{R}$ is the pressure range, and the algorithms `max` and `min` are the maximum and minimum values of the time series p_{eps}, respectively.

The calculation of rg_p does not take into account the spatial distribution of pressure range. Therefore, in this thesis, the pressure variability is defined as:

$$P_{var,j} = \texttt{max}(p_{eps,j}) - \texttt{min}(p_{eps,j}),\ \forall j \in N_n \tag{3.5}$$

where $P_{var} \in \mathbb{R}^{n_n}$. The average pressure variability of a network is therefore defined as:

$$\overline{P}_{var} = \frac{1}{n_n} \sum_{j=1}^{n_n} P_{var,j} \tag{3.6}$$

where $\overline{P}_{var,j} \in \mathbb{R}$ is the average pressure variability. Although pressure variability is not investigated in detail in this thesis, it is reported on as one of the potential benefits of operating a dynamic topology. This is being investigated in other work on valve control, for example, by Pecci et al. (2015).

3.5.2 Resilience to Failure

A selection of the performance indicators related to resilience to failure (Alegre et al., 2006), and used extensively in industry and by regulators, are:

- % Operational water points;
- % Adequacy of pressure of supply;
- % Continuity of supply;
- % Water interruptions;
- % Interruptions per connection (No./1000 connections/year);
- Bulk supply interruptions (No./delivery point/year);
- % Population experiencing restrictions to water service;
- %Days with restrictions to water service;
- Service complaints per connection (No. complaints/1000 connections/year);
- % Pressure complaints;
- % Continuity complaints;
- % Interruption complaints;

amongst others. Some performance indicators are more applicable than others, depending on the type of analysis carried out (Farley and Trow, 2003). The in-depth investigation of all resilience indicators used in industry and throughout the academic literature is beyond the scope of this thesis. What is of more relevance, is the suitable selection of resilience indicators that facilitate the performance of a dynamic topology to be measured and compared with other established and emerging network configurations.

One good indication of all the resilience indicators presented above (Alegre et al., 2006) is the % of demand met (d_{met}) during a failure incident where pressure is not high enough to meet nominal demand (d). This is the ratio of the actual demand supplied (d_{act}) in pressure deficit conditions to the demand that would be supplied normally:

$$d_{met} = 100 \times \sum_{j=1}^{nn} \frac{d_{act,j}}{d_j} \tag{3.7}$$

The demand met is equivalent to the Volume-Reliability factor from (Gupta and Bhave, 1994) for a single period simulation. In order to calculate d_{met}, a pressure-driven simulation using the GGA method (Section 2.9.2) is undertaken with the demand-pressure relationship given in (2.43), Section 2.9.1.

Another type of index, that is popular in analysis and resilience design (Prasad and Park, 2004; Reca et al., 2008), is the reliability index $I_r \in \mathbb{R}$ defined by Todini (2000):

$$I_r = \frac{\sum_{j=1}^{n_n} d_j(h_j - \underline{h_j})}{\sum_{i,j=1,\ \forall i \in \mathcal{R}}^{n_o} q_i h_{0,j} - \sum_{j=1}^{n_n} d_j \underline{h_j}} \tag{3.8}$$

where $\underline{h_j}$ is the minimum allowable hydraulic head to ensure a good level of customer service and the set $\mathcal{R} \subseteq N_p$ contains the links that are outflows from reservoirs. Todini's index measures how close a WDN operates to a specified minimum allowable head i.e. the numerator of (3.8). It is therefore a measure of how much "excess" pressure is present in the network. As indicated by Todini (2000), excess pressure in the network can help a network overcome certain types of failure, such as small to medium bursts, by ensuring there is enough pressure to meet customer demand in addition to additional head losses introduced by the burst. By using the product of nodal heads and nodal demands, an index that varies between 0 and 1 can be achieved. Todini's index also captures implicitly the redundancy of the network, both in terms of how many loops exist internally in the network, as well as how many independent sources (reservoirs) are connected to the network, which is another factor important for determining network resilience (Yazdani et al., 2011). The reason for this is that, unless the redundancy (additional links) are at hydraulic balance points, the additional

paths for water to take will always result in a reduction of frictional energy losses occurring (Section 3.4.2). The reduced frictional energy losses result in a network with a higher pressure (assuming no PRV control is actuated in the network), which is detected in Todini's index.

Another useful index is the reserve capacity, presented by Wright et al. (2015*c*). The reserve capacity is the solution to the following NLP:

$$\max_{\mu,q,h} \mu, \tag{3.9a}$$

$$\text{Subject to: } A_{11}(q)q + A_{12}h + A_{10}h_0 = 0, \tag{3.9b}$$

$$A_{12}^T q - \mu d = 0, \tag{3.9c}$$

$$\underline{h}_j - h_j \leq 0, \ \forall j \in N_n \tag{3.9d}$$

where $\mu \in \mathbb{R}$ is a demand multiplier. The solution to (3.9), defined as μ_{max}, is the maximum demand multiplier that can be applied to the demand of the network, with the hydraulic equations satisfied in (3.9b) and (3.9c), and without violating the minimum service pressure constraint in (3.9d). Demand multipliers are often used in industry to scale the entire network demand for peak summer days, when water consumption goes up.

Reserve capacity is a well established measure of performance for transportation networks. It first appears in a paper by Webster (1958), and is developed later by Allsop (1972), where the concept was generalized for transport networks. Allsop (1972) calculated the reserve capacity μ_{max} by solving a linear program that maximizes μ subject to the linear constraints of the network. Wong and Yang (1997) extended the concept of reserve capacity to include general signal controlled networks, which resulted in a non linear program. In order to solve this, a sequential linear programming method was used to calculate μ_{max}. In their example network, the maximum flow multiplier was 1.688, therefore the reserve capacity is 68.8% of the current network demand. The reserve capacity was also calculated by Chen et al. (1999), where the degradation of link capacity was taken into account due to factors such as bad weather, type of traffic and roadway type. Chen et al. (1999) used an iterative incremental method to calculate μ_{max}. Chen et al. (2013) extended this work further by removing the assumption that demand patterns have uniform growth when calculating μ_{max}. The use of the reserve capacity has been used extensively in the efficient design of road networks (Yang and H. Bell, 1998; Zhang and van Wee, 2012; Chen et al., 2011).

A method for solving (3.9) for μ_{max} was presented by Wright et al. (2015*c*). In comparison to d_{met} in (3.7), μ_{max} can also be used to analyse critical pressure scenarios, where $h < \underline{h}$ in (3.9d). Here, $\mu_{max} < 1$. Unlike d_{met} however, if a network experiences a failure that reduces its resilience, but not the extent that $h < \underline{h}$ is true, μ_{max} will capture this reduction in resilience, whereas d_{met} will

still report 100% demand met. Like Todini's index, μ_{max} is also a measure of how much excess pressure is in the network. Therefore, in a single index, the reserve capacity can:

- Provide intuitive insight into network resilience;
- Detect and analyse networks in a state of failure with critical pressure;
- Analyse how resilient a network is in normal operation;
- Compare the resilience of both different configurations and different networks, whereas Todini's index can only be used to analyse different configurations on a single network.

The main disadvantage of the reserve capacity is that not all changes in redundancy will influence μ_{max}, despite the added redundancy potentially improving resilience in its vicinity. This is an advantage of Todini's index: any change in redundancy will be captured.

3.6 DMA Design

The main requirement for the set up of DMAs is a good understanding of the hydraulic behaviour of the overall network (Morrison et al., 2007). A hydraulic model is therefore an important tool in the set up of DMAs (Chapter 2).

The initial, general approach adopted for settings up DMAs on a large complicated network is to identify the water sources and trunk mains, and discretize the network at this higher level and work down until DMAs are formed on the smallest of mains at customer level (Morrison et al., 2007). The aim is to facilitate control at the trunk mains levels (for example, pump operations) without compromising on flexibility at the customer/DMA level. A key objective for this initial stage is to identify legal requirements (e.g. fire fighting capacity) and local customer requirements (e.g. critical customers, commercial users) so that the DMAs do not interfere with the quality of service. Once the hydraulic requirements of each DMA are understood, the boundary and size of the DMAs can be established.

3.6.1 Critical Customers and Regulations

The requirements of critical customers and regulations are first established. Critical customers can include hospitals, schools, industrial users, properties with vulnerable customers, and high rise buildings that require more pressure than low rise buildings. Once identified, assessments can be made about the level of service they require. This could be providing a higher than normal supply pressure, or providing more supply routes for critical customers to mitigate the

consequences of failure. Meeting regulations is undertaken in a similar way: identify the requirement and make arrangements to meet it. For example, fire flow capacity is critical for utilities in North America (Section 3.9), and additional DMA inlets are often installed to add this capacity in supply (Section 4.2.1).

3.6.2 Establishing the DMA Boundary

The DMA boundary must be established in order to close the isolation (boundary) valves. As discussed in Section 3.4, the permanent closure of isolation valves in water supply networks should be limited in order to avoid negative effects such as reduced resilience to failure, increased energy losses and stagnant water building up in the network. Setting up DMAs whilst limiting the number of boundary valves closed is therefore a challenging problem. When setting up a DMA, natural boundaries should be used where possible to reduce the number of isolation valves closed. Natural boundaries include rivers, streams, railway lines, city topography and major roads (Morrison et al., 2007).

After establishing natural DMA boundaries, the remainder of the boundary should ideally be set up at hydraulic balance points. A hydraulic balance point is a point in the network where the flow rate of water is zero (or close to zero). Therefore, closing an isolation valve at this point will not disrupt the natural hydraulic behaviour of the network (i.e. frictional energy losses will not be increased). Identifying the hydraulic balance points can be undertaken using a calibrated hydraulic model. Automated DMA design uses this principle of energy loss minimisation to design DMA boundaries (Section 3.6.7), a similar concept to closing boundary valves at hydraulic balance points.

Other considerations for closing isolation valves should be based on the size of main and location of large consumers (Sturm and Thornton, 2005). In order to reduce the build up of stagnant water at permanently closed boundary valves, isolation valve should ideally be closed on smaller mains. It is also better to close isolation valves near large consumers, since these users will draw more water away from the dead ends of the network and reduce water residence times.

Finally, the contours of the network area should also be used to establish DMA boundaries. The elevation across a DMA is important because the level of pressure set up (either through pumping, or valve control) for a DMA is dependent on the elevation of customers. If there is a wide range of elevation in a DMA, enough pressure will be needed to provide for customers at high elevations, but there will be excess pressure for customers at lower elevations and therefore additional leakage. It is therefore recommended that DMAs are formed on areas with a similar elevation (Morrison et al., 2007; Meyer et al., 2009). Automated DMA design approaches have also adopted the elevation across DMAs into the

calculation of optimised DMA boundaries (Section 3.6.7).

3.6.3 DMA Size

The DMA size will influence the effectiveness of leakage estimation and burst identification. If a DMA is sized too large, the ability to detect new bursts is reduced, since a bigger DMA will also have a higher background leakage and higher uncertainty in the legitimate customer demand (Morrison et al., 2007). Whilst small DMAs will improve the ability to detect bursts, discretizing the network too finely will exacerbate the disadvantages of DMAs (Section 3.4), and also increase DMA installation costs (flow meters, PRVs). DMAs therefore typically contain between 500 and 3,000 customer connections (Farley and Trow, 2003), with a general maximum bound of 5,000 connections (Morrison et al., 2007; Kunkel and Sturm, 2011).

It is not important that all DMAs are the same size (Morrison et al., 2007). Instead, determining the exact size of the DMA will generally be undertaken based on hydraulic, logistic and economic factors. The natural hydraulics of the network should not be altered extensively (Section 3.6.2). The budget for DMA installation also needs to be considered, since smaller DMA require the installation of more flow meters and PRVs (Morrison et al., 2007).

The requirements for a DMA can differ globally due to differences in metering, infrastructure and regulation.

In North America, the mains are much larger due to regulations placed on fire flow (Section 3.9). Therefore DMAs need to be larger in order to increase the fluid velocity at DMA inlets and accurately measure the flow. The networks in North America are also more looped than the UK due to the grid like nature of streets. Consequently, the DMA boundary can be more difficult to establish, more isolation valves need to be closed, and the DMAs are more likely to cascade i.e. the outlet of one DMA forms the inlet of another (Sturm and Thornton, 2005). This is in contrast to the UK, where a more dendritic topology is present. Cascading DMAs can present additional challenges in pressure management because head losses can be high across the cascading DMAs. Pressure sustaining valves (PSV) are sometimes used in cascading DMAs to ensure pressure upstream is sufficiently high enough to maintain a good level of service.

In the UK, around 60% of customers are not metered (Ofwat, 2013). Consequently, any leakage occurring on pipes that are within the boundary of the property will be almost undetectable to the water company carrying out ALC (Section 3.3.1). Water companies in the UK therefore generally try to reduce the size of their DMAs in order to more easily capture leakage on customer-owned pipes (Sturm and Thornton, 2005). In general, it is the customer's responsibility

to pay for repair work on leaking pipes within their property boundary.

The location of customer meters can also be taken into account in networks where all/most customers are metered. If the customer meters are installed at street level, the DMA size should be larger, because leakage can be detected on the customers pipework and charged for accordingly. If the meters are installed within properties, smaller DMAs may be more suitable in order to more effectively capture this leakage, as is done in the UK.

With all of these consideration taken into account, the DMA should then be sized as small as possible, subject to constraints on the increased cost of more flow meters, in order to improve leakage estimations (Morrison et al., 2007). The number of inlets/outlets, taking into consideration critical customers and regulation (Section 3.6.1), should also be minimised in order to reduce the cost of flow metering, reduce the risk of error accumulation in flow measurements, and reduce the complexity of the leakage analysis (Farley, 2012).

3.6.4 Critical Points

The critical point (CP) of a DMA is defined as the point in the network where pressure is closest to a minimum allowable pressure in the network $P_{min} \in \mathbb{R}$. This is related to $\underline{h_j}$ in (3.8) for most nodes j such that $P_{min} = \underline{h_j} - z_j$. Some nodes require a pressure higher than P_{min} however (Section 3.6.1). Water companies aim to operate their networks with a pressure equal to or above P_{min} to ensure an acceptable level of customer service. Most nodes in a DMA will have the same minimum allowable pressure, therefore the critical point is often the point of the DMA with the lowest pressure. For DMAs that have customers with specific pressure requirements, this might then become the critical point.

By identifying the CP of a DMA, water companies can ensure with a high degree of certainty that pressure elsewhere in the DMA is also adequate. In the set up of DMAs, it is beneficial to identify the CP and its distance to the DMA inlet, since the frictional energy losses of water along this path will dictate the performance of pressure management in the DMA (Section 3.7).

3.6.5 Flow Meter Installation

Leakage monitoring is undertaken using a flow meter installed at inlets/outlets. The meter is typically installed in-line with the pipe in a chamber. Well established flow meter technology includes mechanical (turbine) meters, electromagnetic meters and ultrasonic meters (Farley and Trow, 2003). Insertion flow meters that use vortex shedding (Cla-Val, 2015*b*) or electromagnetism (Bermad, 2015) are also emerging.

A mechanic meter is the simplest to manufacture and is therefore often used in developing countries. It has a large flow range, which makes it suitable as a DMA inlet/outlet meter with an accuracy of approximately 5%, depending on the manufacturer. It should however be installed in conjunction with a strainer, which protects the turbine from suspended particles. This requires a larger chamber and therefore increases costs.

Electromagnetic meters are becoming more cost efficient and offer very good bidirectional flow accuracy (±0.2% from ABB (2015)). They require very little maintenance but do however require a power source (battery, solar power, turbine energy). Electromagnetic flow meters do no require strainers, and therefore cost and space savings can be made. Ultrasonic meters, whilst accurate, are not cost effective. Ultrasonic clamp-on meters exist and are useful for the temporary acquisition of flow data.

An insertion flow meter is retrofitted to a control valve or pipe using an insertion point. Therefore no additional chamber is needed for its installation. This makes insertion flow meters cost effective and also beneficial if physical space is a constraint. Insertion meters are now becoming widely available. Example include the use of the vortex shedding phenomenon to capture flow data (Cla-Val, 2015*b*) and the use of an insertion electromagnetic meter that can capture bidirectional flow data with ±2% accuracy (Bermad, 2015).

Another approach to measuring flow is the measurement of pressure differential across a valve with known head loss characteristics and valve stem position (Atmanand and Konnur, 1996). The main drawback of this approach is the acquisition of valve characteristics, which can vary even between valves in the same manufacturer's product range.

Out of all flow meter solutions, electromagnetic meters are the most appropriate for use at dynamic boundary valves due their ability to accurately measure bi-direction flow. Where space is a constraint, an insertion flow meter could provide a good solution at the expense of losing some accuracy in the flow reading.

3.6.6 Zero Pressure Test

Before the DMA becomes operational (i.e. monitoring night lines, pressure managing the DMA), it is important to perform a "zero pressure test" once all the boundary valves have been identified and closed permanently. The zero pressure test then involves closing the inlet/outlet(s) of the DMA, and monitoring the pressure in the DMA. If the pressure drops, it means the zone has been isolated successfully. If the pressure does not drop, this suggests that there is an unknown feed into the DMA that needs to be identified before the DMA can become operational (Meyer et al., 2009). It is also good practice to check the

status of all internal isolation valves of the DMA to ensure they are in the correct position and operating correctly (Kunkel and Sturm, 2011).

3.6.7 Automated DMA Design

Methods exist for automated DMA design that minimise energy losses using graph theory and heuristics (Di Nardo and Di Natale, 2011; Perelman et al., 2015). Clustering nodes based on their elevation in order to form DMAs has also been proposed (Herrera et al., 2010). Finally, mathematical programming approaches for optimally placing valves have been investigated in the literature (Pecci et al., 2015). Such approaches can have a strong influence in the design of new DMAs that are both resilient and provide good pressure management. However, water companies are less likely to use such methods to drastically redesign their current DMAs, unless strong operational improvements can be shown. This is because the water companies have been operating their WDNs for long periods of time in their current configurations, and they have built up a comprehensive understanding of leakages across all DMAs. By reorganizing the structure of their DMAs, they lose this knowledge.

3.7 Approaches to Pressure Management

Pressure management at DMA level involves the installation of a PRV at the DMA inlets (Section 3.3.2). Since most DMAs are single-feed (Section 3.10), a single PRV can be installed to reduce pressure downstream within the DMA. The outlet pressure of the PRV must be sufficient to ensure the minimum pressure threshold P_{min} is not violated and guarantee a good level of customer service. A number of commercially available options for implementing and optimising PRV control are available (Technolog, 2015; i2O, 2015*a*; Palmer, 2015). These approaches are most commonly implemented on single-feed DMAs, and this section is dedicated to this type of configuration. Some water companies and researchers are exploring multi-feed pressure management DMA control, which is discussed in Section 4.2.1.

3.7.1 Fixed Outlet Pressure Reducing Valve

A PRV operating with a fixed outlet pressure profile is the simplest form of pressure management available to water companies and is the most commonly used form of control. It is typically implemented hydraulically using a pilot valve on a bypass of the PRV as shown in Figure 3.2, resulting in a highly reliable control solution. The area of the seat (where the inlet pressure is acting) is smaller than the cover chamber area, therefore the PRV will close fully if the

cover chamber is connected only to the inlet pressure via the bypass. Under normal PRV operation (outlet pressure lower than inlet pressure), the bypass carries water from the inlet to the main valve cover chamber and outlet via a pilot valve, therefore venting some of the cover chamber pressure. The PRV outlet pressure set point can be configured by varying the resistance of the pilot valve. Once configured, if outlet pressure drops during operation below the set point, the pilot valve opens further, which vents the valve cover chamber and opens the main valve to increase the outlet pressure back to the set point. If the outlet pressure increases above the set point, the pilot valve closes further, which adds pressure to the cover chamber and closes the main valve, which reduces the outlet pressure back to its set point. Strainers are used in the bypass to stop debris from affecting control, and flow control check valves are used in the bypass to limit the opening/closing speed of the main valve. The opening/closing speed can affect the stability of the valve, and should be set such that the valve is both stable in operation and reacts to network changes efficiently (Prescott and Ulanicki, 2004).

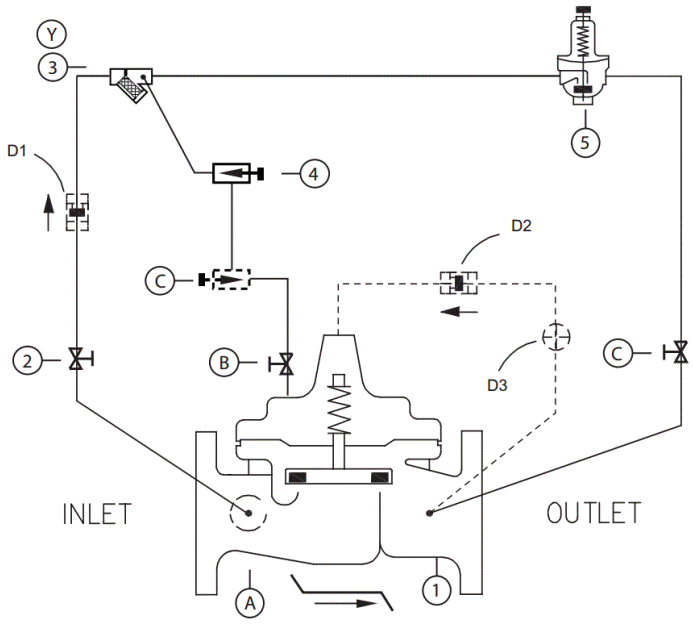


Figure 3.2: The schematic of a pressure reducing valve (Cla-Val, 2015*d*) with components: (1) main valve, (2) isolation valve, (3) strainer, (4) check valve flow control for main valve opening speed, (5) pilot valve, (A) strainer, (B) isolation valve, (C) check valve flow control for main valve closing speed, (Y) strainer and (D) check valve with isolation valves.

The PRV is typically set up to maintain pressure at the CP of the network at or just above P_{min} during peak demand hours. At other times, the pressure at the CP will therefore be higher than P_{min}. The major disadvantage of using constant outlet PRVs is that a fixed outlet pressure profile will not always be optimal for a network. This is most apparent during low demand hours, where

frictional energy losses become small and the pressure in the network becomes high. A fixed outlet PRV can be close to optimal however for DMAs that do not have high frictional head losses (for example, due to newly laid pipes, or a DMA of small size).

3.7.2 Timer Controlled Outlet Pressure

The main disadvantage of using a fixed outlet PRV for pressure management is the excess in pressure it will typically provide, which is most apparent during the night when demand is low. A timer controlled outlet pressure PRV is the simplest approach used to address this disadvantage. By installing a simple time controlled switch that induces a bias pressure in the pilot valve of the PRV, the outlet pressure can be varied with the time of day. This control approach is sometimes called "time modulation" (Awad et al., 2008), and it is considered as an advanced PRV control option (Nicolini and Zovatto, 2009).

There are two potential disadvantages of time modulated PRVs when compared to fixed outlet PRVs. First, the additional components required to bias the pressure in the pilot valve at discrete times adds complexity to what would otherwise be a fixed outlet PRV. As with any system, additional components can impact the reliability of the system. Second, pressure is one measure of the network's resilience to failure (Section 3.5.2). A time modulated PRV follows an open-loop schedule, programmed to keep pressure low. This inherently reduces the resilience of the network to failure. For example, if a failure occurs in the network at night (e.g. a burst, fire flow), it is possible that pressure will become critically low and affect demand. The open-loop control of the PRV will not react to this failure. Nevertheless, the simplicity of this advanced pressure management option and the reductions in leakage it could achieve over a fixed outlet PRV might outweigh its disadvantages, depending on the priorities of the water company.

3.7.3 Flow Modulation

Flow modulation is another advanced PRV control option where the flow is measured locally at the PRV, and its outlet pressure is varied based on a predetermined flow-outlet pressure function. This function is commonly called a "flow modulation curve" (Ulanicki et al., 2008) or "regulation curve" (Nicolini and Zovatto, 2009). It is also sometimes referred to as a lookup table, when discrete points of the function are used. Measuring flow locally at the PRV provides an approximation of the level of demand occurring within the DMA, and therefore the frictional head losses. The flow modulation curve is based on this relationship to vary pressure in the network based on the extent of head loss occurring.

Like time modulation, the change in PRV outlet pressure is achieved by biasing the pilot valve pressure. The biasing pressure can be undertaken electronically (i2O, 2015*a*) or hydraulically (Aquavent, 2015). A hydraulic biasing pressure mechanism uses a pilot tube connected to the outlet of the PRV, which converts the main valve flow to a dynamic pressure (AbdelMeguid et al., 2011).

Flow modulating PRVs can improve network resilience to failure by introducing a form of feedback into the control. As is shown in Chapter 7, if a failure occurs such as a burst or fire flow, the flow modulating PRV detects this increase in demand through the measurement of flow into the DMA, and increases its outlet pressure. The increase in outlet pressure is unlikely to be optimal, this depends on how the flow modulation curve was calculated and the type of failure occurring. However, the increase in outlet pressure will mitigate some of the consequences of failure (as defined by the performance indicators in Section 3.5.2). This is acknowledged in industry, where flow modulation is often used to ensure a sufficient fire flow is available (LaLonde, 2004; Sturm and Thornton, 2005; Lalonde et al., 2008; Kunkel and Sturm, 2011).

The calculation of a flow modulation curve can be undertaken through the engineering judgement of the DMA managers (Sturm and Thornton, 2005). For optimal flow modulation curves, optimisation methods linked with a hydraulic model (Ulanicki et al., 2000) or statistical methods (i2O, 2015*a*) should be used. The flow modulation curve is generally produced with the aim of minimising pressure (or leakage) in the DMA whilst still maintaining a minimum service level.

Optimisation methods that use a hydraulic model for the calculation of optimal open loop control are discussed in Section 6.3. Flow modulation curves can then be fitted to the open loop control schedules (Ulanicki et al., 2000). The calculation of optimal flow modulation curves is undertaken off-line, and the flow modulating PRV is programmed with this function in order to actuate the control. The control is classed as decentralised (Ulanicki et al., 2000), since the flow modulation valve derives its control locally based on the flow. In order for the flow modulation curves to work effectively, the hydraulic model used in the optimisation method needs to be calibrated to a sufficient degree. This is undertaken by monitoring pressure and flow in the network and adjusting model parameters accordingly (Section 5.5). Since the control optimisation is carried out off-line, fluctuations in the stochastic nature of customer demand and uncertainty in the efficiency of valve actuation and model parameters could cause sub-optimal control. In practice, these effects are minimal, as shown in Chapter 7.

Statistical methods are also emerging for the calculation of optimal flow modulation curves (i2O, 2015*a*). Since no hydraulic model is used, a pressure logger

needs to be installed at the critical point of the network. For a single-feed DMA, maintaining pressure at the CP close to P_{min} is equivalent to minimising pressure or leakage in a single-feed DMA, subject to minimum pressure constraints (Section 4.1). By monitoring the PRV outlet pressure and flow, and using pressure data from the CP, a flow modulation curve can be calculated. The pressure data at the CP is transmitted to the PRV periodically. The flow modulating PRV therefore operates predominantly using local information only. To overcome some uncertainty in the stochastic nature of the network, demand influences, such as weekend/week day patterns, are used by the system to better maintain the pressure at the CP close to P_{min}. It is unclear to what extent this improves performance in comparison to a flow modulation curve calculated off-line only. A statistical approach to the calculation flow modulation curves is demonstrated in Figure 3.3, together with a flow modulation curve that demonstrates how the outlet pressure of a flow modulation PRV increases when demand and therefore frictional head losses increase.

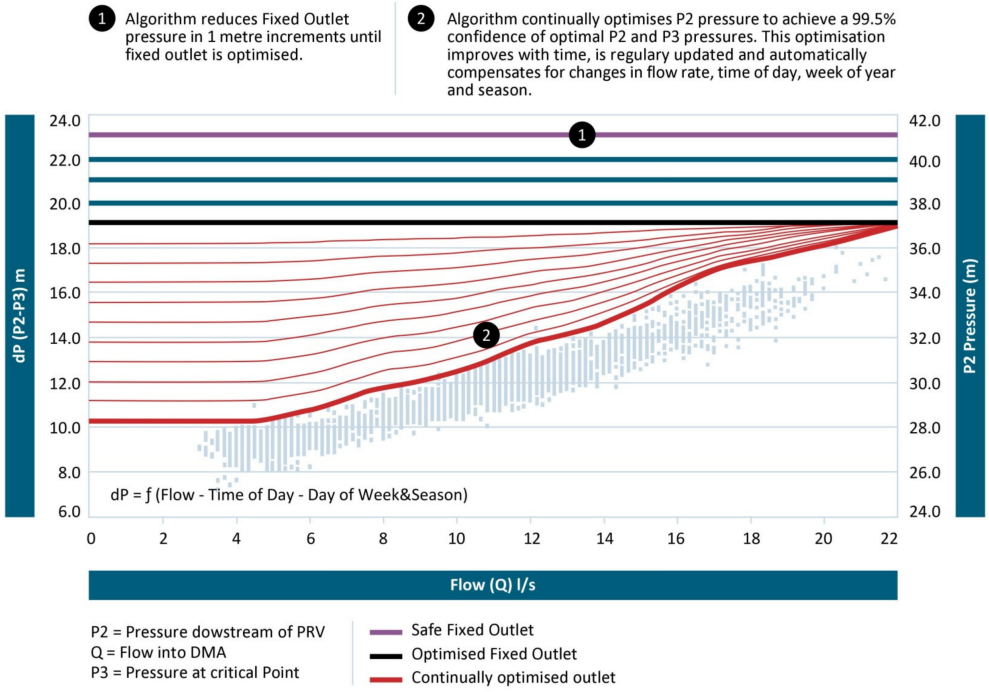


Figure 3.3: An example of a flow modulation curve and a statistical approach for its calculation, where $P2$ is the PRV outlet pressure and $P3$ is the CP pressure

Compared with time modulated PRVs, additional components are required for flow modulation (e.g. a flow meter and system for biasing pressure based on a flow signal). This could reduce the reliability of the PRV control. One mitigation of flow modulation PRV failure is a minor modification to the control curve. In the event that the flow meter fails or the flow signal is lost, the measured flow will typically become zero. To mitigate the consequences of this particular failure, it is good practice to program the look up table with a suitably high pressure at

zero flow.

Flow modulation PRVs are less common than fixed outlet PRVs. However, more interest in this technology is building as water resources becomes more scarce and regulation of leakage becomes more stringent. For example, Matthews (2012) reports that two hundred flow modulating PRVs were recently ordered in one UK water company, which is a substantial investment in advanced pressure management.

3.7.4 Closed loop

Flow modulation is often implemented with the objective of regulating the CP pressure close to P_{min}. Another approach to achieving this is to install a pressure logger at the CP and transmit feedback to the PRV control. This approach therefore eliminates the uncertainty in using hydraulic models, statistics, and demand estimation from flow measurements. The main disadvantages of this approach is the need to install and continuously power telecommunications and a pressure logger at the critical point, and the reduced reliability and cost of continuously transmitting control signals.

3.7.5 Hybrid Methods

Variants of the preceding types of control are also emerging. For example, by measuring pressure at the CP, a pressure-time profile can be produced for the PRV without the need to continuously transmit control adjustments. An alarm can be created at the CP should pressure violate a prescribed threshold, and the PRV control is adapted (for example, by adjusting the control to flow modulation or closed loop).

3.8 Alternatives to the DMA

Farley (2012) has reported on a number of alternative technologies for leak identification and localisation. These are categorized into three main groups: correlating noise loggers, multi-parameter logging, and advanced hydraulic modelling.

Correlative noise loggers are installed in clusters and identify and locate leakage by monitoring noise levels. It was reported that Thames Water reduced their nightline by 22% using this method. Another example of its implementation is in the city of Abu Dhabi, UAE (Farley, 2012). In Dubai however, it is apparent that zoning and pressure management schemes are also desirable (Dubai Electricity & Water Authority, 2015).

Multi-parameter logging involves the installation of loggers capable of measuring flow, pressure and noise simultaneously, at discrete locations. This facilitates the detection of leakage and bursts at low demand hours by analysing the different measurements against reference values. The approach is similar to the deployment of correlative noise loggers, except that more parameters are used to make leakage estimations. Thames Water was again reported as having investigated this technology (Farley, 2012).

Advanced hydraulic models are also being investigated for leakage identification (Farley, 2012), although there are no reports on real case studies that have been successful on a large scale. A summary of simulation based methods for leakage detection is provided by Puust et al. (2010).

Whilst alternative methods exist for leak localization, none are available that can replace the performance or cost effectiveness of the DMA. This is either due to high costs involved with some of the technology, such as noise correlators that can be impractical for extensive deployments (Farley, 2012), or the inadequate performance of other approaches such as those based on transient analysis (Puust et al., 2010). The DMA also facilitates valve control for pressure management (Section 3.3.2), whereas other approaches do not. This will invariably lead to higher leakage rates and a higher burst frequency.

3.9 Global Trends in DMA Installation

Farley (2012) states that he was involved in the design of what were probably the first two DMAs to be installed worldwide, in 1982 in the UK. Since then, the UK has rapidly extended their use of DMAs such that they are now ubiquitous. Japan has also made leakage management a priority since the 1980s, and DMAs are extensively used. Networks in Japan are also designed to take into account factors such as elevation (Lambert, 2001). Australia also take a proactive approach to leakage management (Sturm and Thornton, 2005). The rest of the world has been slower to adopt leakage management practices, although this mentality is changing due to rising populations, infrastructure decay, and a decline in water resources (Section 1.1).

In Europe, it is reported that most countries are starting to implement DMAs (European Commission, 2015). This is likely to be related to new recommendations given by the EU for water to be managed more efficiently (European Union, 2015). Advanced pressure management and DMAs are also being installed in Cyprus (Charalambous and Isaia, 2013).

In the USA there are approximately 52,000 water companies (US Environmental Protection Agency, 2007), some providing solely for very small rural communities, and others providing for entire cities. Most water companies in the USA

take a reactive approach to leakage management i.e. leaks are fixed when they are visible on the surface (Kunkel and Sturm, 2011). This is likely to be attributed to three factors:

1. First, the regulators of US water companies do not generally encourage or enforce the reduction of leakage, although this is starting to change (Sturm and Thornton, 2005). Without regulation, and with an abundant amount of water at their disposal, the most cost efficient option for water companies would be to take a reactive, not proactive, approach to leakage management.

2. As a result of the regulations placed on fire flow requirements, the mains sizes in the USA are much larger than those found in the UK, which were designed only to meet customer demand. The disadvantage of large diameter mains is that low flow velocities occur in the pipes, which makes flow metering more difficult. The selection and position of flow meters is therefore more critical in the USA than in the UK (Morrison et al., 2007). The DMA size therefore needs to be large enough to acquire high minimum night flows (Sturm and Thornton, 2005). It is also likely that DMAs in the USA will be cascading due to the highly looped street layout. All of these factors make DMA implementation more difficult, as highlighted in Section 3.6.

3. The leakage in the USA, as a percentage of total input, actually appears to be one of the lowest in the world. In (Farley and Trow, 2003), real losses are quoted as being approximately 6% of the total system input in California. In comparison, England and Wales (where proactive leakage management has been undertaken for decades) have real losses of approximately 25% of system input. This will partly be down to both the condition of infrastructure and pressure in the network. However, as discussed in Section 3.5.1, reporting the real losses as a percentage of total input is not an effective approach to understanding the extent of leakage on a network. Consumption in the USA is very high, partly due to the high network pressure available for fire flow. As a result, the leakage appears to be low, and this could influence the adoption of pressure and leakage management in the USA.

Some water companies in North America are starting to introduce proactive leakage management schemes. In 2005, the only two water companies in North America to practice proactive leakage detection were Halifax Regional Water Commission (Canada) and the Pennsylvania American Water Company Wilkes-Barre/Scranton (Sturm and Thornton, 2005). A number of other American utilities were also testing leakage management approaches including areas of Birmingham, AL; Dallas, TX; Placerville, CA; and Seattle, WA (Sturm and Thornton, 2005). In 2011, it was reported that a DMA set up in Philadelphia

(Pennsylvania) was one of the first to be set up in USA (Kunkel and Sturm, 2011). With some parts of American experiencing a severe drought (Howitt et al., 2014), which has been linked to global warming (Swain et al., 2014), the interest in proactive pressure and leakage management is increasing. One example is in California, where IBM (2015) are working with a water utility to optimise PRV control for a network serving 600,000 people.

In South Africa, a number of very successful pressure managed DMA schemes exist (McKenzie and Wegelin, 2010). The City of Cape town was the first city in South Africa to introduce a large scale pressure management scheme in 2001 (Meyer et al., 2009). The pressure management scheme was a success, and extended to other areas including Guguletho, Atlantis, Mfuleni, Delft, Mitchells Plain, Belhar, Langa and Eersterivier. It was reported that approximately $8 million per year was saved as result of reduced leakage (Meyer et al., 2009). (Seago et al., 2007) report that the Infrastructure Leakage Index (Section 3.3.1) for 30 water companies in South Africa is only marginally above the world average.

3.10 Case Study: Analysis of Large Scale Networks

One key objective of this chapter is to estimate the current status and operation of DMAs in comparison to design guidelines (Section 3.6). A case study of a real, operational network in the UK is used to undertake this analysis. The case study is shown in Figure 3.4a and its DMA boundaries in Figure 3.4b. Three aspects of DMA status are investigated:

- An estimation of the percentage of single feed DMAs in existence, which are generally recommended in design guidelines as low cost, simple and high accuracy solutions for the design of DMAs.
- The pressure differential across permanently closed boundary valves. If pressure is substantially higher on one side than the other, the boundary valve is not at a hydraulic balance point, because opening the valve would result in a substantial amount of flow occurring. If the pressure differential is minimal, this implies that the boundary valve is at a hydraulic balance point. A high pressure differential across a permanently closed boundary valve indicates that improvements to pressure management can be made.
- The diameter of the closed boundary valves. To reduce water residence time, mainly smaller diameter mains should contain a closed boundary valve (Sturm and Thornton, 2005). Larger diameter mains are also valuable for their high capacity, and used to sustain fire flow (Sturm and Thornton, 2005).

The case study network, summarised in Table 2, consists of 245 DMAs and approximately 3,148km of pipeline in a partly urban, partly rural environment. The network operator reports that of the 245 DMAs, 60% are single feed and not cascading (no outlet). The remaining 40% of DMAs make up cascading DMAs and multi-feed DMAs. An investigation by Herrera et al. (2015) using graph theoretic measures on the same case study found that the total number of single-feed DMAs was also 60%.

To estimate pressure differential across all the valves in the case study network, a hydraulic analysis of the network is undertaken using Infoworks WS 11.0, which is used by the water company that operates the network. The hydraulic model contains the current configuration of the network, including the pumping schedules, pump curves, closed boundary valves, and PRV control. The distribution of pressure differential across all closed boundary valves is shown in Figure 3.4c. Whilst the majority of closed boundary valves have a low pressure differential (i.e. they are placed at hydraulic points, which is considered best practice in DMA design), there is still a substantial number of closed boundary valves (46%) that have a higher pressure differential, some of which are over $40mH_2O$ (including, for example, the experimental programme network as outlined in Chapter 5). A high pressure differential at closed boundary valves indicates that frictional energy losses and pressure management in the network is suboptimal.

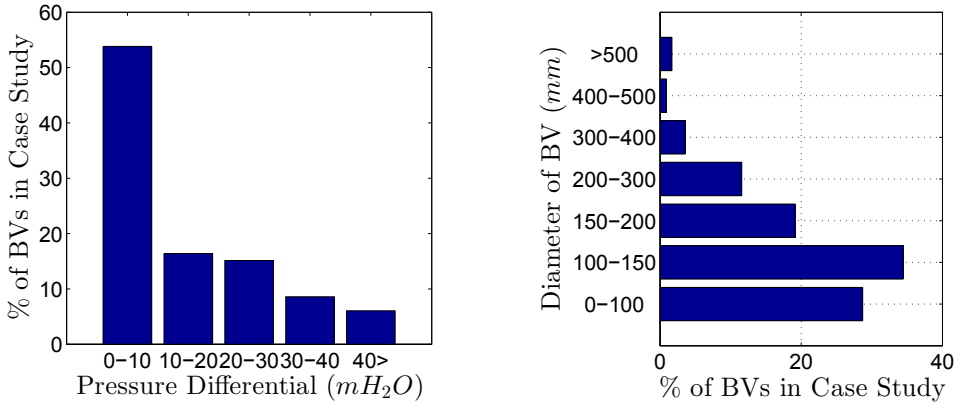
The range of diameters of the closed boundary valves is shown in Figure 3.4d. Although mainly smaller diameter valves are closed at the DMA boundary (29% less than 100mm and 34% between 100-150mm), there are a substantial number of boundary valves above 150mm (37%) that are closed. It is quite common for the size of the inlet main to a DMA to be around 150 - 200mm, therefore there are a number of high capacity routes that are unavailable during failure due to the closed boundary valves.

Table 2: Network information for the case study used to analysis the current state and operation of DMA

Length of Mains	3,148km
Number of nodes	106,116
Number of links	111,093
Number of reservoirs	28
Number of pumps	102
Number of DMAs	245



(a) Case study network (b) DMA boundaries



(c) Pressure differential at closed boundary valves (d) Diameter of the closed boundary valves

Figure 3.4: (a) A real, operational water distribution network consisting of approximately 3,148km of pipeline, (b) the DMA boundaries (red lines), (c) a breakdown of pressure differential at closed boundary valves, and (d) a breakdown of diameter at closed boundary valves

3.11 Conclusion

The DMA has many advantages:

- It is a cost effective solution that facilitates accurate, nightly estimations of leakage levels and its spatially variability at DMA level, used to both identify new bursts and plan pipe replacement/repair.
- DMAs facilitate the simplistic implementation of pressure management by forming discrete zones. PRVs can be installed at the DMA inlets to reduce background leakage and future burst frequencies.
- Logistically, DMAs allow repair work and new technology to be installed without the need to model or investigate the effects of the work on hydraulically connected neighbouring DMAs, which leads to man-hour savings.
- Contaminations can be contained more efficiently and undesirable mixing of water sources is avoided.

Alternative approaches to leakage management, such as noise correlators, are not cost efficient options nor do they facilitate pressure management, contamination containment and logistical improvements in the operation of the network. These advantages are the reasons that water companies around the world are adopting the DMA in order to better manage their water resources, which are diminishing due to increased population sizes and global warming.

However, countries that adopt the DMA will eventually experience its disadvantages that the UK and Japan now face. Large failures in the network can cause thousands of customers to lose their supply to water, consequences which are exacerbated by permanently closed valves. In the UK, poor customer service can result in penalties up to 1% of the water company's revenue: a substantial amount that can inhibit future investment. In addition, there will come a point when water companies are aiming to reduce their AZP to the extent that every meter in pressure head counts. Consequently, the use of larger pressure managed zones, where frictional head losses are smaller, will aid in achieving more efficient pressure management. At the same time however, water companies that are strongly targeting leakage through ALC are aiming to reduce the size of their DMAs. A dynamic DMA topology facilitates all of these objectives.

The disadvantages of operating a dynamic DMA topology include a more complicated control approach (investigated in Chapter 4), a higher cost of installation and maintenance for the dynamic boundary valves and contamination that could spread further than it would in a closed topology DMA network. In regards to water contamination, this disadvantage has to be balanced with the advantages that a dynamic DMA brings in terms of improved pressure management, reduced leakage, and better resilience to failure. The additional cost of

the dynamic boundary valves also needs to be considered in this analysis. This is dependent on the priorities of the water company.

The water companies and their regulators often use performance indicators to compare the performance of different networks and network configurations. This allows that water company to understand how well they are operating their networks, and adopt other approaches if they show improvement in the performance indicators. In terms of network operation, the performance indicators are strongly based on the pressure and leakage of a network, and how well the water company maintains the customers' supply of water. Both of these performance indicators coincide with the benefits of a dynamic topology. In this thesis, performance indicators for average zone pressure, leakage, pressure variability, reserve capacity of the network, and the extent that customer demand is affected during failure, are used to benchmark a dynamic topology with other established and emerging pressure management options. Out of the approaches available in pressure management, the use of fixed outlet PRVs is the most common form of pressure management, and the use of flow modulating PRVs, where pressure is controlled based on the head losses in the network, is an emerging form of advanced pressure management. These two approaches to pressure management are used to benchmark a dynamic topology in the experimental investigation carried out in Chapter 7.

The case study network analysed in this chapter has highlighted that 60% of its 245 DMAs are single-feed. As recommended in DMA design guidelines, single feed DMAs are more cost efficient and provide more accurate leakage estimations. The analysis has also highlighted that the DMAs can have a considerably high pressure differential at the closed boundary valves (46% of all closed boundary valves). This indicates that the closed boundary valves are not at the hydraulic balance points of the network, and that the pressure management of the DMAs is suboptimal. Whilst automated DMA design approaches promote the placement of closed boundary valves at hydraulic balance points, the water companies are unlikely to change their DMA structure because they will lose many years of knowledge on asset condition and leakage statistics. Due to the ever increasing expansion of networks, housing developments, changes in demand, and changes in operation, it is not possible to maintaine closed boundary valves at hydraulic balance points. The use of dynamic boundary valves could be beneficial in this respect. Finally, the analysis on the case study indicated that the boundary valves are often closed on large diameter mains (37% of all closed boundary valves), which are high capacity backup supply routes during failure. With all these considerations in mind, the design and installation of a dynamic topology is carried out on a real, operational network that is a subset of the case study network analysed in this chapter. This experimental programme is outlined in Chapter 5.

4 Control of Multi-feed Pressure Managed Zones

4.1 Introduction

The optimal valve control of a water distribution network with multiple control points and inlets would be achieved with the following:

- Ubiquitous sensor placement in order to accurately estimate the state of the network;
- Real-time communication between a central controller and all sensors and actuation points (i.e. centralised control);
- A sufficiently fast and reliable global optimisation solver for updating valve control settings based on the current state estimation for the entire network.

At any point in time, the network state can be estimated and optimal control for all valves can be calculated, transmitted, and actuated. This sequence can be repeated at all points in time to optimally control the network.

In reality, optimal control is difficult to achieve for a number of reasons. First, sensors are expensive and installation is restricted to the availability of access points (hydrants, chambers, etc.), and so they can only be sparsely placed. It is therefore only possible to estimate the state of the network based on limited data. Second, power and cost constraints make real-time sensor communication generally unviable for most networks. Finally, due to the non-convex nature of WDN optimisation problems (Chapter 6), efficiently and reliably finding the global optimum is a challenging problem, although a local optimum is often sufficient.

The optimal control of a PRV at the inlet of a single-feed DMA does not face many of the above challenges in optimal control. Consider the optimal control problem of minimising pressure for a single-feed DMA, subject to minimum pressure constraints. Then, at any point in time, there is only one setting for the PRV that supplies high enough pressure in the DMA to satisfy these constraints and minimise the objective function. It can be concluded that pressure at the critical point of the DMA will be equal to the minimum allowable pressure. Therefore, if the critical point is static (does not change location diurnally under normal network conditions), optimal PRV control can be achieved by using just one sensor placed at the critical point transmitting data to the PRV. This approach also circumvents the need for an optimisation solver. Near-optimal control that does not use regular data transmission from the CP can also be implemented. This is achieved by monitoring the flow locally at the PRV, which is an indication of energy losses in the DMA and therefore pressure at the critical point. The PRV

outlet pressure is then varied using the flow measurement and a pressure-flow relationship for optimal network pressure (i.e. flow modulation, as discussed in Section 3.7.3). A network that consists of many single-feed DMAs can all therefore be controlled independently and optimally with many decentralised PRV controllers.

The operation of water distribution networks with dynamic topology involves the pressure management of large, multi-feed, interacting DMAs, therefore it is more difficult to introduce the simplifications and assumptions used to optimally control single-feed DMAs. This is predominantly because the consequences of control undertaken in a DMA are no longer isolated, since other DMAs are also connected. For example, measuring flow locally at the PRV to estimate energy losses in the DMA no longer necessarily indicates the level of demand in the DMA, since there are other inlets to the same DMA. In addition, optimal pressure management is more challenging to calculate because there are multiple PRVs and consequently multiple combinations of valve settings that all give satisfactory performances. An optimisation solver for multi-feed optimal control is therefore generally required.

This chapter addresses the following objectives in order to understand the challenges of optimal control in multi-feed pressure managed DMAs and make reasonable assumptions and simplifications in order to undertake control:

- Review case studies where multi-feed, pressure managed DMAs have been undertaken and explore the challenges experienced in these case studies (Section 4.2);
- Review potential control approaches for networks with dynamic topology (Section 4.3);
- Explore unstable modes of valve operation and demonstrate the "valve interaction phenomenon" with hydraulic data from the experimental programme (Section 4.4).

The final part of the chapter proposes a novel control methodology, termed "Time Varying Flow Modulation", for the optimal pressure management of WDNs with dynamic topology (Section 4.5). This control methodology is used in the experimental programme network to actuate near optimal control.

4.2 Review of Multi-feed Pressure Managed DMA Practices

4.2.1 Multiple Flow Modulating PRVs

One approach to achieve optimal control in multi-feed networks is the operation of multiple flow modulating PRVs. The successful implementation of this

approach is dependent on two factors: The existence of flow modulation curves and the proximity of flow modulating PRVs in the network.

As with flow modulation in single-feed DMAs (Section 3.7.3), if the optimal outlet pressure of each PRV in a multi-inlet network can be correlated with the flow through each PRV for an extended period of time (at least 24 hours to capture the full diurnal behaviour of the network), then control curves exist and can be fitted for each PRV (flow modulation). In the literature, it is noted that the flow modulation curves do not always exist in multi-feed networks. Ulanicka et al. (2001) report on one example. In the simulated case study, Ulanicka et al. (2001) use an optimisation method to minimise the cost of water supplied (i.e. reduce leakage) for a multi-feed network for two PRVs. When weighting the cost of water at both sources equally, Ulanicka et al. (2001) found that no flow modulation curves exist. Ulanicka et al. (2001) proposed weighting the cost of water through one of the PRVs to overcome this problem. After rerunning the optimisation method, flow modulation curves could then be calculated, and the PRV with the smaller cost of water became the dominant feed into the network. Since the problem formulation had been weighted, flow modulation curves can be produced but at the expense of the objective function. A similar control approach is used in a number of experimental case studies (Section 4.2.2).

The use of multiple flow modulating PRVs in close proximity and supplying the same DMA can result in PRV interaction (Ulanicki et al., 2000). This is due to an increase in flow output from one PRV causing a reduction in flow at the other PRV, eventually shutting it down (Yates et al., 2014). This type of behaviour is shown in Section 4.4.2 using hydraulic data from the experimental programme. One solution, as proposed by (Ulanicki et al., 2000) and implemented in an experimental case study by Yates et al. (2014), is to transmit flow data between all network inlets. It is then possible to accurately establish the total demand in the network, which facilitates the flow modulating PRVs to both supply the zone. It is however difficult to establish in which situations valve interaction could occur in order to install this type of communications. Furthermore, the need to continuously send flow data across the WDN reduces the reliability of this control system and therefore valve stability is not guaranteed at all times.

4.2.2 Combining Flow Modulating and Fixed Outlet PRVs

A simple and common approach to pressure managing a multi-feed DMA in practice is the use of a single flow modulating PRV with additional fixed outlet PRVs (Sturm and Thornton, 2005; Lalonde et al., 2008; Kunkel and Sturm, 2011). The flow modulating PRV is often referred to as the “master” or “primary” control valve, since it monitors and reacts to demand changes in the DMA. It is also the feed that is used to monitor the minimum night flow. The supporting fixed

outlet PRVs are often referred to as "slave" or "backup" control valves, and support the master control valve by opening when pressure in the district become too low, for example, during peak demand times or fire flow situations. This approach simplifies the control problem and would result in suboptimal pressure management, as discussed in Section 4.2.1.

Sturm and Thornton (2005) report on a single feed DMA with two PRVs installed in parallel at the inlet, one primary and one backup. The backup PRV in (Sturm and Thornton, 2005) has a set point outlet pressure lower than the set point of the primary PRV. Since the PRVs are installed in parallel, both PRVs have the same inlet and outlet pressure pressure. Therefore, the primary PRV will maintain the outlet pressure at its set point. The backup PRV will remain closed in an attempt to reach its set point. Only in situations where the flow through the primary PRV is too high for it to maintain its set point (i.e. its outlet pressure drops such that the primary PRV becomes fully open), will the secondary valve then open, because the outlet pressure is now lower than its set point. Section 3.7.1 and Figure 3.2 describes in more detail the control process of a fixed outlet PRV. The master/slave valve setup was tested by Sturm and Thornton (2005) by opening fire hydrants in the network, and with some tweaking of the valve opening/closing response to avoid "valve swing", a stable operation was achieved.

Lalonde et al. (2008); Kunkel and Sturm (2011) also report on the implementation of a pressure management scheme with one master PRV operating with flow modulation and slave PRVs used in the same manner as Sturm and Thornton (2005), i.e. to open at peak demand times and fire flow situations. The slave valves were located at different sides of the DMA to the master PRV. Check valves can also be used to achieve this type of control at backup inlets, although the check valve will not regulate pressure when operational, whereas a backup PRV will maintain its set point (Sturm and Thornton, 2005).

4.2.3 Model Predictive Control

Model predictive control (MPC) for WDN control is a centralised form of control (Ulanicki et al., 2000) and involves the periodic finite-time optimisation of the future state of the WDN model and the calculation and implementation of optimal valve settings based on this future horizon. The future state of the WDN is often estimated using a demand forecaster (Ulanicki et al., 2000; Skworcow et al., 2010). Since the optimisation is carried out periodically, frequent transmission of hydraulic data (for forecasting) and control settings (for actuating the optimal control over the future horizon) is necessary, which makes this approach less accessible for water utilities. A time-horizon that is too long could result in suboptimal control occurring, particularly if a failure occurs before the next control update.

Ulanicki et al. (2000) investigated MPC for PRV control that minimises the cost of water input (including leakage). The MPC approaches used a commercial optimisation solver, a skeletonised network model (to improve computational efficiency) and a demand forecaster. A one hour horizon was used. Skworcow et al. (2010) investigated MPC for combined pump scheduling and valve control. The objective function was the minimisation of costs associated with pumping and leakage. A one hour horizon was again used. This MPC approach was tested using real data from a SCADA system, however the calculated optimal control was not actuated in the network due to limitations in remote-control infrastructure.

4.3 Control Options for WDNs with Dynamic Topology

4.3.1 Model Predictive Control

Model predictive control (MPC) is one control option for WDNs with dynamic topology. A framework for its implementation (Figure 4.1) was proposed by Wright et al. (2014*a*), which incorporated the following features:

- Continuous high-resolution pressure data used to identify steady, pseudo-steady and unsteady-state hydraulic conditions which can either lead to suboptimal control or could result from the control actuation. Optimal valve control is facilitated by the existence of steady and pseudo-steady hydraulic conditions;
- Fail-safe control settings that are established for each network controller, and are defined as a network configuration previously used by the water company that has been proven to be robust and safe. This may not include open DMA boundaries, but is dependent on the type of failure that occurred. For example, sectorisation would be an appropriate mitigation action in response to a water quality incident, whereas open pressure zones might be a more suitable response to a hydraulic failure resulting in low pressure. Detected hydraulic instabilities are analysed to identify the source;
- Retrospective snippets of high-resolution time-synchronised data are retrieved upon request to facilitate a root-cause analysis and the prompt diagnosis of valves operation and control instabilities (Hoskins and Stoianov, 2014);
- Incident optimisation initiated by the detection of network failures and deviations from expected hydraulic conditions.

Due to limitations in the frequency at which valve settings can be remotely updated (which is constrained by the power generation of the micro-turbine),

the implementation of MPC is not explored further in this thesis. MPC is however one of the most appealing options for network control due to its ability to actuate optimal control without the constraints of valve interaction or the existence of optimal flow modulation curves.

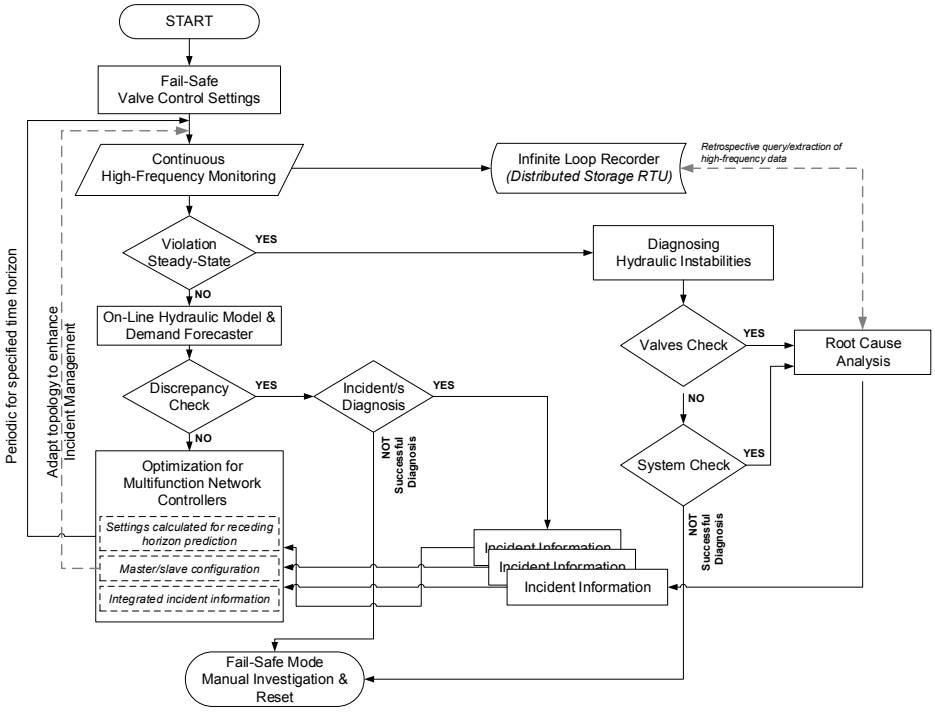


Figure 4.1: Using the multifunction network controllers in a model predictive control framework (Wright et al., 2014*a*)

4.3.2 Decentralised Control

Since it is not possible to implement a centralised form of control with the technology used in this thesis, a decentralised form of valve control is sought.

The use of flow modulation curves at all control valves in the network could, in theory, be implemented for optimal control. This approach has two major disadvantages however:

- Flow modulation curves might not exist for all control valves in the network (Ulanicka et al., 2001);
- Flow modulating PRVs in close proximity to each other are likely to interact (Ulanicki et al., 2000).

Since the PRVs at DMA inlets and dynamic boundary valves are generally in close proximity to each other, the chances of valve interaction are high, therefore this control option is not explored further in this thesis. Instead, a master/slave valve arrangement is investigated, where the master control valves use flow modulation (as undertaken in other investigations outlined in Section 4.2.2), and the

slave control valves follow an open-loop control profile. Unlike the case studies in Section 4.2.2 however, the slave valves do not close when a flow reversal occurs. Bidirectional flow and control is facilitated using the pilot control bypass system (Section 1.2 and Section 5.4.1).

The most efficient type of open-loop control at slave valves requires investigation. Out of the options available, the slave control valves could:

- Follow a flow schedule, i.e. a flow control valve;
- Follow an outlet pressure schedule (either fixed or variable over time), i.e. pressure control valve;
- Follow a stem position profile, i.e. position control valve.

By using flow control at dynamic boundary valves, the total net flow into the DMA will generally be known at all times. Consequently, the flow modulating PRV (master valve) will be able to follow its control curve efficiently. This is possible because the locally measured flow at the master valve, minus any flows at dynamic boundary valves (which are known a priori), must be the demand change within the DMA. This network configuration is shown in Figure 4.2, where the master control valve detects a change in flow that deviates from its current measure q_m. The change in flow reading must be the change in demand in the DMA (Δd) since all other inlets have a fixed flow, therefore the master PRV varies its outlet pressure accordingly.

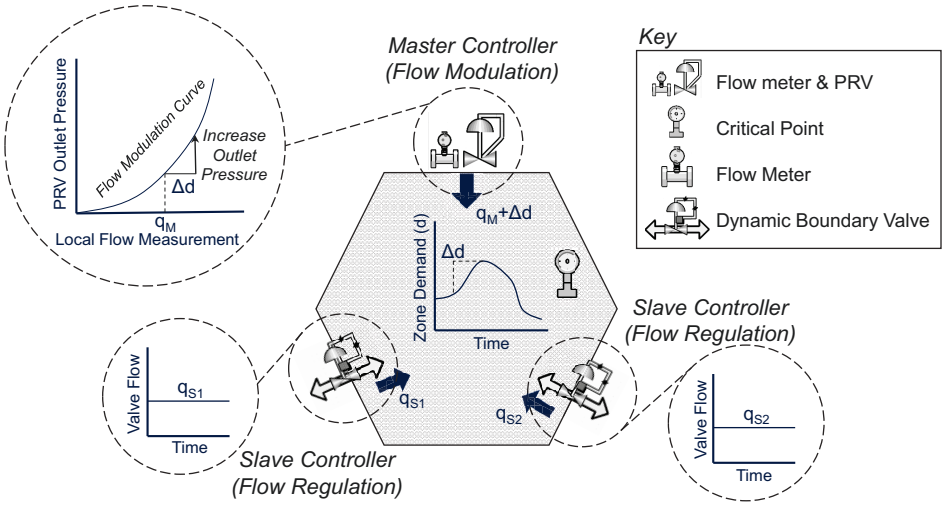


Figure 4.2: Master/Slave arrangement with Flow Modulating PRVs and FCVs

The main disadvantage of using flow control at dynamic boundary valves is its control in failure conditions. Since the flow is predefined, this might restrict the performance of the network to react to a failure. In addition, it might not always be possible for the flow control valve to maintain its flow set point, which would result in suboptimal control of the flow modulating (master) PRV. For

these reason, this control approach is not explored further in this thesis.

The use of either pressure control or position control at the dynamic boundary valves would result in a variable flow occurring through the DMA boundary. Consequently, suboptimal control at the flow modulating (master) PRV could occur. In Section 6.5.2, optimal open-loop control was calculated for the experimental programme network, where the objective function was the minimisation of AZP. The optimal open-loop valve settings and simulation results showed that:

- The upstream and downstream pressure at the dynamic boundary valves was quite consistent between the hours 06:00 - 00:00. Therefore the flow through the dynamic boundary valves (whether they control pressure or stem position), will also be consistent.
- The dynamic boundary valves close partially at night (00:00 - 06:00).

It was decided that a position control schedule would be most appropriate for implementing these optimal open-loop settings at the dynamic boundary valves for the following reasons:

- In order to monitor the minimum night flow, the dynamic boundary valves must shut down. Since the optimal open-loop valve settings indicated that the dynamic boundary valves should shut down at night to minimise AZP (regardless of minimum night flow monitoring), a position control schedule would facilitate this operation in a simple way.
- In failure situations where pressure becomes critically low on one side of a dynamic boundary valve fixed at a certain % opening, the high pressure differential will force more flow though to the critical pressure area and help restore its pressure, therefore minimising the disruption to customers and mitigating the consequences of failure. The is true regardless of which side of the dynamic boundary valve a failure occurs. Any other form of control at the dynamic boundary valve would require a more complicated approach to detect and react to this type of failure.
- It is useful when first implementing a dynamic DMA topology to only pass a small amount of flow through to a neighbouring DMA, whilst still maintaining improved network resilience as described above. Only passing a small amount of flow between DMAs minimises flow reversals in the network initially, which can be useful for minimising the risk of discolouration for the customer. The regular occurrence of flow reversals does not present this risk since the network becomes well conditioned to the flow reversals. The use of position control at dynamic boundary valves facilitates a small amount of water to be passed between DMAs. The use of flow control valves would also facilitate this. However, it would be more complicated to guarantee a certain flow range using pressure control valves.

The operation of dynamic boundary valves with a position schedule is shown in Figure 4.3. This control option is investigated both in simulation (Section 6.5.3) and experimentally on a real, operational network (Chapter 7). Flow data from the experimental programme, where a dynamic boundary valve follows a position control schedule, shows that the flow is quite consistent between DMAs (Figure 4.4). Consequently, the flow modulating (master) PRVs can efficiently follow their control curves.

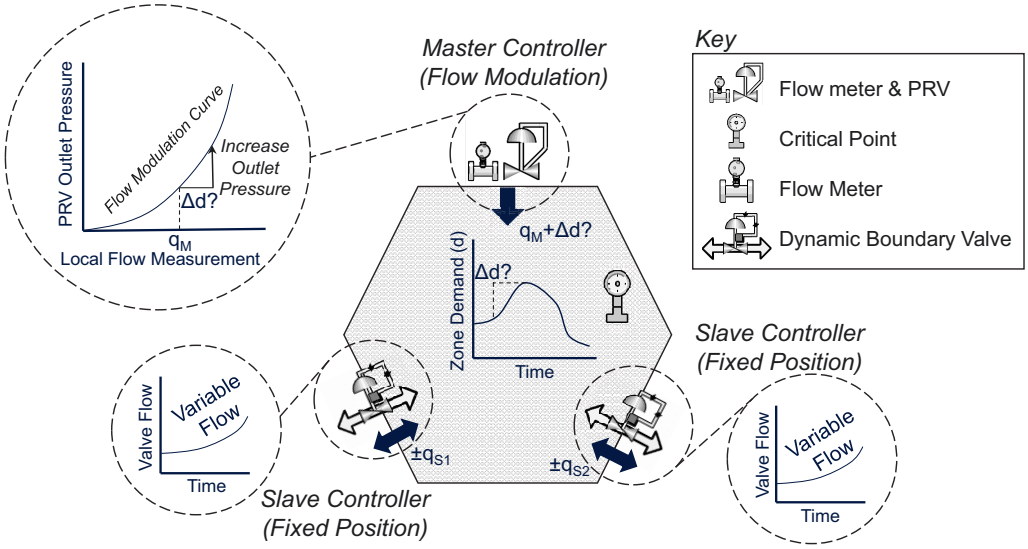


Figure 4.3: Master/Slave arrangement with flow modulating PRVs and fixed position valves

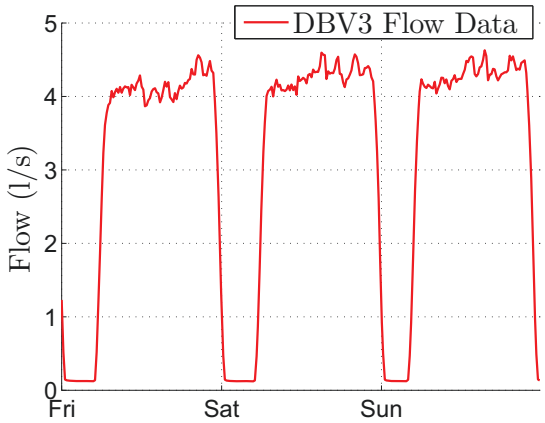


Figure 4.4: Data showing a consistent flow of approximately 4l/s through the dynamic boundary valve in the experimental programme when operating as a slave controller with fixed stem position (40%), attributed to the fact that pressure variability is low in the network

4.4 Undesirable Valve Behaviour

Two forms of undesirable valve behaviour related to multi-feed control are described in this subsection. The first is when a valve becomes dynamic (not steady-state) in its operation, potentially causing pressure transients to propagate through the network. Multi-feed networks can be susceptible to this (Prescott and Ulanicki, 2004). The second form is when flow modulating PRVs supply the same area, and one valve forces the other to close by increasing its flow output.

4.4.1 Valve Oscillations

A control valve can become dynamic in operation in both single-feed and multi-feed DMAs. In both single-feed and multi-feed DMAs, unsteady behaviour can be caused by (Hoskins and Stoianov, 2014):

- Pressure transients caused by large industrial users or pumping. For example, Figure 4.5 shows a pressure data at 128samples/s that demonstrates a PRV in a single-feed DMA becoming unstable due to a pressure transient (Hoskins and Stoianov, 2014).
- Incorrect set up or installation of the PRV (i.e. the valve's needle valve is configured such that the valve reacts too fast to hydraulic changes, the valve is incorrectly sized, etc.)

It has also been reported that multi-feed valve control is more prone to dynamic valve behaviour as a result of multiple valves controlling the same DMA (Prescott and Ulanicki, 2004). In this study, a simple looped network with two fixed outlet PRVs at either end of the network was simulated using a transient model. The same network with just a single PRV feeding the network was also investigated. The investigation involved changing demand in the network (0.1l/s per node for approx. 25 nodes) and observing how the PRV(s) react for different levels of PRV opening speed. In both scenarios oscillations of the PRV(s) outlet pressure occurred. In the single-feed case, oscillations were $\approx 1mH_2O$, and in mulit-feed case $\approx 1.5mH_2O$. The oscillations also took longer to diminish in the multi-feed case.

Valve oscillations were also analysed by Ulanicki and Skworcow (2014), where the high rate of change of outlet pressure with respect to a change in valve opening %, particularly when the valve was nearly closed, was identified as the cause. With more control valves in operation for a dynamic DMA topology configuration, low flows (valve opening %) and possibly oscillations could be more common, which motivates the need to accurately model and optimise the valve control in order to avoid such situations.

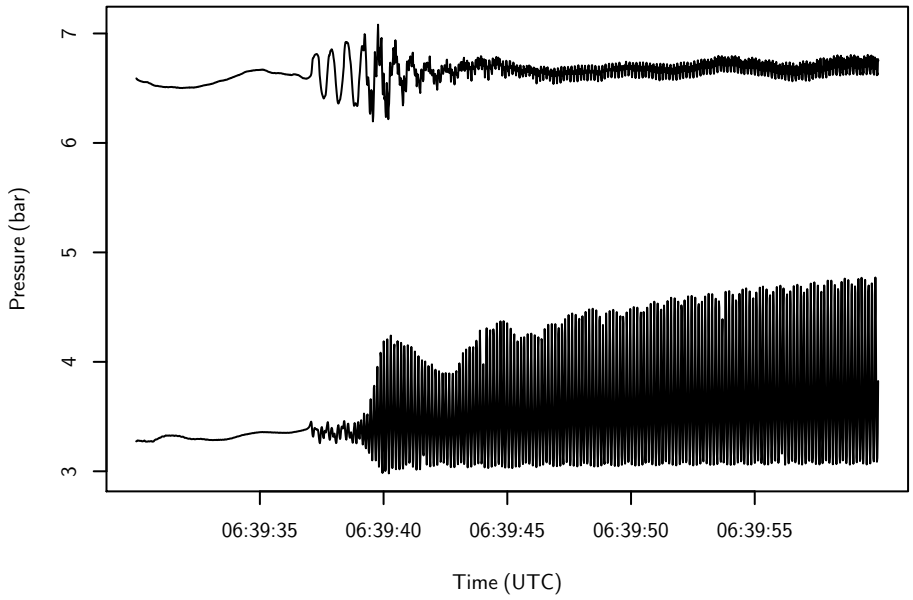
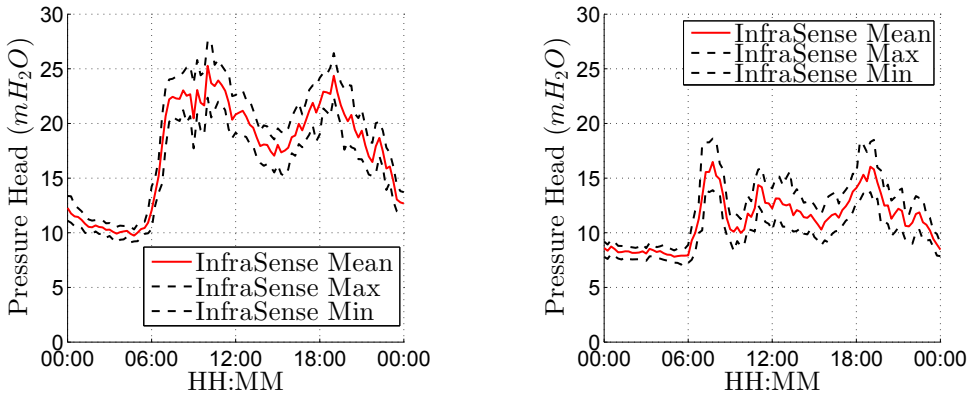


Figure 4.5: PRV dynamic behaviour in a single-inlet DMA caused by a pressure transient (Hoskins and Stoianov, 2014)

The steady state control of networks with dynamic topology is a key objective in this thesis. Without steady state hydraulic conditions, it is not possible calculate or actuate steady state optimal control. Transient conditions also have damaging affects on the network such as pipe fatigue and discolouration (Hoskins and Stoianov, 2014). For this reason, sensors monitoring pressure at 128 Samples/s are deployed in the experimental investigation carried out in this thesis in order to guarantee a stable control at valves. Figure 4.6 demonstrates PRV control for the experimental investigation carried out in Chapter 7. The pressure data, plotted at 15 minutes, has maximum and minimum bounds that represent 128 samples/s. In both cases, the bounds on outlet pressure are approximately $2.5mH_2O$ above and below the mean outlet pressure. A stable operation for both a single and multi-feed network is therefore achieved.



(a) Single-Feed

(b) Multi-Feed

Figure 4.6: Pressure monitoring at 128 samples/s at a PRV for (a) a single-inlet network and (b) multi-inlet network

4.4.2 Interaction of Flow Modulating PRVs

The use of multiple flow modulating PRVs in close proximity and supplying the same DMA can result in PRVs competing. This behaviour is due to an increase in flow output from one PRV causing a reduction in flow at the other PRV, eventually shutting it down. This type of behaviour was captured with hydraulic data in the experimental programme (Section 5).

The interaction of flow modulating PRVs is shown in Figure 4.7. The network at the time was operating with flow modulating curves determined in an adhoc way at PRV 1 and PRV 2. Figure 4.7 shows that some days (Sunday, evening Monday, Tuesday, Thursday), PRV 1 would be the dominant supply for the network, whereas other days (Monday morning and afternoon, Wednesday), PRV 1 would be the dominant supply.

Unpredictable control such as the valve interaction demonstrated in Figure 4.7 should be avoided. When the PRV control was updated with optimal flow modulation curves produced in Chapter 6, this behaviour was no longer observed. There is still great uncertainty however in determining the occurrence of valve interaction.

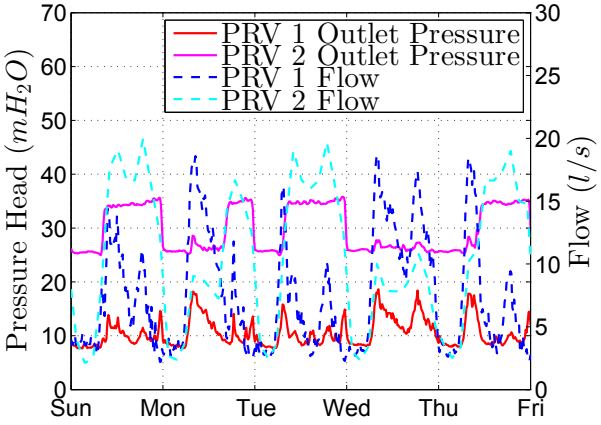
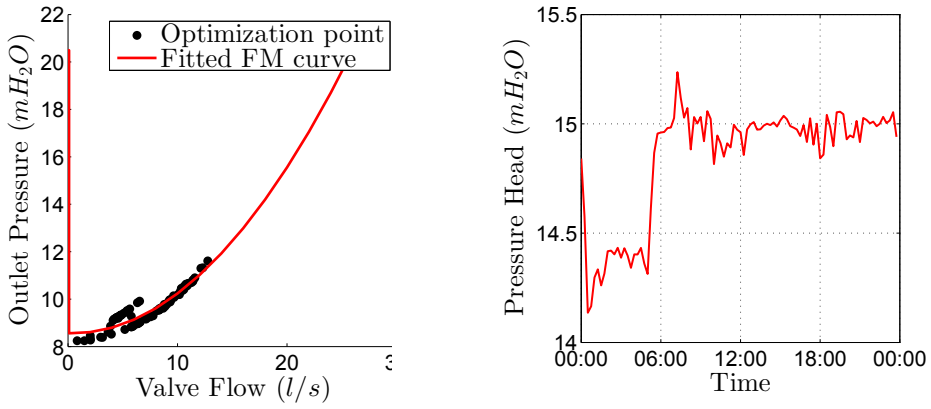


Figure 4.7: (a) Data (outlet pressure and flow) for PRV 1 and PRV 2, showing that PRV 2 is dominant on Sun, Tue and Thur, and PRV 1 is dominant on Wed and parts of Tue.

4.5 Time Varying Flow Modulation Control

In this section, a new control methodology is proposed for water distribution networks with dynamic topology. It was determined in Section 4.2.1 that flow modulation curves can only be produced if the flow and optimal outlet pressure of a PRV for an extended period of time is correlative. For the network in the experimental programme, it is possible to fit flow modulation curves to optimal points calculated (see Chapter 6). This is also demonstrated in Figure 4.8, where optimal PRV settings were calculated that minimise AZP over a 24 hour period. The dynamic boundary valves open to a stem position of 80% during the day, and are closed at night between 02:00-05:00.



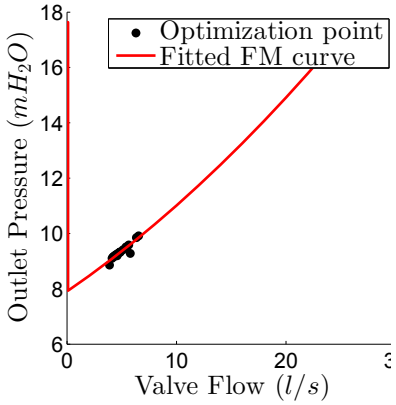
(a) Single flow modulation curve

(b) CP 1 Pressure

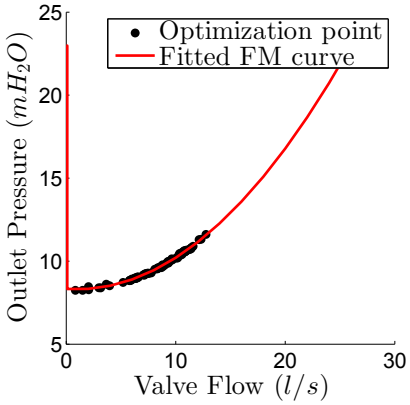
Figure 4.8: (a) Fitting a single flow modulation curve to optimal open loop settings at PRV 1 and (b) pressure at the CP when using just a single flow modulation curve for PRV 1 whilst operating a dynamic topology that opens to 80% in the day and closes at night

The flow modulation curve in Figure 4.8a is not a perfect fit for the optimal control points (defines as the series of optimal PRV outlet pressures and corresponding PRV flows in an extended period simulation). The result of this is seen at the critical point, where pressure at night has dropped below $P_{min}(= 15mH_2O)$ by approximately $0.6 - 0.8mH_2O$. It is therefore proposed that two flow modulation curves are fitted to the optimisation points in Figure 4.8a. The first flow modulation curve is used when the topology is closed at night. The second flow modulation curve is used during the day, when the dynamic boundary valves open up. Therefore, the flow modulation curves changes based on the dynamic topology of the network.

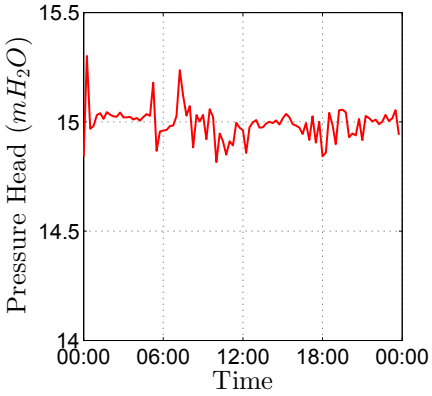
The results of implementing different flow modulation curves at different times, depending on the topology of the DMAs, is demonstrated in Figure 4.9. Instead of the single (sub-optimal) flow modulation curve being fitted to optimal open-loop control settings in Figure 4.8a, two flow modulation curves have been fitted, which results in an optimal actuation of the valve settings. The first flow modulation curve is shown in Figure 4.9a and is used at night (02:00-05:00) whilst the dynamic boundary valves are closed. Outside of these hours, when the dynamic boundary valves are open, the flow modulation curve in Figure 4.9b is used. As shown in Figure 4.9c, the pressure at the CP is now fluctuates closer to the minimum allowable pressure P_{min}. A constant pressure at the CP equal to P_{min} is not achieved however. This is due to the use of a position control valve at the dynamic DMA boundary, which leads to some variation in flow between DMAs (as discussed in Section 4.3.2) and minor variations between the flow modulation curve and optimisation points in Figure 4.9 ($\approx 0.1mH_2O$).



(a) Nighttime flow modulation curve



(b) Daytime flow modulation curve



(c) CP 1 Pressure

Figure 4.9: In order to obtain a better fit of flow modulation curve, it is proposed that a (a) Nighttime flow modulation curve is used for when the DMA topology is closed, (b) a daytime flow modulation curve is used for when the DMA topology is open, and (c) pressure at the CP 1 which is more stable at its minimum allowable pressure

4.6 Conclusion

Achieving optimal control in water distribution networks is a challenging problem because sensor placement is sparse and remote communications are generally limited to periodic transmission due to power constraints. These challenges will persist until sensor placement and continuous communication become more financially viable.

For single-feed DMAs, many of these challenges are avoided because the hydraulics of the network are less complicated. By maintaining pressure at the critical point of the network close to a minimum allowable pressure P_{min}, it is possible to minimise pressure or leakage throughout the DMA in an optimal way using a single PRV at the DMA inlet. Optimal control can be achieved by installing a pressure sensor at the CP which transmits data to the PRV, or near-optimal control can be achieved by calculating a flow modulation curve. The flow modulation curve facilitates a PRV to alter its outlet pressure based on a locally measured flow, which is an indication of customer demand in the DMA and therefore frictional head losses occurring in the network. Therefore it is possible to maintain pressure at the CP close to P_{min} without continuously monitoring or transmitting pressure data at the CP. For a single-feed DMA, the flow modulation curves can be calculated using a calibrated hydraulic model and optimisation method, or statistically using pressure data from the CP.

For multi-feed networks, it is difficult to introduce the same simplifications used to achieve optimal control in single-feed DMAs because:

- There is no guarantee that flow modulation curves exist for multiple PRVs controlling one DMA. There could be many combinations of valve control that all give satisfactory performance.
- Measuring flow at a PRV no longer guarantees that a change in flow is a change in customer demand in the DMA.
- Multiple flow modulating PRVs in close proximity can interact with each other, causing unpredictable behaviour in the network, as demonstrated in Section 4.4.2.

Using statistics to understand the hydraulics of a multi-feed network is a complicated task with no clear solution. A hydraulic model and optimisation method is therefore generally necessary to achieve optimal control in a multi-feed network.

Due to limitations in valve communication, a centralised control method is not viable in this thesis. In order to actuate near optimal control in a network with dynamic topology, a decentralised approach is explored. A novel control approach for a network with dynamic topology, termed "time varying flow modulation", is proposed. The flow modulation curves used at PRVs change based

on the time of day and whether the dynamic DMAs are hydraulically connected or not. The use of position control valves at the dynamic DMA boundary facilitates:

- A resilient network because position control facilitates bidirectional flow in the direction of pressure criticality. If pressure is low on one side of the dynamic boundary (due to high demand, bursts, fire flow, etc.), the change in pressure differential at the position control valve will help sustain pressure in this area.
- A consistent flow through the DMA boundary in times of normal operation. This facilitates the flow modulating PRVs to efficiently follow their flow modulation curves, whereas a variable flow can cause flow modulation PRVs to shut down unexpectedly.

The principles in multi-feed network control established in this chapter are used to set up an experimental programme on a real, operational network, outlined in Chapter 5, and inform the control optimisation carried out in Chapter 6.

5 Experimental Programme

5.1 Introduction

In order to investigate the benefits and challenges of operating a dynamic topology and validate analytical work, an experimental programme is set up on a real, operational water distribution network in the UK. This unique facility combines the installation of the technology briefly outlined in Section 1.2 within an operational WDN and facilitates the implementation and investigation of pioneering developments in DMA and WDN management. At present, this WDN is operating with a dynamic topology.

The experimental programme, termed "Field Lab", has two aims relevant to this thesis:

1. Develop, assess and demonstrate a novel concept of dynamically reconfigurable DMAs for improving the redundancy and resilience to failure of water distribution networks:
    - Dynamically, remotely and safely adjust the topological connectivity of DMAs;
    - Enable faster response to mitigate the consequences of mechanical and hydraulic failures and minimise the number of affected customers (e.g. the new Ofwat regulations for the maximum period of unplanned interruptions of supply);
    - Facilitate the improved pressure management of WDNs by automatically aggregating DMAs;
    - Facilitate leakage monitoring using the minimum night flow by automatically segregating DMAs;
    - Support the implementation of smaller or larger sized DMAs for improved leak detection, while resolving associated problems with redundancy in supply, resilience and water quality;
    - Assess the impact/constraints of the proposed scheme;
2. Test novel tools for modelling, optimisation and control that support the implementation of dynamically reconfigurable DMAs:
    - A novel approach of integrating PRV control within null space algorithms and used to improve the computational performance of control optimisation algorithms (described in Sections 2.7 and Section 6.4.1)
    - A novel control strategy (time varying flow modulation) for implementing optimal control more efficiently in a network with dynamic

topology (described in Section 4.5)

- A novel optimisation algorithm based on SCP that calculates optimal control efficiently (by using the null space algorithm) and with reliable convergence, even for large, complex networks (described in Chapter 6).

This chapter describes the set-up and installation of the field lab. It is based on two internal reports between Imperial College London, Bristol Water plc, and Cla-Val Ltd.

5.2 Network Description and Motivation

The network that was identified as a suitable location to set up the proposed experimental programme consists of two neighbouring DMAs that are hydraulically separated by three permanently closed boundary valves (V1, V2 and V3) as shown in Figure 5.1. The DMAs each have a single inlet and supply a total of approximately 8,000 properties. The inlets are connected to a telemetry system that acquires flow and pressure data at 15 minute intervals. A number of non-continuous flow meters are also located throughout the field lab network. The area has a large variation in elevation ($\approx 80m$, Figure 5.19) and the critical point is marked in Figure 5.1. Before the installation of the dynamic boundary, a pressure management scheme was being investigated for these DMAs by the water company to address the following problems:

- Significant diurnal variability in pressure (average zone night pressure (AZNP) is approximately $75mH_2O$);
- Low pressure during peak demand hours (with pressures dropping to $10mH_2O-15mH_2O$ in some areas, see Figure 5.2);
- Customer complaints due to the low pressure and pressure variability in the area;
- A high number of critical customers including two hospitals and an area consisting of large commercial users being fed from a single-feed, single point of failure inlet;
- High pressure differential at the closed boundary valves ($\approx 50mH_2O$ at V3 and $\approx 10mH_2O$ at V1).

A hydraulic simulation prepared by the water company showing the low pressure during peak hours is shown in Figure 5.2 which confirms the customer complaints. The network suffers from high frictional head loss in cast iron mains and a 10" - 7" cross section as shown in Figure 5.2. A number of pressure management options were considered and investigated in order to address these

challenges.

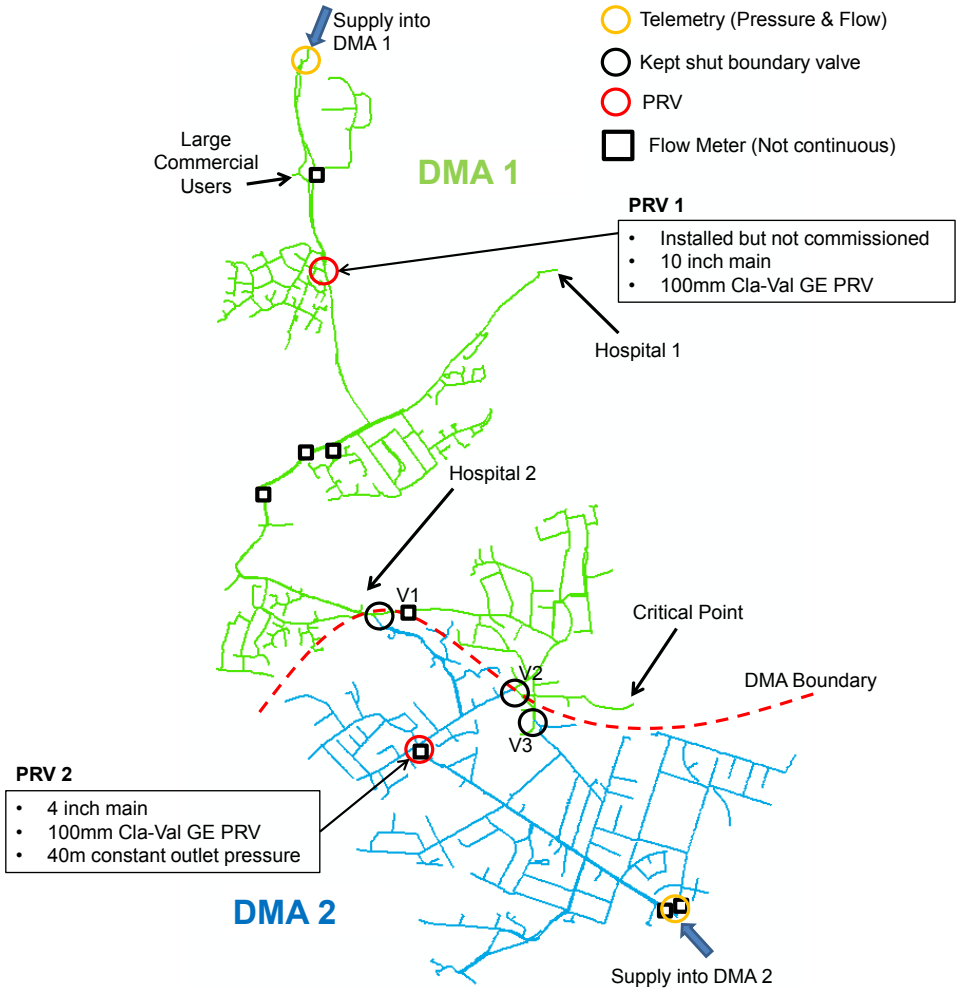


Figure 5.1: Network configuration of the experimental programme before installation of the dynamic boundary and associated technologies

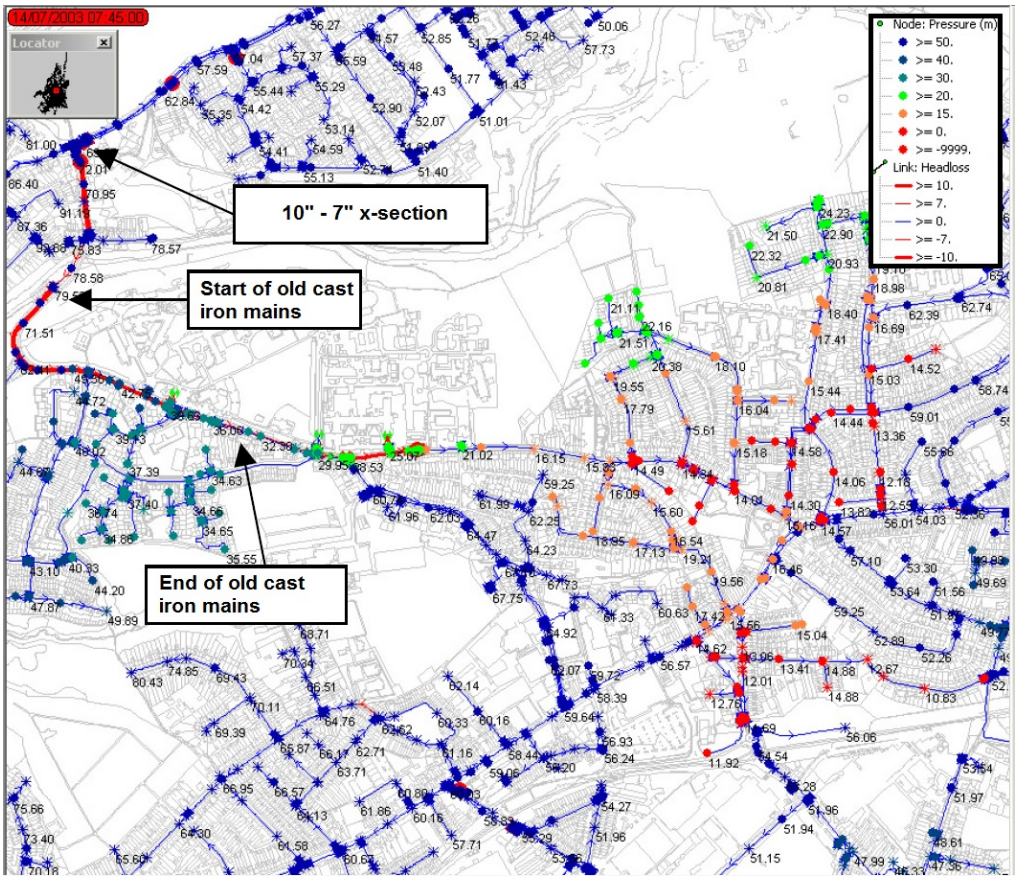


Figure 5.2: Simulation of the field lab network by the water company using Infoworks WS, prior to the installation of the dynamic boundary, that confirms low pressure complaints from customers. Low pressure is experienced in the network due to high frictional head losses in cast iron mains

5.3 Design

5.3.1 Initial Model Calibration

In order to investigate design options for the experimental programme and their viability and performance, a hydraulic model must be calibrated. Calibration involves varying model parameters in order to sufficiently minimise discrepancies between the modelled variables and corresponding measurements. Due to limitations in time at the beginning of the project (when the design options were considered), a manual calibration approach was adopted for the initial model calibration, and there was not time to investigate all model discrepancies. A more thorough calibration process was undertaken at a later date prior to calculating optimal control in the experimental programme, and is discussed in Section 5.5.

Hydraulic data (pressure and flow data) was collected in December 2011 and March 2012 to calibrate the hydraulic model used by the water company. The calibration results are shown in Figure 5.3. The model fits acquired data to within $1mH_2O$ pressure head in most areas, however there were irregularities

with a difference in the pressure head of $\approx 2mH_2O - 6mH_2O$. These irregularities were later investigated, where isolation valves that should have been fully open were found closed or partially closed.

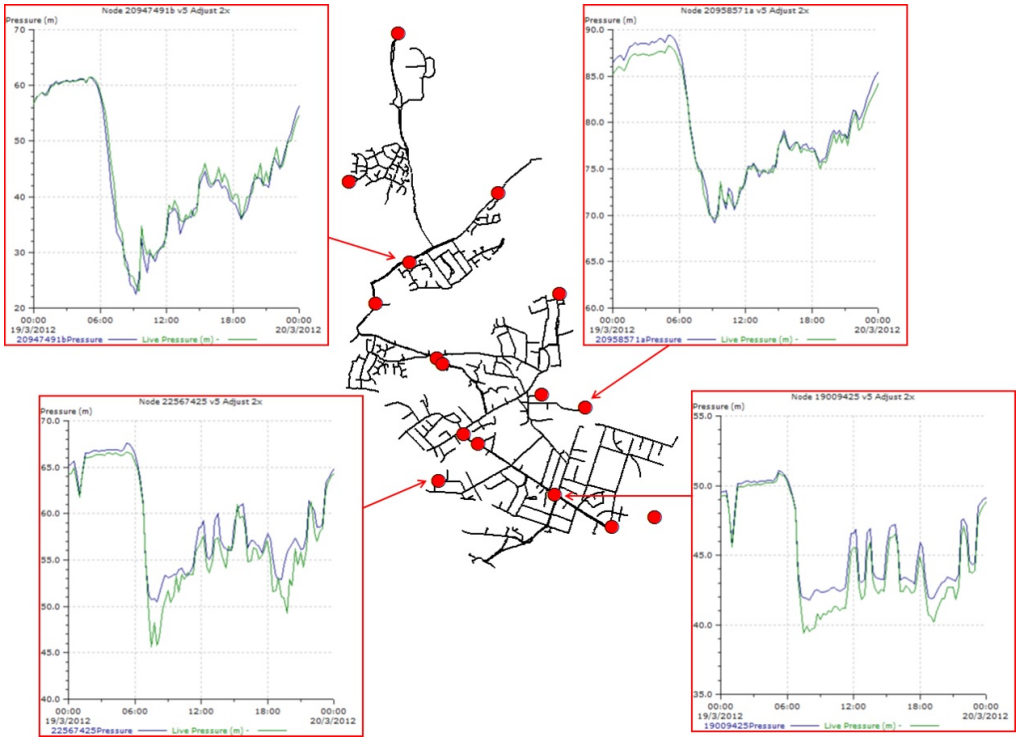


Figure 5.3: Initial calibration of the hydraulic model for investigating the design options of the field lab site (red dots: locations where hydraulic data was acquired)

5.3.2 Candidate Options

The options investigated for the pressure management of the network are outlined below. All options, except the first, included the reinforcement of the 10" - 7" cross section shown in Figure 5.2 with 180mm polyethylene. It was advised that PRV 2 should maintain a constant outlet pressure of $40mH_2O$ for all design options, due to a high rise building being located just downstream of this location and uncertainty in their pressure requirements. This constraint was later lowered to $25mH_2O$. For the options that include a dynamic boundary valve, its control schedule is fully open 05:30-00:00 and closed otherwise.

- Option 1: DMA rezone: A rezone of a district area from DMA 2 to DMA 1 was proposed, as shown in Figure 5.5. Resilience to Hospital 2 is increased because a supply is available via both DMA 1 and DMA 2. The DMA topology is fixed and closed.
- Option 2: Fixed, closed DMA topology and PRV 1 operating with time modulation (Figure 5.7). The original DMA boundary is maintained.

- Option 3: A dynamic boundary valve installed at position V1 only and PRV 1 operating with time modulation (Figure 5.8). The original DMA boundary is maintained.
- Option 4: A dynamic boundary valve installed at position V3 only and PRV 1 operating with time modulation (Figure 5.9). The original DMA boundary is maintained.
- Option 5: Two dynamic boundary valves installed at positions V1 and V3 and PRV 1 operating with a fixed outlet pressure profile (Figure 5.10). The original DMA boundary is maintained.

None of the design options included the installation of a dynamic boundary valve at position V2 (Figure 5.1). According to the pipe diameter distribution of the experimental programme network (Figure 5.4), V2 is positioned on a larger diameter main than V1 or V3. As discussed in Chapter 3, larger diameter mains should not contain a closed boundary valve in order to reduce residence time of the water and provide a high capacity route for water during failure. Therefore V2 would have been an ideal choice for a dynamic boundary valve. Unfortunately, after investigating further, V2 is located on a heavy traffic road that had also just had its entire road surface rehabilitated. The installation of a chamber containing the dynamic boundary valve and equipment was not appropriate, and V2 was dismissed as a potential option for installing a dynamic boundary valve.

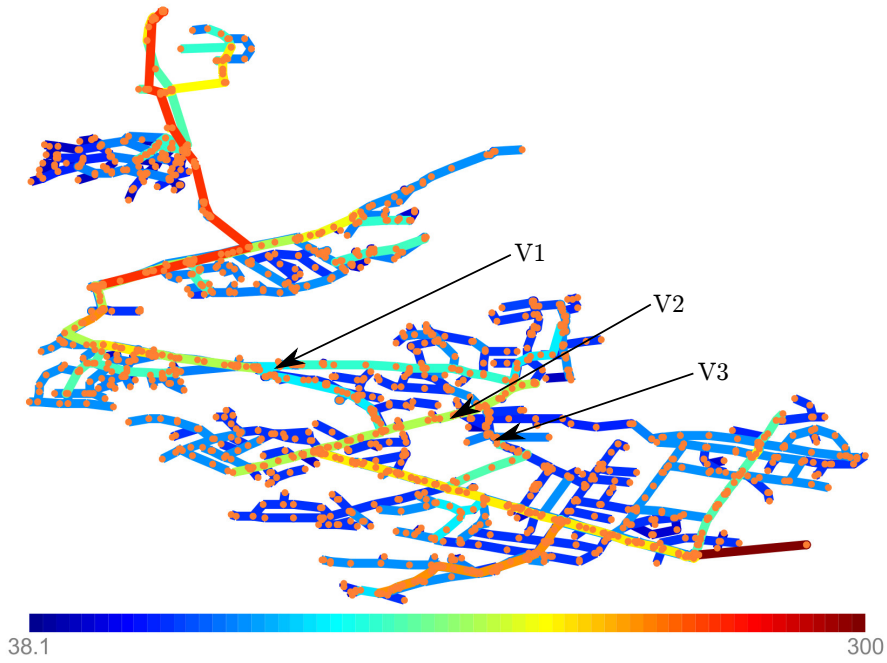


Figure 5.4: The distribution of pipe diameter across the experimental programme network. Larger pipes provide larger capacity for flow.

A number of other pressure management options were also investigated by the water company, and are detailed in a separate report. The conclusion of this report is that a dynamic topology provided the lowest AZP as well as greater security of supply to the hospitals. This thesis only outlines the most promising design options.

5.3.2.1 Option 1: DMA rezone

The DMA rezone is shown in Figure 5.5. Resilience to Hospital 2 is increased because a supply is available via both DMA 1 and DMA 2. The DMA topology is fixed and closed.

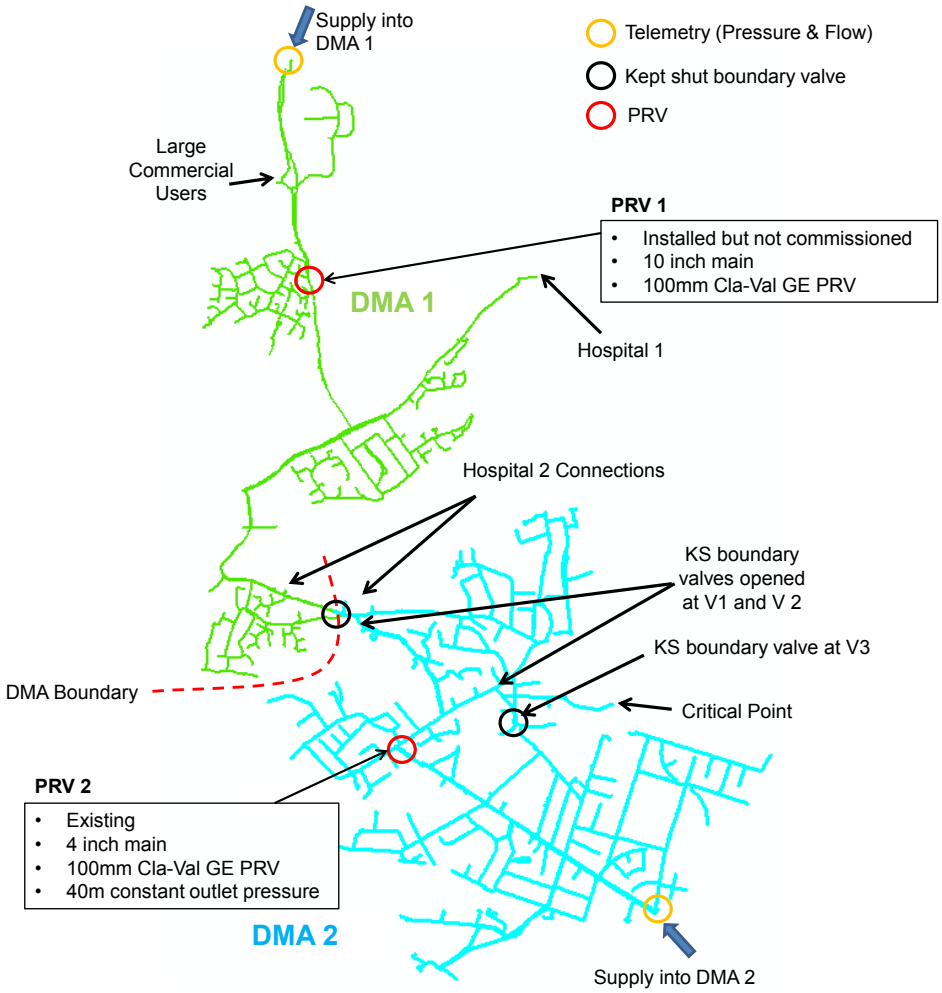


Figure 5.5: Option 1: DMA rezone + 2 PRVs

The model calibration (Section 5.3.1) resulted in friction factors increasing substantially to account for the 19th century mains in this area. As a result, the model suggested that Option 1 would result in low pressures at peak time as shown in Figure 5.6, even with PRV 2 fully open. Furthermore, the model suggests that even with the PRV 1 nearly fully closed, pressure is still moderately high at the boundary of DMA 1 (around $30mH_2O$). For these reasons, Option

1 was dismissed.

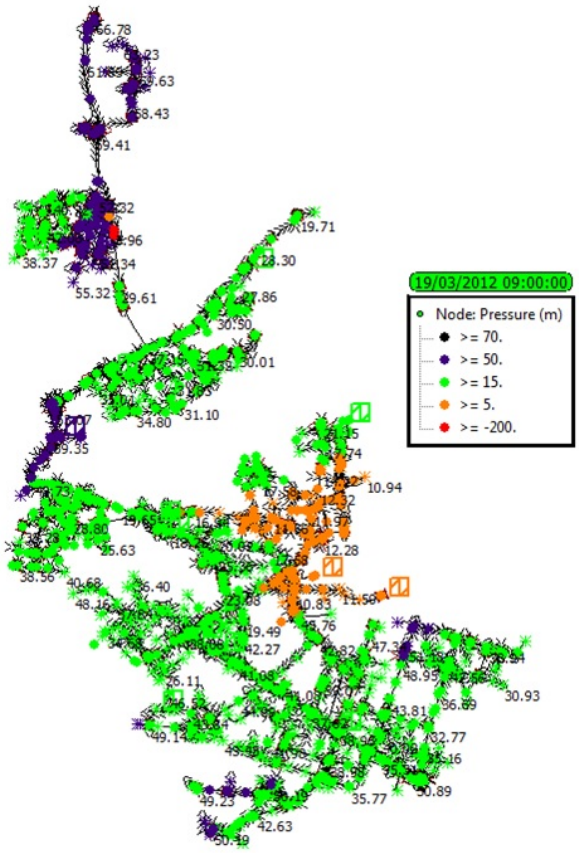


Figure 5.6: Low pressure simulated when rezoning the DMAs in the design process for Option 1

5.3.2.2 Option 2: Fixed, closed DMA topology

This option keeps the original DMA boundary, in a closed, static configuration. A time varying outlet is introduced at PRV 1 with a three step profile. Alternatively, flow modulation could be used. This option is shown in Figure 5.7 along with the three-step profile necessary to keep pressures at the critical point above $15mH_2O$. At peak times (7:00 - 12:00), the PRV outlet at Stoke Lane needs to be moderately high ($40mH_2O$) due to the long route to the critical point with high head losses due to 19th century mains.

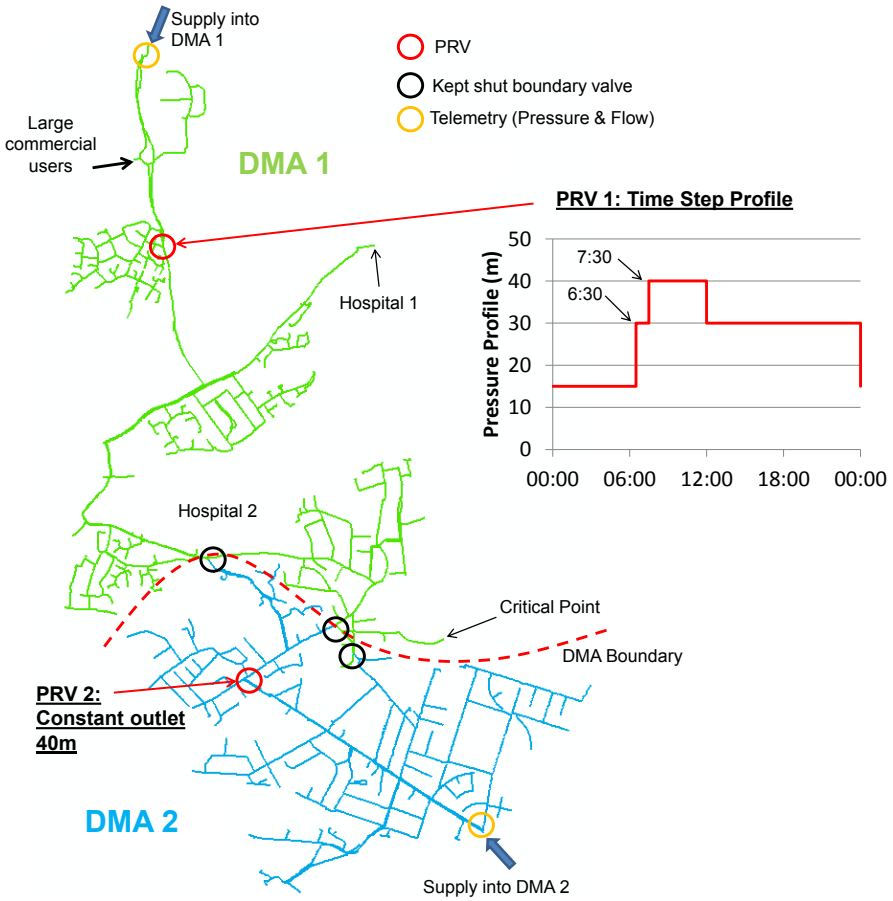


Figure 5.7: Option 2: Original DMA topology (closed) + Constant Outlet PRV + Time Varying Outlet PRV

5.3.2.3 Option 3: A dynamic boundary valve installed at position V1 only

A dynamic boundary valve is installed at position V1 only, as shown in Figure 5.8. The original DMA boundary is maintained. There is still a long supply route from the inlet to DMA 1 to the critical point, therefore a time step profile is still necessary at PRV 1 to maintain pressure at the critical point above $15mH_2O$. Due to the hydraulic connection at location V1, the profile is $5mH_2O$ lower than Option 2. The hydraulic connection between DMA 1 and 2 at the location V1 also provides extra security to Hospital 2.

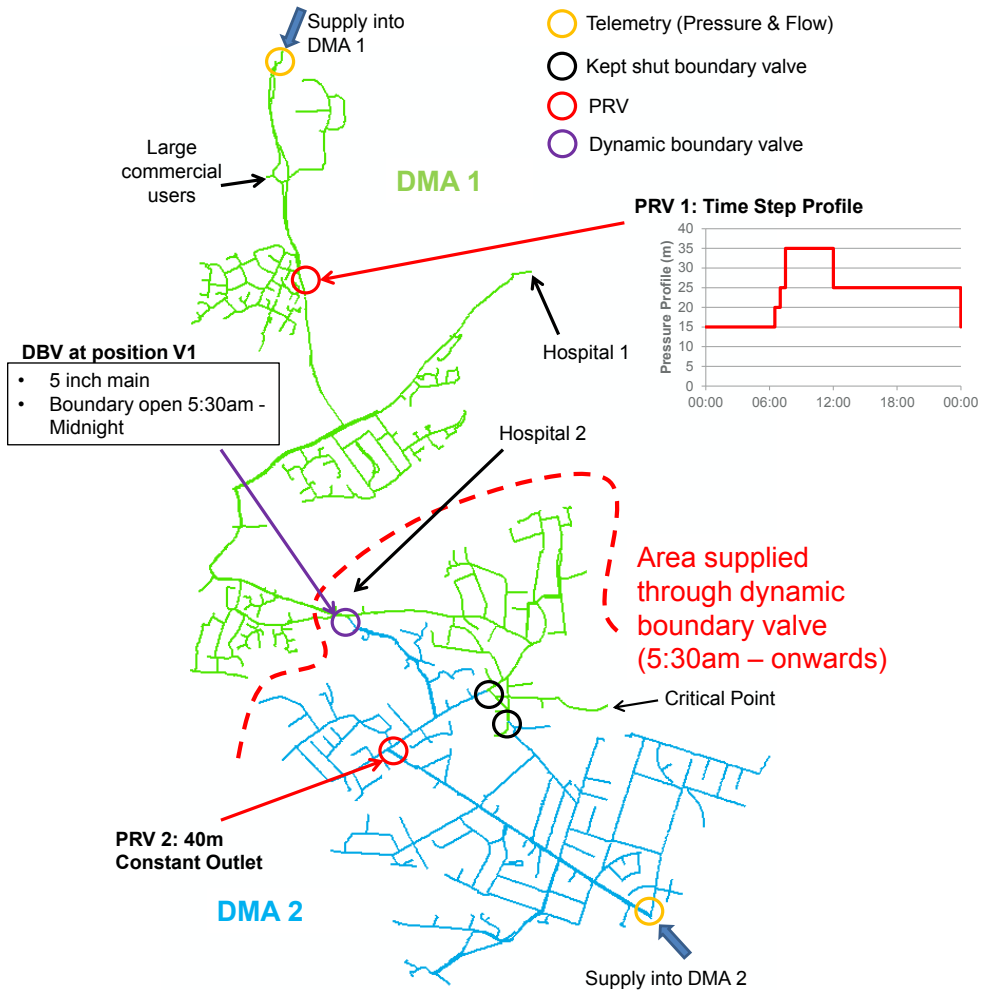


Figure 5.8: Option 3: Dynamic boundary valve at location V1, PRV 1 following a time varying outlet profile, and PRV 2 fixed outlet pressure

5.3.2.4 Option 4: A dynamic boundary valve installed at position V3 only

A dynamic boundary valve is installed at position V3 only, as shown in Figure 5.9. The original DMA boundary is maintained. The connection between DMA 1 and DMA 2 is close to the critical point of DMA 1, therefore the outlet pressure of PRV 1 can be $10mH_2O$ lower than Option 3 at peak demand hours.

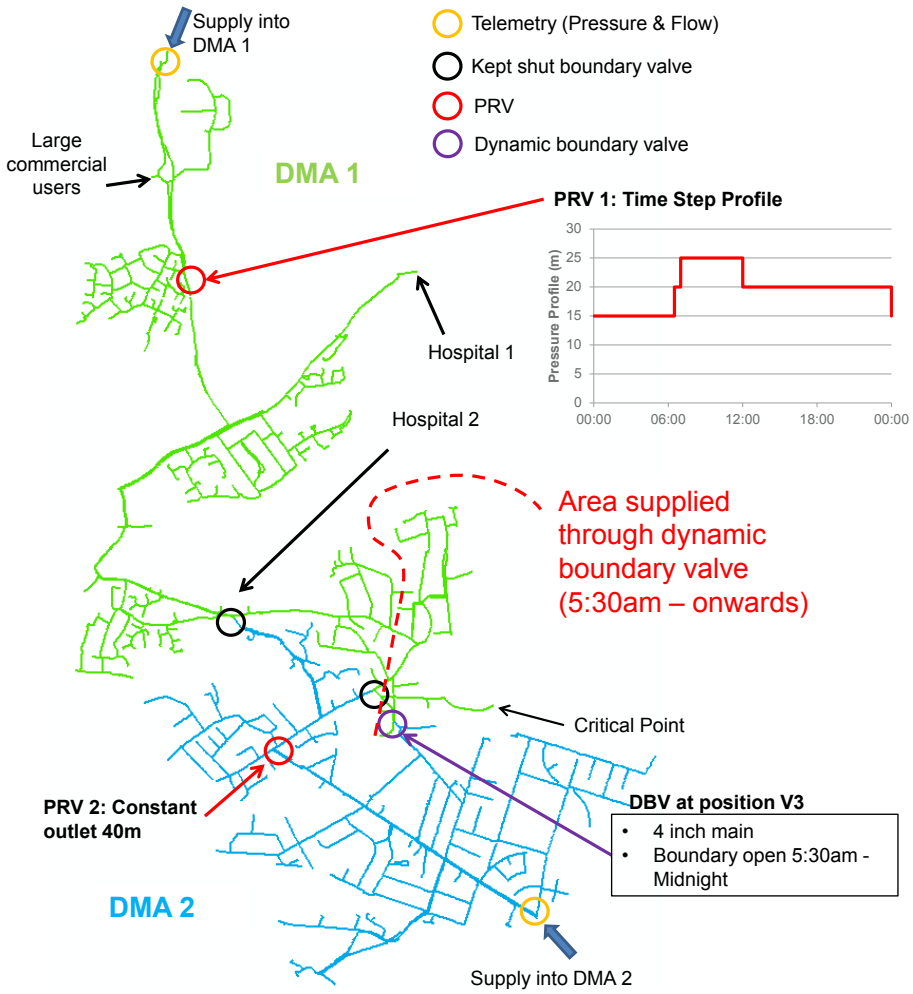


Figure 5.9: Option 4: Dynamic boundary valve at location V3, PRV 1 following a time varying outlet profile, and PRV 2 fixed outlet pressure

5.3.2.5 Option 5: Two dynamic boundary valves installed at positions V1 and V3

Two dynamic boundary valves are installed at position V1 and V3, as shown in Figure 5.10. The original DMA boundary is maintained. With two DBVs installed, a constant outlet ($15mH_2O$) PRV at Stoke Lane is sufficient for keeping pressure at the critical point above $15mH_2O$. Furthermore, Hospital 2 has added security of supply through the dynamic boundary valves placed at both V1 and V3.

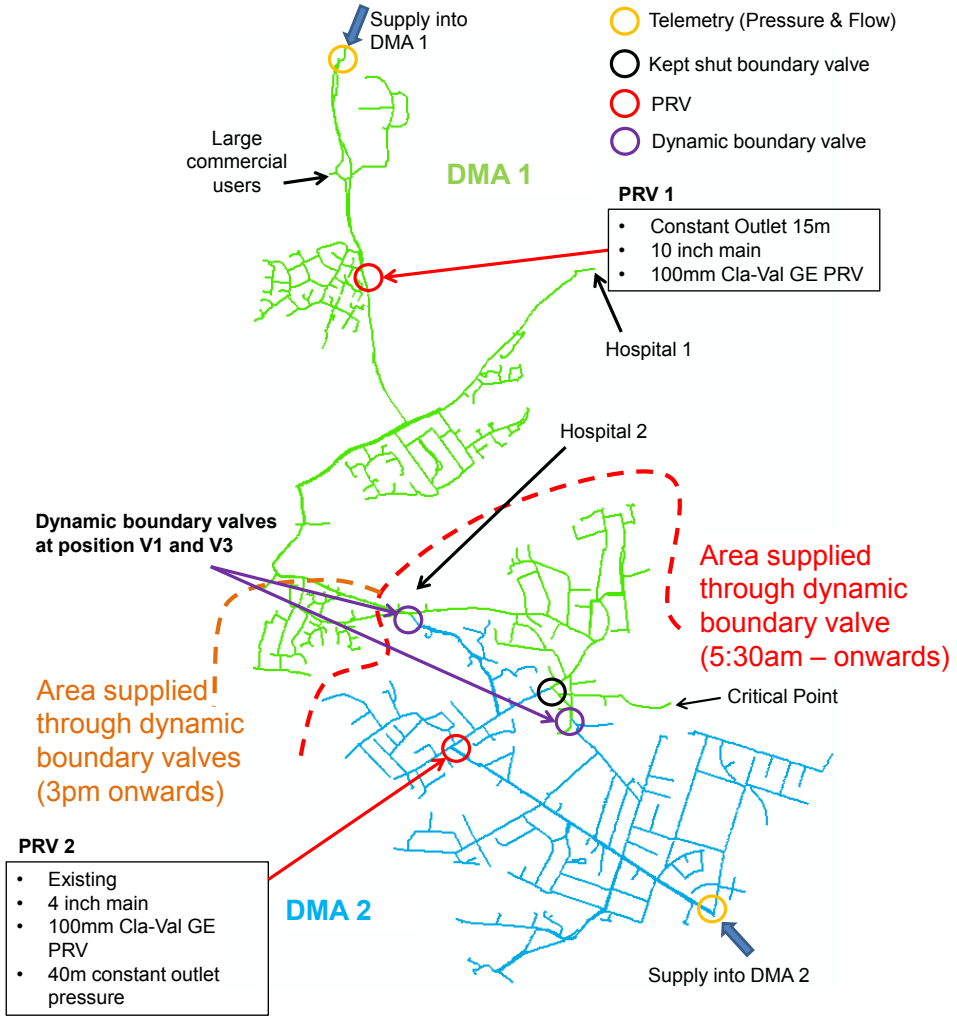


Figure 5.10: Option 5: 2 Dynamic boundary valves at locations V1 and V3, PRV 1 and PRV 2 following a fixed outlet profile

5.3.3 Pressure Management

A box plot of average daytime (07:30 - 21:45) nodal pressure (P_{av}) is shown in Figure 5.11, and a box plot of the diurnal pressure variability of nodes (P_{var}) is shown in Figure 5.12. These results are also summarised in Table 3. It is observed that the installation of two dynamic boundary valves (option 5) results in the lowest P_{av} ($42.3mH_2O$, which is a $4.8mH_2O$ reduction over a closed DMA topology in Option 2). Installing two dynamic boundary valves also results in the lowest $\overline{P}_{var}$ out of all options (Table 3), although installing just a single DBV at position V3 (Option 4) results in a smaller spread of P_{var} (Figure 5.12).

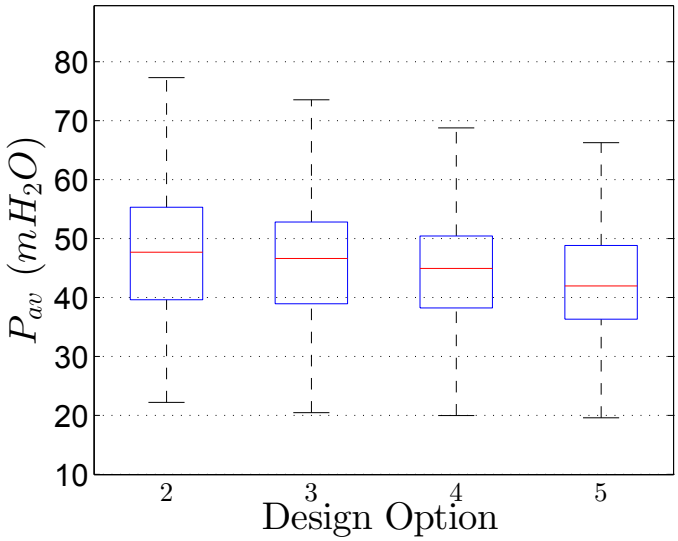


Figure 5.11: A comparison of average daytime nodal pressure (P_{av}) for the potential design options

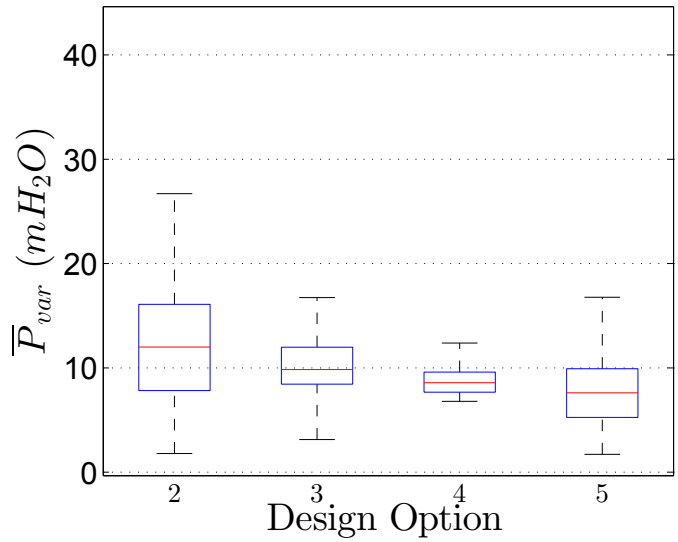


Figure 5.12: A comparison of pressure variability ($\overline{P}_{var}$) for the potential design options

Table 3: Pressure management comparison for different design options

	Option 2	Option 3	Option 4	Option 5
P_{av} (mH_2O)	47.1	45.8	44.5	42.3
$\overline{P}_{var}$ (mH_2O)	11.7	10.1	8.5	8.2

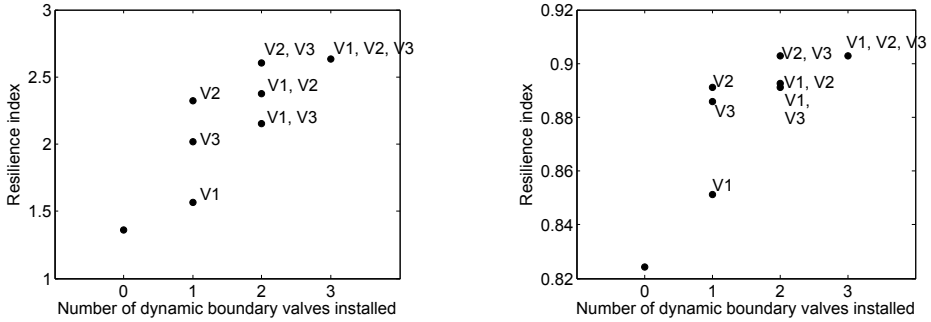
5.3.4 Resilience to Failure

The resilience to failure was analysed for the different design options by:

- Using resilience indexes that capture the redundancy of a network gained by installing dynamic boundary valves;
- Simulating different failure scenarios and calculating d_{met}, i.e. how many customers have been affected.

Two resilience indexes are used to investigate the potential design solutions: the reserve capacity and Todini's resilience index (Section 3.5). Each design solution involves the addition of a link or multiple links to the boundary of the DMAs in positions V1, V2 and/or V3, as shown in Figure 5.1.

The results are shown in Figure 5.13. The reserve capacity highlights that hydraulically connecting the two DMAs facilitates more demand to be met. Installing just a single valve shows that valve V2 achieves the strongest improvement in resilience by adding 90% to the reserve capacity, followed by V3 adding 60% in reservce capacity. Valve V1 only adds a 20% increase in reserve capacity. Installing both V2 and V3 results in a reserve capacity increase of 120%. Adding a valve at V1 in addition to V2 and V3 only adds 3%, highlighting that V1 does not produce a strong improvement in reserve capacity. Both the reserve capacity and Todini's resilience index produce a set of design options without any contradictions. The reserve capacity has the advantage that the design options are more intuitive. The advantage of Todini's index is that it will always detect changes in redundancy, provided that the change in redundancy results in a different flow regime in the network.



(a) Reserve Capacity (μ_{max})

(b) Todini's Index (I_r)

Figure 5.13: A comparison of resilience indexes: (a) Design options produced using the developed resilience index (b) Design options produced using Todini's resilience index

An assessment of resilience was also made in simulation by first assessing the impact of a burst to pressure in the network, and second by assessing how much

customer demand can be supplied in the event that critical mains are closed. For this analysis, pressure-driven hydraulic simulations must be carried out (Section 2.9) in order calculate the total demand met d_{met} for a pressure critical scenario that reduces the customers' supply.

The burst is simulated next to Hospital 2 with a flow rate of $5l/s$ at 08:30. Figure 5.14 shows a comparison of pressure when operating 2 DBVs and a kept shut (KS) boundary. More nodes experience pressures below $15mH_2O$ for the KS valve option. When operating a closed DMA boundary, 95.5% of customer demand was met, compared to 99.1% when operating a dynamic boundary.

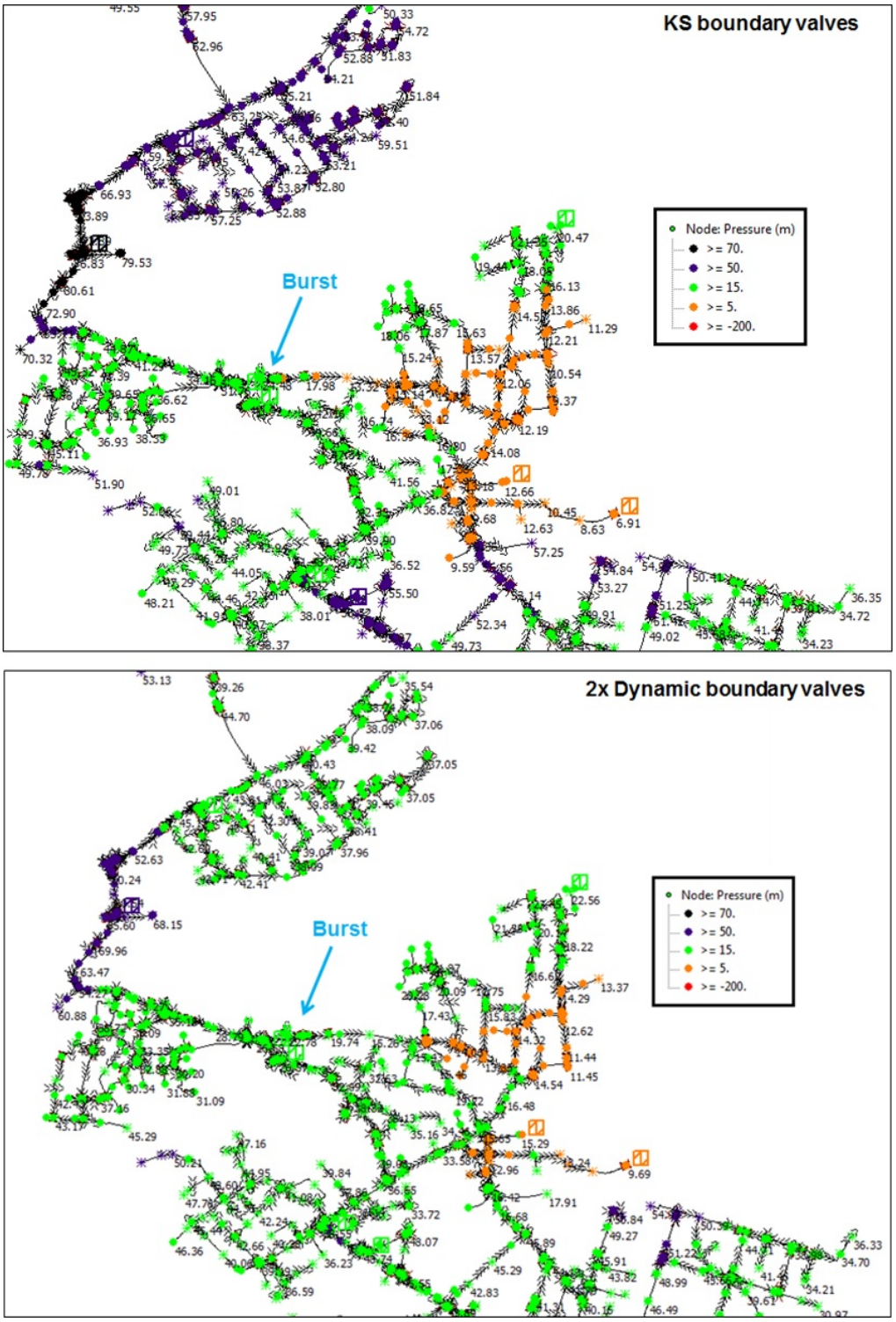


Figure 5.14: A burst simulation at 8:30am comparing a kept shut (KS) boundary valve configuration, and a dynamic boundary valve configuration

The pipe closures shown in Figure 5.15 as a result of a complete pipe failure and/or isolating bursts have been analysed. For each of the five closures, the pressure-driven analysis is implemented to estimate the actual water supplied to customers. The analysis has been completed for the case where two dynamic boundary valves have been installed, and the case where all boundary valves are kept shut.

The percentage of demand met has been calculated for each scenario. PRVs were set to fully open in both scenarios. In all 5 cases, dynamic boundary valves supplied more demand at all times than kept shut boundary valves, demonstrating a prompt response to failure and minimising the number of affected customers. The biggest improvement in supplied demand was observed in scenarios 1 and 2 where the major supply line into DMA 1 is closed. In these scenarios, critical customers such as Hospital 1 and Hospital 2 would still able to receive water.

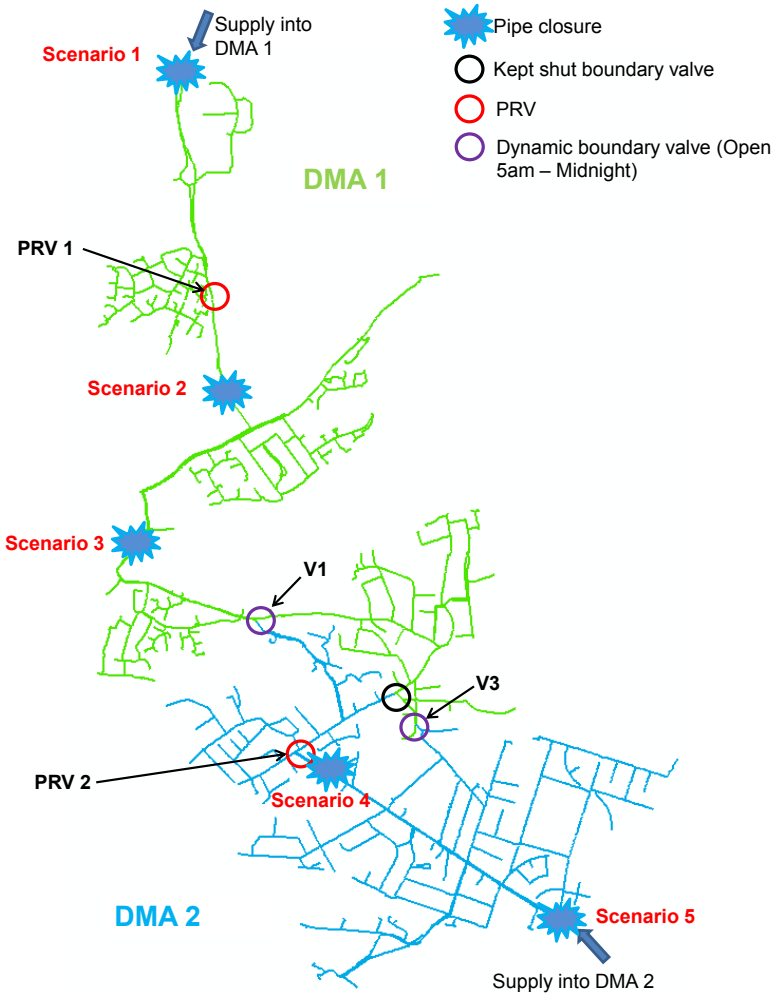


Figure 5.15: Pipe closure scenarios

Table 4: Analysing % demand met during pipe closure scenarios for the design of the experimental programme

	Demand Met (d_{met}) (%)	
Network Config.	KS Topology	Dynamic Topology
Scenario 1	54.6	90.4
Scenario 2	68.0	100.0
Scenario 3	77.8	100.0
Scenario 4	84.4	100.0
Scenario 5	45.4	70.2

5.3.5 Conclusions

Based on the results, the water company decided to implement a dynamic topology in the network with two dynamic boundary valves, and two PRVs upgraded with the same technology as the dynamic boundary valves (Section 5.4), in order to take advantage of reduced network pressure, reduced diurnal pressure variability, and improved network resilience to failure. The implementation happened over an extended period of time, with a substantial amount of work undertaken by all parties involved (Bristol Water plc, Cla-Val Ltd. and Imperial College London) to:

- Develop and test the novel bidirectional pilot valve system;
- Calibrate sensors and control actuators;
- Install chambers for the housing of the control valves;
- Test the bidirectional flow metering;
- Install kiosks by the PRV and dynamic boundary valve chambers, used to house a dedicated communication link, a real-time logging system, mains power, and other related equipment;
- Flush the hydrants in DMA 1 and DMA 2 to prepare the network for flow reversals;
- Deploy logging equipment, identify inconsistencies, and calibrate the hydraulic model for use in control optimisation

The technology and set-up is outlined in Section 5.4.

5.4 Technology

The implementation of the dynamic topology incorporates a number of recent developments in sensing and control technology. An overview of this technology and its location in the experimental programme is shown in Figure 5.16. Since the initial investigation, a small area of customers had been rezoned on to DMA 2, as shown in Figure 5.16, due to unrelated operational issues. Furthermore, another PRV was installed at the inlet of DMA 2 (Figure 5.16), however it could not be fully commissioned due to insufficient inlet pressure at DMA 2, a result of unrelated remedial work being undertaken upstream of DMA 2. The experimental results undertaken in this thesis do not therefore include PRV 3 in the investigation.

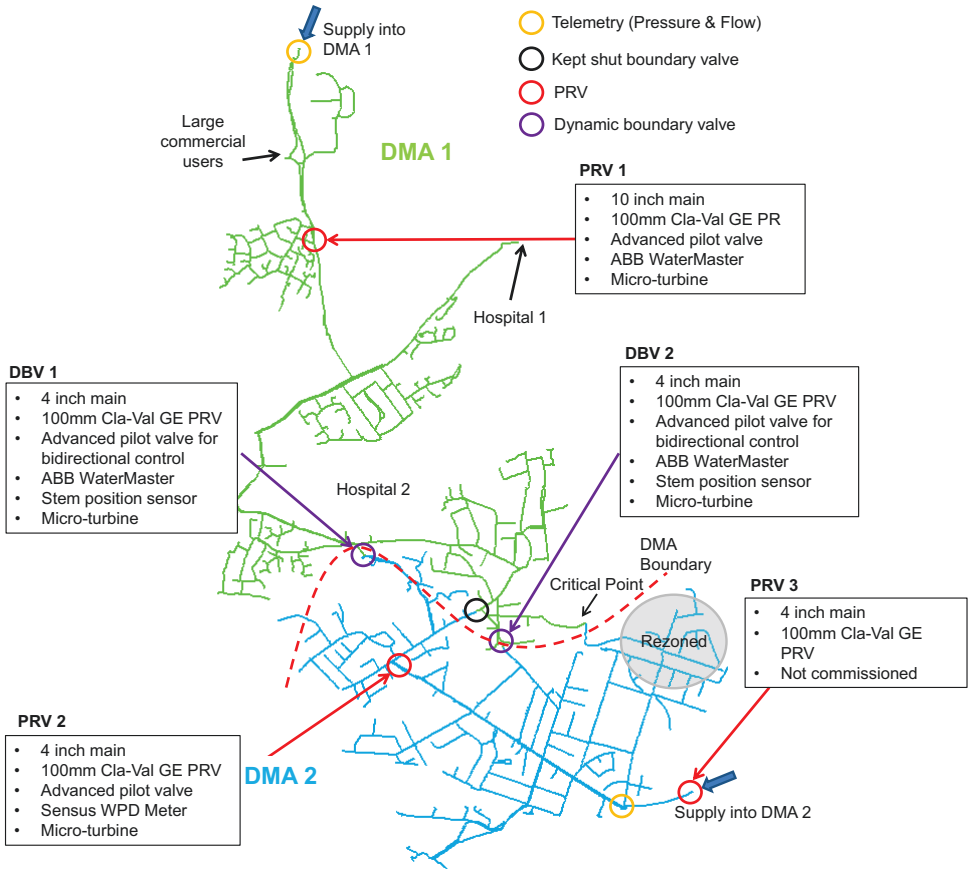


Figure 5.16: An overview of the experimental programme for the investigation of dynamic topologies for adaptive networks, showing the installed equipment

5.4.1 Pilot Valve for Bidirectional Control

A schematic of the novel pilot valve and bypass system (Cla-Val, 2015*a*) that facilitates bidirectional flow and control at the dynamic boundary valves is shown in Figure 5.17, and a key for its components is shown in Table 5.

A PRV would typically shut down when flow reversals occur (i.e. the PRV acts as a check valve when the outlet pressure is higher than the inlet pressure). This is not a desirable form of control at the dynamic boundary, where flow and control should be bidirectional for optimal pressure management and resilience to failure, as discussed in Chapter 4.

The bidirectional flow and control of the dynamic boundary valves is achieved by installing two bypasses on the control valve (instead of just one, as is used for a typical PRV in Figure 3.2, Section 3.7.1) together with a number of check valves that ensures the flow of the bypass is only occurring in one direction at any time. As shown in Figure 5.17, if flow is L-R, then the check valves stop flow into the reverse flow bypass, and the dynamic boundary valves acts like a standard PRV, where flow goes from the inlet, via "4C" to the chamber, and via

the pilot valve to the outlet. If flow reverses (R-L), the check valves stop flow in the standard bypass, and instead, flow takes the route via "4D" to the chamber, and via the pilot valve and "4A" to the outlet.

Pressure, flow, and stem position sensors placed on the valve facilitate the dynamic boundary valve to operate as a PRV, flow control valve, or position control valve, respectively. The desired set point is maintained using the sensors and the electronic autonomous controller (No. 5, in Figure 5.17).

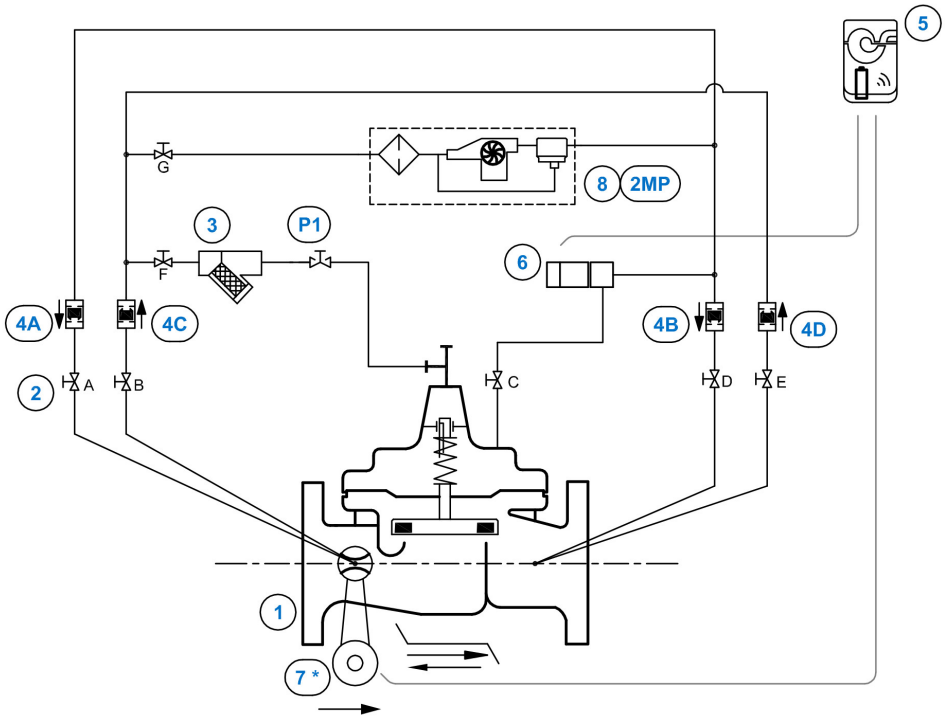


Figure 5.17: Schematic of a position control valve set up for bidirectional flow, to be used as a dynamic boundary valve

Item	Description	Quantity
1	Main valve	1
2	Isolation ball valve	7
3	Strainer	1
4	Check valve	4
5	Electronic autonomous controller	1
6	Flow control	1
7*	Insertion flow meter (*One direction only as indicated)	1
8	Turbine MP	1
P1	Isolation ball valve (Optional)	1
2MP	Double turbine MP (Optional)	1

Table 5: Key for Figure 5.17, which shows a bidirectional control valve for the dynamic DMA topology

5.4.2 High Speed Pressure Monitoring (128S/s)

In the experimental programme, pressure is monitored at 128 samples/s with a time synchronization of 2ms (Hoskins and Stoianov, 2014). This gives a unique insight into the hydraulic conditions of WDNs not available when using the industry standard (1 sample / 15 minutes). Since multi-feed networks and more advanced control options could cause dynamic hydraulics (Section 4.4), the high frequency data is used to guarantee all control is undertaken in a steady manner. By streaming the data in real-time over dedicated communication links at all control valve locations (Section 5.4.5), visibility of the network conditions is known at all times.

The high speed pressure data is also used to:

- Accurately calculate performance indicators for the network (Section 3.5);
- Calibrate the hydraulic model (Section 5.5), which is used for control optimisation (Chapter 6). The high frequency data can also validate or invalidate the steady state assumption used in the hydraulic modelling (Section 2.1).

5.4.3 Flow Meters

In order to accurately monitor bidirectional flow at the dynamic boundary valves, electromagnetic flow meters are used (see Section 3.6.5 for details on flow meter selection). The flow meters used in the experimental programme with the dynamic boundary valves are ABB WaterMaster electromagnetic meters (ABB, 2015), which have an accuracy of $\pm 0.2\%$. In addition, an insertion flow meter (Cla-Val, 2015*b*) is also installed at dynamic boundary valve sites.

The DMA inlets, which provide flow data via the telemetry (Figure 5.16), only have an accuracy of $\pm 5\%$. This can introduce error in the hydraulic modelling and control.

5.4.4 Turbine for Energy Harvesting

All control valves in the experimental programme have a micro-turbine for energy harvesting (Cla-Val, 2015*c*). The micro-turbine is installed on the valve bypass (Figure 5.17) and is powered by the pressure differential of the valve. A pressure differential of $\approx 4mH_2O$ is required across the valve to keep the battery charged.

The micro-turbine and battery power pressure sensors located at the inlet and outlet of the valve, pilot biasing, the insertion flow meter, and remote communications used to remotely update the control valve settings and acquire hydraulic

data. The sensors, which are not related to those in Section 5.4.2, have a maximum logging rate of 1 sample/s. The maximum frequency that valve settings can be updated is once every 9 minutes, although this was not tested. The constraints on logging and remotely updating valve settings come from the power consumption of the CPU used in the electronic autonomous controller (Figure 5.17) and from powering the GSM antenna (Section 5.4.5).

So that the experimental programme is not constrained by power generation, mains power is also installed at all control valve sites, which powers the dedicated communications (Section 5.4.5) and ensures that hydraulic data at 128S/s (Section 5.4.2) is always available.

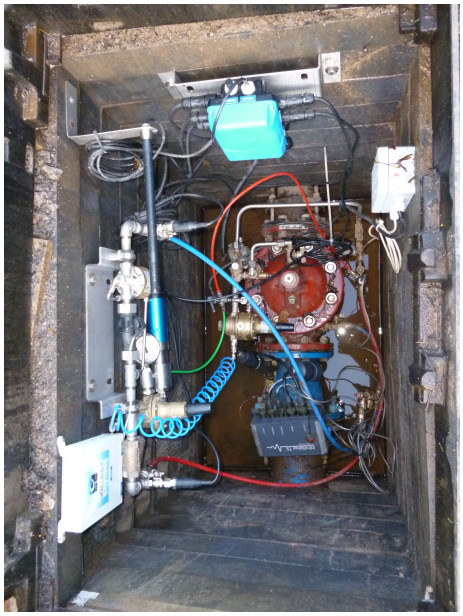
5.4.5 ADSL and GSM Telecommunications

Two forms of communication are available in the experimental programme: ADSL and GSM.

A dedicated ADSL link was installed at all control valves. This facilitates:

- Real-time availability of the high speed pressure data (Section 5.4.2), used to guarantee that all control is steady;
- Update of the model parameters in near real-time (Section 2.8), which improves the accuracy of the hydraulic modelling and control.

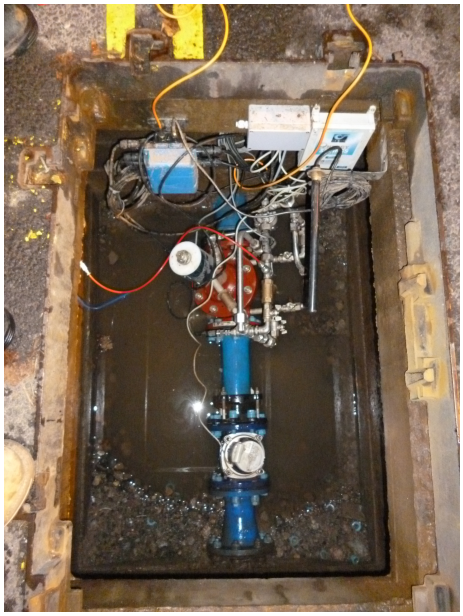
In addition, GSM is used to remotely update control valve settings and recieve hydraulic data from the sensors powered with the turbine (Section 5.4.4).



(a) PRV 1



(b) PRV 2



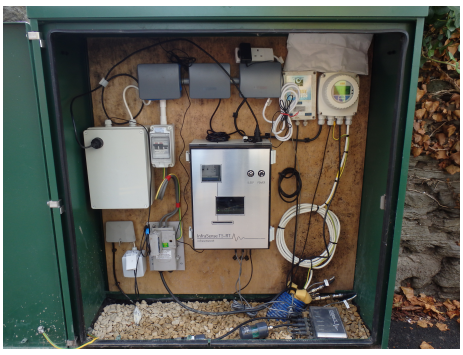
(c) DBV 1



(d) DBV 2



(e) Chamber and empty kiosk



(f) Kiosk with real-time logging and comms.

Figure 5.18: Equipment installation for the experimental programme: (a) PRV 1, (b) PRV 2, (c) DBV 1, (d) DBV 2, (e) PRV chamber and empty kiosk and (f) the kiosk fully equipped with ADSL, mains power and real-time pressure sensing

5.5 Hydraulic Model Calibration

As discussed in Section 5.3.1, model calibration involves varying model parameters in order to sufficiently minimise discrepancies between the modelled variables and corresponding measurements. This process is imperative for undertaking model-based control and model observability (i.e. given a certain number of loggers, establishing whether it is possible to estimate all other variables in the network.

The network model was manually calibrated using all available data from the equipment in Section 5.4. An additional 22 battery powered, high speed InfraSense TS (Hoskins and Stoianov, 2014) pressure sensors (up to 128 samples/s, 2ms time synchronisation) were also deployed with locations shown in Figure 5.19. The InfraSense TS loggers facilitate a unique form of model calibration, where the suitability of a steady-state model can be compared with transient conditions of the network.

The extended period simulation of the network uses 15 minute intervals. Since the pressure data is acquired at 128 S/s, a pressure envelope that represents transient pressure conditions can be created (Hoskins and Stoianov, 2014). The envelope consists of:

- Mean: The average pressure over the 15 minute period, used to compare the steady-state model with pressure data
- Max/Min: the maximum and minimum pressure data over the 15 minute period, used to establish the applicability of using a steady state hydraulic model, and investigate potential discrepancies between model and data.

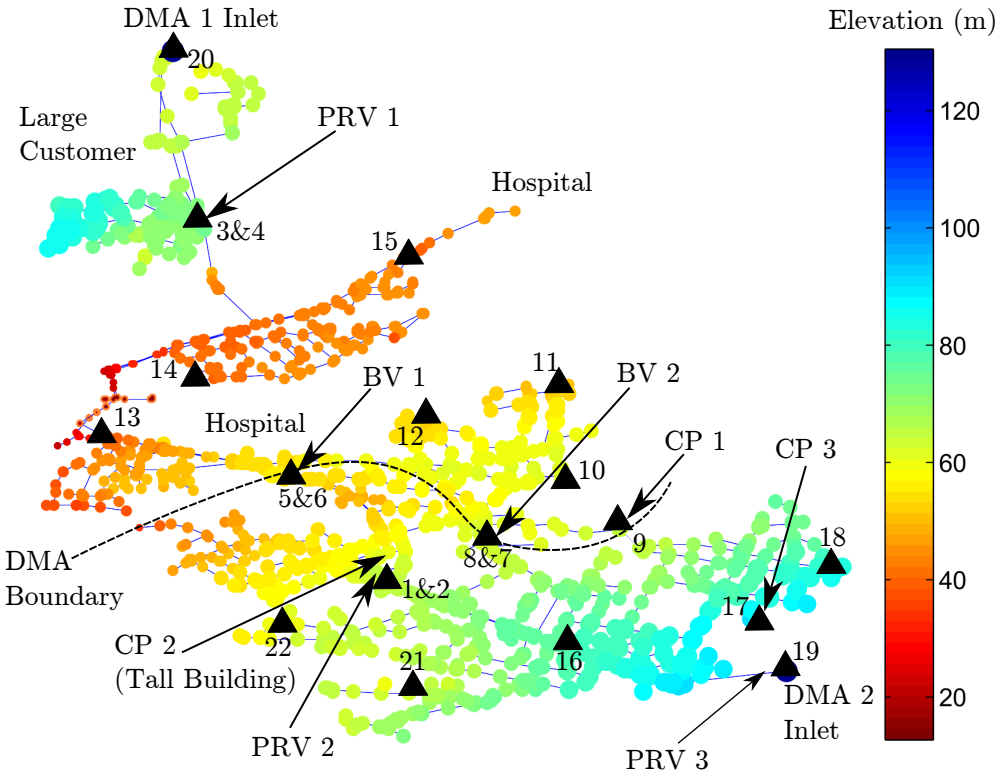
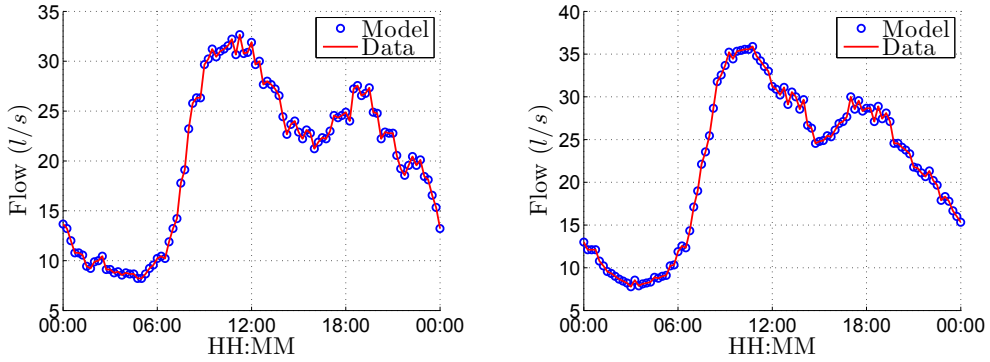


Figure 5.19: The locations of InfraSense TS pressure loggers (black triangles) sampling at up to 128S/s and used for hydraulic model calibration and insight into the hydraulic behaviour of the experimental programme during normal operation and failure situations. Control valves have two loggers installed, where the number notation is: First number (inlet), second number (outlet), both boundary valves have flow directions northerly

The calibration of the hydraulic model involves (1) updating the customer demand profiles using flow data and (2) altering the friction factor for pipes until the modelled pressure fits the measured pressure at the InfraSense TS locations to within an acceptable tolerance.

The first step of calibration involves updating the customer demand profiles using flow meter data, a process that is undertaken for the calibration as well as in near real-time for data analysis (Section 2.8). The demand patterns are updated according to the flow meter data and the distribution of customers located across the network. This produces a hydraulic model that agrees exactly with observed flow data as shown in Figure 5.20.



(a) DMA 1 Inlet

(b) DMA 2 Inlet

Figure 5.20: Calibrating demand profiles with inlet flow data

The friction factors in the hydraulic model are calibrated so that modelled pressure aligns with measured pressure at all logged locations shown in Figure 5.19. The calibration is undertaken manually, although a breadth-first search is used to select the links between known hydraulic head points (pressure logged points) in order to automate part of the calibration process. A guide to Hazen-Williams roughness coefficients from (Bhave, 1991), as shown in Table 6, is used to help select the roughness coefficients. The calibration is undertaken for a 24 hour period. A summary of the calibration results are found in Table 7, and plots that compare the model and pressure data are shown in Appendix A.

Table 6: Hazen-Williams coefficients for pipes of varying age and condition (Bhave, 1991)

Trend	Pipe Diameter (mm)	75	150	300	600	1200
30 years old						
1	slight	100	106	112	117	120
2	moderate	83	90	97	102	107
3	appreciable	59	70	78	83	89
4	severe	41	50	58	66	73
60 years old						
1	slight	90	97	102	107	112
2	moderate	69	79	85	92	96
3	appreciable	49	58	66	72	78
4	severe	30	39	48	56	62
100 years old						
1	slight	81	89	95	100	104
2	moderate	61	70	78	83	89
3	appreciable	40	49	57	64	71
4	severe	21	30	39	48	54

Recommended guidelines for hydraulic model calibration are given by AWWA Engineering Computer Applications Committee and others (1999). These are:

1. At least 100% of readings within $2mH_2O$
2. At least 95% of readings within $0.75mH_2O$
3. At least 85% of readings within $0.5mH_2O$

Since data is collected at high frequencies, it is immediately apparent that a steady state hydraulic model can not achieve the recommended tolerences given in the 2nd and 3rd items above. In this thesis, another tolerance is given, which is:

- At least 100% of readings within $1mH_2O$

In addition to these criteria, it is recommended that at least 10% of nodes are logged for pressure to complete the calibration (AWWA Engineering Computer Applications Committee and others, 1999). However, due to limitations in the availability of resources, only 1% of nodes are logged in this project, which is equal to 22 nodes/loggers.

The hydraulic model agrees with all pressure data measurements to within the first threshold guideline laid out by (AWWA Engineering Computer Applications Committee and others, 1999), and to within $1mH_2O$ on average at 100% of logged nodes:

- 100.00% of readings within $2mH_2O$
- 100.00% of readings within $1mH_2O$
- 61.11% of readings within $0.75mH_2O$
- 44.44% of readings within $0.5mH_2O$

Logger ID	Mean Pressure Difference Over 24 Hours
1	0.25
2	0.00
3	0.12
4	0.00
5	0.05
6	0.61
7	0.81
8	0.22
9	0.82
10	0.83
11	0.82
12	0.81
13	0.56
14	0.21
15	0.29
16	0.13
17	0.66
18	0.82
19	0.00
20	0.02
21	0.14
22	0.81

Table 7: Summary of calibration results for the experimental programme network (Figure 5.19

The manual calibration outlined above provided sufficiently good accuracy (as shown in Table 7) for the calibration problem. However, an automated calibration process, formulated as an optimization problem (Brdys and Ulanicki, 1994), would likely improve accuracy and reduce the amount of time needed to undertake future calibration tasks. Other calibration methods in the literature include non-linear programming (Ormsbee, 1989) and evolution algorithms (Kapelan et al., 2003). Due to limitations in time and a requirement to prioritise other aspects of the dynamic DMA topology investigation, an automated approach to model calibration was not undertaken. The automation of model calibration is an interesting problem, and the combination of real time data and simulation of hydraulic conditions provides the foundations for more advanced forms of model calibration.

5.6 Conclusion

This chapter has detailed the design and installation of a dynamic DMA topology on a real, operational network supplying approximately 8,000 properties across two DMAs.

A number of design options were considered for the DMAs that were experiencing high night time AZP, low pressure and customer complaints during peak demand hours, high diurnal pressure variability, and low resilience to failure due to the single-feed nature of the DMAs and a number of critical customers located in the area, including two hospitals and a large commercial customer. The design options were explored using a manual approach and the performance indicators outlined in Section 3.5 to compare different network configurations.

The design options explored included conventional fixed topology DMAs and pressure management, and a number of dynamic topology options that would hydraulically connect the two DMAs. The investigation found that the installation of two dynamic boundary valves resulted in the best performance across all indicators used:

- An average daytime AZP of $42.3 mH_2O$, compared to $47.1 mH_2O$ for the closed DMA topology option, a 10.2% reduction;
- An average pressure variability P_{av} of $8.2 mH_2O$, compared to $11.7 mH_2O$ for the closed DMA topology option, a 29.9% reduction;
- More customer demand met during a medium burst event, 99.1% for a dynamic topology compared to 95.5% for the closed DMA topology option;
- Maintaining more customer demand during all pipe closure scenarios including, in some cases, 100% of demand met comped to 68 – 84.4% for the closed DMA topology option.

It was decided to install two dynamic boundary valves and a number of other technologies, including electromagnetic flow meters for bidirectional flow metering at the DMA boundary, 22 high speed (128 samples/s) pressure loggers for guaranteeing a stable operation of control valves and to understand the hydraulic behaviour of the network when operating a dynamic topology, and telecommunications for receiving hydraulic data in real time and updating control settings periodically. The dynamic boundary valves use the novel pilot valve bypass system that facilitates bidirectional flow and control at the DMA boundary.

An extensive model network calibration was carried out once the dynamic DMA had been installed. Calibration is important for carrying out model based control optimisation and for calculating performance indicators. The calibration made use of all available data streams. A good degree of model calibration was achieved, where the average discrepancy was $\leq 1 mH_2O$ for all logged data

points. However, it is recommended that future work should focus on automatic large scale network calibration in order to improve the calibration results.

6 Control Optimisation

6.1 Introduction

The optimal operation of water distribution networks with dynamic topology requires an optimisation method for the calculation of valve control (Chapter 4).

The dynamic aggregation of DMAs can result in very large, complex networks being used in the optimisation method. This increases the computational time required to find an optimal solution, and also increases the risk of convergence issues occurring. The optimisation method to be used for calculating valve control for this type of network should therefore be:

- Computationally efficient i.e. reasonable solution times;
- Reliable in convergence.

Since the technology used in this thesis for valve monitoring and control could, in future work, be used in real-time control, these objectives could also support the use of other control options such as centralised control.

In this chapter, a novel optimisation algorithm based on SCP is proposed that satisfies these objectives. The main advantage of the proposed approach over other optimisation methods is its reliable, efficient convergence to an optimal point for real, complex networks. This is achieved by using strictly feasible iterations, therefore the algorithm is termed Strictly Feasible Sequential Convex Programming (SFSCP). The SFSCP method has the following features that also makes it attractive for real-time control under normal conditions and control in failure conditions:

- Hydraulically and operationally feasible iterations that facilitate early termination of the optimisation algorithm with valid valve settings. This is useful for situations where a solution is subjected to certain time constraints in real-time control.
- An exact representation of the hydraulic model can be used without simplification or skeletonization. This is particularly useful when a failure occurs in the network and critical pressure reduces the amount of demand supplied to customers. By using an exact representation of the network, customers that have been affected can be identified and located more accurately, and pressure optimised to mitigate consequences.

The structure of this chapter is as follows:

- A generalised valve control optimisation problem is outlined in Section 6.2, and a review of optimisation methods for its solution is undertaken in Section 6.3;

- The proposed SFSCP algorithm is detailed in Section 6.4 for the minimisation of AZP;
- Results that demonstrate the convergence of SCP and the pressure management performance of a dynamic topology are shown in Section 6.5;
- Reliable convergence of SFSCP is demonstrated in Section 6.6 and compared with other valve control optimisation approaches;
- Finally, conclusions are made in Section 6.7.

6.2 General Overview of Problem Formulation

Optimal valve control is calculated by solving a series of optimisation problems that represent steady state conditions of the water distribution network at different points in time. The solutions to the steady state optimisation problems results in an extended period simulation and a corresponding schedule of optimal open-loop control settings for each valve.

An optimisation problem for the arbitrary objective function f that finds optimal valve control in a single steady state simulation is as follows:

$$\min f(x) \tag{6.1a}$$

$$\text{Subject to: } g(x) = 0 \tag{6.1b}$$

$$c(x) \leq 0 \tag{6.1c}$$

where x are the variables of the system (i.e. pipe flows, nodal heads, valve settings), $g(x)$ are equality constraints that must include the steady state hydraulic model of the network (either demand-driven or pressure-driven as outlined in Chapter 2) and $c(x)$ are inequality constraints that should include service requirement constraints (for example, providing a minimum level of pressure for customers) and also physical constraints on some network elements (such as check valves that limit flow to a single direction).

The hydraulic model parameters (customer demand and fixed head nodes) in the optimisation method are determined with recent hydraulic data to avoid suboptimal control occurring (Section 2.8). For example, hydraulic models exist for weekend days, week days, or different seasons.

Since the hydraulics that make up the equality constraints are non linear (i.e. frictional energy losses in (2.3), the valve model in (2.32), leakage model in (2.44)), the optimisation problem is classed as a non-linear programming problem (NLP). The objective function could also be non-linear if, for example, a non-linear leakage function is minimised.

6.3 Review of Optimization Methods for Valve Control

Research on optimal valve control in water distribution networks can be categorised into four main areas. These methods are:

1. Sequential linear programming;
2. Sequential quadratic programming;
3. Other NLP methods from commercial or open-source packages;
4. Evolutionary algorithms.

The optimisation methods for valve control have generally been studied with the intention of reducing either pressure or leakage in WDNs. A related operational optimisation problem is pump scheduling for reducing energy costs, and proposed optimisation methods include linear programming (Jowitt and Germanopoulos, 1992), heuristics (Ormsbee and Reddy, 1995), dynamic optimisation (Ulanicki et al., 2007), a hybrid genetic algorithm (Van Zyl et al., 2004), a direct solver approach (Skworcow et al., 2010), and a combined greedy algorithm and linear programming technique (Giacomello et al., 2012). Significantly less research has been conducted on valve control, which might be attributed to the fact that its benefit in previous work has been limited to pressure and leakage reduction, whereas pump scheduling may provide water companies with greater financial incentives over advanced leakage management. The benefits gained by the valve control proposed in this thesis however are not limited to pressure and leakage, but also include strong improvements in network resilience with the dynamic topology.

6.3.1 Sequential Linear Programming

Sequential linear programming (SLP) was one of the first approaches used to solve optimal valve control problems in WDNs and has been studied extensively by researchers. The approach solves the general form of the NLP in (6.1) iteratively as follows:

1. At the first iteration, set $k = 1$ and choose an initial solution in the search space (x_k).
2. Construct a linear program (LP) by linearising g (and f is necessary) in (6.1), using either a first order Taylor expansion (i.e. the Newton method in Chapter 2) or a linear theory method, around the solution x_k and solve the LP for x_{k+1} using a LP solver
3. Update the iteration counter $k = k + 1$ and repeat the previous step until the difference in successive solutions of $x_{k+1} - x_k$ is sufficiently small.

Bargiela (1984) applied a SLP method using a Taylor expansion linearisation to minimise the sum of nodal heads. The method used warm starting and converged (to an unspecified tolerance) in 5-7 iterations for networks of size up to 32 nodes, 3 sources, and 3 control valves. Trust regions were used in this method to aid the convergence.

Germanopoulos and Jowitt (1989) applied SLP with a linear theory type linearisation, also to minimise the sum of nodal heads. The constraints representing the hydraulic model included pressure-driven leakage, whereas the constraints in (Bargiela, 1984) included just the demand-driven hydraulic equations. Germanopoulos and Jowitt (1989) modelled each control valve i located between nodes a and b with the following relationship:

$$q_i = V_i r_i \mathtt{sgn}(h_a - h_b)|h_a - h_b|^{0.54}, \ \forall i \in N_v \tag{6.2}$$

where $V_i \in [0, 1]$ is the valve opening and `sgn` is the sign of the expression. The valve model in (6.2) is nonlinear and must be linearised in a SLP method. The SLP method proposed by Germanopoulos and Jowitt (1989) used warm starting and converged to a tolerance of 0.02l/s in 10-12 iterations for a small 7 node network, and 5-21 iterations for a 25 node network that was also used by Bargiela (1984). One interesting result from Germanopoulos and Jowitt (1989) was that peak demand simulations converged the quickest, in 5 iterations, then average demand with 14 iterations, and then low demand with 21 iterations.

Jowitt and Xu (1990) achieved faster convergence using the SLP method used by Germanopoulos and Jowitt (1989) by modifying the linearisation of the valve model in (6.2). This new formulation included the valve settings at iteration k in the calculation of x_{k+1}, whereas Germanopoulos and Jowitt (1989) did not include the valve settings at iteration k to calculate x_{k+1}.

The wide availability of LP solvers that efficiently solve very large problems make SLP methods an attractive option for certain optimisation problems for water distribution networks. The main drawback of SLP is that there is no guarantee on convergence for valve control problems, and divergence can occur for large, complex networks (Section 6.6).

6.3.2 Sequential Quadratic Programming

Sequential quadratic programming (SQP) is another iterative approach to solving NLP problems. An SQP approach solves the general form of the NLP in (6.1) iteratively as follows:

1. At the first iteration, set $k = 1$ and choose an initial solution in the search space (x_k).

2. Construct a quadratic program (QP) by forming a quadratic approximation of (6.1a). The objective function f can be approximated using a second-order Taylor series expansion estimation around the current point x_k, and non linear constraints in g can be linearised using either a first order Taylor expansion or a linear theory method around the solution x_k. Solve the QP with a QP solver, which are computationally as cheap to use as linear program solvers.

3. Update the iteration counter $k = k + 1$ and repeat the previous step until the difference in successive solutions of $x_{k+1} - x_k$ is sufficiently small.

Vairavamoorthy and Lumbers (1998) used the network from Jowitt and Xu (1990) to demonstrate a SQP method that minimises the difference between nodal pressure and the nodal minimum allowable pressure. This minimisation problem was constructed as a quadratic objective function:

$$\min \sum_{i=1}^{n_n} (h_i - \underline{h}_i)^2 \tag{6.3}$$

where $\underline{h} \in \mathbb{R}^{n_n}$ are the minimum allowable heads for nodes to ensure a minimum quality of customer service. Vairavamoorthy and Lumbers (1998) propose this objective function as a more efficient method of reducing pressure in the network. For example, allowing minor violations of a minimum allowable head at certain nodes might result in a large reduction in the objective function of pressure minimisation. Since it is not known a priori which nodes should or could have a relaxation of the minimum allowable pressure constraint, Vairavamoorthy and Lumbers (1998) use the objective function in (6.3) to facilitate minor violations in the minimum allowable pressure constraints but also penalise these violations. Since the objective function in (6.3) is quadratic, an SQP method is used to achieve better convergence compared to an SLP method (Vairavamoorthy and Lumbers, 1998).

In addition to proposing a novel objective function for the minimisation of pressure, Vairavamoorthy and Lumbers (1998) propose a decomposition of the NLP to reduce the dimensions of the QP solved at each iteration. This resulted in the decision variables x in the QP approximation of (6.1) only containing the valve settings.

6.3.3 Other Non Linear Program Solvers

Many other NLP solvers exist (both comnercial and open source) that try to find an optimal solution based on gradient information of the objective function and constraints.

Ulanicki et al. (2000) solved an NLP for optimal PRV control that minimises the cost of water supplied (i.e. minimise leakage). The NLP was solved using

a commercial NLP solver called CONOPT (Drud, 1994), which is based on the generalised reduced gradient (GRG) method. A GRG method solves an NLP problem by separating the decision variables (x) into two types (Habib, 2010): basic (x_b) and non-basic (x_{nb}), with reference to (6.1). Given a starting feasible point $x^{k=1}$, a feasible step in the equality constraint search space of the NLP in (6.1) can be made using a first order Taylor expansion of (6.1b):

$$g'(x^k)(x - x^k) + g(x^k) = 0, \tag{6.4}$$

Since the current point is feasible, $g(x^k) = 0$, therefore:

$$g'(x^k)(x - x^k) = 0, \tag{6.5}$$

However, (6.5) can't be solved because the system is under-determined. In order to overcome this problem, the Jacobian $g'(x^k)$ is partitioned into two parts, the first corresponding to the basic variables ($g'_b(x^k)$, simplified as J) and the second to the non-basic variables ($g'_{nb}(x^k_{nb})$, simplified as W). Therefore, (6.5) becomes:

$$J(x_b - x^k_b) + W(x_{nb} - x^k_{nb}) = 0, \tag{6.6}$$

If it is assumed that J is invertible (which is not always the case, for example, due to zero flows as discussed in Section 2.6), the basic variables at the next step in the search space can be defined in terms of the non-basic variables and basic variables at the current point:

$$x_b = x^k_b - J^{-1}W(x_{nb} - x^k_{nb}) \tag{6.7}$$

Therefore, the general objective function f in (6.1) can be approximated as:

$$\bar{f}(x_b; x_{nb}) \simeq f(x^k_b - J^{-1}W(x_{nb} - x^k_{nb}); x_{nb}) \tag{6.8}$$

Since both x_b and x_{nb} are a function of x_{nb}, the chain rule for partial derivatives can be used to estimate the gradient (termed the reduced gradient) of (6.8):

$$\frac{\partial \bar{f}}{\partial x_{nb}} = \frac{\partial f}{\partial x_{nb}} + \frac{\partial f}{\partial x_b}\frac{\partial x_b}{\partial x_{nb}} \tag{6.9}$$

From (6.7), (6.9) becomes:

$$\frac{\partial \bar{f}}{\partial x_{nb}} = \frac{\partial f}{\partial x_{nb}} - \frac{\partial f}{\partial x_b}J^{-1}W \tag{6.10}$$

The reduced gradient can be used to then minimise an objective function in conjunction with a line search method and a suitable stopping criteria (for example, using the Karush Kuhn Tucker conditions for a necessary condition of an optimal point).

For large networks, Ulanicki et al. (2000) used a model skeletonization technique proposed by Ulanicki et al. (1996) to improve the computational performance

of GRG. The model simplification method was extended more recently (Martinez Alzamora et al., 2012). The PRVs were solely located on the boundary of the network in the case study. Each PRV outlet pressure could therefore be modelled as a source node with a fixed head to be determined by the NLP solver (Ulanicki et al., 2000). Ulanicki et al. (2008) extended this work to include PRVs also located within the network. Since these PRVs have a variable head upstream node, it is not possible to consider these PRVs in the same way as boundary PRVs. Ulanicki et al. (2008) therefore modelled internal PRVs by varying the valve resistance in a similar way to the work in (Germanopoulos and Jowitt, 1989; Jowitt and Xu, 1990). Skworcow et al. (2010) also used CONOPT and a skeletonized network model for the combined optimisation of PRVs and pump scheduling.

In addition to directly solving the NLP problems, reformulation of (6.1) has also been proposed. Eck and Mevissen (2013) and Eck and Mevissen (2012) consider the simultaneous optimization of valve placement and settings, and valve settings only for fixed locations, respectively. An approximation of the Hazen-Williams relationship using a quadratic function was made. Two variables representing flows in opposite directions were then assigned to each pipe but with a complementarity condition to ensure at least one of the flows is zero. This approach therefore avoids the discontinuity at $q_i = 0$ when using the Hazen-Williams head loss formula, and results in a quadratically constrained optimisation problem. Two case studies were used: the small illustrative network from Jowitt and Xu (1990) and a larger network ('Exnet') consisting of approximately 1,900 nodes introduced to the research community as a more realistic WDN model by Farmani et al. (2004). The quadratic approximation resulted in a pressure and flow solution that generally agreed well with hydraulic simulation solutions from EPANET although some reported errors were as high as 0.75l/s. The recorded solution time for optimising the settings of 4 control valves in 'Exnet' was 121 seconds.

The use of a NLP solver for the valve control problem in early work of this thesis resulted in occasional convergence problems (Wright et al., 2014*a*). In this thesis, the GRG method was not used because of the need to invert the Jacobian matrix, uncertainty in how regularization methods applied to the Jacobian can affect convergence, and a main objective of the thesis which is to explore computationally efficient methods (such as the null space algorithm) for the scalable implementation of dynamic DMA topologies. This would not be possible if a package such as CONOPT were used. An investigation into the convergence of different NLP solvers would however be beneficial in future research.

6.3.4 Evolutionary Algorithms

Evolutionary algorithms (EA) are metaheuristic optimisation methods. EA attempts to find local optimal (or potentially global) points to an optimisation problem by taking a selection of initial starting point solutions and assessing the strength of these solutions with a fitness function. The solutions are then combined based on their fitness to produce new solution points. The process then repeats until the change in the fitness function is below a specified tolerance. The process of combining the solutions determines to some extent the class of EA. The most commonly studied class is the genetic algorithm (GA), where solutions are combined based on processes inspired by inheritance and mutation. A hydraulic simulation is typically used to assess solution points in GA methods applied to water distribution network problems. Savic and Walters (1995) investigated the optimised valve settings of isolation valves for the minimisation of leakage using GA and the linear theory method for hydraulic simulation. Isolation valves were selected as the decision variable because they are abundant in most networks and could therefore be a cost effective solution to minimising leakage. Araujo et al. (2006) investigate the design and operation problem of placing control valves for the minimisation of pressure, linked with the hydraulic simulator EPANET (Rossman, 2000). Nicolini and Zovatto (2009) also investigate the design and operation problem of placing control valves, but with two objectives of minimising leakage explicitly and minimising the number of valves placed. It is challenging to incorporate multiple objectives into an optimisation problem solved deterministically (i.e. SLP, SQP), whereas GA facilitates multiple objectives in a more simplistic way (Tang et al., 1996). This is therefore one of the advantages of using GA.

Whilst heuristics such as GA are highly applicable to design problems and often find good solutions in the search space, they can exhibit unpredictable behaviour which makes them generally unsuitable for real time control applications (Tang et al., 1996). This might explain why GA has in general only been applied to design problems or combined design/operational problems. For this reason, GA is not explored further in this thesis for the control of water distribution networks with dynamic topology.

6.4 Sequential Convex Programming for PRV Control

The optimisation method proposed in this section meets the objectives outlined in Section 6.1 by approximating the original NLP in (6.1) with a number of convex sub-problems. By fixing and linearising certain optimisation variables, sub-problems can be formed in a way that make use of efficient linear program solvers and null space algorithms, both of which lead to fast and reliable iter-

ations that remain in the hydraulically and operationally feasible search space. To facilitate the use of LP solvers and null space algorithms, a novel approach to modelling PRVs in the optimisation method is proposed and outlined in Section 6.4.1.

Maintaining convexity of the sub-problems formed from (6.1) results in an optimisation method that comes under the framework of sequential convex programming. Although SCP has been acknowledged as a suitable and efficient method for very large scale optimization and control problems (Zillober et al., 2004; Quoc et al., 2012), it has not yet been applied to water distribution networks.

6.4.1 Novel Valve Model for Optimal Control

In the literature, a control valve is commonly represented with a highly non linear model shown in (6.2). Although this equation can successfully be linearised (Germanopoulos and Jowitt, 1989; Jowitt and Xu, 1990), it is possible to model a control valve without introducing additional non-linear behaviour (Wright et al., 2014*a*).

The control valve is modelled using the following convex equations and set:

$$\Delta h_i = \xi_{0,i} \frac{8 q_i^{n_i}}{g \pi^2 d_i^4} + \eta_i, \ \forall i \in N_v \tag{6.11a}$$

$$-q_i \leq 0, \ \forall i \in N_v \tag{6.11b}$$

$$-\eta_i \leq 0, \ \forall i \in N_v \tag{6.11c}$$

$$n_i = 2, \ \forall i \in N_v \tag{6.11d}$$

$$A_{11}(i,i) = \xi_{0,i} \frac{8 q_i}{g \pi^2 d_i^4}, \ \forall i \in N_v \tag{6.11e}$$

where $\eta \in \mathbb{R}^{n_v}$ is a linear head loss variable and $\xi_0 \in \mathbb{R}^{n_v}$ is the valve minor loss coefficient when fully open. Because η_i is not a function of q_i, it is necessary to invoke an inequality constraint at all control valves so that energy losses are in the direction of the flow, as shown in (6.11b) and (6.11c). The valve minor losses exponent is in (6.11d), and the valve minor loss is combined with the system of network equations by using (6.11e).

The control valve is modelled as a regular valve (see (2.32) and (2.33) in Section 2.7) that is fully open and has minor head losses, plus an additional head loss (η_i) determined during control optimisation. In comparison to other approaches of incorporating PRVs in control optimisation algorithms, this novel approach has the following advantages:

- Fast, efficient null space algorithms can be used since η is independent of all other variables (Section 2.7);
- The requirement to linearise highly non linear valve models such as (6.2) is eliminated. The use of (6.2) also leads to uncertainty in achieving a

global optimum or good local optimum, since these can only be found using many, different starting points in the optimisation method (Vairavamoorthy and Lumbers, 1998). In contrast, the valve model in (6.11) is convex. The optimisation search space can be explored by switching the inequality constraints for any control valve and solving the NLP again, although typically the control valves (both PRVs at the boundary of the network, and dynamic boundary valves) have a well defined flow direction during normal network conditions. It is proposed that this approach of finding other local optima in the optimisation search space is superior to solving an NLP many times with different, random starting points in order to find a other local optima.

- By using η to simulate a valve closing, the valve resistance does not become extremely high (r_i in (2.32), Section 2.7) if/when a control valve becomes fully closed during the optimisation iterations, which could cause numerical/convergence problems.
- Both boundary PRVs and internal PRVs can be modelled and optimised. Approaches for the modelling of PRVs internal to networks using a fixed head node (e.g. Bhave (1991, p. 175) in Section 2.7) require the manual manipulation of the network topology and hydraulic equations.

6.4.2 Problem Formulation

The mass and energy conservation laws that describe the water distribution system with the inclusion of control valves (described in Section 6.4.1) are defined by the set of equations:

$$g_1(q,h,\eta) := A_{11}(q)q + A_{12}h + A_{10}h_0 + A_{13}\eta = 0, \tag{6.12}$$

$$g_2(q) := A_{12}^T q - d = 0, \tag{6.13}$$

As explained in Section 6.2, steady state control is considered, therefore source heads (h_0) and demands (d) are fixed for a single NLP. The general form of the NLP in (6.1) is now rewritten as follows, where PRV settings η are determined that minimise the average zone pressure (AZP), which consequently reduces leakage and future burst frequency in the network:

$$\min_{q,h,\eta} f(q;h;\eta) := \sum_{j=1}^{n_n} \omega_j h_j, \tag{6.14a}$$

$$\text{Subject to: } g_1(\cdot) = 0 \tag{6.14b}$$

$$g_2(\cdot) = 0 \tag{6.14c}$$

$$-q_i \leq 0,\ \forall i \in N_v \tag{6.14d}$$

$$-\eta_i \leq 0,\ \forall i \in N_v \tag{6.14e}$$

$$\underline{h}_j - h_j \leq 0,\ \forall j \in N_n \tag{6.14f}$$

where $g_1(\cdot)$ and $g_2(\cdot)$ are the conservation equations (6.12) and (6.13), respectively, and the inequality constraints (6.14d) and (6.14e) come from the physical constraint that PRVs regulate pressure in a single direction.

The inequality constraints in (6.14f) represents operational limits on the minimum service head at each node. For nodes that contain customer connections (denoted by the set $N_c \subseteq N_n$), the minimum service head must be equal to the minimum service pressure P_{min}. For this study, P_{min} has been set to $15mH_2O$ based on the operational practice adopted by the UK water industry for aggressive leakage reduction but acceptable customer service. The value of P_{min} can be altered according to the practices of the water company and needs of their customers. The relation between the minimum service pressure and $\underline{h}$ for nodes containing customer connections is as follows:

$$\underline{h}_j = z_j + P_{min},\ \forall j \in N_c \tag{6.15}$$

As suggested by Vairavamoorthy and Lumbers (1998), minor violations in the pressure constraints at nodes without customer connections are permitted in order achieve the lowest possible objective function:

$$\underline{h}_j = z_j + P_{min} - \zeta_j,\ \forall j \in N_n \setminus N_c \tag{6.16}$$

where $\zeta \in \mathbb{R}^{n_n}$ is a minor pressure violation vector.

Let the optimisation variables in (6.14) be reformulated as $x := [q^T\ h^T\ \eta^T]^T$ and the equality constraints that represent the hydraulic conservation equations in (6.14b)–(6.14c) be $g(x) := [g_1(x)^T\ g_2(x)^T]^T \in \mathbb{R}^{n_p+n_n}$. Also, let the hydraulic feasibility region be defined by the set

$$\mathbb{E} := \{x \in \mathbb{R}^{n_p+n_n+n_v} : x \text{ satisfies (6.14b), (6.14c), (6.14d), and (6.14e)}\}. \tag{6.17}$$

Similarly, the inequality feasibility region for the PRV setting and customer service constraints is defined by the following set:

$$\mathbb{F} := \{x \in \mathbb{R}^{n_p+n_n+n_v} : x \text{ satisfies (6.14d), (6.14e) and (6.14f)}\}. \tag{6.18}$$

A point $x \in (\mathbb{E} \cap \mathbb{F})$ is therefore both hydraulically feasible (all conservation equations and PRV requirements are met) and operationally feasible (pressure at all nodes is at or above the minimum allowable pressure).

6.4.3 Remarks on Problem Formulation

The optimisation problem in (6.14) contains a large number of non-linear equality constraints due to the frictional head loss relationship in (6.14b). The optimisation problem (6.14b) is also non-convex due to the head loss relationship for pipes in (6.14b).

A function $g_i(x) : \mathbb{R}^{n_p+n_n+n_v} \rightarrow \mathbb{R}$ is convex if the following inequality is true for all $x_1, x_2 \in \mathbb{R}^{n_p+n_n+n_v}$ and $0 \leq \alpha \leq 1$ (Boyd and Vandenberghe, 2004):

$$g_i(\alpha x_1 + (1-\alpha)x_2) \leq \alpha g_i(x_1) + (1-\alpha)g_i(x_2) \tag{6.19}$$

The head loss relationship (6.14b) does not satisfy this relationship due to the absolute function used to define A_{11} and the fact that flow in pipes is bidirectional (q is not constrained to be positive or negative for pipes). Therefore the NLP in (6.14) is non-convex.

The non-convexity of the NLP can also be shown by observing the feasibility set ($\mathbb{E} \cap \mathbb{F}$). As with functions, a set C is defined as convex if the following relationship is true for any two points $x_1, x_2 \in C$ with $0 \leq \alpha \leq 1$:

$$\alpha x_1 + (1-\alpha)x_2 \in C \tag{6.20}$$

An example of a non-convex set is shown in Figure 6.1. A line segment, made from two points that are within the set, is not fully contained in the set. Therefore the set is non-convex.

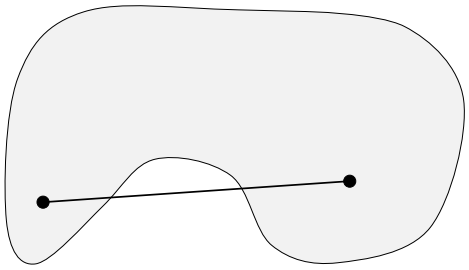
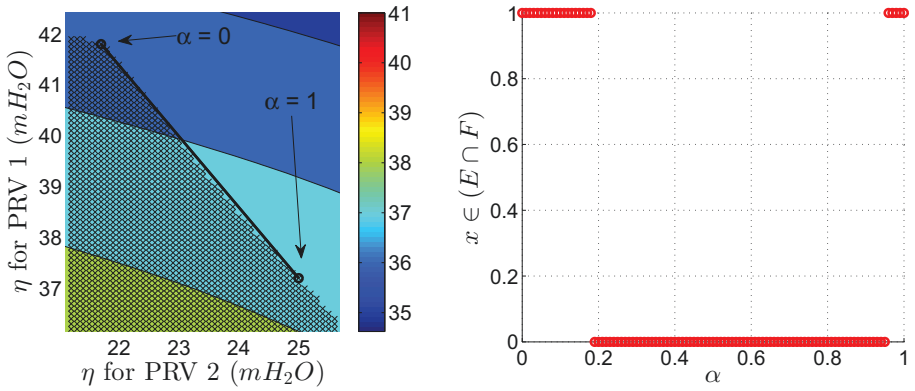


Figure 6.1: A convex set example taken from (Boyd and Vandenberghe, 2004, Sec. 2.1.4).

The non-convexity of ($\mathbb{E} \cap \mathbb{F}$) for (6.14) is shown in Figure 6.2a with $n_v = 2$, i.e. two control valves are present in the network. The contours represent the objective function (AZP) and hydraulically feasible set $\mathbb{E}$, where PRV settings η are varied along each axis. The shaded area represents the operationally and hydraulically feasible set $\mathbb{E} \cap \mathbb{F}$. A line segment between two feasible points shows that not all of the line is in $\mathbb{E} \cap \mathbb{F}$. This is highlighted in Figure 6.2b, where α is plotted against a true (1), false (0) test on $x \in (\mathbb{E} \cap \mathbb{F})$. Both ends of the line segment ($\alpha = 0, 1$) are in the set ($\mathbb{E} \cap \mathbb{F}$), whereas in the middle of the line segment, they are not. Therefore $\mathbb{E} \cap \mathbb{F}$ is not a convex set and the NLP in (6.14) is not convex.



(a) Non-convex search space

(b) Feasibility of line segment

Figure 6.2: Demonstrating that the NLP in (6.14) is non-convex. In (a), The contours represent the objective function (AZP) and hydraulically feasible set $\mathbb{E}$, where PRV settings η are varied along each axis. The shaded area represents the operationally and hydraulically feasible set $\mathbb{E} \cap \mathbb{F}$. A line segment between two feasible points shows that not all of the line is in $\mathbb{E} \cap \mathbb{F}$, as highlighted in (b).

A sequential convex programming method solves a non-convex NLP problem by sequentially solving convex approximations (sub-problems). The convexity of each approximation means each sub-problem can be solved accurately and efficiently. SCP methods differ from other sequential optimisation methods (SLP, SQP) because they preserve convexity in the problem, even if this convexity is non-linear (Dinh and Diehl, 2010). The novel control valve model proposed in Section 6.4.1 facilitates these convex approximations. For the NLP defined in (6.14), two convex sub-problems can then be formed, termed sub-problem A and B.

6.4.4 Sub-Problem A

When the SCP framework (Dinh et al., 2011) is applied to (6.14), the algorithm structure is as follows:

Step 1. Choose a hydraulically and operationally feasible $x^1 \in (\mathbb{E} \cap \mathbb{F})$, Set $k = 1$

Step 2. Solve the following convex sub-problem to obtain x:

$$\min_x \; c^T x \tag{6.21a}$$

subject to:

$$g'(x^k)(x - x^k) + g(x^k) = 0, \tag{6.21b}$$

$$x \in \mathbb{F} \tag{6.21c}$$

where the coefficient vector c contains the vector of weights w_i and $g'(x^k)$ is the Jacobian of the constraint matrix g.

Step 3. Set $\Delta x^k := x - x^k$ as a search direction. If $\|g(x)\|_\infty \leq \epsilon_N$ and $\|\Delta x^k\|_\infty \leq \lambda_{tol}$ (where λ_{tol} is a specified tolerance), then terminate. Otherwise, find an appropriate step size $\alpha \in [0, 1]$. Set $x^{k+1} := x^k + \alpha \Delta x^k$, set $k := k + 1$ and go back to Step 2.

The sub-problem (6.21) is formed by linearising the equality constraints, specifically (6.14b). The equality constraint (6.21b) has the expression:

$$\begin{aligned} NA_{11}(q^k)(q - q^k) + A_{11}(q^k)q^k + A_{12}h + \\ A_{10}h_0 + A_{13}\eta = 0, \end{aligned} \tag{6.22a}$$

$$A_{12}^T q - d = 0, \tag{6.22b}$$

With x^k being a known constant at the current iteration k, the constraints (6.22) are all linear in the unknown x. Therefore, the resulting optimisation problem (6.21) has a linear objective and linear equality and inequality constraints; it is, therefore, a convex program and can be solved efficiently (Luenberger and Ye, 2008). In this thesis, a solver developed by Forrest (2006) is used to obtain a solution. The step size α in the SCP algorithm can either be fixed at each iteration k or updated based on a merit function (Dinh et al., 2011).

6.4.5 Sub-Problem B

A second, convex approximation can also be formed from the original NLP in (6.14) by fixing η in (6.12). It can then be shown that (6.14b) and (6.14c) are a convex system of equations (called sub-problem B). Sub-problem B is solved using a null space algorithm with control valves modelling incorporated (Algorithm 1, as outlined in Section 2.7).

The convexity and uniqueness of the solution to sub-problem B was established by Todini and Pilati (1988) and Wright et al. (2014*a*), but for completeness the derivation is reviewed here with the inclusion of valve control using η. The convexity of sub-problem B is established by showing that its solution satisfies the Karush Kuhn Tucker (KKT) conditions of the following NLP:

$$\min_q \sum_{i=1}^{n_p} \frac{r_i |q_i|^{n_i+1}}{(n_i+1)} + q_i(A_{10,i}h0 + A_{13,i}\eta), \tag{6.23a}$$

$$\text{Subject to: } A_{12}^T q - d = 0 \tag{6.23b}$$

where $A_{10,i}$ and $A_{13,i}$ denote the i^{th} row of A_{10} and A_{13} respectively. Since the objective function in (6.23a) is strictly convex (since r_i and n_i are always positive) and subjected only to linear equality constraints as shown in (6.23b), this NLP is convex. A solution q^* that satisfies the KKT conditions is therefore

a global optimum and unique. The KKT conditions for this NLP consist of (6.23b) and the Lagrangian (denoted Λ):

$$\Lambda(q_i^*, \lambda^*) = r_i \partial \frac{|q_i^*|^{n_i+1}}{(n_i+1)} + A_{10,i}h0 + A_{13,i}\eta + A_{12,i}\lambda^* \in 0, \ \forall i \in N_p \qquad (6.24)$$

where λ^* are the Lagrange multipliers and $\partial|q_i^*|$ denotes a sub-gradient of $|q_i^*|$ (Rockafellar, 1997). Since the sub-gradient of $|q_i^*|$ is -1 if $|q_i^*| < 0$, +1 if $|q_i^*| > 0$ and $[-1, 1]$ if $|q_i^*| = 0$, it can be seen that (6.24) is equivalent to (6.14b) where the Lagrange multipliers of (6.24) represent the unknown nodal heads h at the solution q^*. Therefore, for a fixed η, sub-problem B is convex and has a unique solution.

6.4.6 Full Step Sequential Convex Programming

In (Wright et al., 2014*a*) and (Wright et al., 2014*b*), an SCP method that uses sub-problem A and sub-problem B was investigated. The SCP method starts with iteration $k = 1$ at Step 1 of sub-problem A, which requires a hydraulically and operationally feasible $x^k \in (\mathbb{E} \cap \mathbb{F})$. This is found by solving sub-problem B, a system of hydraulic equations consisting of (6.14b) and (6.14c) with $\eta^1 = 0$ (i.e. the control valves are fully open). It is assumed that there is sufficient pressure provided at source nodes to satisfy all pressure constraints at customer nodes, and that pressure minimisation using valve control is appropriate. If this is not true, then at the first iteration $k = 1$, $x^k \notin (\mathbb{E} \cap \mathbb{F})$ will hold, and a failure is likely to have caused low pressure to occur in the network, which should be investigated.

Next, the LP at Step 2 of sub-problem A is solved, and a full step line search ($\alpha = 1$) at Step 3 is undertaken to get x^{k+1}. Although the iterates x^{k+1} that solve (6.21) satisfy the linear equality constraint(6.14c), they would not satisfy the non-linear equality (6.14b) and so would not be hydraulically feasible. In an attempt to achieve reliable convergence, an approximate approach to 'project' x^{k+1} back on to the set $\mathbb{E}$ is used by solving Sub-problem B with η^{k+1}. Finally, the convergence check at Step 3 is undertaken. If satisfied, the SCP method terminates, otherwise, the method updates the iteration counter $k = k + 1$ and returns to Step 2. Since no line search is undertaken in Step 3, the method is called a full step sequential convex programming method (Dinh et al., 2011). A visualisation of the method is shown in Figure 6.3.

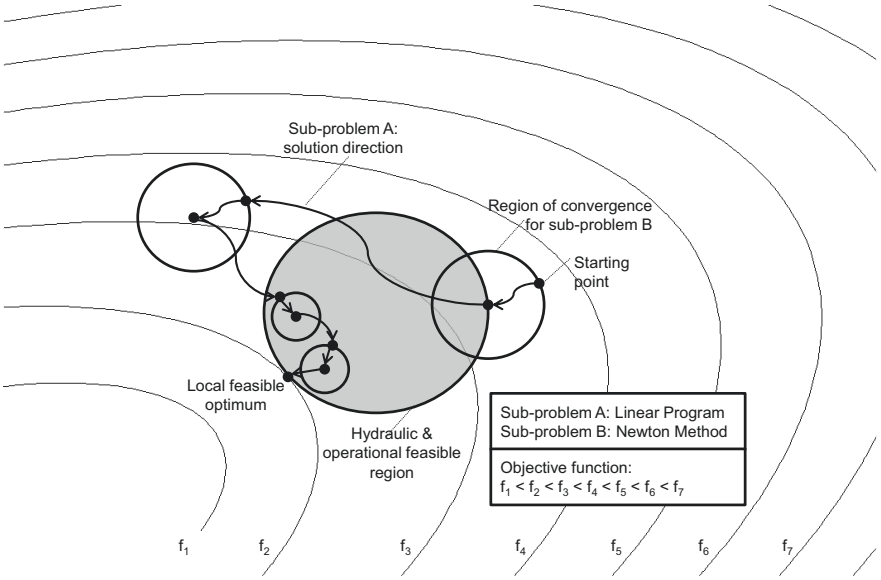
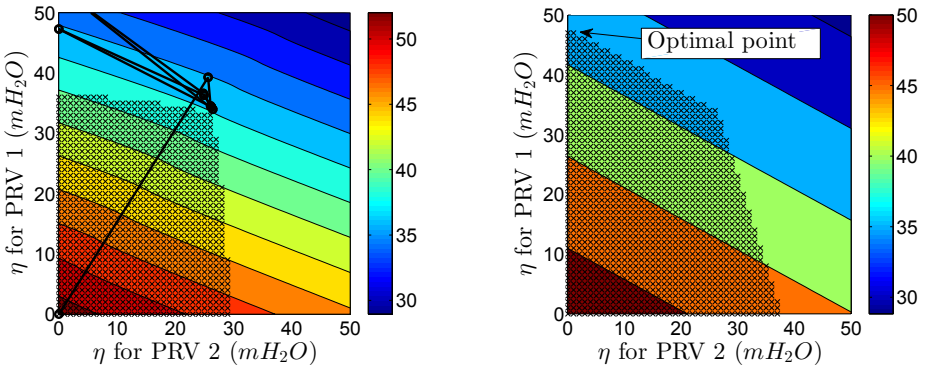


Figure 6.3: Visualisation of the η search space for SCP (Wright et al., 2014*a*)

It was shown by Wright et al. (2014*a*) that this approach worked well most of the time. However, the method sometimes fails to converge to a feasible solution for the original optimisation problem (6.14). For example, η^{k+1} computed at Step 2 would sometimes result in a solution that violates (6.14f) when projected onto $\mathbb{E}$, which occasionally led to convergence difficulties. One example of this is shown in Figure 6.4a. Here, the SCP method from Wright et al. (2014*a*) is applied to the case study in Figure 6.8. The contours represent the objective function when only two control valves are optimised and the shaded region represents the feasible region ($\mathbb{E} \cap \mathbb{F}$) i.e. the space where the constraints (6.14b) – (6.14f) are all satisfied. The optimisation method takes steps outside of the feasibility region initially, and eventually oscillates in the infeasible search space. This either resulted in an infeasible solution after the maximum number of iterations or in suboptimality when the final solution was 'projected' onto the feasibility region. It is shown in Figure 6.4b why this behaviour occurs. Figure 6.4b shows the search space for the LP at Step 2 of Sub-problem A. The optimal point of the LP consists of an η that is not in $\mathbb{E} \cap \mathbb{F}$, as shown in Figure 6.4a.



(a) Objective function f (contours), and feasible space $\mathbb{E} \cap \mathbb{F}$ (shaded areas)

(b) f (contours) and LP search space

Figure 6.4: (a) Solution space $\mathbb{E}$ and objective function f (contours), and feasible space $\mathbb{E} \cap \mathbb{F}$ (shaded areas). Cycling in convergence in the infeasible area of the search space occurs with SCP (b) Objective function f (contours) in the LP search space (Sub-problem A). The solution to a linear program results in iterations outside of the feasible area in the non-linear search space of (a)

6.4.7 Strictly Feasible Sequential Convex Programming

The use of strictly feasible iterates is developed to achieve reliable convergence (Wright et al., 2015*a*). In the spirit of feasible direction descent methods (Bertsekas, 1999, Sec 2.2), a sequence of feasible iterates is generated by using line searches along descent directions. A simple line search is used to guarantee a decrease in the objective function and feasibility at each iteration, which together guarantee convergence to a local minima. This method is therefore termed strictly feasible sequential convex programming (SFSCP). The SFSCP algorithm can only guarantee convergence to locally optimal solutions because the original problem is non-convex.

For a given feasible iterate x^k, a feasible direction at x^k is a non-zero vector d^k that guarantees $x^k + \alpha d^k$ is feasible for all $\alpha \in (0, \theta]$ with some $\theta > 0$ that is sufficiently small. From Figure 6.4a, the first iterate of the SCP method is taken along a feasible descent direction. Since the descent direction is one that reduces pressure heads, taking a full-step in this direction can violate the minimum pressure constraints (6.14f). Moreover, if the feasible iterate is on the boundary of the feasibility space $\mathbb{E} \cap \mathbb{F}$, where the constraints (6.14f) are active, the descent directions may not even be feasible. Like feasible interior point methods (Nocedal and Wright, 2006), it is proposed that iterates are strictly feasible by approaching the boundary of $\mathbb{E} \cap \mathbb{F}$ from the interior of the constraints (6.14f). Unlike interior point methods, a barrier function is not used but rather strict feasibility is enforced in the 'projection' stage of the SCP approach.

In this new approach, the valve settings η, which are computed by solving the linear program in Step 2 of the k^{th} iteration in the SCP algorithm, are not used directly to find a 'projection'/solution in $\mathbb{E}$ via hydraulic simulations. Instead, η is used to form a feasible descent direction, and a line search is performed to find a next iteration that is guaranteed to be both feasible in $\mathbb{E} \cap \mathbb{F}$ and lower in objective function value.

Line search methods are used in optimisation to determine step sizes that minimise or decrease the objective function $f(\cdot)$ along a search direction. With the search direction defined as:

$$\Delta\eta^k = \eta - \eta^k, \tag{6.25}$$

a line search is used to find a step-size α that guarantees a reduction in objective function value by evaluating:

$$f(q^{k+1}, h^{k+1}, \eta^k + \alpha\Delta\eta^k) = \sum_{j=1}^{n_n} \omega_j h_j^{k+1} \tag{6.26}$$

and checking that the next iterate x^{k+1} is strictly feasible with respect to all the constraints, i.e. $x^{k+1} \in (\mathbb{E} \cap \mathbb{F})$. Since it is not always possible to find a feasible descent direction from an iterate on the boundary of the feasible set, initial iterations of the optimisation method are restricted from getting too close to the infeasible space – the iterates will be in the interior of the feasible region at all iterations of a strictly feasible optimization method. In order to discourage initial iterations from becoming close to the infeasible space, $\epsilon -$ feasibility is enforced. At the k^{th} iteration of the SCP, the line search considers feasibility that is $\epsilon(k)$ of (6.14f) as follows:

$$\underline{h}_j - h_j + \epsilon(k) \leq 0,\ \forall j \in N_n,\ \epsilon(k) > 0 \tag{6.27}$$

where $\epsilon(k)$ decreases with SCP iteration number as

$$\epsilon(k) = \frac{1}{k^2}. \tag{6.28}$$

As can be seen from (6.28), $\epsilon(k) \to 0$ as k increases. Therefore, the inequality (6.27) becomes arbitrarily close to (6.14f) as a local optimum is approached on the boundary. It is also clear that an x^{k+1} that satisfies (6.14b), (6.14c), (6.14d), (6.14e) and (6.27), is also in the set $E \cap \mathbb{F}$.

The type of line search used in this paper is partly inspired by the Armijo rule from the Wolfe conditions and Backtracking line search principles.

An Armijo method enforces a sufficient descent in the objective along the descent direction (Bertsekas, 1999). Since a full step will not necessarily maintain strict feasibility of all constraints, instead it is only required that $f(\cdot)$ decreases. For

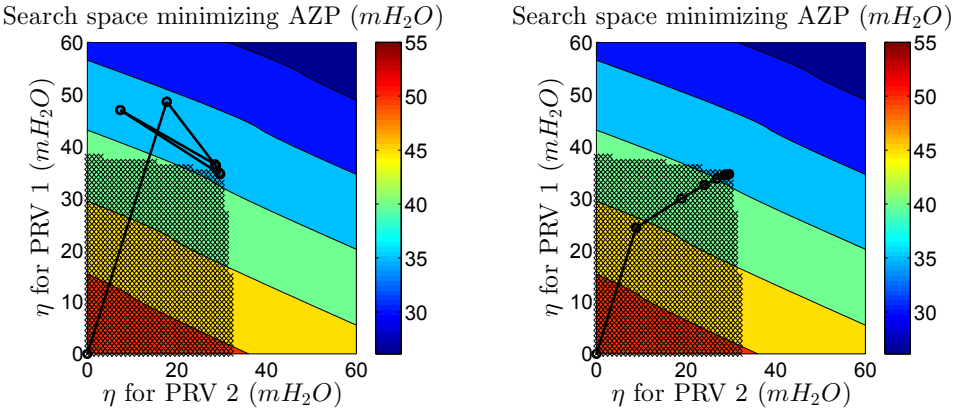
practical purposes this works well, since $f(\cdot)$ decreases rapidly along the search directions $\Delta\eta^k$ as seen in Figure 6.4a, and quickly gets very close to a local minimum.

In Backtracking line searches, initially the full step is taken (i.e. $\alpha = 1$) and subsequently reduced until a stopping condition is satisfied (Boyd and Vandenberghe, 2004). The same principle is used in this paper by first taking a unit step ($\alpha = 1$) and updating α subsequently until the line search stopping criteria are satisfied. The stopping criteria is that the next iterate is feasible ($\mathbb{E} \cap \mathbb{F}$) and that it has a lower objective.

The line search is carried out using a two step process as follows. For the first iteration of the line search, $\alpha = 1$ and

1. Compute $f(\cdot, \eta^k + \alpha\Delta\eta^k)$
2. IF $f(\cdot, \eta^k + \alpha\Delta\eta^k) < f(\cdot, \eta^k)$ AND the next iterate is feasible, then $\eta^{k+1} = \eta^k + \alpha\Delta\eta^k$ ELSE set $\alpha = \alpha/2$, return to return to step 1

A comparison of the convergence of the SCP method and SFSCP method is shown in Figure 6.5. In Figure 6.5a, the SCP method does not converge after the iterates go outside of the strictly feasible set. The SFSCP method improves the convergence as shown shown in Figure 6.5b. Here it is guaranteed that each step both decreases $f(\cdot)$ and is strictly inside the feasible set $\mathbb{E} \cap \mathbb{F}$ shown by the shaded area. In the latter iterations of the optimisation, allowing the $\epsilon(k)$ to become sufficiently small enables the solutions to get arbitrarily close to the local optima. A practical stopping criteria that the relative decrease in the objective function is within some tolerance λ_{tol} is used here, i.e. termination is triggered when $\frac{f^k - f^{k+1}}{f^k} < \lambda_{tol}$. In the examples, it was found that a value of 10^{-3} for λ_{tol} was sufficiently small. The SFSCP method is summarised in Algorithm 3, where a hydraulic simulation that solves (2.5) and (2.2) is denoted by HS.



(a) SCP

(b) SFSCP

Figure 6.5: (a) Cycling in convergence in an infeasible area when using SCP (b) Strictly feasible steps to aid convergence in SFSCP

Input: Network parameters (A_{12}, A_{21}, A_{10}, A_{13}, h_0, d, r)
Result: Optimal valve settings (η)
Initialization: Set $\eta = 0$, $k = 1$;
h^k, $q^k \longleftarrow$ Algorithm 1 with input (η^k);
while $(f^k - f^{k+1})/f^k > \lambda_{tol}$ **and** $k \leq k_{max}$ **do**
    $\eta \longleftarrow$ Step 2, Sub-problem A;
    $\Delta\eta^k \longleftarrow \eta - \eta^k$;
    Set $\alpha = 1$;
    h^{k+1}, $q^{k+1} \longleftarrow$ Algorithm 1 with input ($\eta^k + \alpha\Delta\eta^k$);
    while $f^{k+1} > f^k$ **or** $x^{k+1} \notin \mathbb{E} \cap \mathbb{F}$ **do**
        $\alpha \longleftarrow \alpha/2$;
        h^{k+1}, $q^{k+1} \longleftarrow$ Algorithm 1 with input ($\eta^k + \alpha\Delta\eta^k$);
    end
    $\eta^{k+1} \longleftarrow \eta^k + \alpha\Delta\eta^k$;
    $k \longleftarrow k + 1$
end

Algorithm 3: SFSCP

6.5 Results

6.5.1 Small Illustrative Example

The developed SFSCP optimisation algorithm is first demonstrated by optimising valve settings for a variant of the simple network presented in Todini (2003). The network is modified slightly to include a single PRV at the inlet to the network as shown in Figure 6.6. This small illustrative network serves two purposes. First it shows how an optimisation method works for PRV control, and second it provides an example network that is replicable.

The network consists of 9 variable head nodes with an allocated demand that varies according to a data-derived time-dependent demand factor (shown in Figure 6.7). The network has one critical point indicated in Figure 6.6, which does not move spatially with the diurnal demand factor. The node and link properties of this network are shown in Table 8 and Table 9 respectively.

The developed SFSCP optimisation algorithm for minimizing AZP was applied to this network and the optimised PRV settings are shown in Figure 6.7. The minimum allowable pressure P_{min} is set to $20mH_2O$ and the optimal solution shows this pressure is maintained at the critical point node throughout the extended period simulation (Figure 6.7). As expected, the outlet pressure of the PRV increases as the demand increases in order achieve P_{min} consistently at the critical point.

The SFSCP algorithm converged at every time step. Out of the 96 steady state NLPs, 80 NLPs converged in 10 iterations and 16 NLPs converged in 9 iterations. In comparison to (Wright et al., 2014*a*) where the SCP method was applied to the same network, convergence was achieved for every NLP with 2 iterations to exactly the same solution. This demonstrates that, whilst SFSCP has strong improvements in convergence for complicated, large scale networks, it adds unnecessary complexity and computational effort for small networks. On the other hand, since the network is small, the additional computational time required to solve the network is minor.

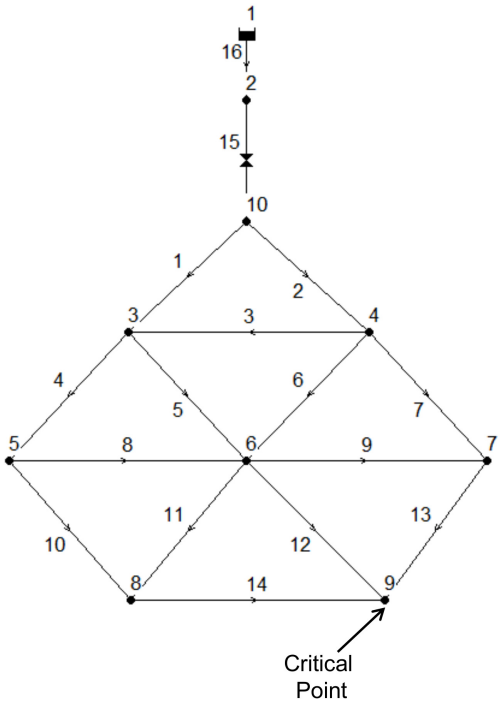


Figure 6.6: Small illustrative example network taken from Todini (2003)

Node	Elevation (m)	Demand (l/s)
1	150	-98
2	85	0
3	80	2
4	90	2
5	70	4
6	80	30
7	90	30
8	90	20
9	100	10
10	85	0

Table 8: Details of the nodes in the simple example shown in Figure 6.6

Link	Length (m)	Diameter (mm)	HW Coefficient
1	1000	300	65
2	1000	500	65
3	1000	150	70
4	1000	250	70
5	1000	200	70
6	1000	200	65
7	1000	250	65
8	1000	150	80
9	1000	150	90
10	1000	250	70
11	1000	150	80
12	1000	150	65
13	1000	200	65
14	1000	150	65
15 (PRV)	n/a	400	n/a
16	1000	500	65

Table 9: Details of the links in the simple example shown in Figure 6.6

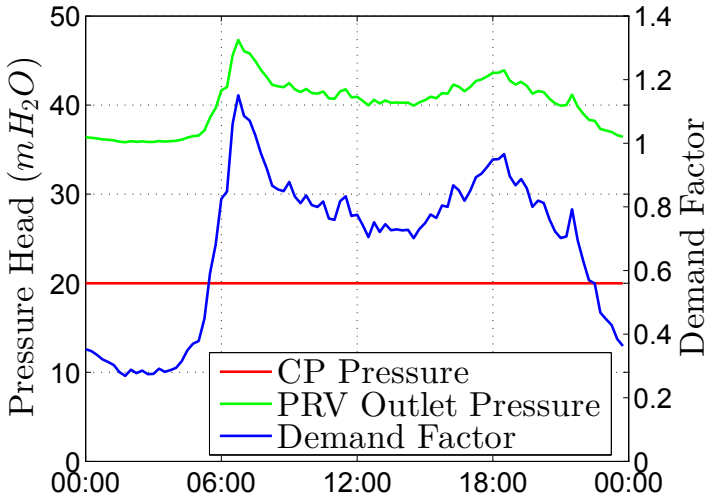


Figure 6.7: Optimisation results for small illustrative network shown in Figure 6.6

6.5.2 Experimental Programme Network (2 PRVs + 2 PRV Boundary Valves)

In this sub-section, SFSCP is applied the the experimental programme network, shown in Figure 6.8, where the dynamic boundary valves are simulated as PRVs (i.e. an optimal outlet pressure is to be determined by SFSCP). The network

consists of 2,374 nodes, 2,434 link, 2 PRVs and 2 dynamic boundary valves (acting as PRVs).

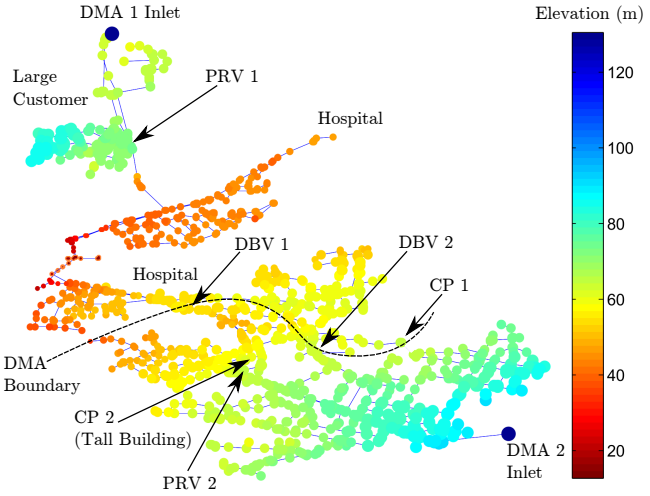


Figure 6.8: The hydraulic model of the network where the experimental programme is located. In this model, 2 PRVs are active.

Modelling the dynamic boundary valves as PRVs is similar to to the approach used in many case studies for multi-feed network control (Section 4.2.2), where mutliple PRVs supply a zone, and close if not required. The PRVs used in SFSCP must have a flow direction selected (Section 6.4.1). Generally all PRVs, and most DBVs, will have a very well defined flow direction. However, it is still possible to explore the optimisation search space for better local optimal points. One example of this is shown in Figure 6.9. Here, the flow direction of DBV 1 is explored by calculating optimal valve settings for an extended period simulation and comparing the optimal objective function (AZP). In Figure 6.9, it is clear that DBV 1 with a northerly flow direction facilitates a lower AZP in the network.

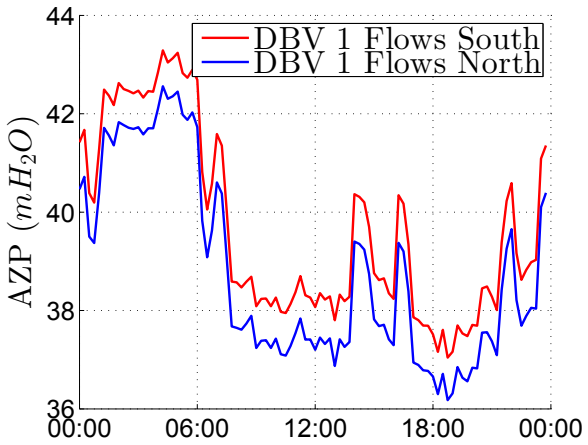
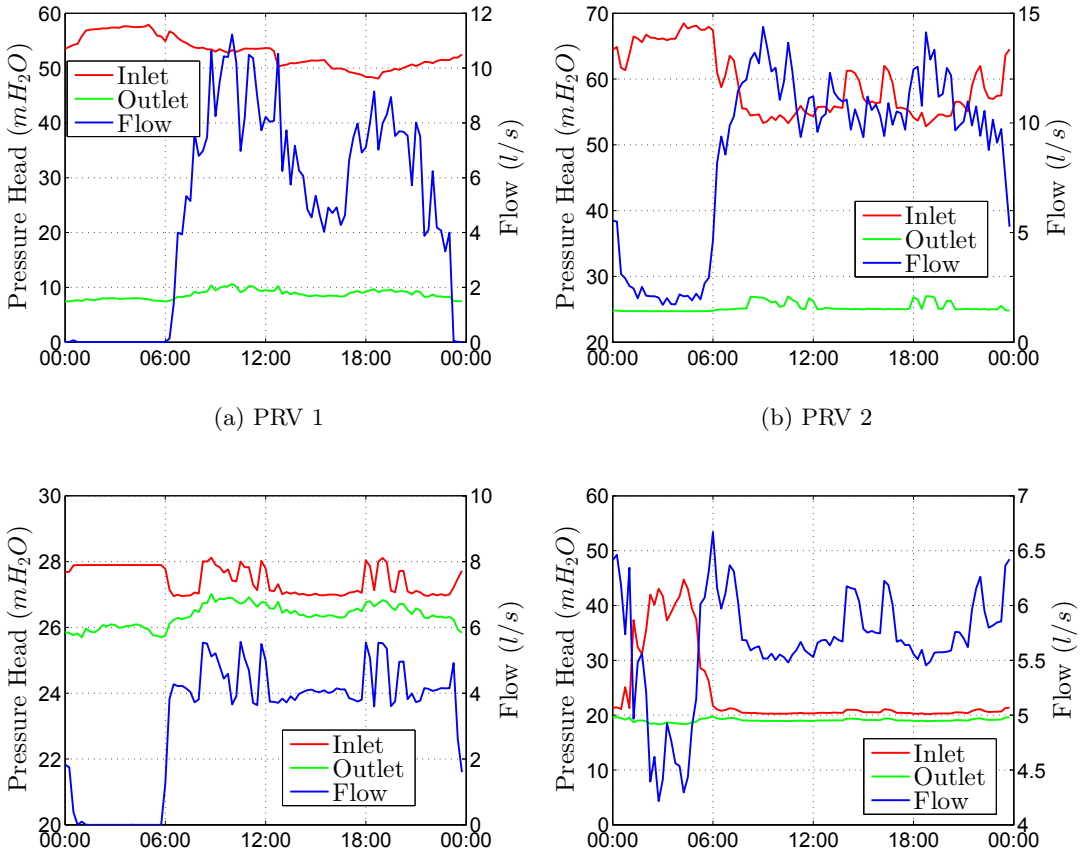


Figure 6.9: Exploring the solution search space. A more optimal AZP is achieved if DBV 1 controls pressure and flow in a northwards direction.

The control results for minimising the AZP in the experimental programme network are shown in Figure 6.10. Both PRV 1 and PRV 2 (Figure 6.10a and Figure 6.10b respectively) greatly reduce pressure at their outlets in order to minimise AZP. At the dynamic boundary valves, the pressure reduction is equal to that of a fully open valve (i.e. η is zero) from approximately 06:00-11:30 (Figure 6.10c and Figure 6.10d). This result is expected, since demand is high during the day and frictional energy losses should be reduced by increasing redundancy in the network as much as possible (i.e. by opening the boundary valves fully). During the night, it is observed that the head drop across DBV 2 increases, therefore the boundary valves is now partially closed. At DBV 1, the flow drops to zero, therefore this boundary valve is closed.



(a) PRV 1

(b) PRV 2

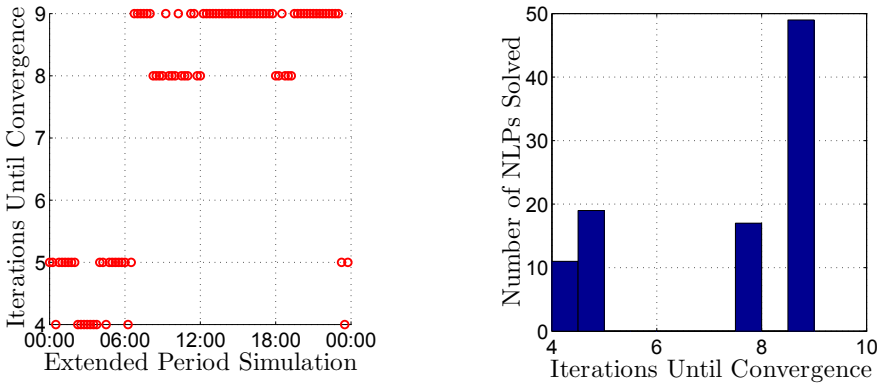
(c) DBV 1

(d) DBV 2

Figure 6.10: Optimal PRV settings for the experimental programme operating with 2 PRVs and 2 dynamic boundary valves

The convergence of the SFSCP algorithm that obtained the results in Figure 6.10 is shown in Figure 6.11. Every NLP out of 96 (which represents a single day split into 15 minute single period simulations) converged successfully. In Figure 6.11b, a histogram shows that the iterations required for convergence range from 4 to 9, with an average value of 7. In Figure 6.11a, it is shown that more iterations are required during day time hours when demand is high. The opposite behaviour

was observed with the SLP method presented by Germanopoulos and Jowitt (1989), where more iterations were required during low demand hours.



(a) EPS

(b) Occurrence of required iterations

Figure 6.11: Convergence of SFSCP plotted as (a) an extended period simulation which shows more iterations seem to be required during day time hours and (b) a histogram showing that the iterations required range from 4 to 9, with an average value of 7.

In Chapter 5, the optimal operation of a dynamic topology is compared with two other network configurations. These configurations, with reference to Figure 6.8, are as follows:

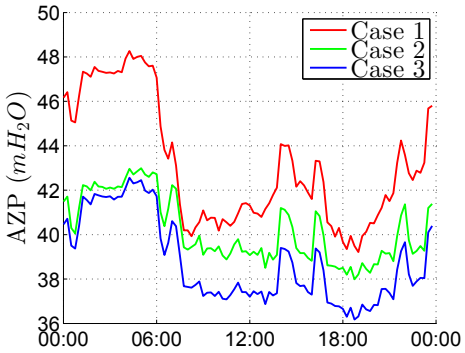
- Closed boundary valves and constant outlet PRVs (PRV 1 and PRV 2) i.e. the most typical form of pressure management
- Closed boundary valves and modulating PRVs (PRV 1 and PRV 2) i.e. an advanced form of pressure management that is emerging (Section 3.7.3)
- Optimised valve settings at PRV 1, PRV 2, DBV 1, DBV 2 (dynamic topology).

The PRV settings for case one are chosen so that the pressure at the CP 1 during peak demand hours is close to but does not violate the minimum allowable pressure ($15mH_2O$). For case two, settings for PRV 1 and PRV 2 are determined using the SFSCP method. For case three, the dynamic topology, settings for PRV 1, PRV 2, DBV 1, and DBV 2 are all determined using the SFSCP method.

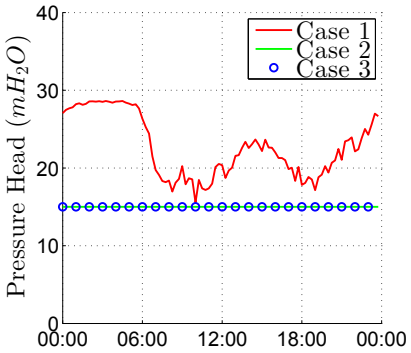
The comparison of the three cases is shown in Figure 6.12 and Table 10. Day-time hours are defined as 06:00-21:00 and night time hours as 21:00-06:00. The following observations are made:

- The pressure at the critical point Figure 6.12b is consistently controlled at the minimum allowable pressure in the network ($15mH_2O$) for case 2 and case 3. This is expected, since the SFSCP method was used in case 2 and case 3 to minimise pressure in the network.

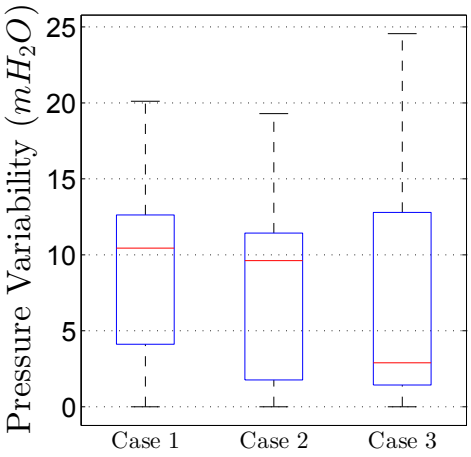
- Although pressure at the critical point is identical for case 2 and case 3, operating a dynamic topology (case 3) reduces day time AZP by approximately $2mH_2O$ over case 2. This is a similar reduction in AZP between case 1 and case 2 (i.e. switching from fixed outlet PRVs to flow modulating PRVs in a closed topology network) as shown in Table 10.
- In percentages, compared to case 1, case 2 reduces daytime AZP by 4.8%, and case 3 reduces daytime AZP by 8.9%.
- During peak demand hours, the pressure management performance of flow modulation (case 2) is similar to the fixed outlet configuration (case 1), as shown in Figure 6.12a. This is because fixed outlet PRVs are configured to supply enough pressure at peak demand times. At non peak demand times, a fixed outlet PRV therefore typically supplies too much pressure in the network, whereas flow modulating PRVs can be configured to reduce excess pressure at all times. At night time, this is most apparent. Table 10 shows that AZP during the night for case 1 is $4.5mH_2O$ higher than the flow modulating PRV configuration (case 2).
- The pressure variability is plotted in Figure 6.12c. Although approximately 12.5% of nodes experience a higher pressure variability in case 3, the mean pressure variability for case 3 is lower ($7.3mH_2O$ in case 3 compared to $7.8mH_2O$ and $9.6mH_2O$ for cases 1 and 2 respectively). The lower pressure variability can be attributed to the lower frictional energy losses occurring in a multi-feed network (case 3). Consequently, the optimal outlet pressure at PRVs is lower. The nodes that experience a higher pressure variability are located around DBV 2, which closes at night and causes a change in pressure upstream (as shown in Figure 6.10d).
- The pressure variability of case 1 and case 2 is similar (Figure 6.12c). This might be due to the fact that, whilst a fixed outlet PRV keeps pressure upstream of the network constant (i.e. at the PRV outlet), a flow modulating PRV keeps pressure downstream of the network constant (i.e. at the CP). Depending on the network, this is likely to result in a similar pressure variability in both configurations.



(a) AZP



(b) CP 1 Pressure



(c) Dirunal Pressure Variability

Figure 6.12: Optimal PRV settings

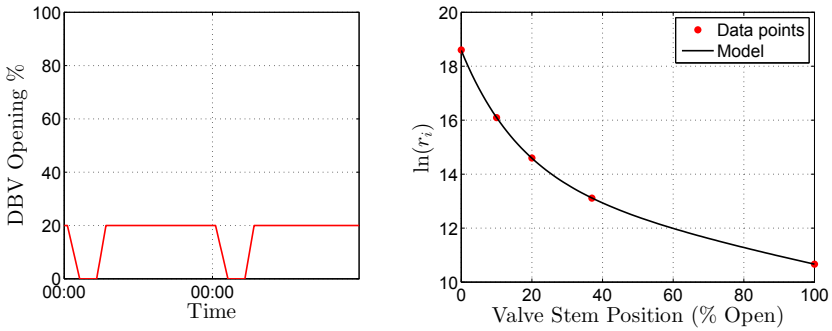
Table 10: Summary of pressure management results for the operation of the experimental programme under three different configurations

	Case 1	Case 2	Case 3
AZP (Day) (mH_2O)	41.5	39.5	37.8
% Reduction compared to Case 1	n/a	4.8%	8.9%
AZP (Night) (mH_2O)	46.0	41.5	40.6
% Reduction compared to Case 1	n/a	9.8%	11.7 %
Mean Pressure Variability $\overline{P}_{var,j}$ (mH_2O)	9.6	7.8	7.3
% Reduction compared to Case 1	n/a	18.8%	24.0%

6.5.3 Experimental Programme Network (2 PRVs + 2 Position Control Boundary Valves)

In Section 6.5.2, optimal open loop PRV settings were determined for the dynamic boundary valves in the experimental programme. The open loop optimal PRV settings indicated that the dynamic boundary valves should be fully opened from approximately 06:00-11:30 (Figure 6.10c and Figure 6.10d), and either closed or partially closed at other times (night). In addition, leakage monitoring is undertaken at night, and the dynamic boundary valves should close to facilitate a more accurate estimation. Finally, in Section 4.3.2, it was established that the dynamic boundary valves are well suited to being controlled as stem position control valves, which would provide a prompt response to failure, irrespective of which DMA the failure occurs. Based on all these conclusions, the dynamic boundary valves are modelled as position control valves with an open-loop position schedule, and optimal valve settings are calculated for all other PRVs in the network.

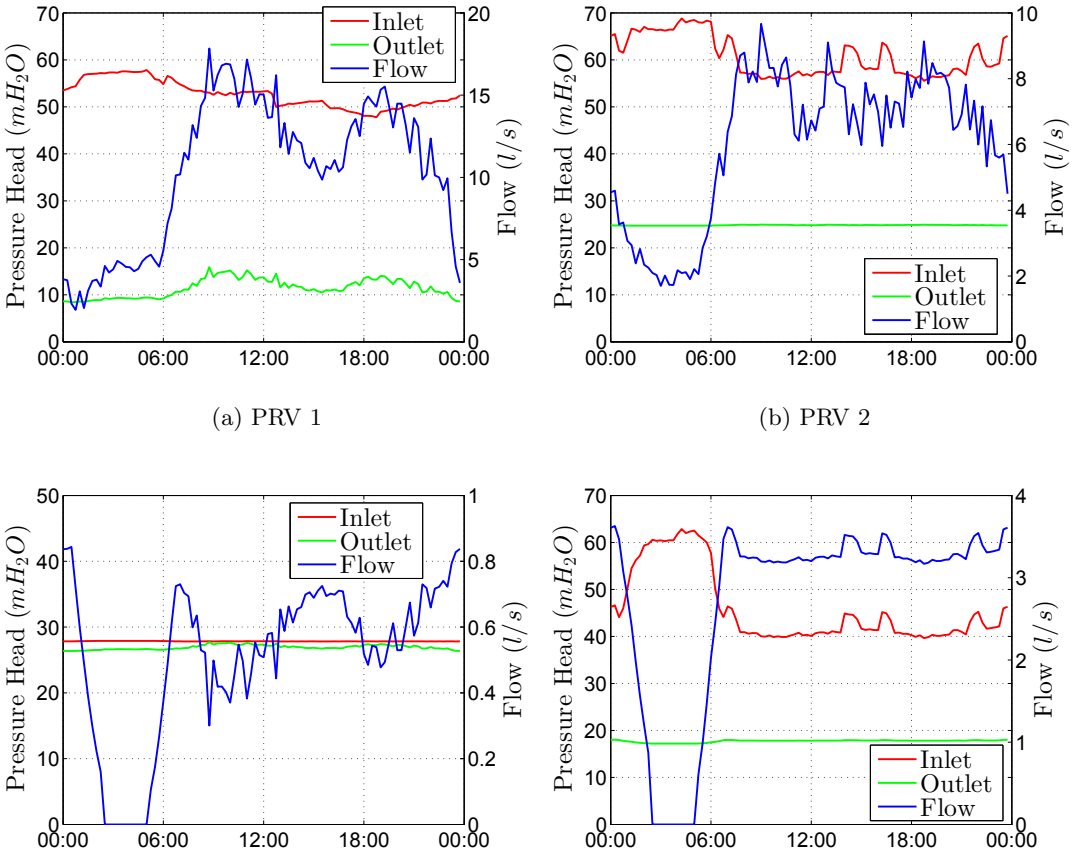
For the experimental investigation of the dynamic topology (Chapter 5), the dynamic boundary valves are limited to an opening of 20% in order to safely test the technology and slowly introduce the network to new flow reversals. This sub-section therefore outlines the application of SFSCP when the dynamic boundary valves open to 20% daily, and close at night. The opening schedule is shown in Figure 6.13a. Since the valve resistance $r \in \mathbb{R}^{n_v}$ now changes according to the opening schedule (Section 2.7), a relationship between the opening % and $r \in \mathbb{R}^{n_v}$ must be determined. This was done by fitting a curve to known data points of flow against valve head drop, either acquired from the experimental programme or from the valve manufacturer. The valve stem position - resistance model is shown in Figure 6.13b. Therefore, for each NLP solved with SFSCP in the optimised extended period simulation, the valve resistance is updated in the model according to the opening schedule (Figure 6.13).



(a) DBV Schedule (b) DBV Model

Figure 6.13: (a) A stem position opening schedule for the control of the dynamic boundary valves and (b) a valve model fitted to the available data points from the experimental programme

The optimised PRV outlet pressure profiles are shown in Figure 6.14a and Figure 6.14b. It is observed that each PRV outlet pressure is correlative to the PRV flow, therefore it is possible to establish and implement a flow modulation curve, i.e. the relationship between outlet pressure and flow. This facilitates near optimal valve settings to be actuated locally on each PRV. The flow modulation curves constructed are shown in Figure 6.15. The hydraulic simulation results for the boundary valves are shown in Figure 6.14c and Figure 6.14d. It is seen that the dynamic boundary valves provide a route for water between the two DMAs during the day, therefore minimising frictional energy losses in the network. At night the boundary valves close down automatically and the flow between DMAs reduces to zero, which facilitates an accurate and simplistic minimum night flow analysis.



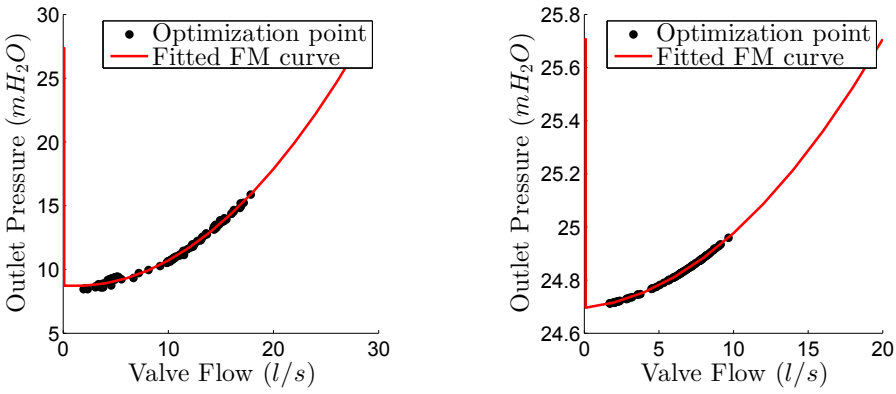
(a) PRV 1

(b) PRV 2

(c) DBV 1

(d) DBV 2

Figure 6.14: Optimal PRV settings for the experimental programme operating with 2 PRVs and 2 dynamic boundary valves opening to 20% as shown in Figure 6.13a.



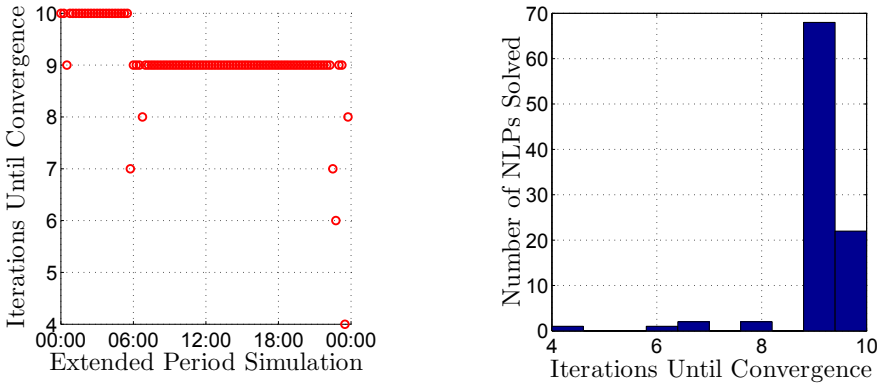
(a) PRV 1

(b) PRV 2

Figure 6.15: Fitted flow modulation curves to PRV 1 and PRV 2 open loop settings from Figure 6.14

The convergence of optimising two PRVs whilst two dynamic boundary valves follow a position control schedule is shown in Figure 6.16. In every NLP, the

SFSCP algorithm converges, most commonly with 9 iterations. The inclusion of position control valves does not therefore affect the stability in convergence of SFSCP.



(a) EPS

(b) Occurrence of required iterations

Figure 6.16: Convergence of SFSCP when DBVs follow an open loop stem position schedule. (a) An extended period simulation that shows the iterations required at each time step and (b) a histogram showing the most common number of iterations required for convergence

6.5.4 Experimental Programme Network (3 PRVs + 2 Position Control Boundary Valves)

In this sub-section, the experimental programme network is used to investigate the following:

- The network performance if the boundary valves are opened beyond 20%
- The performance of the network when a new PRV (called PRV 3), which was installed at the inlet to DMA 2, becomes operational (as explained in Section 5.4).
- Extensive testing of the convergence of the SFSCP algorithm.

The network, with PRV 3 installed, is shown in Figure 6.17. Optimal valve settings are determined for PRV 1 - 3 over a 24 hour period. The dynamic boundary valves follow the predefined opening/closing schedule (open 07:00 - 00:30 and fully shut 02:30 - 05:30), using the valve opening-resistance relationship in Figure 6.13b to update the model parameters for the dynamic boundary valves. As before, the 24 hour period is discretized into 15 minute steady state periods, which results in 96 separate NLPs to solve. This process is then repeated for 11 different levels of BV % opening ranging from 0% (i.e. a closed topology DMA network with optimal flow modulating PRVs) and 100%. In total, 1056 NLPs are solved reliably and efficiently, with the SFSCP algorithm converging in 9 iterations on average. In Figure 6.18, the convergence of SFSCP (blue

line), in comparison to SCP (red line), is compared for the optimal control of three PRVs. The 3D search space represents the objective function f and the hydraulically feasible set $\mathbb{E}$, and the shaded region represents the operationally and hydraulically feasible set $\mathbb{E} \cap \mathbb{F}$. It is observed that SFSCP efficiently finds an optimal point on the edge of the feasible space $\mathbb{E} \cap \mathbb{F}$, whereas SCP cycles in the infeasible search space and does not converge.

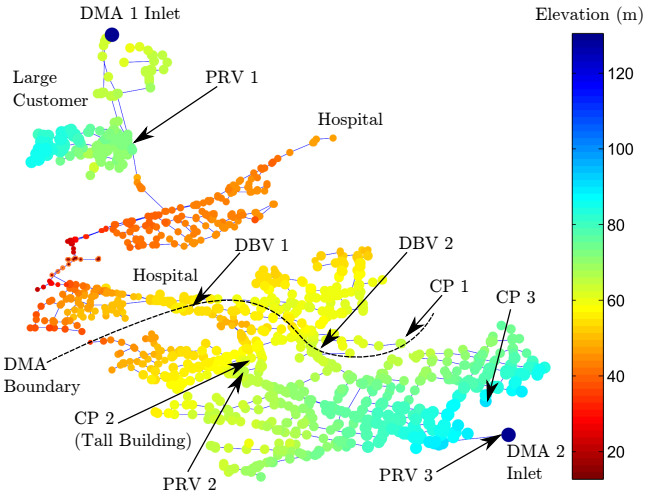


Figure 6.17: The hydraulic model of the network where the experimental programme is located. In this model, 3 PRVs are active.

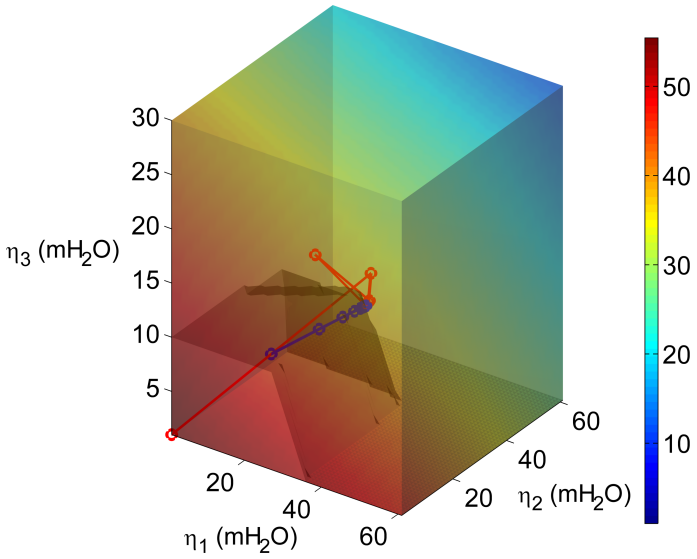
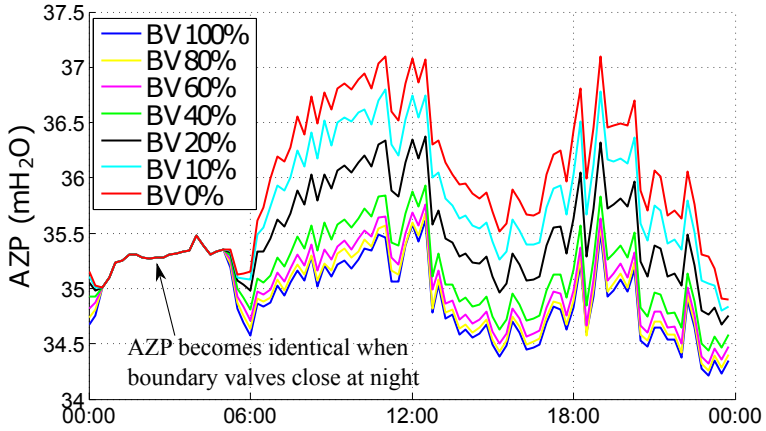


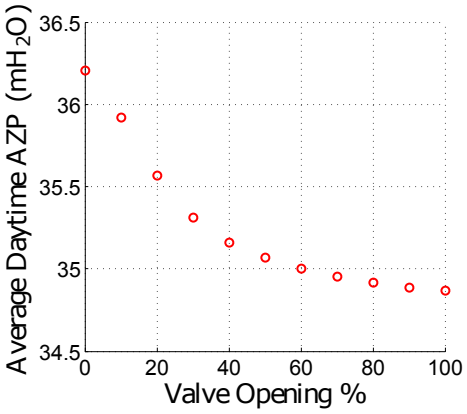
Figure 6.18: Search space of AZP showing the convergence properties of SCP (red line) and SFSCP (blue line) (Wright et al., 2015*d*)

The AZP throughout the 24 hour period at different % BV openings are shown in Figure 6.19a. It is seen that when the boundary valves are allowed to open further, the optimally controlled AZP reduces. The difference between opening 0% (i.e. a closed DMA topology) and 100% opening is 3.7%, which is an AZP reduction of approximately $1.5mH_2O$. At night, when the boundary valves close

down during the operation of a dynamic topology, the AZP becomes equivalent in all simulations. In order to simplify results, the average daytime AZP (07:00 - 00:00) is plotted in Figure 6.19b for different BV % openings.



(a) AZP over 24 hours



(b) Average daytime AZP

Figure 6.19: AZP results when the SFSCP algorithm is applied to the experimental programme network for different levels of dynamic boundary valve opening %. (a) AZP over a 24 hour period and (b) average daytime AZP.

6.6 Comparison with Other Optimisation Approaches

In this sub-section, the convergence of SFSCP is compared with three other optimisation approaches, all of which are used to minimise AZP. The comparison is made in order to highlight the benefit of restricting the iterations of the SFSCP to the feasible (hydraulically and operationally) set. The three other optimisation methods in the comparison are:

1. Sequential linear programming (SLP), using linear theory to linearise (6.14b) in the original NLP. This approach is identical to that presented in (Germanopoulos and Jowitt, 1989; Jowitt and Xu, 1990), except for the difference in the valve model used, difference in objective function, and use of demand/head driven leakage modelling. In this method, warm starting is used. This method is denoted "SLP-LT".

2. Sequential linear programming (SLP), using a first order Taylor expansion to linearise (6.14b) in the original NLP. This approach is identical to that presented in (Bargiela, 1984), except for the difference in the valve model used and difference in objective function. In this method, warm starting is used. This method is denoted "SLP-NR".

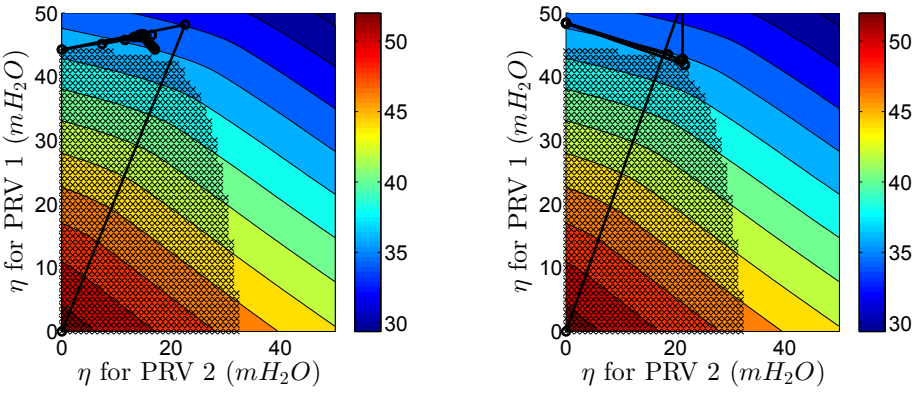
3. Sequential convex programming (SCP), using linear theory to linearise (6.14b) in the original NLP. This approach is identical to that presented in (Wright et al., 2014*a*). Warm starting is inherent in this method. This method is denoted "SCP-LT".

The network model used for the comparison is the experimental programme network. The network is shown in Figure 6.8 and has the following configuration:

- A single period, steady-state snapshot of the network is considered, representing peak demand at 08:15 in the morning;
- The dynamic boundary valves (DBV) are open to a fixed position of 80%
- The optimisation method finds the optimal outlet pressure for PRV 1 and PRV 2 for the single-period network, where the objective function is the minimisation of AZP, as shown in (6.14a).
- A minimum allowable pressure of $15mH_2O$ is placed at all nodes with a customer connection.

The iterations and convergence for the network configuration detailed above are shown in Figure 6.20. Only SFSCP converges to a local optimum, whereas all other optimisation approaches tested failed to converge. Out of all methods, SLP-LT performed most poorly. This is likely to be related to the type of linearisation used in LT, where gradient information is not used (Todini and Rossman, 2012). Although the iterations of SLP-NR and SCP-LT come close to the optimal point, their progress is not steady, and the next iterations results in a point that is very far from the optimal point and in an infeasible area.

In addition to this test, the optimisation approaches are tested for another single period at 12:00. PRV settings are once again determined, all other parts of the test are identical to before. The results of the comparison of optimisation methods are shown in Table 11. This time, SLP-NR and SCP-LT did converge, along with SFSCP. SLP-LT, which had the poorest performance from the first test, once again did not converge. Aside from this, all optimisation methods converged to the same optimal point, with identical PRV settings and objective function value. SCP-LT converged the fastest, in 3 iterations, and SFSCP and SLP-NR converged in 9 iterations.



(a) SLP-LT

(b) SLP-NR

(c) SCP-LT

(d) SFSCP

Figure 6.20: A comparison of optimisation methods. The contours represent the objective function (AZP) and hydraulically feasible set $\mathbb{E}$, where PRV settings η are varied along each axis. The shaded area represents the operationally and hydraulically feasible set $\mathbb{E} \cap \mathbb{F}$. The black line is the iteration path of the optimisation solver for (a) SLP-LT, (b) SLP-NR, (c) SCP-LT and (d) SFSCP.

Table 11: Comparison of optimisation methods for another steady simulation where all methods except SLP-LT converge to the same local optimal point

Method	Objective Func. (mH_2O)	PRV Settings η^T (mH_2O)	Iterations for convergence
SLP-LT	n/a	n/a	100
SLP-NR	36.51	[43.8, 22.4]	9
SCP-LT	36.51	[43.8, 22.4]	3
SFSCP	36.51	[43.8, 22.4]	9

6.7 Conclusion

The dynamic aggregation of DMAs results in the formation of very large networks, complicated further by interaction between multiple sources, control valves and large consumers that impact the hydraulic conditions extensively. Consequently, an optimisation method for valve control that is computationally efficient and converges reliably is required in such networks.

In this chapter, an optimisation algorithm based on SCP for valve control is outlined that is computationally efficient, and provides good convergence properties in comparison to other optimisation methods, such as linear theory or Newton based SLP. The SCP method achieves reliable convergence by guaranteeing that each iterate is strictly within a hydraulically and operationally feasible set, therefore it is termed strictly feasible SCP. SFSCP also takes advantage of efficient LP solvers and null space algorithms and can therefore be used for networks ranging from small to very large in size.

In order to take advantage of the computational efficiency of null space algorithms, a novel approach to including control valves in the hydraulic model constraints has been developed. The valve model is fully convex, therefore the optimisation search space, which is non-convex due to the head loss relationship of pipes, can also be more efficiently searched for a better local or the global optimum. It is proposed that this approach is more efficient for finding better optimal points than repeatedly solving the optimisation problem with different, random starting points as required by other approaches where the valve model is non-convex.

The SFSCP algorithm is used to optimise control valves in the experimental programme network. The optimal open-loop schedules can be used to create flow modulation curves, which are used for actuating control in the experimental investigation (Chapter 7). Based on the optimisation and modelling results alone:

- Daytime AZP reductions of 8.9% ($3.7mH_2O$) can be achieved when operating a network with dynamic topology compared to a closed topology network controlled with two fixed outlet PRVs (the most common approach to pressure management).
- AZP reductions of 4.3% ($1.7mH_2O$) are made with a dynamic topology in comparison to a closed topology network optimally controlled with two flow modulating valves (an emerging form of advanced pressure management), i.e. the reductions in daytime AZP achieved going from fixed to flow modulating PRVs on a closed topology network, is approximately the same reduction as going from flow modulating PRVs to a dynamic topology.

- AZP reductions of 3.7% ($1.5mH_2O$) can be achieved when operating a network with dynamic topology, in comparison to a closed topology network optimally controlled with three flow modulating valves.

Future work on valve control could focus on further comparisons of optimisation algorithms, particularly GRG. The comparison should include both reliability in convergence and computational speed. The use of alternative objective functions for valve control related to performance indicators such as resilience to failure and water quality is also a relatively unexplored area of research.

7 Experimental Investigation of Pressure Management and Network Resilience

7.1 Introduction

This chapter details the three week, phased experimental implementation of different network configurations in a real, operational network (Chapter 5), and analyses their performances. The phases/configurations are:

- Phase 1: Closed, static DMA boundary and two fixed outlet PRVs. This is the most commonly implemented form of pressure management used by water companies to reduce leakage and future bursts (Section 3.7.1).
- Phase 2: Closed, static DMA boundary and two flow modulating PRVs. This is an emerging form of advanced pressure management that is less common but is gaining popularity (Section 3.7.3).
- Phase 3: Dynamic DMA boundary and two flow modulating PRVs. This approach has been shown analytically to provide further pressure reductions and better resilience to failure in comparison to closed DMA approaches.

Each phase was in operation for one week, where 2 days were used to set up and test that the equipment was operating correctly, and the experimental investigation was carried out over the remaining 5 days. The 5 day periods are as follows:

- Phase 1: Wednesday 23rd – Sunday 27th July 2014
- Phase 2: Wednesday 17th – Sunday 21st September 2014
- Phase 3: Thursday 9th – Monday 13th October 2014

Two aspects of operation were investigated over the 5 day period:

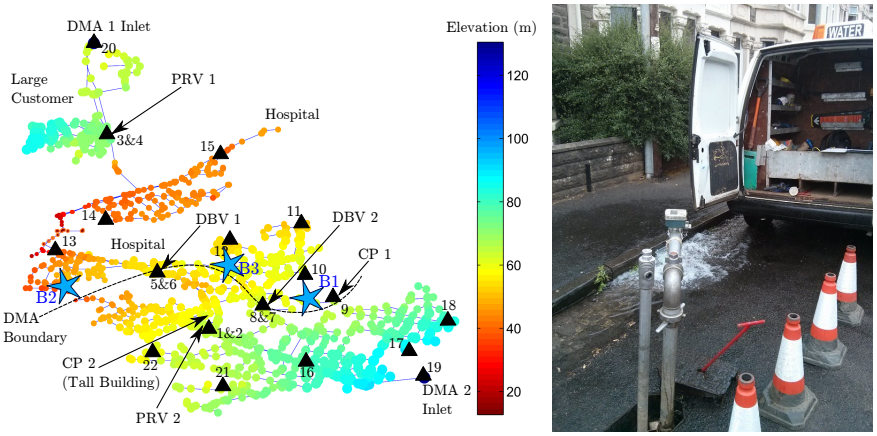
- The pressure management performance and associated leakage performance. The pressure management is assessed just for a single, weekend day for each phase, and is detailed in Section 7.2. The total water input over each 5 day phase is also used in the investigation in order to estimate leakage rates.
- The resilience of failure to medium sized, artificially generated bursts in the network, created by operating fire hydrants (Figure 7.1b). Three bursts, each at different locations as shown in Figure 7.1a, were generated for each phase. The first two bursts were generated on Day 1 of the 5 day phase, and the final burst was generated on day 2 of the 5 day phase. The artificial burst and resilience assessment is carried out in Section 7.4.

In addition to the planned artificial bursts, a real, major burst occurred on a 35 inch trunk main, upstream of the inlet to DMA 2. Consequently, thousands of customers were disconnected from their water supply across many DMAs of the network. At the time, the experimental programme was being prepared for phase 3, and a dynamic topology was in partial operation with just one dynamic boundary valve opening daily. The inlet pressure at DMA 2 was affected by this incident, and the resilience of the (partially operating) dynamic DMAs is assessed in Section 7.4.2.

7.2 Pressure Management

In this subsection, each phase is experimentally investigated to establish its performance for:

- AZP;
- Average diurnal pressure variability $\overline{P}_{var}$;
- Leakage estimates using the minimum night flow (Farley and Trow, 2003);
- Flow reversals.



(a) Locations of the artificial bursts and loggers

(b) Artificial bursts generated by operating fire hydrants

Figure 7.1: (a) Elevation plot of the experimental programme network and its schematic, InfraSense TS locations (black triangle), and artificial burst locations (blue star) created by operating fire hydrants and (b) a photograph of the artificial bursts generated by operating fire hydrants.

The specific set up of the each phase/configuration, with reference to Figure 7.1a, is as follows:

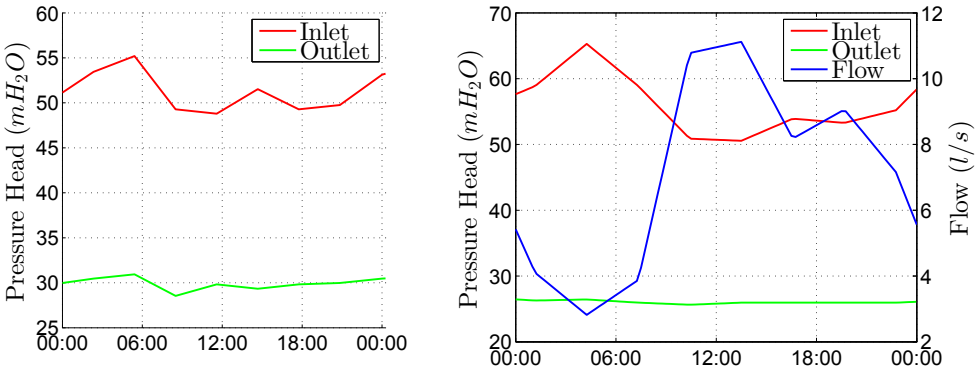
- Phase 1: The boundary valves DBV 1 and DBV 2 are closed at all times. The two DMAs are therefore not hydraulically connected. PRV 1 has a fixed outlet pressure of $30mH_2O$ which results in a pressure at CP 1 during

peak demand hours of approximately $20mH_2O$. The minimum allowable pressure at this node is $15mH_2O$. The approximate buffer of $5mH_2O$ is to proivde the network with some additional resilience in the case of failure. Excess network pressure is one way to increase the network's resilience to failure (Todini, 2000).

- Phase 2: As with Phase 1, boundary valves DBV 1 and DBV 2 are closed at all times. PRV 1 and PRV 2 follow a flow modulation look up table which was obtained using a hydraulic model and SFSCP optimisation method (Section 6.4.7). The flow modulating PRVs results in a consistent pressure at CP 1 of approximately $15mH_2O$, which is the minimum allowable pressure. The network can operate closer to the minimum allowable pressure (unlike configuration 1) because flow modulating PRVs will react to some failure situations such as bursts and fire flow by increasing the outlet pressure due to the increase in monitored flow (Section 3.7.3).
- The operation of phase 3 introduces a dynamic boundary. DBV 1 and DBV 2 open to 20% during the day, and automatically shut at night between 02:00-05:00 so that leakage monitoring practices can be undertaken. PRV 1 and PRV 2 also use flow modulation curves calculated using SFSCP. As before, flow modulation results in a consistent pressure at CP 1 of approximately $15mH_2O$.

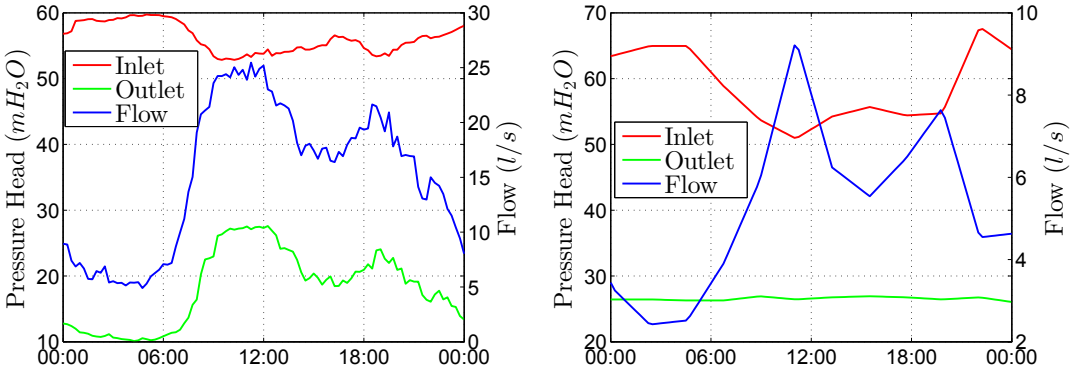
7.2.1 AZP and Pressure Variability

The AZP and pressure variability are assessed for a single day (different to the days where artificial bursts are generated). The data collected at PRV 1 and PRV 2 for phase 1 and phase 2 are shown in Figure 7.2 and Figure 7.3 respectively, and data for PRV 1, PRV 2, DBV 1 and DBV 2 are shown in Figure 7.4. The data presented is generally acquired from the InfraSense loggers (Figure 7.1a), however at times the data from these were unavailable, and instead data from the Cla-Val loggers (Section 5.4.1) was used instead, which has a lower sampling rate.



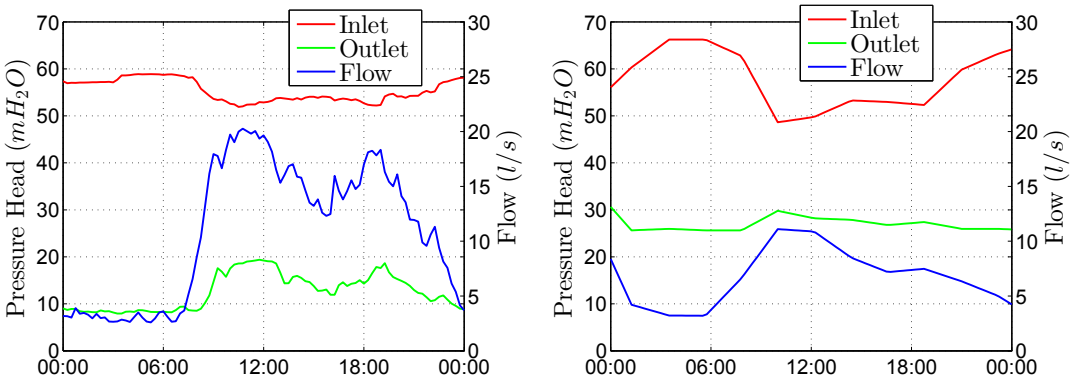
(a) PRV 1 (b) PRV 2

Figure 7.2: Data at the control valves during phase 1. Flow data is unavailable at PRV 1 for this period.



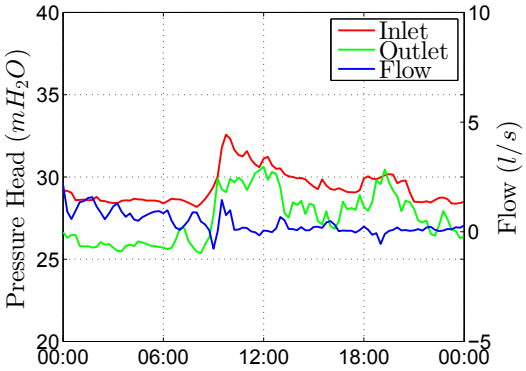
(a) PRV 1 (b) PRV 2

Figure 7.3: Data at the control valves during phase 2.

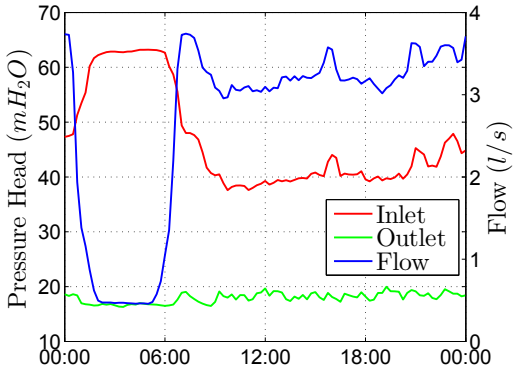


(a) PRV 1

(b) PRV 2



(c) DBV 1



(d) DBV 2

Figure 7.4: Data at the control valves during phase 3

The data acquired at the control valves for phases 1-3 (Figure 7.2 - Figure 7.4) is used to simulate the control valves in an extended period simulation, using the method outlined in Section 2.7. Each simulation/phase also uses the parameter update described in Section 2.8, to update the demand and source head for each phase. The AZP and pressure variability are then calculated, based on the extended period simulation, and shown in Figure 7.5a and Figure 7.5c respectively. The pressure at the CP (data) is also plotted in Figure 7.5b. The following observations are made:

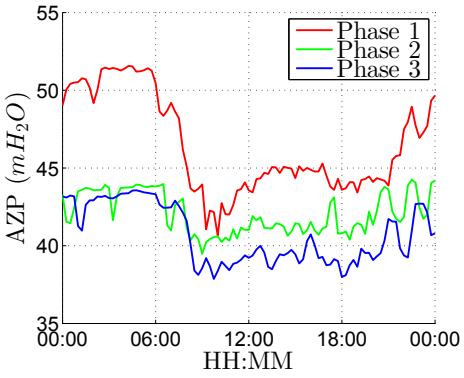
- The pressure at the critical point Figure 7.5b is consistently controlled at the minimum allowable pressure in the network ($15mH_2O$) for both phase 2 and phase 3. This is expected, since both phase 2 and phase 3 used optimised flow modulation curves at PRVs.
- Although pressure at the critical point is $\approx 15mH_2O$ for phase 2 and phase 3, operating a dynamic topology (phase 3) reduces day time AZP by approximately $1.7mH_2O$ compared to phase 2, which is a 4.1% reduction. It is observed that the CP pressure is slightly lower in phase 3 than phase 2 however, due to uncertainty in valve actuation, logging errors, and uncer-

tainty in the model parameters used to calculate the control curves. To obtain a less biased estimate of daytime AZP for phase 3, the AZP at 03:00 for phase 2 and 3 is compared, when the dynamic boundary valves are closed. At 03:00, the difference in AZP is $\approx 0.4mH_2O$. Therefore a more accurate estimate of the daytime AZP reduction between phase 2 and phase 3 is $1.7mH_2O - 0.4mH_2O = 1.3mH_2O$, a 3.1% reduction over phase 2. The difference between this result and the analytical result in Section 6.5.2 is predominantly due to fact that the dynamic boundary valves only open to 20% in the experimental programme, whereas in simulation they were fully open.

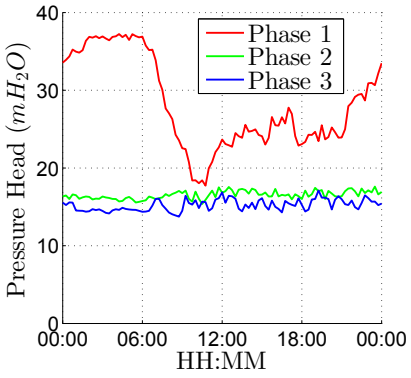
- During peak demand hours, the pressure management performance of flow modulation (phase 2) is similar to the fixed outlet configuration (phase 1), as shown in Figure 7.5a. This is because the fixed outlet PRVs in phase 1 were configured to supply enough pressure at peak demand times. At non peak demand times, this fixed outlet pressure provides too much pressure for the demand conditions, therefore there is excess pressure in the network, whereas the flow modulating PRV in phase 2 has reduced its outlet pressure based on the customer demand. At night time, this is most apparent. Table 12 shows that AZP during the night for phase 1 is $6.5mH_2O$ higher than the flow modulating PRV configuration (phase 2), and the CP pressure is almost $20mH_2O$ higher.

- The pressure variability is plotted in Figure 7.5c. The range in pressure variability is similar for all phases. Both phase 2 and phase 3 have a mean pressure variability of $\approx 10.2mH_2O$. Approximately 10% of nodes in phase 3 have higher pressure variability than phase 1 and phase 2, due to the opening/closing of DBV 2, which has a high pressure differential of approximately $40mH_2O$ (Figure 7.4d).

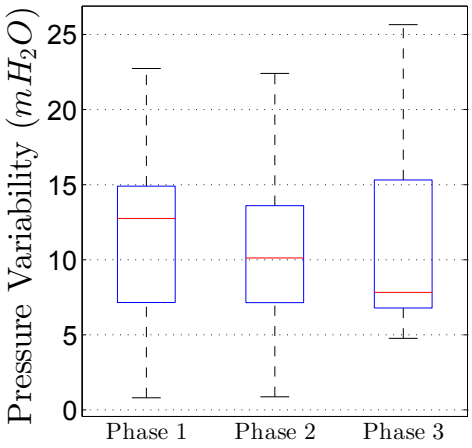
In the analysis, daytime hours are defined as 06:00-21:00 and night time hours as 21:00-06:00.



(a) AZP



(b) CP 1 Pressure



(c) Dirunal Pressure Variability

Figure 7.5: Pressure management comparison during the three phase experimental programme

Table 12: Summary of pressure management results for the three phase operation of the experimental programme

	Phase 1	Phase 2	Phase 3
AZP (Day) (mH_2O)	44.6	41.4	39.7
% Reduction compared to Phase 1	n/a	7.2%	11.0%
AZP (Night) (mH_2O)	49.7	43.2	42.5
% Reduction compared to Phase 1	n/a	13.1%	14.5%
Mean Pressure Variability $\overline{P}_{var,j}$ (mH_2O)	11.6	10.2	10.3
% Reduction compared to Phase 1	n/a	12.1%	11.2%

In order to validate that the model is a true representation of the hydraulic data used at each phase, a validation of the calibration (originally carried out in Section 5.5) is provided in Table 13. For all phases, pressure measurements are on average within $2mH_2O$ of the model, and phase 2 and phase 3 are within $1mH_2O$. More details on the model calibration and validation are shown in Appendix B. The accuracy achieved is adequate to draw valid conclusions from the data, although it highlights the need for optimal model calibration, which can be used for validating results as well as undertaking accurate model-based control.

	Phase 1	Phase 2	Phase 3
% of readings within $2mH_2O$	100.0	100.0	100.0
% of readings within $1mH_2O$	61.5	100.0	100.0
% of readings within $0.75mH_2O$	38.5	61.1	100.0
% of readings within $0.5mH_2O$	38.5	44.4	50.0
Average discrepancy over 24H (mH_2O)	0.62	0.42	0.34

Table 13: Pressure data and model comparison. Logger locations are shown in Figure 5.19, Section 5.5

7.2.2 Background Leakage Estimation

An approximation of background leakage can be made based on the experimental data acquired in Section 7.2.1. The approximation uses the leakage-pressure relationship outlined in (2.44). As detailed in Section 2.8, the aggregated demand and leakage in the network is updated for all simulations using the inlet flow data (i.e. Figure 5.20, Section 5.5 where the inlet flow data and model agree exactly). Therefore, the coefficients in (2.44) can be calibrated using the demand driven model.

The leakage-pressure relationship in (2.44) contains the coefficient ϕ_j and the exponent ψ_j. Although ψ_j often takes an assumed value (1.5 is commonly used for background leakage), it has also been shown to vary based on the network and type of pipes present (Farley and Trow, 2003).

In order to establish an estimate of ϕ_j and ψ_j for the experimental programme network, the AZP is plotted against an estimate of leakage based on the minimum night flow (Figure 7.6). In order to estimate the leakage at night, an estimate of legitimate night demand is required. One estimate of legitimate customer demand during the period 02:00-04:00 is 1.7 litres/property/hour (Farley and Trow, 2003). In the experimental programme, a more accurate estimate based on billing records is 2.7 litres/property/hour. There are 7,904 properties in the experimental programme network, therefore during the period 02:00-04:00 legitimate customer use is approximately 6.0l/s (water flow rate into the network).

Subtracting this value from the actual measured flow therefore gives an estimate of the leakage occurring. The leakage estimate is plotted against the night AZP (02:00-04:00) during all phases of the experimental programme (Figure 7.6). A curve of best fit is plotted against the data. A limit is placed on $\phi_j \geq 0$ and $\psi_j \geq 0.5$, which are the minimum values found in the literature. The best fit gives $\phi_j = 1.15 \times 10^{-3} m^{0.6}/s$ and $\psi_j = 2.4$. The R-square value is 0.68, which is considered sufficient for an estimation of leakage, where many factors contribute and great uncertainty in parameters is present. More specifically, the error in Figure 7.6 can be attributed to:

- Model uncertainty when calculating the night AZP. The validation of model calibration is presented in Table 13 in order to understand the uncertainty in the model. Uncertainty in the model includes factors such as the unknown spatial customer demand, the assumption that leakage is assigned proportionately to the customer demand at nodes (Ulanicka et al., 2001), errors in the friction factors and errors in sensor measurements that are used to calibrate the model.
- Discrepancies in the assumption that leakage is directly related to the AZP. Whilst it is clear that there is a relationship between AZP and leakage (Figure 7.6), many other factors also affect leakage (Kleiner and Rajani, 2002).
- Changes in the condition of the pipes between each phase, which would result in a different level of leakage. Since there was not a large period between the different phases, this factor should be minimal.

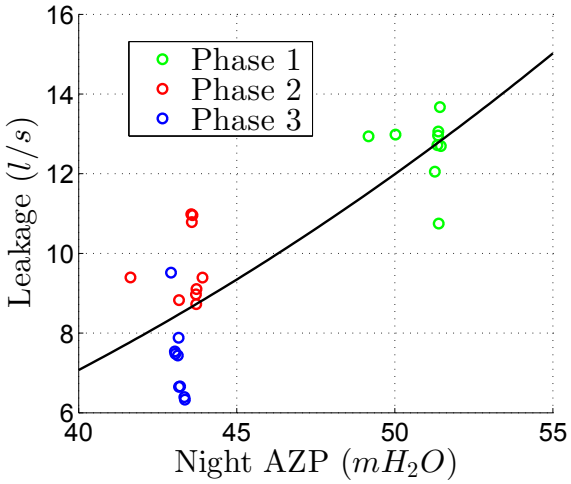
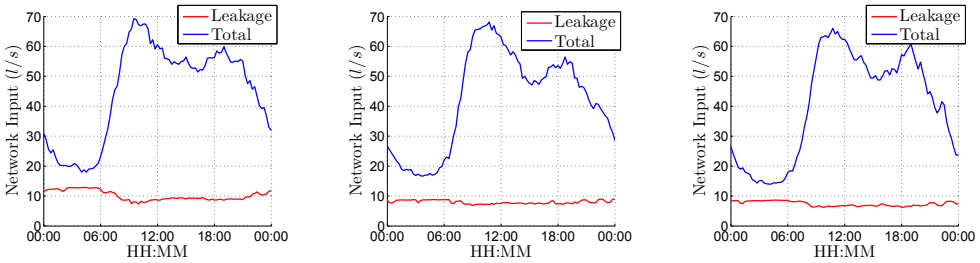


Figure 7.6: Estimating a leakage-pressure relationship using the night AZP (R-square value = 0.68)

The AZP-leakage curve in Figure 7.6 is used to estimate leakage throughout the day. The leakage and total input over a 24 hour period is shown in Figure 7.7.

Integrating the leakage over the full 5 day period therefore gives the total leakage for each phase, which can be compared with the total water input for this period. The results are shown in Table 14. Approximately 1 million litres less are used between phase 1 and phase 2, and between phase 2 and phase 3. This however is not a valid comparison, since demand fluctuates based on many factors, including seasonal variations. The leakage estimates however will give a more accurate indication of the amount of water saved as a result of pressure management. In Table 14, there is 0.94Ml less leakage during phase 2 compared with phase 1, and a further 0.25Ml less leakage during phase 3, compared to phase 2. In summary, in comparison to the use of fixed outlet PRVs on a closed DMA boundary, which is the most common form of pressure management in industry, flow modulating PRVs and a closed DMA boundary results in 21.4% less leakage, and a dynamic topology results in 27.2% less leakage. The average reduction in leakage when using statistically calculated flow modulation curves is 20% (i2O, 2015*b*), therefore the leakage calculations carried out in this section is consistent with other case studies.



(a) Phase 1 (b) Phase 2 (c) Phase 3

Figure 7.7: Demonstrating leakage in comparison to DMA input for the three phase programme

Table 14: Leakage estimation using the model and data over a 5 day period

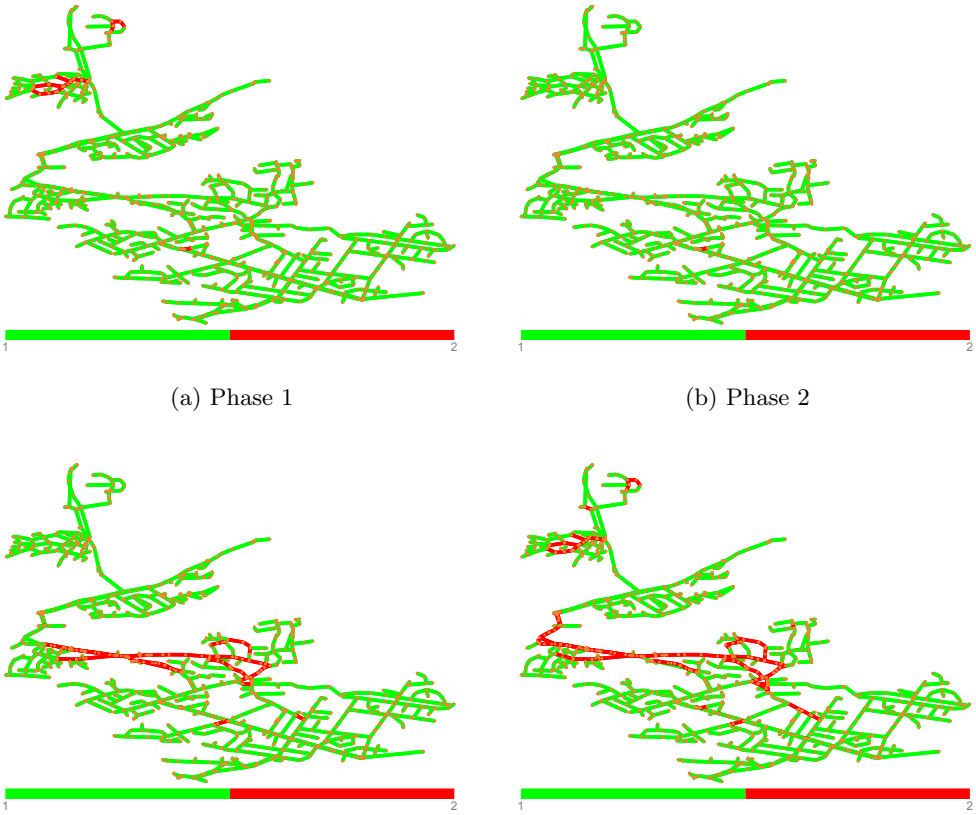
	Phase 1	Phase 2	Phase 3
Total DMA Input (Data)	19.9Ml	18.9Ml	17.8Ml
% Reduction compared to Phase 1	n/a	5.5%	10.9%
Total Leakage (Model)	4.38Ml	3.44Ml	3.19Ml
% Reduction compared to Phase 1	n/a	21.4%	27.2%

7.3 Flow Reversals

One of the disadvantages of closed topology DMAs is the well defined flow direction that most of the pipes experience. The pipes becomes well conditioned to the flow direction, and consequently any flow reversal that occurs due to operational changes or bursts can result in water discolouration for customers (Section 3.4.3).

In Figure 7.8, the flow reversal that occurred during the phased experimental investigation are plotted. When the DMA boundary is closed at all times (phase 1 and phase 2), there are a minimal number of flow reversals that occur in the network as part of the normal, diurnal hydraulic changes. In comparison, during phase 3 there were a high number of flow reversals occurring around the DMA boundary every day (Figure 7.8c). More flow reversals can also be achieved by opening the boundary valves to 100% (Figure 7.8d, simulated results) or by configuring PRVs to periodically shift the hydraulic balance point in a network with dynamic topology from one end of the network to the other, thereby achieving flow reversals in many pipes of the network.

Flow reversals that occur on a periodic basis allow the network and its pipes to become better conditioned to new flow conditions. Consequently, if a failure occurs that causes a flow reversal, the risk of discolouration for customers is minimised. For networks that do not often experience such flow reversals, the risk of discolouration is substantially increased. Further work is required to investigate the effects of a dynamic DMA topology on water quality.



(a) Phase 1

(b) Phase 2

(c) Phase 3

(d) Simulated DBV 100% Open

Figure 7.8: Analysing the flow reversals of the three phase programme

7.4 Resilience to Failure

7.4.1 Medium Sized Bursts (Hydrant Flushing)

The resilience to failure is tested during the three phase programme by flushing hydrants to simulate medium burst events (Zan et al., 2014).

In (Wright et al., 2014*a*) it was shown in simulation that medium bursts (approx. 5l/s) reduced pressure further in a closed DMA topology network than in a dynamic topology network, at areas close to the critical point. For example, Figure 7.9 shows a comparison of pressure for a dynamic topology and a closed DMA topology. Pressure drops severely in the closed DMA network, whereas the dynamic topology maintains a good level of pressure.

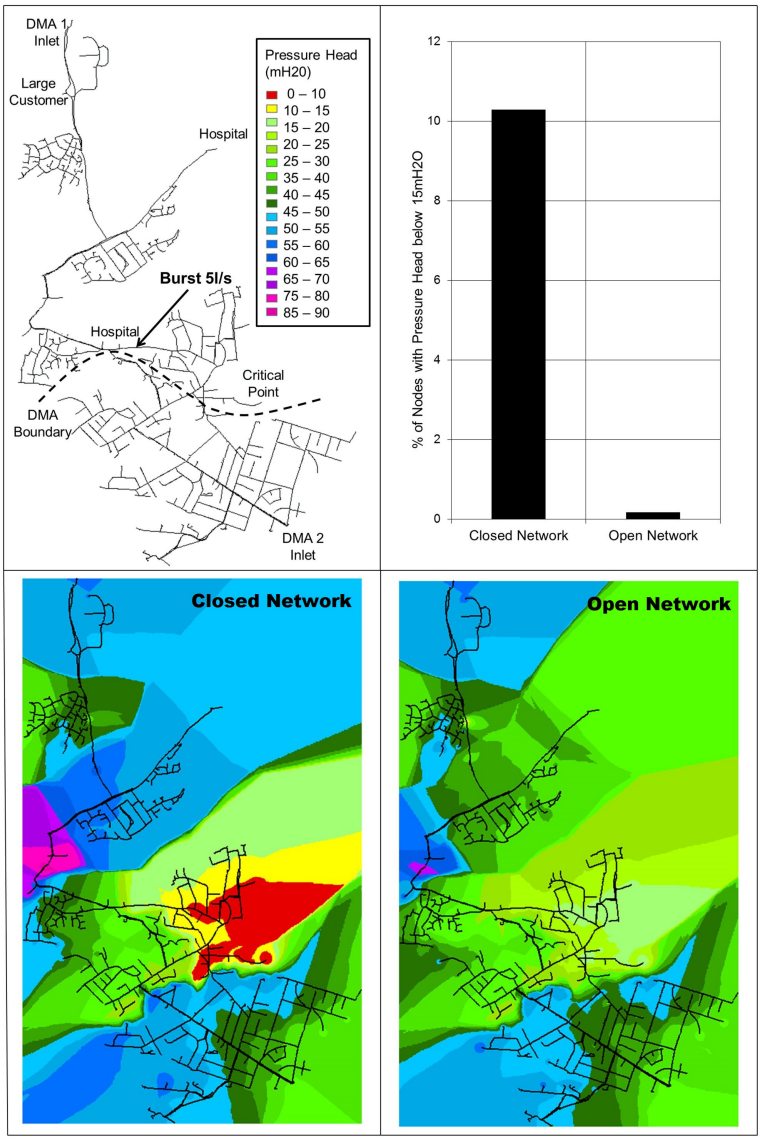


Figure 7.9: Analysis of network resilience to a medium burst event (Wright et al., 2014*a*)

The locations of the three artificially generated bursts are shown in Figure 7.1a. As explained in Section 7.1, three artificial bursts are generated for each phase. The burst flow rate is controlled at 5l/1 by varying the orifice of the hydrant (Figure 7.1b). The impact of each burst is most apparent at the CP of the network, as shown in Figure 7.10. The following observations are made:

- Burst 1 is near CP 1 and hence is a critical burst location. Furthermore, the burst occurs between 09:00 - 12:00 which overlaps with peak demand hours, making the burst particularly critical during the first hour. During phase 1 (fixed outlet pressure PRVs, closed DMAs), pressure drops substantially by 11.1$mH2O$, from 23.8$mH2O$ to 12.7$mH2O$ and remains at this approximate pressure level for the duration of the burst until 12:00. This is because a fixed outlet PRV does not react to increases in demand. The start of burst 1 for phase 1 was delayed because the water technician

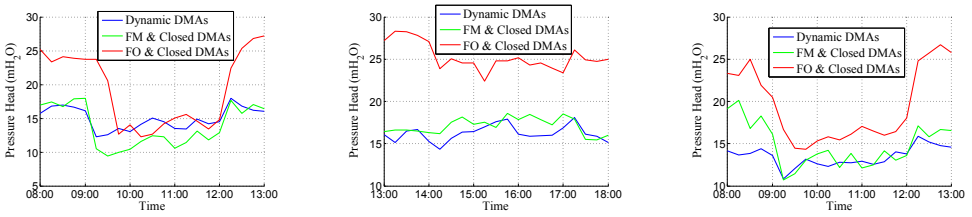
could not access the fire hydrant due to a parked vehicle, and the hydrant was finally opened at 09:20. Pressure during configuration 2 (flow modulating PRVs, closed DMAs) also becomes critical during burst 1, dropping by $8.6mH2O$, from $18.0mH2O$ to $9.4mH2O$. The pressure does recover slightly, increasing to levels between $10.6mH2O$ and $13.1mH2O$. The recovery in pressure is due to the flow modulating PRV detecting an increase in demand and consequently increasing its outlet pressure. Network resilience during phase 3 (dynamic topology) performs the best during burst 1. Pre-burst pressure is $16.1mH_2O$, and this drops by only $3.8mH_2O$ to $12.3mH_2O$. Pressure then recovers due to the flow modulating PRVs to levels between $13.0mH2O$ and $15.1mH2O$.

- Burst 2 is further upstream in the DMA within an area of high pressure and is therefore a less critical burst location. The burst was also carried out at non-peak demand hours (14:00 - 17:00). During phase 1, pressure drops from $27.1mH_2O$ to $23.9mH_2O$ and remains approximately at this pressure for the duration of the burst. During phase 2 and phase 3, pressure at CP 1 is similar. During phase 3, pressure drops momentarily to $14.3mH_2O$ before returning above $15mH2_O$ for the remainder of the burst. No other pressure drops below $15mH_2O$ are observed.

- Burst 3 is in a less critical location than burst 1, but more critical than burst 2 due to its closer proximity to the critical point. The burst also occurs between 09:00 - 12:00, making the first hour particularly critical. During phase 1, pressure drops substantially from $20.5mH_2O$ to $14.5mH_2O$. Pressure recovers slightly due customer demand reducing after peak-demand hours. At the end of the burst (12:00), pressure increases to $25mH_2O$. During phase 2, pressure drops from $16.1mH_2O$ to $10.7mH_2O$. A small recovery in pressure is made since the flow modulating PRVs react to demand increases, and pressure averages $13.3mH_2O$ for the duration of the burst. During phase 3, pressure at the CP on this day was being maintained slightly lower than $15mH_2O$ before the burst occurred. To ensure a fair test, ideally pressure at CP 1 would have been higher than this during normal operation. Nevertheless, the burst was simulated at 09:00 and pressure dropped from $13.6mH_2O$ to $10.8mH2_O$ and then recovered due to the flow modulating PRVs, averaging at $12.9mH_2O$. for the remainder of the burst. This is similar performance to phase 2, despite operating pre-burst with a lower pressure at the critical point.

The dynamic topology has demonstrated better resilience to failure by maintaining a higher pressure during all artificially generated bursts. This is important for maintaining a good level of customer service, particularly when pressure starts to drop further below $10mH_2O$, which will severely reduce the satisfactory amount

of water available to customers (Section 2.9).



(a) Burst location 1 (b) Burst location 2 (c) Burst location 3

Figure 7.10: Artificially generated bursts produced by operating fire hydrants under different network configurations. FM = Flow modulation and FO = Fixed Outlet (Wright et al., 2015*b*)

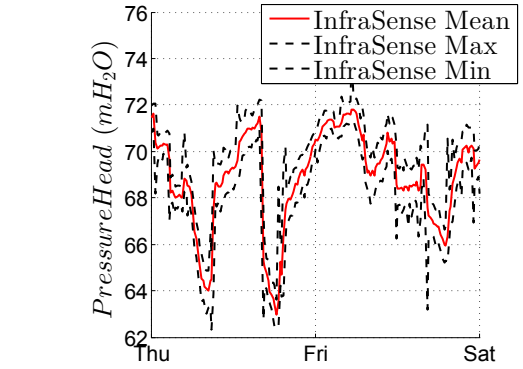
7.4.2 Large Burst Incident

A real, major burst occurred upstream of DMA 2 on a 35 inch trunk main during the experimental investigation which resulted in a supply failure to DMA 2. This event was detected by the high density of logging equipment in place in the experimental programme. For example, the inlet pressure head at DMA 2 is plotted in Figure 7.11b. Prior to the burst, a number of periodic pressure transients are captured with fluctuations of approximately $20mH_2O$. These transients occur as a result of an electronically operated valve opening and closing at the inlet of a nearby reservoir, upstream of DMA 2. The burst occurs at approximately 17:00 and the pressure drops to zero at the inlet of DMA 2 (Figure 7.11b). The inlet to DMA 1 was unaffected by the burst (Figure 7.11a).

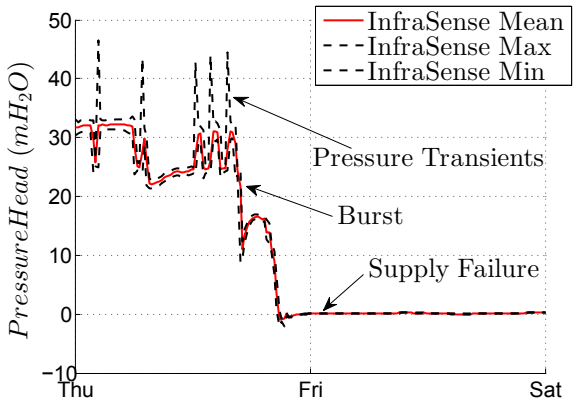
At the time of this incident, the dynamic topology was in partial operation, with DBV 1 opening during the day and closing at night for leakage detection practices, and DBV2 closed at all times. The dynamic topology maintained the supply of water to 1,400 properties that would otherwise have been without water because DMA 1, which was fully operational, was able to supply DMA 2 through the dynamic boundary valve DBV1.

An overview of the network pressure is shown in Figure 7.12a during the real burst incident. The flow at DBV 1 is plotted in Figure 7.12b. The boundary valve is closed during the early hours of Thursday to measure the minimum night flow and undertake leakage localization. The boundary valve then opens at 06:00, ready for the increase in consumption throughout the day. During the morning peak, optimal pressure management is maintained by supplying DMA 1 from DMA 2, as indicated by the positive flow at BV 1 in Figure 7.12b. The real burst then occurs later that day at 17:00. The flow at BV 2 is now negative, indicating that DMA 1 is supplying DMA 2. At night, BV 1 is kept open. Demand decreases and the flow drops to approximately $1l/s$. The following day, DMA 1 continues to supply DMA 2 via BV 1 with a flow of approximately

$8l/s$ for 1,400 properties that would otherwise have been without water unless a manual intervention was carried out.

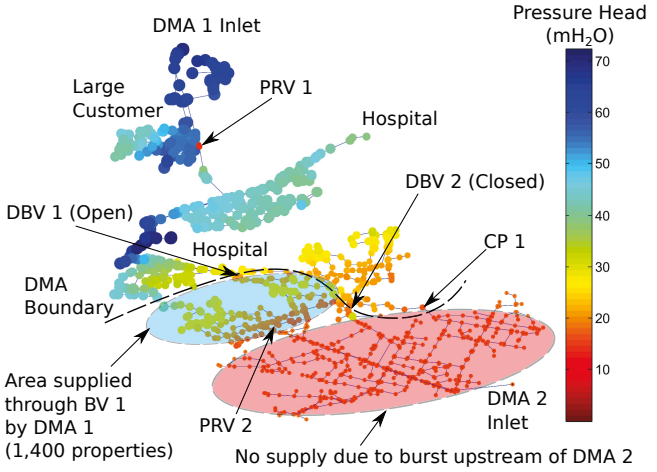


(a) DMA 1 Supply

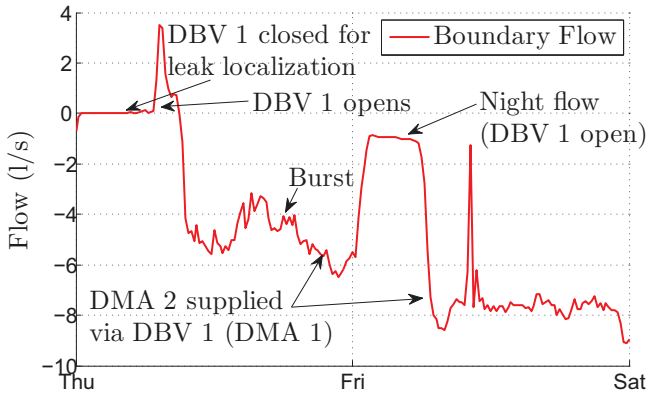


(b) DMA 2 Supply

Figure 7.11: A comparison of DMA 1 and DMA 2 inlet pressure heads during the occurrence of a real burst



(a) An overview of the network pressure and events during the real burst



(b) Boundary flow at BV 1

Figure 7.12: (a) An overview of the network during the real burst incident. The top DMA, which was not affected by the burst, supplies the neighbouring DMA with an alternative supply of water (b) the boundary flow at DBV 1 which supplies the affected DMA

7.5 Conclusion

This chapter has demonstrated the successful operation of a WDN with dynamic topology on a real, operational network. The experimental data, acquired in a three phase implementation, has validated analytical work and demonstrated improvements in pressure management and resilience to failure when operating a dynamic topology (phase 3). This was compared to:

- Phase 1: Fixed outlet PRVs and a closed DMA topology, which is the most commonly implemented form of pressure management (Section 3.7.1);
- Phase 2: Flow modulating PRVs and a closed DMA topology, which is an emerging form of advanced pressure management that is becoming more popular (Section 3.7.3).

The improvements are summarised as:

- AZP reductions of 4.1% compared to phase 2, and 11.0% compared to phase 1;
- Leakage reduction of 7.3% compared to phase 2, and 27.2% compared to phase 1;
- A higher number of flow reversals, which conditions the pipes to future bursts or hydraulic changes. The risk of discolouration of the customers' water supply during failure is therefore reduced;
- Pressure sustained at approximately $13mH_2O - 15mH_2O$ during the most critically placed, artificially generated burst, compared to phase 2 where pressure was $10.6mH_2O - 13.1mH_2O$ and during phase 1 $\approx 12.7mH_2O$.
- 1,400 properties (39% of all properties in DMA2) that maintained their water supply during a real, major burst, that would otherwise have been without water if a fixed, closed DMA network topology had been in operation.

The dynamic boundary valves were limited to a 20% opening daily during this initial experimental investigation. Analytical work in this thesis has demonstrated that opening the dynamic boundary valves further will produce further improvements in pressure management and resilience to failure.

8 Conclusion

The DMA is a valuable tool for leakage management. By permanently closing boundary valves, water companies can firmly establish the hydraulic behaviour in their networks and consequently make leakage estimations. No other technology available today can offer this type of information for the cost of setting up DMAs. Globally, countries that are becoming committed to reducing their leakage are turning to DMAs as the preferred option for leakage management. DMAs also facilitate:

- Simplistic pressure management by forming discrete zones where PRVs can be installed to reduce background leakage and future burst frequency;
- Repair, replacement and installations that can be implemented without the need to model or investigate the effects of the work on hydraulically connected neighbouring DMAs, which leads to man-hour savings;
- Contaminations containment and the prevention of undesirable mixing between water sources.

However, the DMA has substantial drawbacks that limit the effectiveness of pressure management and the quality of service provided. Major burst incidents on the ageing infrastructure can cause thousands of properties to lose their supply to water, consequences which are exacerbated by permanently closed valves and reduced redundancy in connectivity. In the UK, poor customer service can result in penalties up to 1% of the water company's revenue. Since providing a good customer service can also result in up to 0.5% of revenue reward, substantial savings can be made and used to invest in a better network infrastructure. Water companies are also investing in more advanced pressure management solutions in order to reduce leakage and comply with ever stricter regulations. The use of larger pressure managed zones, where frictional head losses are smaller, can aid in achieving more efficient pressure management. However, the approach adopted so far by water companies has generally been focused on optimising pressure for single-feed DMAs. At the same time, water companies that are strongly targeting leakage through ALC are aiming to reduce the size of their DMAs, an activity that will require more valve closures and further reductions in redundancy and network resilience.

This thesis introduces a novel approach to the operational management of water distribution networks, where DMAs are dynamically aggregated for improved pressure management, reduced leakage, and stronger resilience to failure, and segregated for leakage monitoring at discrete times, thereby facilitating DMAs of any size to be used without introducing its disadvantages. The performance of a dynamic topology in pressure management and resilience to failure is bench-

marked against two other approaches to pressure management. The first is the use of fixed outlet PRVs in a closed, static DMA topology, which is the most common form of pressure management used by water companies. The second is the use of flow modulating PRVs on a closed, static DMA topology, which is an emerging form of pressure management that has become more popular with water companies over the last five years. The performance of DMAs with dynamic topology is assessed analytically and experimentally through the design and set-up of a dynamic topology on a real, operational network serving approximately 8,000 properties. The analytical and experimentally validated results establish:

- AZP reductions of 11.0% when operating a dynamic topology compared to the most common form of pressure management, fixed outlet PRVs and a closed DMA topology;
- AZP reductions of 4.1% when operating a dynamic topology compared to emerging technologies such as flow modulation and a closed DMA topology;
- A 27.2% reduction in leakage when operating a dynamic topology compared to fixed outlet PRVs and a closed DMA topology;
- A 7.3% reduction in leakage when operating a dynamic topology compared to flow modulating PRVs and a closed DMA topology;
- Pressure sustained by approximately $2 - 3mH_2O$ during medium sized burst incidents when operating a dynamic topology;
- Substantial improvements in resilience to real, major burst incidents, where thousands of properties can maintain their supply of water.

The dynamic aggregation of DMAs results in the formation of very large networks, complicated further by interaction between multiple sources, control valves and large consumers that impact the hydraulic conditions extensively. Consequently, an optimisation method for valve control that is computationally efficient and converges reliably is required in such networks. An optimisation algorithm with computationally efficient and reliable performance is therefore developed. Its main advantage over other optimisation approaches is its reliable convergence to an optimal point for real, complex networks. In order to take advantage of the computational efficiency of null space algorithms, a novel approach to including control valves in the hydraulic model constraints has been developed. The valve model is fully convex, therefore the optimisation search space, which is non-convex due to the head loss relationship of pipes, can also be more efficiently searched for a better local optimal point or the global optimum. It is proposed that this approach is more efficient for finding better local optimal points than repeatedly solving the optimisation problem with different, random starting points as required by other approaches where the valve model is non-convex. In order to implement the optimised valve settings, time varying

flow modulation is proposed for actuating near optimal control at PRVs based on the dynamic aggregation of DMAs.

This thesis has demonstrated that a network with dynamic topology provides strong improvements in pressure management and resilience to failure. These improvements have been validated analytically and experimentally on a real, operational network. Computational tools have been developed and proposed in order to successfully implement and operate the network with dynamic topology. Although its operation requires more advanced model simulation and optimisation algorithms, in the long term this offers substantial benefits in terms of understanding the network behaviour, optimising network performance and improving the water company's response to failures.

8.1 Novel Contributions

The novel contributions of this thesis are as follows:

1. A novel approach to pressure and incident management has been proposed and implemented on a real, operational UK network supplying approximately 8,000 properties;
2. An analytical and experimental investigation into the performance of the dynamic topology has demonstrated a 27% reduction in leakage over the most common approach to pressure management, and strong improvements in network resilience to failure where 1,400 customers maintained a supply during a real, major burst incident;
3. A novel optimisation algorithm for valve control has been developed and strong convergence properties have been demonstrated when compared to other approaches for valve control in large networks formed from the dynamic aggregation of DMAs;
4. The development of a novel, convex valve model that can be integrated into efficient null space algorithms, and is used in order to improve the computational performance of the proposed valve control optimisation algorithm;
5. A novel approach for implementing near optimal control in DMAs with dynamic topology, where time varying flow modulation curves are used based on the dynamic connectivity of DMAs;
6. An extensive review of the current and emerging forms of pressure and DMA management from around the world;
7. A case study using a real large scale network (3,148km of pipeline) demonstrating the current state of DMAs, their compliance to DMA design guide-

lines, and identification of how a dynamic DMA topology can improve their operational performance;

8. A novel resilience index (the Reserve Capacity) that was used in the design of the dynamic DMA topology;
9. The demonstration of modelling, calibration, and control using high frequency pressure data to validate (or reject) steady state assumptions and improve the network control.

8.2 Future Work

The following areas could be explored in future work related to a dynamic topology:

- A more extensive experimental investigation, ideally lasting one year as recommended in performance indicator guidelines, in order to properly benchmark the performance of different network configurations and approaches.
- MPC would be a powerful control method for multi-feed DMAs and would not depend on the existence of flow modulation curves. This would require continuous (or very regular) communication with monitoring and control devised. The possibility of valve interaction would also be eliminated. Other decentralised control options, such as combing flow modulation with fixed outlet or flow control PRVs, could also be of interest in situations where real-time communication is not available.
- An investigation into optimal control in conjunction with automatic or optimised model calibration that uses high frequency pressure data to validate the existence of steady state conditions. The actuation of model-based control requires a sufficiently calibrated model. In this thesis, the calibration was undertaken manually. Identifying the level of model calibration required, and the optimal location of sensors necessary, are related research questions.
- The implementation and benefits of reducing the variability in diurnal pressure when operating a dynamic DMA topology. Pressure variability has been linked to burst frequency in the literature. The reduced frictional energy losses in a multi-feed network can reduce pressure variability, and this was demonstrated in the experimental programme when operating a dynamic DMA topology.
- Further validation of the optimisation algorithm proposed in this thesis in comparison to other methods, such as the reduced gradient method.

There are many optimisation approaches that exist in the literature, however there is a very limited amount of work available on how optimisation methods compare.

- Other benefits or challenges of operating a dynamic topology should also be explored. For example, water contamination and the mixing of water from different sources, which is undesirable but also aggravated by a dynamic topology. Flow reversals and the effect this has on the network can also be investigated. For example, the self-cleansing of networks by artificially inducing ubiquitous flow reversals could provide strong improvements in the resilience to water quality failure.
- A cost-benefit analysis of all financial improvements and costs, undertaken over an extended period of time. In reality, this type of work will most likely need to be undertaken within a water company, since it requires in-depth knowledge of the costings for water treatment, man-hours, turnover, and the size and frequency of penalties. This type of information can be sensitive, and is generally unavailable to the public or research communities.

Bibliography

ABB (2015), 'Watermaster: Electromagnetic flow meter'. [Online; accessed 25-08-2015].
URL: *http://www.abb.com/product/seitp330/ab1ce5818482e4dec1257bdd003003ae.aspx*

AbdelMeguid, H., Skworcow, P. and Ulanicki, B. (2011), 'Mathematical modelling of a hydraulic controller for prv flow modulation', *Journal of Hydroinformatics* **13**(3), 374–389.

Abraham, E. and Stoianov, I. (2015*a*), 'Efficient preconditioned iterative methods for hydraulic simulation of large scale water distribution networks', *Procedia Engineering* **119**, 623–632.

Abraham, E. and Stoianov, I. (2015*b*), 'Sparse null space algorithms for hydraulic analysis of large scale water supply networks', *Journal of Hydraulic Engineering* p. 04015058.

Abraham, E. and Stoianov, I. (2016), 'An efficient null space inexact Newton method for hydraulic simulation of water distribution networks', *ArXiv e-prints* .

Alegre, H., Association, I. W. et al. (2006), *Performance indicators for water supply services*, IWA publishing.

Allsop, R. E. (1972), 'Estimating the traffic capacity of a signalized road junction', *Transportation Research* **6**(3), 245–255.

Andersen, J. and Powell, R. (1999), 'Simulation of water networks containing controlling elements', *Journal of water resources planning and management* **125**(3), 162–169.

Aquavent (2015), 'Aquai-mod valve controller'. [Online; accessed 19-06-2015].
URL: *http://www.aquavent.net/*

Araujo, L., Ramos, H. and Coelho, S. (2006), 'Pressure control for leakage minimisation in water distribution systems management', *Water Resources Management* **20**(1), 133–149.

Armand, H., Stoianov, I. and Graham, N. (2015), 'Investigating the impact of sectorized networks on discoloration', *Procedia Engineering, Accepted for Publication* .

Atmanand, M. and Konnur, M. (1996), A novel method of using a control valve for measurement and control of flow, *in* 'Instrumentation and Measurement Technology Conference, 1996. IMTC-96. Conference Proceedings. Quality

Measurements: The Indispensable Bridge between Theory and Reality., IEEE', Vol. 2, IEEE, pp. 813–816.

Awad, H., Kapelan, Z. and Savic, D. (2008), Analysis of pressure management economics in water distribution systems, *in* 'Proceedings of the 10th Annual Water Distribution Systems Analysis Conference (WDSA2008)', Vol. 1720.

AWWA Engineering Computer Applications Committee and others (1999), Calibration guidelines for water distribution system modeling, *in* 'Proceedings of the 1999 AWWA Information Management and Technology Conference (IMTech), New Orleans, Louisiana'.

Bargiela, A. (1984), On-line monitoring of water distribution networks, PhD thesis, Durham University.

Barr, D. and Sivaloganathan, K. (1982), 'Solutions of the colebrook-white function for resistance to uniform turbulent-flow'.

BBC News (2014), 'Norwich water main burst: No supplies for 5,000 anglian water customers'. [Online; accessed 20-07-2015].
URL: *http://www.bbc.co.uk/news/uk-england-norfolk-30623742*

Benzi, M., Golub, G. H. and Liesen, J. (2005), 'Numerical solution of saddle point problems', *Acta numerica* **14**(1), 1–137.

Bermad (2015), 'Insertion flow meter (electromagnetic)'. [Online; accessed 21-07-2015].
URL: *http://www.bermad.com/product/product=insertion-flow-meter/cat=101604*

Bertsekas, D. P. (1999), 'Nonlinear programming'.

Bhave, P. R. (1991), Analysis of flow in water distribution networks, *in* 'Analysis of flow in water distribution networks', Technomic Publishing.

Boxall, J. and Saul, A. (2005), 'Modeling discoloration in potable water distribution systems', *Journal of Environmental Engineering* **131**(5), 716–725.

Boyd, S. and Vandenberghe, L. (2004), *Convex optimization*, Cambridge university press.

Brdys, M. A. and Ulanicki, B. (1994), *Operational control of water systems: structures, algorithms, and applications*, Prentice Hall.

Charalambous, S. and Isaia, M. (2013), Leakage reduction by innovative pressure regulation and control, *in* 'Final Conference and Stakeholders Event', Vol. 500, p. 185.

Chen, A., Kasikitwiwat, P. and Yang, C. (2013), 'Alternate capacity reliability

measures for transportation networks', *Journal of Advanced Transportation* **47**(1), 79–104.

Chen, A., Yang, H., Lo, H. K. and Tang, W. H. (1999), 'A capacity related reliability for transportation networks', *Journal of advanced transportation* **33**(2), 183–200.

Chen, A., Zhou, Z., Chootinan, P., Ryu, S., Yang, C. and Wong, S. (2011), 'Transport network design problem under uncertainty: a review and new developments', *Transport Reviews* **31**(6), 743–768.

Chen, N. H. (1979), 'An explicit equation for friction factor in pipe', *Industrial & Engineering Chemistry Fundamentals* **18**(3), 296–297.

Cla-Val (2015*a*), 'D22 pilot controller for position, pressure, flow, and modulation control'. [Online; accessed 20-04-2015].
URL: *http://www.cla-val.co.uk/user/downloads/LIN066DE.pdf*

Cla-Val (2015*b*), 'e-flowmeter for flow measurements based on the vortex shedding phenomenon'. [Online; accessed 20-04-2015].
URL: *http://www.cla-val.co.uk/products/Datasheets/E-FLOWMETER/e-flowmeter%20datasheet%20LIN041DE.pdf*

Cla-Val (2015*c*), 'e-power mp for energy harvesting'. [Online; accessed 20-04-2015].
URL: *http://www.cla-val.co.uk/products/Datasheets/e-power/Power%20Generator%205-6V%20(0.39W-0.75W).pdf*

Cla-Val (2015*d*), 'Pressure reducing valve'. [Online; accessed 22-07-2015].
URL: *http://www.cla-val.co.uk/products/Datasheets/90-01/90GE-01_NGE90-01.pdf*

Collins, M., Cooper, L., Helgason, R., Kennington, J. and LeBlanc, L. (1978), 'Solving the pipe network analysis problem using optimization techniques', *Management Science* **24**(7), 747–760.

Cross, H. (1936), 'Analysis of flow in networks of conduits or conductors'.

Davidson, J. and Bouchart, F.-C. (2006), 'Adjusting nodal demands in scada constrained real-time water distribution network models', *Journal of Hydraulic Engineering* .

Deuerlein, J. W., Simpson, A. R. and Dempe, S. (2009), 'Modeling the behavior of flow regulating devices in water distribution systems using constrained nonlinear programming', *Journal of Hydraulic Engineering* .

Di Nardo, A. and Di Natale, M. (2011), 'A heuristic design support methodology based on graph theory for district metering of water supply networks', *Engineering Optimization* **43**(2), 193–211.

Dinh, Q. T. and Diehl, M. (2010), Local convergence of sequential convex programming for nonconvex optimization, *in* 'Recent Advances in Optimization and its Applications in Engineering', Springer, pp. 93–102.

Dinh, Q. T., Savorgnan, C. and Diehl, M. (2011), Real-time sequential convex programming for nonlinear model predictive control and application to a hydro-power plant, *in* 'Decision and Control and European Control Conference (CDC-ECC), 2011 50th IEEE Conference on', IEEE, pp. 5905–5910.

Drinking Water Inspectorate (2009), 'Drinking water safety: Guidance to health and water professionals'.

Drud, A. S. (1994), 'Conopta large-scale grg code', *ORSA Journal on Computing* **6**(2), 207–216.

Dubai Electricity & Water Authority (2015), 'Guidelines for new development projects: Power & water planning'. [Online; accessed 24-08-2015].
URL: *http://www.dewa.gov.ae/consumers/customerguide/Water_Planning_Guidelines_for_New_Development_Projects_2011.pdf*

Eck, B. J. and Mevissen, M. (2012), Valve placement in water networks: Mixed-integer non-linear optimization with quadratic pipe friction, *in* 'Company Report'.

Eck, B. J. and Mevissen, M. (2013), Fast non-linear optimization for design problems on water networks, *in* 'World Environmental and Water Resources Congress 2013'.

Elhay, S. and Simpson, A. R. (2011), 'Dealing with zero flows in solving the nonlinear equations for water distribution systems', *Journal of Hydraulic Engineering* **137**(10), 1216–1224.

Elhay, S., Simpson, A. R., Deuerlein, J., Alexander, B. and Schilders, W. H. (2014), 'Reformulated co-tree flows method competitive with the global gradient algorithm for solving water distribution system equations', *Journal of Water Resources Planning and Management* **140**(12).

Epp, R. and Fowler, A. G. (1970), 'Efficient code for steady-state flows in networks', *Journal of the Hydraulics Division* **96**(1), 43–56.

European Commission (2015), 'Eu reference document good practices on leakage management wfd cis wg pom', *European Union* .

European Union (2015), 'Eu reference document good practices on leakage management wfd cis wg pom main report'.

Fanner, P. (2010), 'Assessing real water losses: a practical approach'.

Fantozzi, M., Calza, F. and Lambert, A. (2009), Experience and results achieved in introducing district metered areas (dma) and pressure management areas (pma) at enia utility (italy), *in* 'IWA International Specialised Conference Water Loss'.

Farley, M. (2012), Are there alternatives to the dma, *in* 'Water Loss Reduction-Proceedings of the 7th IWA Specialist Conference'.

Farley, M. and Trow, S. (2003), *Losses in water distribution networks: a practitioner's guide to assessment, monitoring and control*, IWA Publishing.

Farmani, R., Savic, D. A. and Walters, G. A. (2004), 'Exnet benchmark problem for multi-objective optimization of large water systems', *Modelling and Control for Participatory Planning and Managing Water Systems* .

Fernández, A. (2011), 'Improving water network management by efficient division into supply clusters', *PhD Thesis, Universitat Politecnica de Valencia* .

Forrest, J. (2006), Clp-coin-or linear program solver, *in* 'Proceedings from the DIMACS Workshop on COIN-OR', pp. 17–20.

Germanopoulos, G. and Jowitt, P. (1989), Leakage reduction by excess pressure minimization in a water supply network, *in* 'ICE Proceedings', Vol. 87, Thomas Telford, pp. 195–214.

Get Surrey (2015), 'Burst water main: Major incident declared as water shortage continues'. [Online; accessed 20-07-2015].
URL: *http://www.getsurrey.co.uk/news/surrey-news/burst-water-main-major-incident-9577495*

Giacomello, C., Kapelan, Z. and Nicolini, M. (2012), 'Fast hybrid optimization method for effective pump scheduling', *Journal of Water Resources Planning and Management* **139**(2), 175–183.

Giustolisi, O., Savic, D. and Kapelan, Z. (2008), 'Pressure-driven demand and leakage simulation for water distribution networks', *Journal of Hydraulic Engineering* **134**(5), 626–635.

Giustolisi, O. and Walski, T. (2011), 'Demand components in water distribution network analysis', *Journal of Water Resources Planning and Management* **138**(4), 356–367.

Gupta, R. and Bhave, P. R. (1994), 'Reliability analysis of water-distribution systems', *Journal of Environmental Engineering* **120**(2), 447–461.

Gupta, R. and Prasad, T. (2000), 'Extended use of linear graph theory for analysis of pipe networks', *Journal of hydraulic engineering* **126**(1), 56–62.

Habib, M. F. (2010), 'Direction generation method based on linearization: Generalized reduced gradient method', *Lecture Slides, University of California, Davis* .

Heart (2015), 'Hailsham: Water supplies hit by huge mains burst'. [Online; accessed 20-07-2015].
URL: *http://www.heart.co.uk/sussex/news/local/hailsham-water-supplies-hit-by-huge-mains-burst/#ZIKxC7qZJiXMv7Er.97*

Herrera, M., Abraham, E. and Stoianov, I. (2015), 'A graph-theoretic framework for assessing the resilience of sectorised water distribution networks', *Water Resources Management* -(-), under review.

Herrera, M., Canu, S., Karatzoglou, A., Pérez-García, R. and Izquierdo, J. (2010), 'An approach to water supply clusters by semi-supervised learning', *Proceedings of International Environmental Modelling and Software Society (IEMSS)* .

Hoskins, A. (2016), *Monitoring the Hydraulic Dynamics in Water Distribution Systems*, EngD Thesis, Imperial College London.

Hoskins, A. and Stoianov, I. (2014), 'Infrasense: A distributed system for the continuous analysis of hydraulic transients', *Procedia Engineering* **70**, 823–832.

Howitt, R., Medellín-Azuara, J., MacEwan, D., Lund, J. and Sumner, D. (2014), 'Economic analysis of the 2014 drought for california agriculture', *prepared for California Department of Food and Agriculture by UC Davis Center for Watershed Sciences and ERA Economics* .

i2O (2015*a*), 'Advanced pressure management'. [Online; accessed 15-03-2015].
URL: *http://www.i2owater.com/*

i2O (2015*b*), 'Advanced pressure management brochure'. [Online; accessed 29-08-2015].
URL: *http://www.i2owater.com/wp-content/uploads/2014/02/i2O_Solutions_Overview_Product_Brief.pdf*

IBM (2015), 'Ibm analytics help sonoma county, california conserve water'. [Online; accessed 25-08-2015].
URL:
https://www-03.ibm.com/press/us/en/pressrelease/37046.wss

Isaacs, L. T. and Mills, K. G. (1980), 'Linear theory methods for pipe network analysis', *Journal of the hydraulics division* **106**(7), 1191–1201.

Jones, S., Shepherd, W., Collins, R. and Boxall, J. (2014), 'Experimental

quantification of intrusion due to transients in distribution systems', *Procedia Engineering* **89**, 1306–1313.

Jowitt, P. W. and Germanopoulos, G. (1992), 'Optimal pump scheduling in water-supply networks', *Journal of Water Resources Planning and Management* **118**(4), 406–422.

Jowitt, P. W. and Xu, C. (1990), 'Optimal valve control in water-distribution networks', *Journal of Water Resources Planning and Management* **116**(4), 455–472.

Kapelan, Z. S., Savic, D. A. and Walters, G. A. (2003), 'Multiobjective sampling design for water distribution model calibration', *Journal of Water Resources Planning and Management* **129**(6), 466–479.

Kleiner, Y. and Rajani, B. (2002), 'Forecasting variations and trends in water-main breaks', *Journal of Infrastructure Systems* **8**(4), 122–131.

Kunkel, G. and Sturm, R. (2011), 'Piloting proactive, advanced leakage management technologies', *Jour. AWWA* **203**(2), 62.

LaLonde, A. (2004), Use of flow modulated pressure management in york region, ontario to reduce distribution system losses, *in* 'AWWA Water Sources Conf'.

Lalonde, A., Au, C., Fanner, P. and Lei, J. (2008), 'City of toronto water loss study and pressure management pilot', *Miya Arison Group, unpublished* .

Lambert, A. (2001), What do we know about pressure-leakage relationships in distribution systems, *in* 'IWA Conf. n Systems approach to leakage control and water distribution system management'.

Larock, B. E., Jeppson, R. W. and Watters, G. Z. (1999), *Hydraulics of pipeline systems*, CRC press.

Luenberger, D. G. and Ye, Y. (2008), *Linear and nonlinear programming*, Vol. 116, Springer Science & Business Media.

Martin, D. and Peters, G. (1963), 'The application of newtons method to network analysis by digital computer', *Journal of the institute of Water Engineers* **17**(2), 115.

Martinez Alzamora, F., Ulanicki, B. and Salomons, E. (2012), 'Fast and practical method for model reduction of large-scale water-distribution networks', *Journal of Water Resources Planning and Management* **140**(4), 444–456.

Martínez-Codina, Á., Castillo, M., González-Zeas, D. and Garrote, L. (2015), 'Pressure as a predictor of occurrence of pipe breaks in water distribution networks', *Urban Water Journal* (ahead-of-print), 1–11.

Matthews, C. (2012), 'South east water makes 1.5m leakage investment', *edie.net* . [Online; accessed 15-08-2015].
URL: *http://www.edie.net/news/4/South-East-Water-makes--15m-leakage-investment/22544/*

May, J. (1994), Leakage, pressure and control, *in* 'BICS International Conf. on Leakage Control, London'.

Mays, L. W. (1999), *Water distribution system handbook*, McGraw-Hill Professional Publishing.

McKenzie, R. and Wegelin, W. (2010), Scope for pressure management in south africa, *in* 'Proceedings of the IWA International Specialised Conference Water Loss 2010'.

Meyer, N., Wright, D. and Engelbrecht, M. (2009), Large scale pressure management implementation in the city of cape town, *in* 'IWA Water Loss Conference'.

Michele, G., Zoran, K. and Dragan, S. (2012), 'Using high performance techniques to accelerate demand driven hydraulic solvers'.

Morrison, J., Tooms, S. and Rogers, D. (2007), 'District metered areas guidance notes', *International Water Association Water Loss Task Force* .

Nicolini, M. and Zovatto, L. (2009), 'Optimal location and control of pressure reducing valves in water networks', *Journal of water resources planning and management* **135**(3), 178–187.

Nielsen, H. B. (1989), 'Methods for analyzing pipe networks', *Journal of Hydraulic Engineering* **115**(2), 139–157.

Nocedal, J. and Wright, S. J. (2006), *Numerical optimization*, Springer Verlag.

O'Day, D. K. et al. (1982), 'Organization and analyzing leak and break data for making main replacement decisions (pdf)', *Journal-American Water Works Association* **74**(11), 588–594.

Ofwat (2007), 'Security of supply 2006-07 report'. [Online; accessed 23-04-2015].
URL: *http://www.ofwat.gov.uk/consumerissues/rightsresponsibilities/standards/gud_pro_gss08.pdf*

Ofwat (2008), 'The guaranteed standards scheme (gss)'. [Online; accessed 15-03-2015].
URL: *http://www.ofwat.gov.uk/regulating/aboutconsumers/sim/prs_web201211sim.pdf*

Ofwat (2012), 'The service incentive mechanism (sim)'. [Online; accessed 15-03-2015].

URL: *http://www.ofwat.gov.uk/regulating/aboutconsumers/sim/prs_web201211sim.pdf*

Ofwat (2013), 'Water meters - your questions answered'. [Online; accessed 17-01-2016].
URL: *http://www.ofwat.gov.uk/wp-content/uploads/2015/11/prs_lft_101117meters.pdf*

Ofwat (2014*a*), 'Setting price controls for 2015-20 final price control determination notice'. [Online; accessed 30-08-2015].
URL: *http://www.ofwat.gov.uk/pricereview/pr14/det_pr20141212outcomes.pdf*

Ofwat (2014*b*), 'Setting price controls for 2015-20 pre-qualification decisions'. [Online; accessed 23-04-2015].
URL: *http://www.ofwat.gov.uk/pricereview/pr14/pap_pos20140310pr14pq.pdf*

Ormsbee, L. E. (1989), 'Implicit network calibration', *Journal of Water Resources Planning and Management* **115**(2), 243–257.

Ormsbee, L. E. and Reddy, S. L. (1995), 'Nonlinear heuristic for pump operations', *Journal of Water Resources Planning and Management* **121**(4), 302–309.

Osiadacz, A. j. and Pienkosz, K. (1988), 'Methods of steady-state simulation for gas networks'.

Özger, M. and Yıldırım, G. (2009), 'Determining turbulent flow friction coefficient using adaptive neuro-fuzzy computing technique', *Advances in Engineering Software* **40**(4), 281–287.

Palmer (2015), 'Pressure control'. [Online; accessed 15-03-2015].
URL: *http://www.hwm-water.com/water-management-products/palmer-environmental-products/pressure-control/*

Pearson, D. and Trow, S. (2005), Calculating economic levels of leakage, *in* 'Leakage 2005 Conference Proceedings'.

Pecci, F., Abraham, E. and Stoianov, I. (2015), 'Mathematical programming methods for pressure management in water distribution systems', *Procedia Engineering* **119**, 937–946.

Perelman, L. S., Allen, M., Preis, A., Iqbal, M. and Whittle, A. J. (2015), 'Automated sub-zoning of water distribution systems', *Environmental Modelling & Software* **65**, 1–14.

Piller, O. and van Zyl, J. E. (2014), 'Modeling control valves in water

distribution systems using a continuous state formulation', *Journal of Hydraulic Engineering* **140**(11), 04014052.

Prasad, T. D. and Park, N.-S. (2004), 'Multiobjective genetic algorithms for design of water distribution networks', *Journal of Water Resources Planning and Management* **130**(1), 73–82.

Prescott, S. L. and Ulanicki, B. (2003), 'Dynamic modeling of pressure reducing valves', *Journal of Hydraulic Engineering* **129**(10), 804–812.

Prescott, S. and Ulanicki, B. (2004), Investigating interaction between pressure reducing valves and transients in water networks, *in* 'Proccedings 49th Int. Scientific Colloquium', Vol. 1, pp. 49–54.

Puust, R., Kapelan, Z., Savic, D. and Koppel, T. (2010), 'A review of methods for leakage management in pipe networks', *Urban Water Journal* **7**(1), 25–45.

Quoc, T. D., Savorgnan, C. and Diehl, M. (2012), Real-time sequential convex programming for optimal control applications, *in* 'Modeling, Simulation and Optimization of Complex Processes', Springer, pp. 91–102.

Reca, J., Martinez, J., Banos, R. and Gil, C. (2008), 'Optimal design of gravity-fed looped water distribution networks considering the resilience index', *Journal of Water Resources Planning and Management* **134**(3), 234–238.

Rockafellar, R. T. (1997), 'Convex analysis. princeton landmarks in mathematics'.

Romeo, E., Royo, C. and Monzón, A. (2002), 'Improved explicit equations for estimation of the friction factor in rough and smooth pipes', *Chemical engineering journal* **86**(3), 369–374.

Rossman, L. A. (2000), 'Epanet 2: users manual'.

Ryaben'kii, V. S. and Tsynkov, S. V. (2006), *A theoretical introduction to numerical analysis*, CRC Press.

Salgado, R., Todini, E. and O'Connell, P. (1988), Comparison of the gradient method with some traditional methods for the analysisof water supply distribution networks, *in* 'Computer applications in water supply: vol. 1—systems analysis and simulation', Research Studies Press Ltd., pp. 38–62.

Savic, D. A. and Walters, G. A. (1995), 'An evolution program for optimal pressure regulation in water distribution networks', *Engineering Optimization* **24**(3), 197–219.

Seago, C., Bhagwan, J. and McKenzie, R. (2007), 'Benchmarking leakage from water reticulation systems in south africa', *Water SA* **30**(5), 25–32.

Shamir, U. Y. and Howard, C. D. (1968), 'Water distribution systems analysis', *Journal of the Hydraulics Division* **94**(1), 219–234.

Simpson, A. (2011), 'Comparing the q-equations and todini-pilati formulation for solving the water distribution system equations', *Water Distribution Systems Analysis (12th: 2010: Tucson, Arizona, USA)* .

Simpson, A. R. (1999), Modeling of pressure regulating devices: The last major problem to be solved in hydraulic simulation, *in* 'Proceedings of 29th Annual Water Resources Planning and Management Conference, ASCE'.

Skworcow, P., Ulanicki, B., AbdelMeguid, H. and Paluszczyszyn, D. (2010), 'Model predictive control for energy and leakage management in water distribution systems'.

Strang, G. (1988), 'A framework for equilibrium equations', *SIAM Review* **30**(2), 283–297.

Sturm, R. and Thornton, J. (2005), Proactive leakage management using district metered areas (dma) and pressure management–is it applicable in north america, *in* 'IWA Leakage 2005 conference proceedings'.

Swain, D. L., Tsiang, M., Haugen, M., Singh, D., Charland, A., Rajaratnam, B. and Diffenbaugh, N. S. (2014), 'The extraordinary california drought of 2013-2014: Character, context, and the role of climate change', *Bull Am Meteorol Soc* **95**(7), S3–S7.

Tabesh, M., Yekta, A. A. and Burrows, R. (2009), 'An integrated model to evaluate losses in water distribution systems', *Water Resources Management* **23**(3), 477–492.

Tang, K.-S., Man, K.-F., Kwong, S. and He, Q. (1996), 'Genetic algorithms and their applications', *Signal Processing Magazine, IEEE* **13**(6), 22–37.

Technolog (2015), 'Regulo'. [Online; accessed 05-06-2014].
URL:
http://www.technolog.com/water/products/pressure-control/12/regulo-sms-gprs-electronic-prv-controller.html

Todini, E. (2000), 'Looped water distribution networks design using a resilience index based heuristic approach', *Urban water* **2**(2), 115–122.

Todini, E. (2003), 'A more realistic approach to the extended period simulation of water distribution networks', *Advances in water supply management* pp. 173–184.

Todini, E. and Pilati, S. (1988), A gradient algorithm for the analysis of pipe networks, *in* 'Computer applications in water supply: vol. 1—systems analysis and simulation', Research Studies Press Ltd., pp. 1–20.

Todini, E. and Rossman, L. A. (2012), 'Unified framework for deriving simultaneous equation algorithms for water distribution networks', *Journal of Hydraulic Engineering* **139**(5), 511–526.

Ulanicka, K., Bounds, P., Ulanicki, B. and Rance, J. (2001), 'Pressure control of a large scale water distribution network with interacting water sources–a case study', *Water software systems: Theory and applications* **2**, 41–53.

Ulanicki, B., AbdelMeguid, H., Bounds, P. and Patel, R. (2008), Pressure control in district metering areas with boundary and internal pressure reducing valves, *in* 'The 10th International Water Distribution System Analysis Conference', pp. 17–20.

Ulanicki, B., Bounds, P., Rance, J. and Reynolds, L. (2000), 'Open and closed loop pressure control for leakage reduction', *Urban Water* **2**(2), 105–114.

Ulanicki, B., Kahler, J. and See, H. (2007), 'Dynamic optimization approach for solving an optimal scheduling problem in water distribution systems', *Journal of Water Resources Planning and Management* **133**(1), 23–32.

Ulanicki, B. and Skworcow, P. (2014), 'Why prvs tends to oscillate at low flows', *Procedia Engineering* **89**, 378–385.

Ulanicki, B., Zehnpfund, A. and Martinez, F. (1996), Simplification of water distribution network models, *in* 'Proc., 2nd Int. Conf. on Hydroinformatics', Balkema Rotterdam, Netherlands, pp. 493–500.

United Nations (2012), 'The united nations world water development 42 report 4: Managing water under uncertainty and risk'.

US Environmental Protection Agency (2007), 'Factoids: Drinking water and ground water statistics for 2007'.

Vairavamoorthy, K. and Lumbers, J. (1998), 'Leakage reduction in water distribution systems: optimal valve control', *Journal of hydraulic Engineering* **124**(11), 1146–1154.

Van Zyl, J. E., Savic, D. A. and Walters, G. A. (2004), 'Operational optimization of water distribution systems using a hybrid genetic algorithm', *Journal of water resources planning and management* **130**(2), 160–170.

Wagner, J. M., Shamir, U. and Marks, D. H. (1988), 'Water distribution reliability: simulation methods', *Journal of Water Resources Planning and Management* **114**(3), 276–294.

Walski, T. (2015), 'Discussion of" knowledge-based optimization model for control valve locations in water distribution networks"', *Journal of Water Resources Planning and Management* .

Water Authorities Association and others (1985), *Leakage control policy and practice*, Water Authorities Association.

Webster, F. V. (1958), Traffic signal settings, Technical report.

Wong, S. and Yang, H. (1997), 'Reserve capacity of a signal-controlled road network', *Transportation Research Part B: Methodological* **31**(5), 397–402.

Wood, D. J. and Charles, C. O. (1972), 'Hydraulic network analysis using linear theory', *Journal of the Hydraulics division* **98**(7), 1157–1170.

World Health Organization (2004), 'Design and operation of distribution networks'.
URL: *http://www.who.int/water_sanitation_health/dwq/en/piped3.pdf*, *note = [Online; accessed 02-12-2014]*

Wright, R., Stoianov, I., Parpas, P., Henderson, K. and King, J. (2014*a*), 'Adaptive water distribution networks with dynamically reconfigurable topology', *Journal of Hydroinformatics* **16**(6), 1280–1301.

Wright, R., Stoianov, I. and Parpas, P. (2014*b*), 'Dynamic topology in water distribution networks', *12th Computing and Control for the Water Industry, Procedia Engineering* **70**, 1735–1744.

Wright, R., Abraham, E., Stoianov, I. and Parpas, P. (2015*a*), 'Control of water distribution networks with dynamic topologies using strictly feasible sequential convex programming', *Water Resources Research* **51**, 99259941.

Wright, R., Stoianov, I. and Parpas, P. (2015*b*), 'Experimental investigation of resilience and pressure management in water distribution networks', *13th Computing and Control for the Water Industry, Procedia Engineering* **119**, 643–652.

Wright, R., Herrera, M., Stoianov, I. and Parpas, P. (2015*c*), 'Hydraulic resilience index for the critical link analysis of multi-feed water distribution networks', *13th Computing and Control for the Water Industry, Procedia Engineering* **119**, 1249–1258.

Wright, R., Abraham, E., Stoianov, I. and Parpas, P. (2015*d*), 'Optimized control of pressure reducing valves in water distribution networks with dynamic topology', *13th Computing and Control for the Water Industry, Procedia Engineering* **119**, 1003–1011.

Yang, H. and H. Bell, M. G. (1998), 'Models and algorithms for road network design: a review and some new developments', *Transport Reviews* **18**(3), 257–278.

Yates, C., R, C. and MacDonald, G. (2014), Advanced pressure management

utilizing automated prv control in a dual supply dma, Canadian Society of Civil Engineering Annual Conference 2014, CSCE, Halifax, Nova Scotia.

Yazdani, A., Otoo, R. A. and Jeffrey, P. (2011), 'Resilience enhancing expansion strategies for water distribution systems: A network theory approach', *Environmental Modelling & Software* **26**(12), 1574–1582.

Zan, T. T. T., Lim, H. B., Wong, K.-J., Whittle, A. J. and Lee, B.-S. (2014), 'Event detection and localization in urban water distribution network', *Sensors Journal, IEEE* **14**(12), 4134–4142.

Zhang, X. and van Wee, B. (2012), 'Enhancing transportation network capacity by congestion pricing with simultaneous toll location and toll level optimization', *Engineering Optimization* **44**(4), 477–488.

Zigrang, D. and Sylvester, N. (1982), 'Explicit approximations to the solution of colebrook's friction factor equation', *AIChE Journal* **28**(3), 514–515.

Zillober, C., Schittkowski, K. and Moritzen, K. (2004), 'Very large scale optimization by sequential convex programming', *Optimization Methods and Software* **19**(1), 103–120.

Appendix A Model Calibration

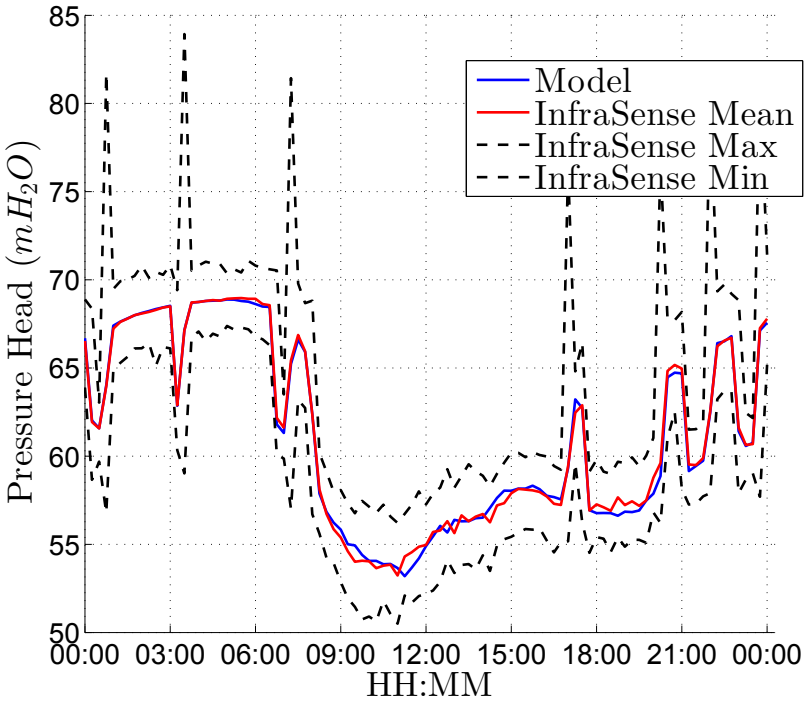


Figure A.1: InfraSense TS Logger ID 1 (See Figure 5.19, Section 5.5 for logger locations)

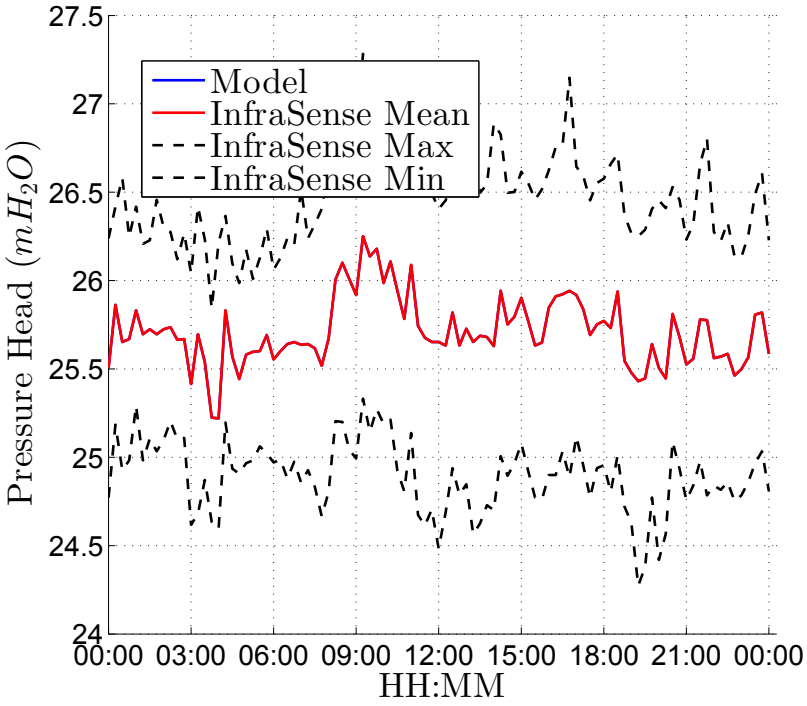


Figure A.2: InfraSense TS Logger ID 2 (See Figure 5.19, Section 5.5 for logger locations)

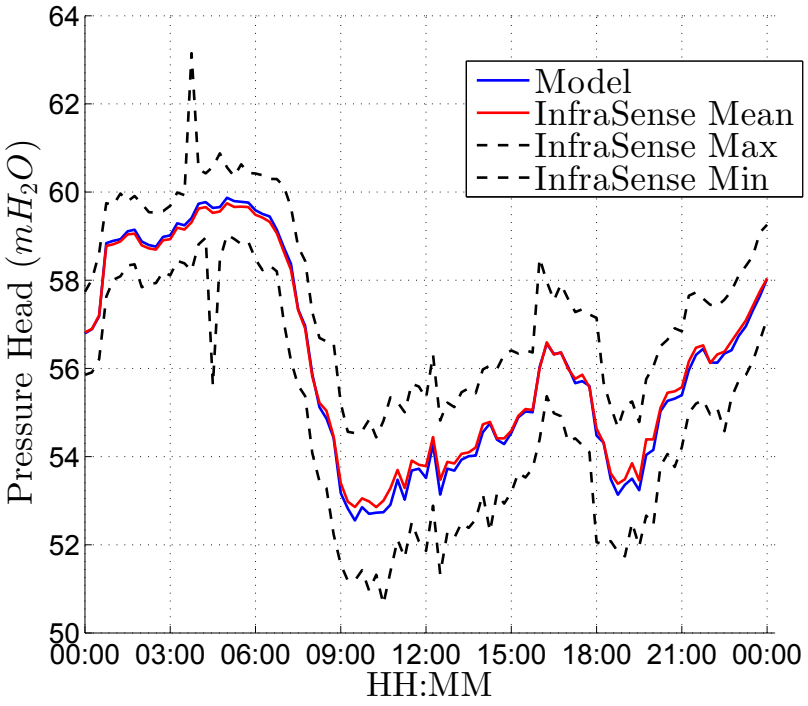


Figure A.3: InfraSense TS Logger ID 3 (See Figure 5.19, Section 5.5 for logger locations)

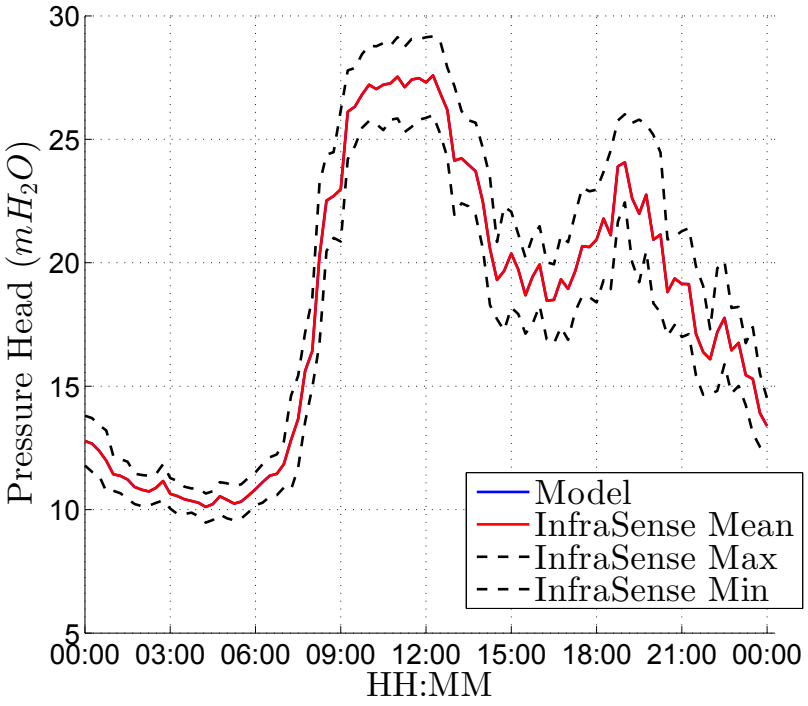


Figure A.4: InfraSense TS Logger ID 4 (See Figure 5.19, Section 5.5 for logger locations)

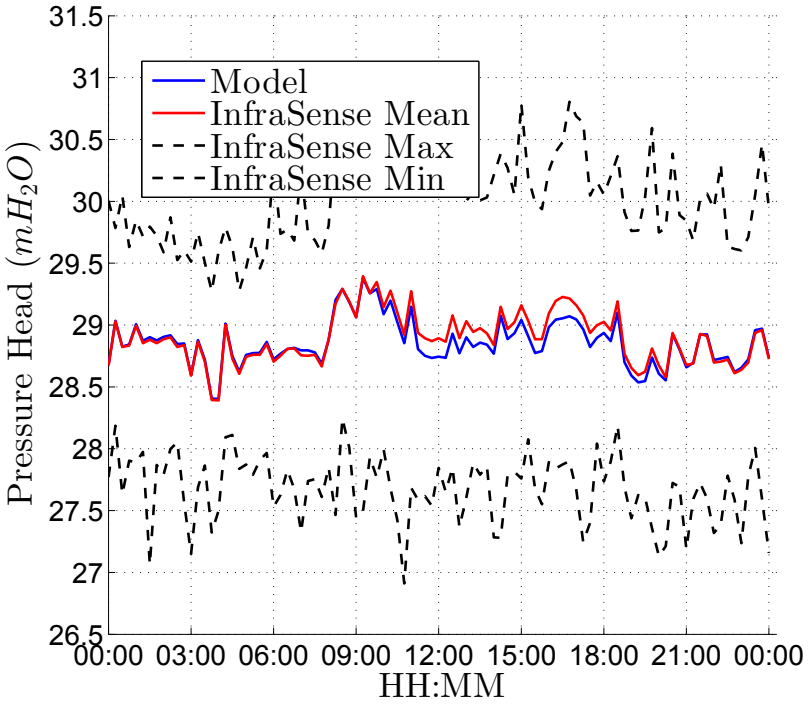


Figure A.5: InfraSense TS Logger ID 5 (See Figure 5.19, Section 5.5 for logger locations)

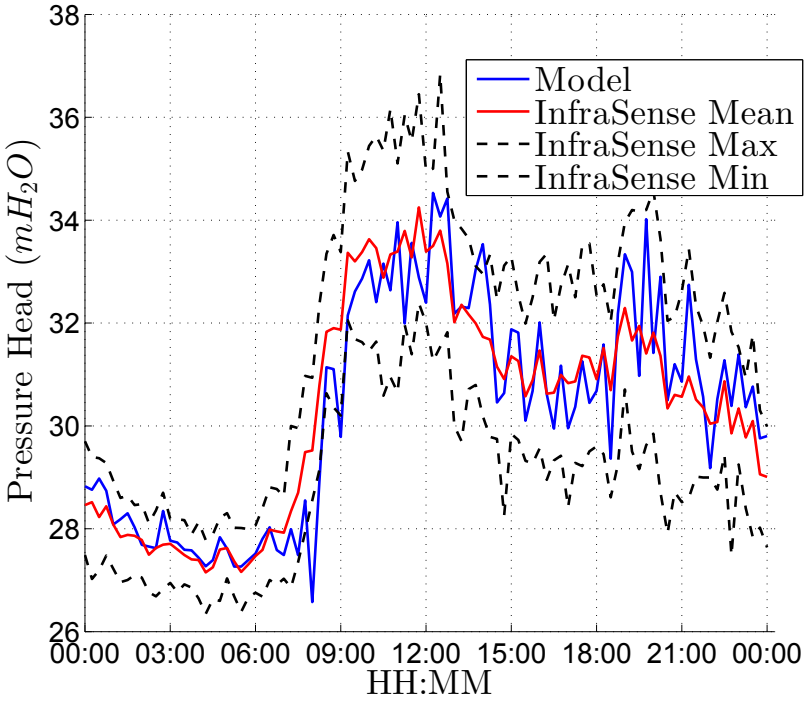


Figure A.6: InfraSense TS Logger ID 6 (See Figure 5.19, Section 5.5 for logger locations)

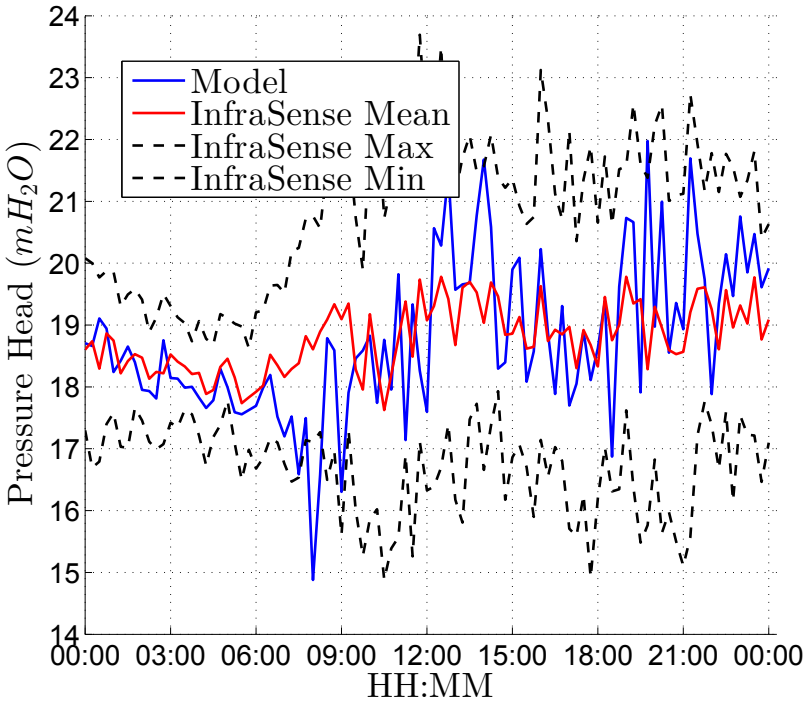


Figure A.7: InfraSense TS Logger ID 7 (See Figure 5.19, Section 5.5 for logger locations)

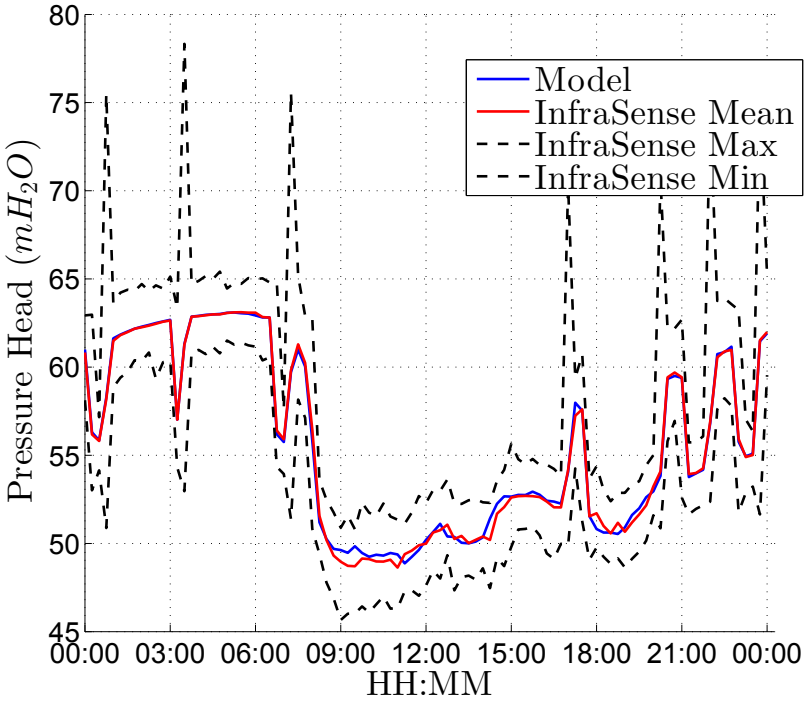


Figure A.8: InfraSense TS Logger ID 8 (See Figure 5.19, Section 5.5 for logger locations)

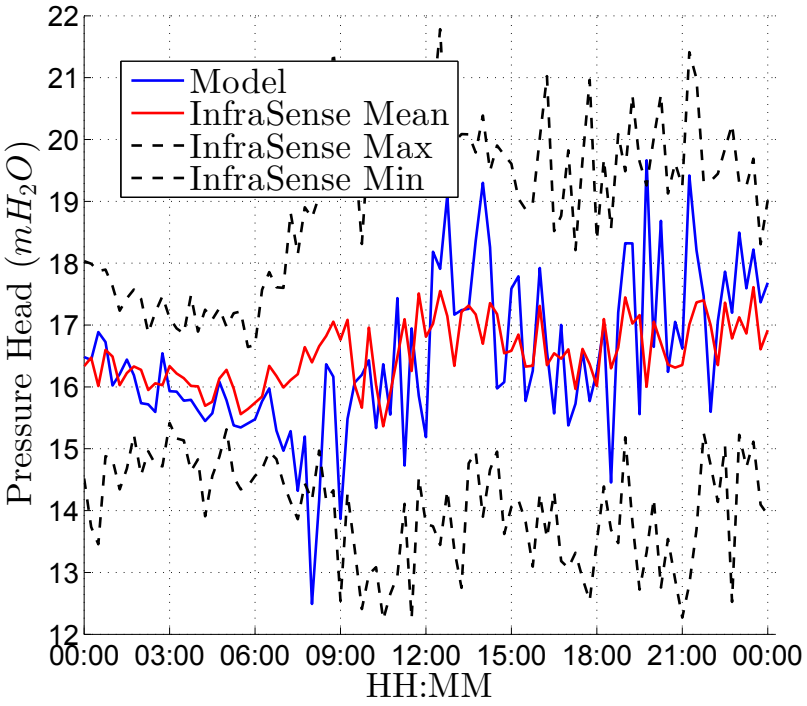


Figure A.9: InfraSense TS Logger ID 9 (See Figure 5.19, Section 5.5 for logger locations)

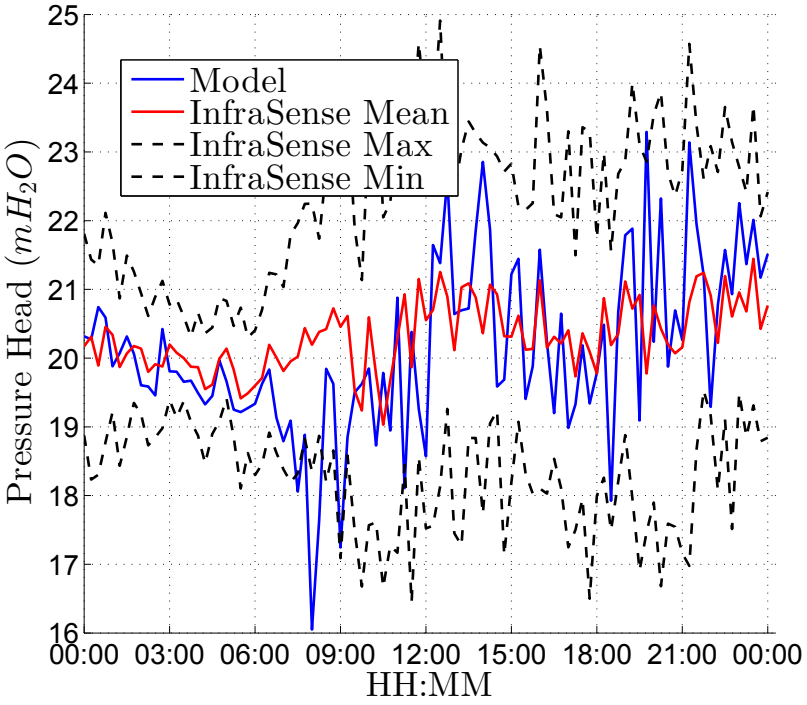


Figure A.10: InfraSense TS Logger ID 10 (See Figure 5.19, Section 5.5 for logger locations)

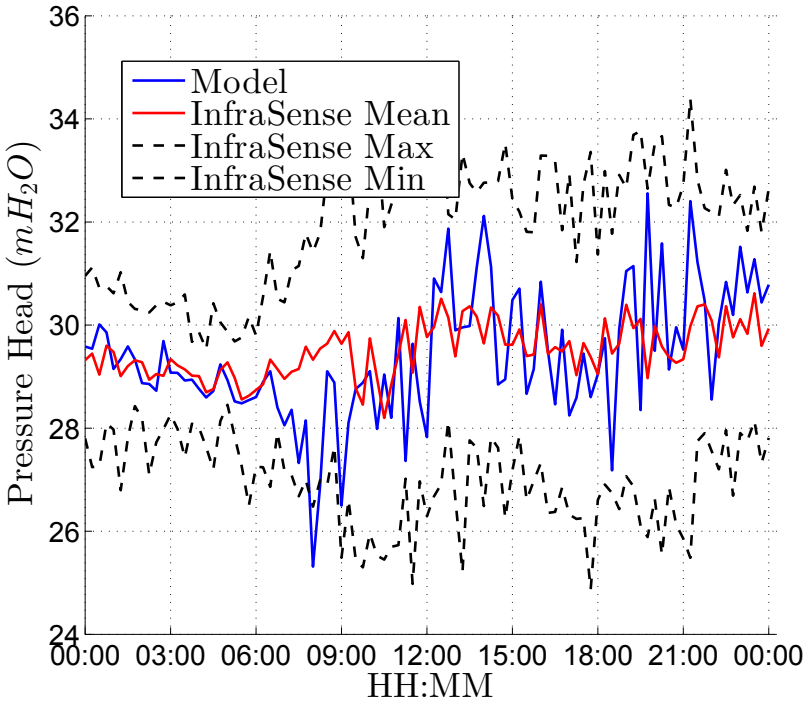


Figure A.11: InfraSense TS Logger ID 11 (See Figure 5.19, Section 5.5 for logger locations)

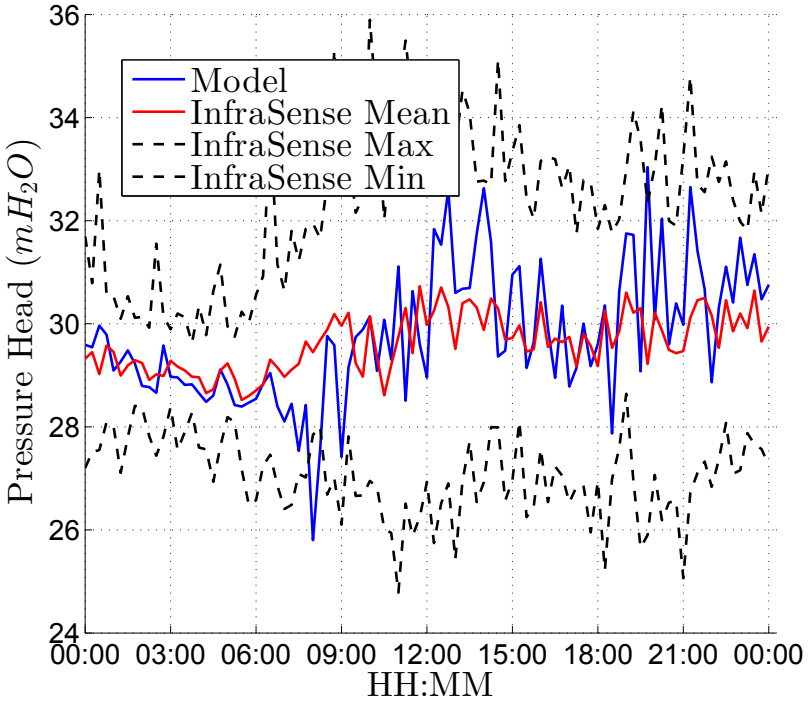


Figure A.12: InfraSense TS Logger ID 12 (See Figure 5.19, Section 5.5 for logger locations)

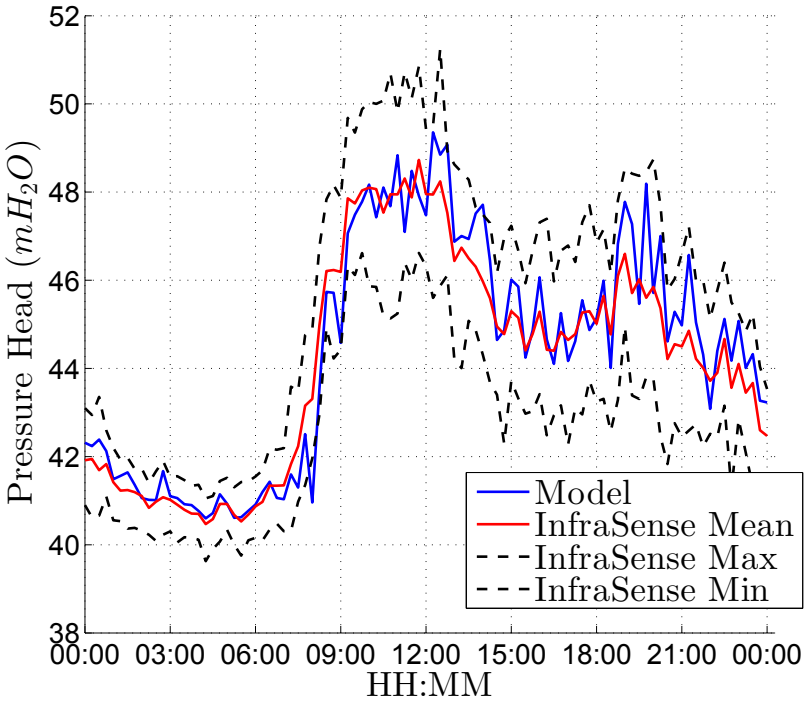


Figure A.13: InfraSense TS Logger ID 13 (See Figure 5.19, Section 5.5 for logger locations)

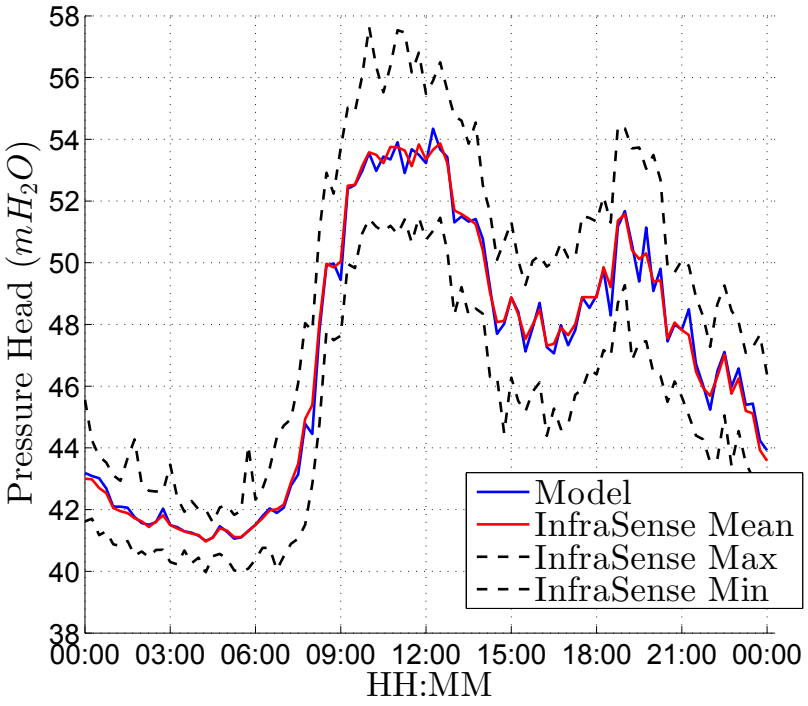


Figure A.14: InfraSense TS Logger ID 14 (See Figure 5.19, Section 5.5 for logger locations)

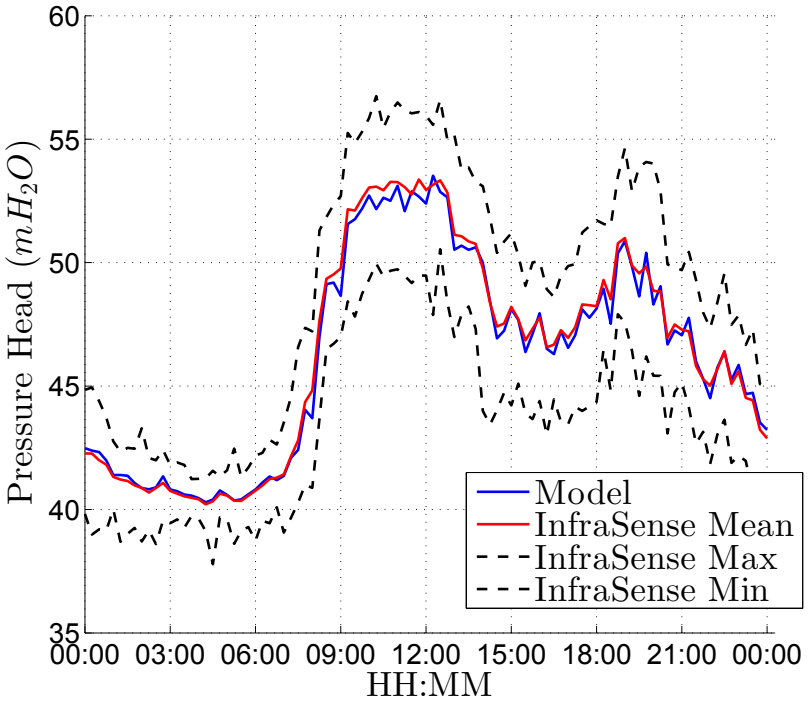


Figure A.15: InfraSense TS Logger ID 15 (See Figure 5.19, Section 5.5 for logger locations)

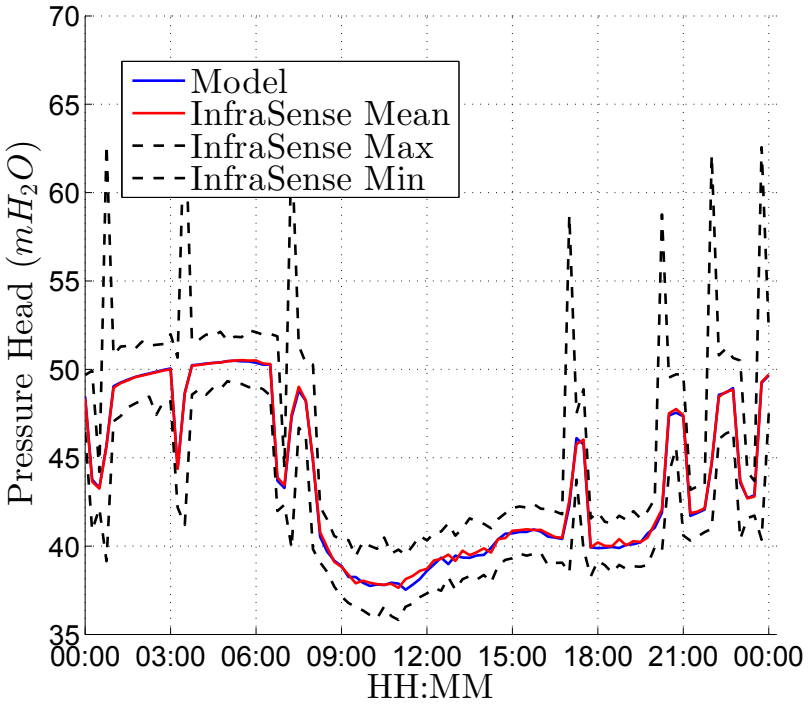


Figure A.16: InfraSense TS Logger ID 16 (See Figure 5.19, Section 5.5 for logger locations)

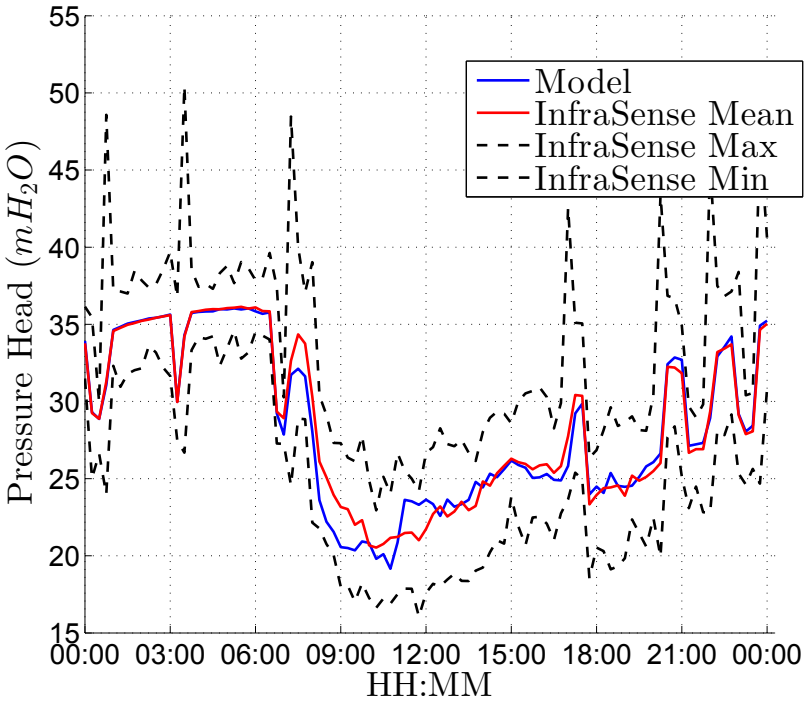


Figure A.17: InfraSense TS Logger ID 17 (See Figure 5.19, Section 5.5 for logger locations)

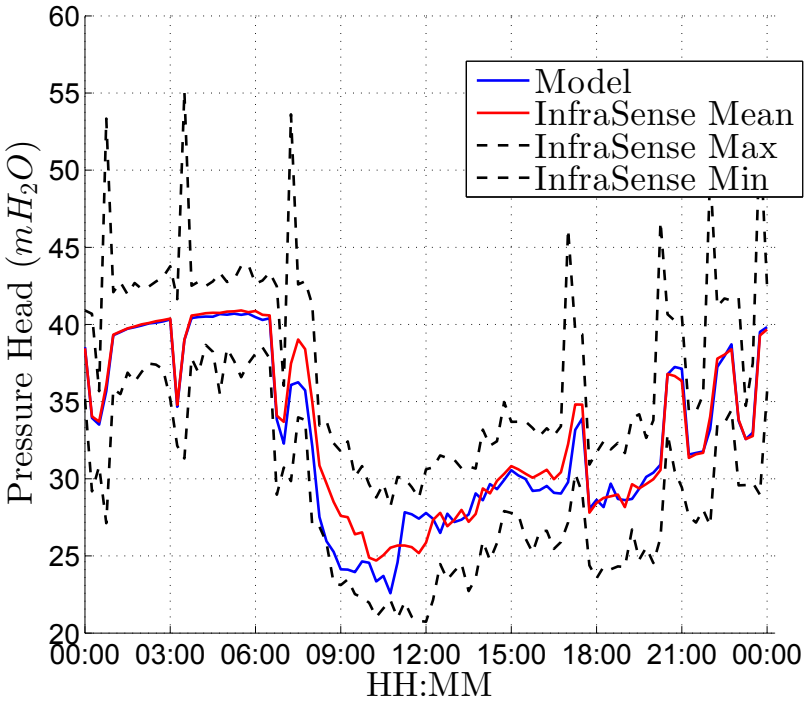


Figure A.18: InfraSense TS Logger ID 18 (See Figure 5.19, Section 5.5 for logger locations)

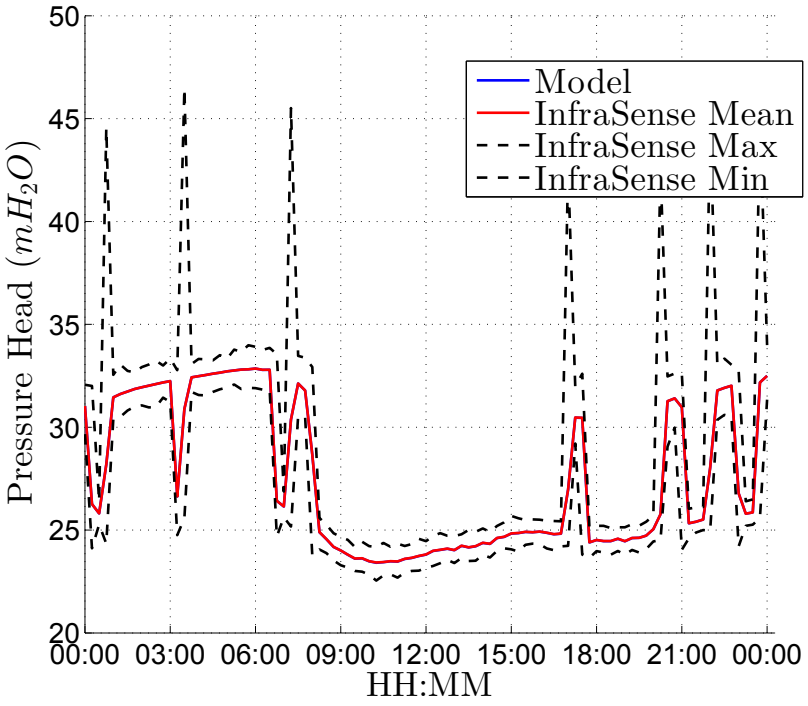


Figure A.19: InfraSense TS Logger ID 19 (See Figure 5.19, Section 5.5 for logger locations)

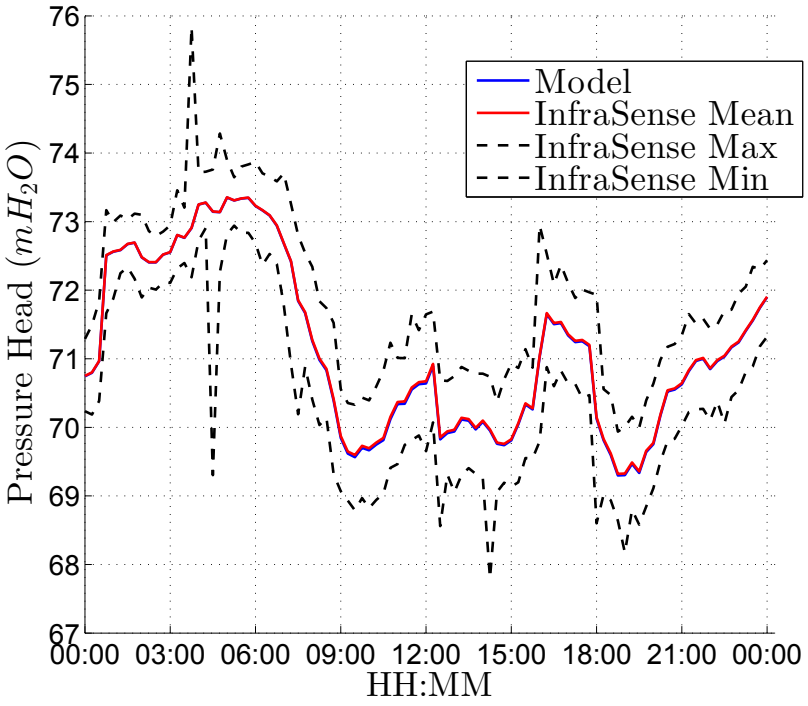


Figure A.20: InfraSense TS Logger ID 20 (See Figure 5.19, Section 5.5 for logger locations)

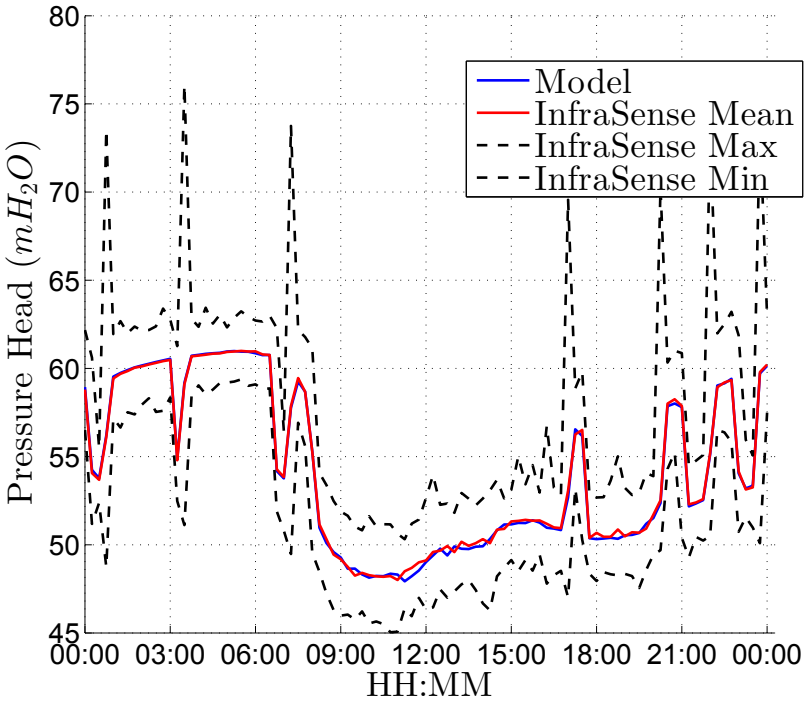


Figure A.21: InfraSense TS Logger ID 21 (See Figure 5.19, Section 5.5 for logger locations)

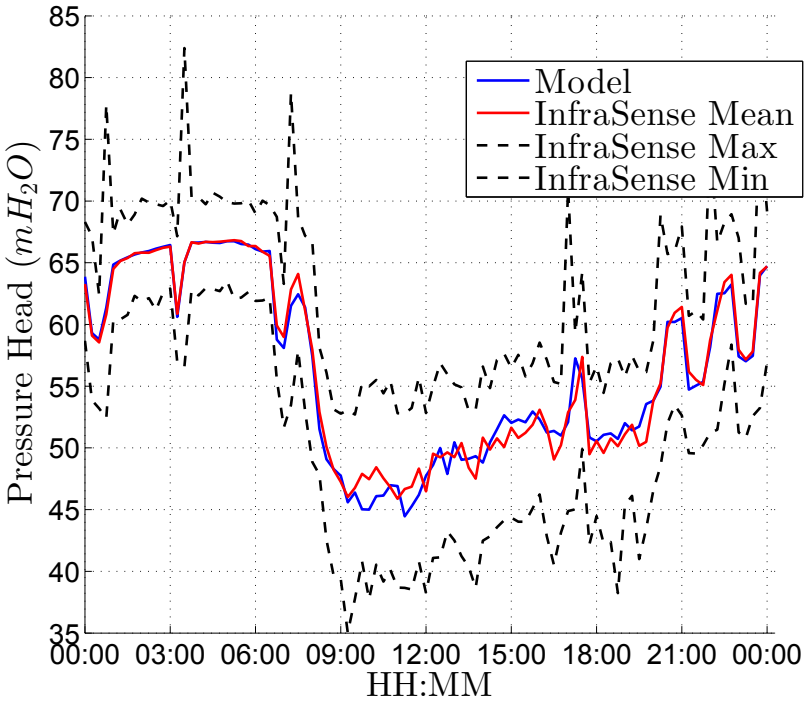


Figure A.22: InfraSense TS Logger ID 22 (See Figure 5.19, Section 5.5 for logger locations)

Appendix B Validation of Model Calibration

Logger ID	Mean Pressure Difference Over 24 Hours
2	0.00
3	0.34
4	0.00
9	1.92
10	1.90
11	1.83
12	1.93
13	0.87
14	0.38
15	0.49
16	0.17
17	0.85
18	0.93
19	0.00
20	0.02
21	0.33
22	1.61

Table 15: Phase 1 pressure data and model comparison. Data at Logger ID 1, 5, 6, 7 and 8 was unavailable during this period. Logger locations are shown in Figure 5.19, Section 5.5

Logger ID	Mean Pressure Difference Over 24 Hours
1	0.31
2	0.00
3	0.11
4	0.00
5	0.07
6	0.58
7	0.81
8	0.39
9	0.81
10	0.83
11	0.82
12	0.78
13	0.55
14	0.20
15	0.26
16	0.15
17	0.66
18	0.82
19	0.00
20	0.02
21	0.15
22	0.82

Table 16: Phase 2 pressure data and model comparison. Logger locations are shown in Figure 5.19, Section 5.5

Logger ID	Mean Pressure Difference Over 24 Hours
3	0.11
4	0.00
5	0.68
6	0.48
7	0.68
8	0.69
9	0.56
10	0.57
11	0.59
12	0.55
13	0.41
14	0.21
15	0.21
16	0.42
17	0.48
18	0.55
19	0.00
20	0.01
21	0.26

Table 17: Phase 3 pressure data and model comparison. Data at Logger ID 1, 2, and 22 was unavailable during this period. Logger locations are shown in Figure 5.19, Section 5.5